Dkt. 37690-II-B/JPW/SHS

IN THE UNITED STATES PATENT AND TRADEMARK OFFICE

Applicants	:	Gary A. Beaudry and Paul J. Maddon	
Serial No.	:	08/484,681	Examiner: P. Gambel
Filed	:	June 7, 1995	Group Art Unit: 1644
For	:	CD4 GAMMA2 AND CD4-IgG2 CHIMERAS	

1185 Avenue of the Americas
New York, New York 10036

Assistant Commissioner for Patents
Washington, D.C. 20231

DECLARATION UNDER 37 C.F.R. §1.132 OF PAUL J. MADDON

I, Paul J. Maddon, M.D., Ph.D, hereby declare that:

1. I am a coinventor of the invention currently being claimed in the subject patent application.

2. I am also Chief Executive Officer of Progenics Phamaceuticals, Inc. ("Progenics") in Tarrytown, New York, the assignee of record of the subject application. A copy of my curriculum vitae is attached hereto as **Exhibit 1**.

3. I am familiar with United States Patent No. 5,565,335 ("'335 patent") issued October 15, 1996 to Daniel J. Capon and entitled Adhesion Variants. Example 2 of the '335 patent purports to be a procedure for obtaining a CD4-IgG heterotetramer which consists of the V1 region of CD4.

4. I am also familiar with PCT International Publication No. WO89/02922 ("PCT Publication"), published April 6, 1989,

the specification of which is identical to that of the '335 patent.

5. I reviewed the PCT publication shortly after it was published in 1989. After reviewing the PCT Publication, particularly Example 2 thereof, I understood that a CD4-IgG heterotetramer which included only the V1 domain of CD4 would be expressed in 293 cells, myeloma cells or other competent cells following the description in the PCT Publication.

6. Also, the common understanding in the field as of October 2, 1987, the earliest date priority of which is claimed in the PCT Publication and the '335 patent, was that a chimeric antibody, such as a CD4-IgG heterotetramer, when expressed in 293, myeloma or other competent cells would be secreted. Copies of scientific publications evidencing that this was the common understanding in the field as of October 2, 1987 are attached hereto as **Exhibits 2-5**.

7. Accordingly, I directed and supervised scientists at Progenics to conduct an experiment to make the CD4-IgG heterotetramer consisting of the V1 domain of CD4 described in Example 2 of the PCT Publication. The experiment is recorded in the laboratory notebook of Ms. Dina Burstein, a technician, and true and accurate copies of the relevant laboratory notebook pages (except that the dates have been redacted) are attached as **Exhibit 6**. The result of this experiment was that the CD4-IgG heterotetramer containing only the V1 domain of CD4 did not secrete, i.e. no chimeric antibody product could be detected when plasmids encoding the heterotetramer were

expressed in Cos cells. Cos cells were known in the field to be capable of being transformed with vector DNA, i.e "competent" as of October 2, 1987, as shown by the scientific papers attached hereto as Exhibits 7-11.

8. The experiments referred to in paragraph 7 are also referenced in the subject patent application at page 40, lines 5-8, where it states that efforts to secrete a heterotetramer having only the V1 domain of CD4 were not successful. That the heterotetramer described in Example 2 of the PCT Publication which consists of only the V1 domain of CD4 did not secrete when expressed in Cos cells was surprising because at the time, it was expected that a CD4-IgG chimeric antibody which included only the V1 domain of CD4 would secrete.

9. Based on the experimental results that the CD4-IgG chimeric antibody containing only V1 did not secrete, it would have been expected that a CD4-IgG heterotetramer containing both the V1 and V2 domains of CD4 would also not secrete since there was no basis as of October 2, 1987 to expect a V1V2 containing chimeric antibody would behave differently from a V1 only containing chimeric antibody.

10. Accordingly, it would not have been obvious to one of ordinary skill in the field as of October 2, 1987 that if one expressed a V1V2 containing chimeric antibody in competent cells, it would secrete, i.e. there was no reasonable expectation of success that a V1V2 containing heterotetramer could be secreted.

11. After the experiment described in paragraphs 7-10, I directed and supervised scientists at Progenics to make a CD4-IgG heterotetramer consisting of both the V1 and V2 domains of CD4. When plasmids encoding this heterotetramer were transfected and then expressed in Cos cells, the very same competent cells from which the chimeric antibody containing only the V1 domain of CD4 did not secrete, unexpectedly the heterotetramer was secreted and therefore, could be, and was, purified. The experiment which resulted in the successful secretion and subsequent purification of the heterotetramer consisting of both the V1 and V2 domains of CD4 is described on page 45, lines 14-32 and in Figure 12 of the subject application.

I hereby declare that all statements made herein of our own knowledge are true and that all statements made on information and belief are believed to be true; and further that these statements were made with the knowledge that willful false statements and the like so made are punishable by fine or imprisonment, or both, under § 1001 of Title 18 of the United States Code and that such willful false statements may jeopardize the validity of the application or any patent issued thereon.

Date: Feb. 26, 2001

Paul D. Maddon

Paul J. Maddon, M.D., Ph.D

ANTIMICROBIAL AGENTS AND CHEMOTHERAPY, Dec. 1991, p. 2580–2586
0066-4804/91/122580-07$02.00/0

VOL. 35, NO. 12

Exhibit (A)

Phase 1 Study of Recombinant Human CD4-Immunoglobulin G Therapy of Patients with AIDS and AIDS-Related Complex

TERI L. HODGES,[1,2]† JAMES O. KAHN,[3,4]‡ LAWRENCE D. KAPLAN,[3,4]‡ JEROME E. GROOPMAN,[1,2]† PAUL A. VOLBERDING,[3,4]‡ ARTHUR J. AMMAN,[5] CAROL J. ARRI,[3,4]‡ LISA M. BOUVIER,[1,2]† JOYCE MORDENTI,[5] ALLEN E. IZU,[5] AND J. DAVIS ALLAN[1,2]†*

New England Deaconess Hospital[1] and Harvard Medical School,[2] Boston, Massachusetts 02215; San Francisco General Hospital, San Francisco, California 94110[3]; University of California at San Francisco, San Francisco, California 94143[4]; and Genentech, Inc., South San Francisco, California 94080

Received 27 March 1991/Accepted 24 September 1991

The safety and pharmacokinetics of recombinant CD4-immunoglobulin G (rCD4-IgG) were evaluated in a phase 1 study with dose escalation. A total of 16 patients, 6 with AIDS and 10 with AIDS-related complex, were evaluated at two university-affiliated hospital clinics. rCD4-IgG was administered once weekly for 12 weeks to four patients each at doses of 0.03, 0.1, 0.3, and 1.0 mg/kg of body weight. Dosing was intravenous for two patients in the 1.0-mg/kg dose group and intramuscular for the remaining patients. Pharmacokinetic, toxicity, and immunologic variables were monitored with all patients. Administration of rCD4-IgG was well tolerated, with no important clinical or immunologic toxicities noted. No subjects required dose reduction or discontinuation of therapy due to toxicity. No consistent changes were seen in human immunodeficiency virus antigen levels in serum or CD4 lymphocyte populations. The volume of distribution was small, and compared with that of rCD4, the half-life of the hybrid molecule was markedly prolonged following intramuscular or intravenous administration. The rate and extent of absorption following intramuscular dosing were variable. Intramuscular administration of rCD4-IgG appears to be inferior to intravenous dosing from a pharmacokinetic standpoint, with lower peak concentrations and variable absorption. After intravenous administration, peak concentrations of rCD4-IgG in serum (20 to 24 μg/ml) that have shown antiviral activity in vitro against more sensitive clinical isolates of human immunodeficiency virus were achieved. The peak concentrations in serum after intramuscular administration were below these levels. Treatment with rCD4-IgG was well tolerated at the doses administered to patients in this study but did not result in significant changes in CD4 lymphocyte counts or p24 antigen levels in serum.

CD4 is a surface glycoprotein of a subset of mature T lymphocytes and serves as the primary receptor for human immunodeficiency virus (HIV) (10, 21, 25, 26) and class II major histocompatibility complex antigen in humans (7, 14, 22). Infection of CD4-bearing cells by diverse strains of HIV type 1 (HIV-1), and by the closely related lentiviruses HIV-2 and simian immunodeficiency virus is mediated by the binding of a viral envelope glycoprotein, gp120, to cellular CD4 (27). The subsequent destruction of CD4 lymphocytes by direct viral cytopathicity, or possibly by immune mechanisms which may not distinguish between infected cells and uninfected cells with free viral gp120 on the surface, is important in the pathogenesis of AIDS (23).

Recombinant soluble CD4 (rCD4), like native CD4, binds viral gp120 with high affinity (11, 13, 18, 29, 30). The antiviral effects of rCD4 have been demonstrated in vitro by the measurement of decreases in both HIV-induced syncytium formation and reverse transcriptase activity (4, 11, 13, 18, 29, 30). In addition, in vivo evidence of rCD4 antiviral activity against simian immunodeficiency virus in rhesus monkeys has been reported (33). Phase 1 clinical trials with patients with AIDS and AIDS-related complex (20, 28) have shown that levels of rCD4 in serum comparable to concentrations that exhibit antiviral effects in vitro are achievable without apparent toxicity; however, rCD4 is rapidly cleared from circulation, with a half-life of approximately 1 h after intravenous dosing and 9 to 11 h after intramuscular or subcutaneous administration (20).

Hybrid molecules incorporating rCD4 that offer improved pharmacokinetics and possibly more potent antiviral activity compared with those of rCD4 (3, 5, 31) have been developed. A recombinant human CD4-immunoglobulin G (rCD4-IgG) hybrid molecule (3, 5) has been shown to bind viral gp120 as readily as rCD4 and to have similar in vitro antiviral activity. Potential advantages of rCD4-IgG relative to rCD4 include a longer serum half-life and Fc-receptor binding by the IgG portion of the molecule, resulting in elimination of HIV-infected cells, as has been shown to occur in vitro (3). On the basis of these data, we conducted a phase 1 evaluation of the safety and pharmacokinetics of rCD4-IgG for patients with AIDS and AIDS-related complex.

MATERIALS AND METHODS

Subjects. Sixteen patients, aged 18 years or older, with a diagnosis of AIDS or AIDS-related complex were enrolled. All had documented HIV infection and total CD4 cell counts of ≤500 cells per mm^3. Centers for Disease Control diagnostic criteria for AIDS were used, and AIDS-related complex was defined as one or more of the following symptoms present for more than 30 days: fever, night sweats, diarrhea without an identifiable pathogen, weight loss of 10% or more

* Corresponding author.
† Present address: Department of Medicine, New England Deaconess Hospital, 185 Pilgrim Road, Boston, MA 02215.
‡ Present address: AIDS Program, Ward 84, San Francisco General Hospital, San Francisco, CA 94110.

of baseline, fatigue, oral ha[illegible]eukoplasia, ral candidiasis, and HIV antigenemia. Subjects were required to be intolerant of or unresponsive to zid vudine therapy or to have declined zidovudine therapy. Entry criteria included a neutrophil count f 1.0 × 10^3/mm^3 or greater, a platelet c unt of 75 × 10^3/mm^3 or greater, total bilirubin of 1.5 mg/dl r less, an aspartate aminotransferase level less than three times the upper limit f normal, a prothrombin time less than 1.5 times that of the control, and a creatinine level of 2.0 mg/dl or less in serum. Patients with serious active opportunistic infections and malignancies other than Kaposi's sarcoma were excluded. Women who were pregnant or breast feeding and subjects with reproductive potential who were unwilling to use effective contraception were also ineligible. Administration of zidovudine, ganciclovir, intravenous acyclovir, interferon, other immunomodulating agents, or experimental therapy was not allowed during the initial phase of the study. Patients with a prior history of *Pneumocystis carinii* pneumonia (PCP) or with a total CD4 count of ≤200 cells per mm^3 were allowed to receive prophylactic therapy for PCP. Suppressive therapy for mucocutaneous candidiasis was allowed. No patient had received any antiretroviral agent, antineoplastic chemotherapy, or immunomodulating therapy for at least 4 weeks prior to entry. This study was approved by the Committees for Human Research at the New England Deaconess Hospital, Boston, Mass., and the University of California, San Francisco. Written informed consent was obtained from all subjects prior to participation.

Study design. This study was a two-center, phase 1, open-label evaluation of the safety and pharmacokinetics of rCD4-IgG. Four patients each were enrolled at doses of 0.03, 0.1, 0.3, and 1.0 mg of rCD4-IgG per kg of body weight. Administration was intramuscular for 14 patients and intravenous for 2 of the 4 patients receiving the 1.0-mg/kg dose. All patients received a single weekly injection of rCD4-IgG at a fixed dose for 12 weeks. Pharmacokinetic studies were performed on days 1 through 7 and with selected patients after 12 weeks.

After completing the initial 12-week phase of the protocol, patients were allowed to continue maintenance therapy administered intramuscularly or intravenously. During the extended maintenance phase of the study, the dose for each patient was escalated to either 0.3 mg/kg twice weekly or 1.0 mg/kg weekly. During this maintenance phase, concomitant zidovudine therapy was permitted, as was systemic chemotherapy for progressive Kaposi's sarcoma.

Clinical and laboratory monitoring. Complete histories were obtained and physical examinations were performed prior to entry and every 2 weeks throughout the study. Safety monitoring at regularly scheduled intervals included complete blood counts with differential and platelets; serum chemistry profiles including sodium, potassium, calcium, uric acid, blood urea nitrogen, creatinine, cholesterol, triglycerides, glucose, lactate dehydrogenase, albumin, alkaline phosphatase, total bilirubin, and aspartate and alanine aminotransferase levels; urinalyses; prothrombin and activated partial thromboplastin times; and chest radiographies and electrocardiographies (at entry). Lymphocyte populations, quantitative immunoglobulins, total serum complement, and anti-rCD4-IgG antibody determinations were followed as immunologic safety parameters.

Human rCD4-IgG. Human rCD4-IgG consisted of a portion of rCD4 including the gp120-binding domain fused to the human IgG1 heavy-chain constant region and was produced by oligonucleotide-directed deletional mutagenesis after insertion int[illegible]a [illegible]ese hamster ovary cell line (5, 16). Th molecule was is lated from cell culture medium and purified by routine methods of protein isolation. The final product was tested f r general safety, purity, and sterility according to guidelines from the Center for Biologics Evaluati n and Research, F od and Drug Administration. The rCD4-IgG was supplied as a sterile lyophilized powder for reconstitution with sterile water t 5 mg/ml by Genentech, Inc., South San Francisco, Calif. The two patients who received the 1.0-mg/kg intramuscular dose required multiple injections. The sites for intramuscular injection were standardized and rotated sequentially between deltoid and gluteal sites n each patient. Patients received their injections from the study nurses and were not allowed to self administer.

Anti-rCD4-IgG antibody. Radioimmunoprecipitation with a modification of the Farr assay (6, 12) was used t detect antibodies to rCD4-IgG. The molecule was radiolabeled with ^{125}I by a modification of the lactoperoxidase method. Specific activity was confirmed by double-antibody enzyme-linked immunoperoxidase assay. A rhesus monkey anti-rCD4-IgG antiserum served as a positive control. Th presence of antibody was defined as a binding level equal to twice that of the negative control.

HIV antigen assay. Serum samples obtained before and during the study were frozen at −70°C and later thawed and tested simultaneously for HIV antigen. A commercial kit (Abbott Laboratories, North Chicago, Ill.) was used t measure HIV antigen in serum. In the laboratory in which the test was performed, an HIV antigen level of greater than 30 pg/ml was considered positive.

Pharmacokinetic analysis. Serum samples were c llected from each patient prior to dosing and at the following times postadministration: 10 and 30 min; 1, 2, 4, 6, 8, and 12 h; and 2, 3, 4, 5, 6, and 7 days. Quantitation of rCD4-IgG levels in serum was accomplished by using an enzyme immunoassay with a monoclonal antibody, Leu 3A, that recognizes the gp120-binding domain and a second antibody specific f r th immunoglobulinlike domain of rCD4 for capture. Immunoreactive protein concentrations were used to construct semilogarithmic concentration-versus-time curves. Exponential equations were fitted to the intravenous and intramuscular data from individual patients by using a weighted nonlinear least-squares parameter estimation procedure (NONLIN84, version 87; Statistical Consultants, Lexington, Ky.). The area under the curve, clearance, initial volume, volume of distribution at steady state, half-life, and mean residence time in the serum following intravenous administration of 1.0 mg/kg were calculated from the coefficients and exponents of the exponential equations, assuming that eliminati n occurred only from the central compartment. The area under the curve and the absorption and elimination half-lives following intramuscular administration were calculated from the fitted data. The bioavailability (expressed as a percentage) following intramuscular administration was calculated for each patient as the ratio of the dose-corrected area under the curve following intramuscular administration to the mean dose-corrected area under the curve following intravenous dosing multiplied by 100. The maximum concentration in serum and time to reach the maximum concentration were observed values.

RESULTS

A total of 18 patients were enrolled. Two patients who each received a single injection of rCD4-IgG are not included in the analysis. One of these patients experienced no adverse

TABLE 1. Patient characteristics at entry

Characteristic[a]	Value
No. enrolled	18
No. evaluated	16
No. male/no. female	16/0
Age (yr)	
Mean	39
Range	29–56
AIDS	
No. of patients	6
No. with OI	5
No. with KS	0
No. with both KS and OI	1
Mean duration of AIDS diagnosis (range)[b]	21 (5–54)
No. with previous therapy with zidovudine	6
Total CD4 (cells/mm^3)	199 (118)[c]
Hemoglobin (g/dl)	14.1 (1.3)[c]
Leukocyte count (10^3 cells/mm^3)	4.6 (0.7)[c]
AIDS-related complex	
No. of patients	10
No. with previous therapy with zidovudine	8
Total CD4 (cells/mm^3)	165 (134)[c]
Hemoglobin (g/dl)	13.6 (1.6)[c]
Leukocyte count (10^3 cells/mm^3)	3.7 (1.2)[c]

[a] OI, opportunistic infection; KS, Kaposi's sarcoma.
[b] Value in months.
[c] Mean (standard deviation).

effects but requested removal from the study for personal reasons on day 5. The other patient was removed from the study when he required hospitalization for an acute exacerbation of a preexisting psychiatric illness on day 1 of the study. Patient characteristics at entry are shown in Table 1. All patients were male, with a mean age of 39 years. Ten patients had AIDS-related complex, and six had AIDS. In those patients with AIDS, the mean duration of AIDS diagnosis was 21 months prior to entry (range, 5 to 54 months). Fourteen patients had received zidovudine therapy in the past.

Of 16 evaluable patients, 15 completed the initial 12 weeks of the study. One patient treated with 0.3 mg/kg was withdrawn from the study at week 6 when there was progression of mild HIV dementia that existed prior to his entering the study. Administration of rCD4-IgG was not interrupted for any other patient during the initial 12 weeks. An opportunistic infection or malignancy developed in three patients during the initial phase of the study, as follows: one patient who had a diagnosis of AIDS-related complex at entry and who was treated with 0.03 mg of rCD4-IgG per kg developed localized Kaposi's sarcoma and PCP at week 9 while receiving aerosolized pentamidine prophylaxis and was successfully treated with intravenous pentamidine, one patient treated with 0.1 mg of rCD4-IgG per kg developed Kaposi's sarcoma at week 8 but did not require systemic therapy, and one patient who had a diagnosis of AIDS-related complex and who was treated with 1.0 mg of rCD4-IgG per kg developed PCP at week 3 while not on prophylaxis (CD4 > 250) and was successfully treated with trimethoprim and dapsone.

During the initial 12 weeks of the study, no intolerable symptoms were reported. Severe asthenia was reported by two patients at days 36 and 52. Since this symptom was present in these patients prior to their entering the study, it was judged to be unrelated to administration of the study medication. All other symptoms were graded mild to moderate and included fever, sweating, dizziness, agitation, depression, paresthesia, tremor, short-term memory loss, myalgia, abdominal pain, back pain, nausea, vomiting, diarrhea, rhinitis, and rash. None of these symptoms were judged to be related to administration of the study medication. The mean body weight for the entire group was unchanged from entry to week 12, and no individual patient sustained a 10% or greater decrease in body weight over the course of the study.

The mean leukocyte count, hemoglobin level, and platelet count for each dose group did not change significantly over the course of the study. Twelve patients had mild to moderate leukopenia (leukocyte count, 1.5×10^3 to 3.9×10^3/mm^3). In all of these patients, the leukopenia was present at entry or was transient. One subject with a leukocyte count of 2.6×10^3/mm^3 at entry had transient severe leukopenia (leukocyte count, 1.0×10^3 to 1.49×10^3/mm^3). Concurrent neutropenia that was mild (neutrophil count, 0.75×10^3 to 1.00×10^3/mm^3) or moderate (neutrophil count, 0.50×10^3 to 0.75×10^3/mm^3) occurred in five patients and one patient, respectively. Progressive decreases in total leukocytes or neutrophils did not develop in any patient with continued rCD4-IgG administration. One patient had moderate anemia (hemoglobin level, 10.0 to 12.0 g/dl), and 11 had mild anemia (hemoglobin level, 12.0 to 14.0 g/dl). The patient with moderate anemia had hemoglobin levels of 9.2 mg/dl at entry, 8.8 mg/dl on day 2, and 9.0 to 10.6 mg/dl during the following 12 weeks. Ten of the patients with mild anemia had either transient decreases or preexisting mild anemia. The hemoglobin level decreased from 13.5 to 11.9 mg/dl coincident with intravenous pentamidine treatment for PCP in one patient. No patient received transfusions during the initial phase. Mild thrombocytopenia (platelet count, 75×10^3 to 100×10^3/mm^3) was seen in three patients. Thrombocytopenia was present at entry in two patients and was transient in a third patient, and it did not progress in any instance.

The mean values for aspartate aminotransferase, alkaline phosphatase, total bilirubin, and creatinine levels for each dose group did not change significantly over the course of the study. The level of aspartate aminotransferase was mildly elevated (50 to 150 IU/liter) in one patient and moderately elevated (151 to 300 IU/liter) in another. The level of alkaline phosphatase was mildly elevated (188 to 375 IU/liter) without concurrent aspartate aminotransferase abnormality in one patient. In each case, therapy was continued and repeat testing 2 weeks later demonstrated resolution of the abnormalities. The only statistically significant change in serum chemistry values was a rise in alkaline phosphatase for all dose groups combined ($P = 0.025$). It should be noted, however, that this rise was not dose related and did not result in mean alkaline phosphatase values above the upper limits of normal. One patient previously diagnosed with Gilbert's syndrome had a total bilirubin level of 1.8 mg/dl at entry and a transient rise to 2.1 mg/dl. No other elevations of levels of alkaline phosphatase or total bilirubin were seen. Creatinine levels in serum rose from 1.2 to 1.7 mg/dl in one patient during intravenous pentamidine therapy and later returned to normal. No other elevations in creatinine levels were noted.

Five patients had prolonged prothrombin times noted on one or more occasions. A prolonged activated partial thromboplastin time was seen in two patients on one or more days.

TABLE 2. Peripheral lymphocyte subset cell counts by dose group[a]

Dose (mg/kg) and cell type	Mean no. of cells/mm³ (SD) at:				P (CI)[b]
	Entry	Day 15	Week 6	Week 12	
0.03					
CD4	269 (134)	249 (116)	227 (120)	226 (124)	0.149 (−115, 28)
CD8	1,133 (471)	1,164 (595)	900 (606)	975 (223)	0.413 (−691, 374)
Total lymphocytes	1,725 (772)	1,775 (806)	1,425 (750)	1,475 (386)	0.348 (−968, 468)
0.1					
CD4	113 (112)	115 (117)	123 (130)	113 (106)	0.975 (−23, 23)
CD8	1,153 (612)	1,162 (572)	1,005 (490)	943 (448)	0.325 (−780, 360)
Total lymphocytes	1,725 (780)	1,650 (686)	1,450 (603)	1,425 (562)	0.259 (−988, 388)
0.3					
CD4	151 (146)	121 (91)	126 (125)	90 (104)	0.395 (−257, 135)
CD8	553 (185)	598 (336)	745 (337)	668 (492)	0.568 (−615, 924)
Total lymphocytes	975 (263)	900 (424)	1,100 (408)	950 (592)	0.909 (−616, 666)
1.0					
CD4	76 (102)	66 (60)	33 (12)	67 (94)	0.395 (−257, 135)
CD8	666 (208)	843 (265)	614 (506)	480 (296)	0.080 (−413, 42)
Total lymphocytes	1,075 (411)	1,350 (465)	1,075 (685)	950 (451)	0.194 (−364, 114)
All dose groups					
CD4	152 (134)	138 (113)	127 (120)	124 (115)	0.102 (−63, 6)
CD8	871 (465)	942 (483)	816 (468)	771 (399)	0.271 (−286, 86)
Total lymphocytes	1,375 (649)	1,419 (651)	1,263 (588)	1,200 (520)	0.069 (−365, 15)

[a] Four patients were in each dose group.
[b] Values are from paired t test of individual values, week 12 compared with entry. Values in parentheses are 95% confidence intervals for observed difference in means, week 12 compared with entry.

In each case, rCD4-IgG administration was continued and repeat testing revealed normal values for both prothrombin and activated partial thromboplastin times. All abnormalities of prothrombin and partial thromboplastin times appeared to be isolated events, most consistent with laboratory error.

Immunologic safety monitoring. T-cell subset analyses are presented in Table 2. Consistent or sustained changes in total lymphocyte, CD4, or CD8 populations were not noted. Serum antibodies to rCD4-IgG were not detected during testing of 179 specimens from 17 patients during the initial phase of administration, including samples from 14 of the 17 patients at week 12. In addition, antibodies to rCD4-IgG have not been detected in any patient receiving prolonged maintenance dosing or in the limited number of patients tested to date at up to 4 weeks following the final injection of rCD4-IgG (1). Additional safety monitoring revealed no consistent changes in quantitative immunoglobulin or total complement levels in serum.

HIV antigen assay. Ten patients had positive HIV antigen determinations in serum at entry. Significant sustained changes in HIV antigen levels in serum were not seen overall. Two patients at the highest dose level (1.0 mg/kg/week) had HIV antigen present at entry. Of these, the patient who received rCD4-IgG intravenously had higher levels of rCD4-IgG in serum and exhibited a decline in HIV antigen levels in serum to less than 50% of the baseline level.

Pharmacokinetic analysis. Peak rCD4-IgG concentrations in serum of 20 to 24 μg/ml were observed 10 min after the 1.0-mg/kg intravenous dose. The initial and steady-state volumes of distribution were small (50 and 76.5 ml/kg, respectively), clearance was slow (1.92 ml/h/kg), the terminal half-life was long (2 days), and the mean residence time in the serum was 40 h. The data obtained following intramuscular administration are summarized in Table 3. The rate and extent of absorption following intramuscular dosing were quite variable; absorption half-lives ranged from 2.4 to 25.8 h, terminal half-lives ranged from 18.6 to 68.3 h, and the bioavailability ranged from 9 to 47%. The mean pharmacokinetic profiles of the four intramuscular-dose groups, a comparison of the mean intramuscular and intravenous pharmacokinetic profiles for the 1.0-mg/kg dose, and a graph comparing concentrations in serum of 0.3 mg of rCD4-IgG and 0.3 mg of rCD4 per kg administered intramuscularly (20) are displayed in Fig. 1, panels A, B, and C, respectively.

DISCUSSION

CD4 immunoadhesins, created by the fusion of rCD4 with the heavy chain of IgG, have been shown in vitro to retain the gp120-binding and HIV-blocking properties of rCD4 (3, 5). In addition, studies with rabbits and monkeys demonstrated that these molecules also possess properties of IgG, most importantly, long plasma half-life and Fc-receptor binding (3, 5). The observed 18.6- to 68.3-h elimination half-life of intramuscularly administered rCD4-IgG is substantially longer than the mean elimination half-life of 9.4 h reported following intramuscular dosing with rCD4 (20). However, absorption following intramuscular administration of rCD4-IgG was quite variable, resulting in low bioavailability and average peak concentrations in serum approximately 10-fold lower than the average peak levels measured in the two patients treated with intravenous rCD4-IgG. Since the terminal half-life following 1.0 mg of intravenous rCD4-IgG per kg was approximately 2 days, it appears that the intramuscular route of administration offers no advantage over the intravenous route from a pharmacokinetic standpoint.

Prior to clinical trials with rCD4-based molecules, theo-

TABLE 3. Pharmacokinetic data obtained after intramuscular and intravenous administration of rCD4-IgG by dose group

Route and dose (mg/kg) (n)	Mean (SD) and range					
	Peak concn in serum (ng/ml)	Absorption half-life (h)	Elimination half-life (h)	Bioavailability (%)	Initial half-life (h)	Terminal half-life (h)[a]
Intramuscular						
0.03 (5)	45 (23), 22–70	7.3 (6.6), 2.4–18.4	37.5 (19.6), 18.6–68.3	23 (15), 14–47		
0.1 (4)	271 (106), 167–380	4.5 (1.4), 2.8–6.2	31.3 (10.2), 22.6–45.5	31 (15), 14–46		
0.3 (4)	461 (255), 165–759	11.0 (10.0), 3.5–25.8	36.9 (16.8), 25.7–61.6	24 (14), 9–38		
1.0 (2)[b]	2,724 (2,756), 776–4,672	8.9 (3.3), 6.6–11.2	33.3 (2.1), 31.8–34.8	21 (9), 14–27		
Intravenous						
1.0 (2)[c]	22,238 (2,811), 20,250–24,225				12 (1.6), 10.8–13.1	50.2 (8.5), 44.2–56.2

[a] The terminal half-life was associated with approximately 43% of the area under the curve.
[b] The 1.0-mg/kg intramuscular dose was described by the sum of three exponentials with a 1-hr lag time. The initial elimination phase (not reported) had a half-life of 9.9 ± 4.8 h (range, 6.5 to 13.2 h).
[c] The mean pharmacokinetic equation is concentration (μg/ml) = 17.5 exp (−0.059t) plus 3.1 exp (−0.014t), where time (t) is in hours.

retical concerns regarding the immunologic safety of this therapy were raised. Antibody-dependent cellular cytotoxicity, mediated by natural anti-gp120 antibodies interacting with soluble viral gp120 bound to healthy "bystander" CD4 cells, has been proposed as one possible mechanism accounting for the CD4-lymphocyte depletion in HIV-infected patients (24). Soluble gp120 is thought to have only a single CD4-binding site which is occupied when gp120 binds to cellular CD4. Since the single CD4-binding site on the gp120 molecule is then unavailable, it is unlikely that rCD4-IgG would be able to bind to gp120 that is attached to uninfected CD4 bearing bystander cells. This is supported by in vitro studies showing that while rCD4-IgG mediated cellular cytotoxicity toward HIV-infected lymphoblastoid cells, uninfected cells preincubated with soluble gp120 were not killed when exposed to rCD4-IgG (5). Further studies of CD4 immunoadhesins using monocyte-macrophage cell lines showed no evidence of enhanced infection in cells expressing high-affinity Fc receptors (3).

In our study, careful monitoring of lymphocyte populations, quantitative immunoglobulins, and complement levels in serum did not reveal evidence of immunologic toxicity. In addition, antibodies against rCD4-IgG were not detected in any patient during therapy or after rCD4-IgG was discontinued. Finally, other laboratory parameters and clinical monitoring did not demonstrate any important toxicity attributable to rCD4-IgG.

Although some individual patients had persistent decreases in HIV antigen levels in serum, overall consistent changes in HIV antigen levels and numbers of CD4 lymphocytes were not observed during the initial phase of study. Further studies are needed to determine whether higher doses at more frequent intervals will result in consistent measurable changes in these parameters. Whether rCD4-IgG-mediated cellular cytotoxicity against HIV-infected cells will be clinically important remains to be determined as well.

The potential role of rCD4-IgG in HIV infection cannot be determined from this safety and pharmacokinetics study, though the apparent lack of toxicity makes it an attractive agent for in vivo trials of combination therapy. In vitro studies using two or three drug combinations of an rCD4 molecule, zidovudine, and recombinant alpha interferon have demonstrated reproducible synergistic inhibition of HIV-1 as measured by p24 antigen assay, reverse transcriptase activity, yields of infectious virus, and indirect immunofluorescence (19). In these studies, concentrations of the rCD4 molecule as low as 0.02 μg/ml combined with subinhibitory concentrations of zidovudine and/or recombinant alpha interferon suppressed HIV-1 replication more effectively and for a longer period than any of the agents used alone (19). A second group of investigators have sh wn that rCD4 concentrations as low as 1 μg/ml combined with subinhibitory concentrations of zidovudine, 2',3'-dide xyinosine, or 2',3'-dideoxycytidine result in synergistic inhibition of HIV-1 without toxicity in vitro (17). Furthermore, rCD4 alone at a concentration of 200 μg/ml has been sh wn to inhibit the spread of the III_B strain of HIV-1 fr m chronically infected pulmonary alveolar macrophages to uninfected peripheral blood mononuclear leukocytes in vitro even in the face of free cell-to-cell contact (15). Finally, the combination of dideoxyinosine and rCD4-IgG has been shown to exhibit synergistic anti-HIV activity in vitro in lymphoid and monocytic cell lines as well as in normal peripheral blood mononuclear leukocytes utilizing both laboratory strains and fresh clinical isolates (8).

One recent report suggests that clinical HIV isolates may be relatively more resistant to neutralization by rCD4 than laboratory strains such as HTLV-III_B (9). The 90% inhibitory dose of an rCD4 for 11 clinical isolates of HIV was 15 to 190 μg/ml, compared with 0.7 μg/ml necessary to inhibit HTLV-III_B. Three of the same clinical strains were tested with a CD4-IgG hybrid molecule and found to be inhibited at concentrations of 2.4 to 40.0 μg/ml (90% inhibitory d se). The relative resistance of clinical isolates of HIV has been confirmed in our laboratory as well (2). However, the peak levels of rCD4-IgG achieved in this clinical trial approach the concentrations needed to inhibit some of the relatively resistant clinical strains, and no dose-limiting toxicity was seen. Further dose escalation studies that are needed t establish the maximal tolerated dose and to assess clinical efficacy are now under way.

The unique mechanism of HIV inhibition and apparent safety of rCD4-IgG suggest that investigation of the agent under special circumstances other than AIDS and AIDS-related complex may also be indicated. rCD4-IgG has been shown to cross the placentae of pregnant rhesus monkeys in amounts similar to those of native IgG (3). Studies to assess the potential for preventing HIV transmission in utero would be of interest (32). Finally, the investigation of a possible role for rCD4-IgG or other compounds that prevent the initial binding and uptake of HIV by target cells in preventing HIV infection following parenteral exposure may be warranted (32).

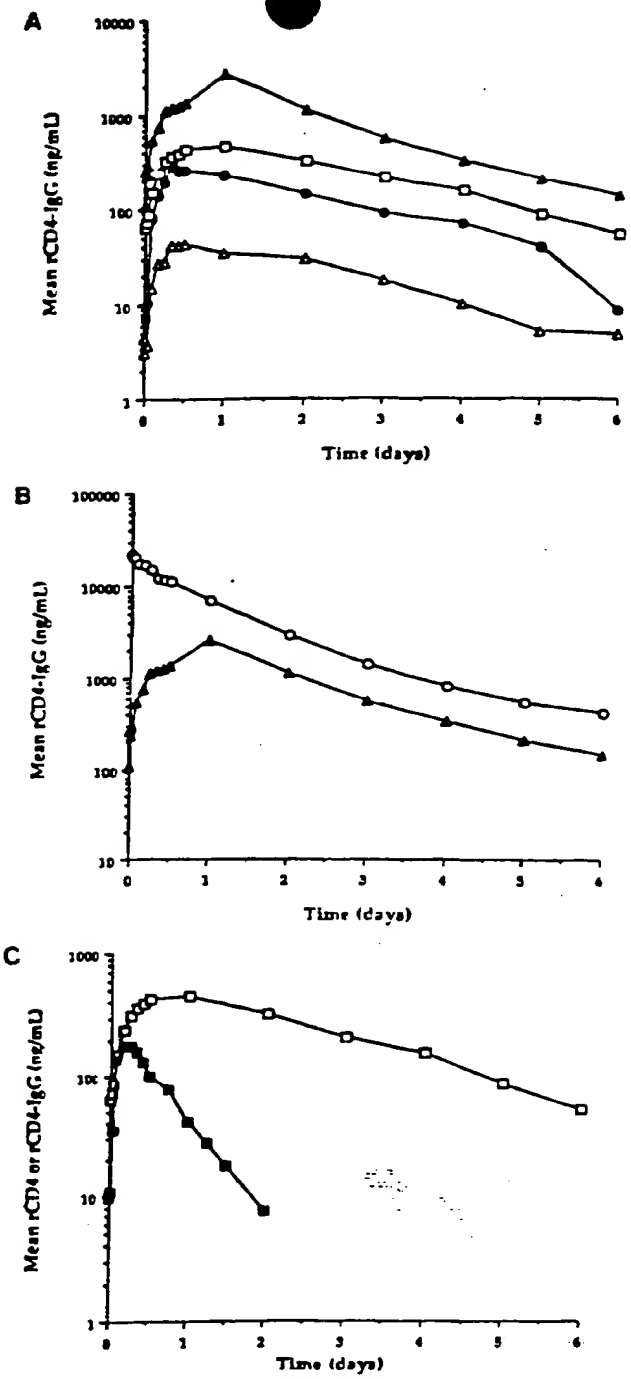

FIG. 1. (A) Mean rCD4-IgG concentrations in serum following intramuscular dosing on day 1. Symbols: △, 0.03 mg/kg; ●, 0.1 mg/kg; □, 0.3 mg/kg; ▲, 1.0 mg/kg. (B) Mean rCD4-IgG concentrations in serum for the 1.0-mg/kg intravenous and intramuscular doses administered on day 1. Symbols: ○, intravenous; ▲, intramuscular. (C) Mean rCD4 (■) and rCD4-IgG (□) concentrations in serum following intramuscular administration of 0.3 mg/kg.

ACKNOWLEDGMENT

This work was supported by a research grant from Genentech, Inc.

REFERENCES

1. Amman, A. J. Personal communication.
2. Byrn, R. A. Unpublished data.
3. Byrn, R. A., J. Mordenti, C. Lucas, D. Smith, S. A. Marsters, J. S. Johnson, P. Cossum, S. M. Chamow, F. M. Wurm, T. Gregory, J. E. Groopman, and D. J. Capon. 1990. Biological properties of a CD4 immunoadhesin. Nature (London) 344:667–670.
4. Byrn, R. A., J. Sekigawa, S. M. Chamow, J. S. Johnson, T. J. Gregory, D. J. Capon, and J. E. Groopman. 1989. Characterization of in vitro inhibition of human immunodeficiency virus by purified recombinant CD4. J. Virol. 63:4370–4375.
5. Capon, D. J., S. M. Chamow, J. Mordenti, S. A. Marsters, T. Gregory, H. Mitsuya, R. A. Byrn, C. Lucas, F. M. Wurm, J. E. Groopman, S. Broder, and D. H. Smith. 1989. Designing CD4 immunoadhesins for AIDS therapy. Nature (London) 337:525–531.
6. Chen, A. B., V. R. Anicetti, T. D. Klassen, W. Berthold, G. Zahn, R. M. Wert, M. D. Geier, and A. J. S. Jones. 1986. A sensitive radioimmunoprecipitation assay for the detection of antibody to recombinant human gamma-interferon: comparison to a bioassay neutralization test. J. Interferon Res. 6:313–320.
7. Clayton, L. K., M. Sieh, D. A. Pious, and E. L. Reinherz. 1989. Identification of human CD4 residues affecting class II MHC versus HIV-1 gp120 binding. Nature (London) 339:548–551.
8. Connolly, K. J., and S. M. Hammer. Personal communication.
9. Daar, E. S., X. L. Li, T. Moudgil, and D. D. Ho. 1990. High concentrations of recombinant soluble CD4 are required to neutralize primary human immunodeficiency virus type 1 isolates. Proc. Natl. Acad. Sci. USA 87:6574–6578.
10. Dalgleish, A. G., P. C. L. Beverley, P. R. Clapham, D. H. Crawford, M. F. Greaves, and R. A. Weiss. 1984. The CD4 (T4) antigen is an essential component of the receptor for the AIDS retrovirus. Nature (London) 312:763–767.
11. Deen, K. C., J. S. McDougal, R. Inacker, G. Folena-Wasserman, J. Arthos, J. Rosenberg, P. J. Maddon, R. Axel, and R. W. Sweet. 1988. A soluble form of CD4 (T4) protein inhibits AIDS virus infection. Nature (London) 331:82–84.
12. Farr, R. S. 1958. A quantitative immunochemical measure of the primary interaction between I*BSA and antibody. J. Infect. Dis. 103:239–262.
13. Fisher, R. A., J. M. Bertonis, W. Meier, V. A. Johnson, D. S. Costopoulos, T. Lui, R. Tizard, B. D. Walker, M. S. Hirsch, R. T. Schooly, and R. A. Flavell. 1988. HIV infection is blocked *in vitro* by recombinant soluble CD4. Nature (London) 331:76–78.
14. Gay, D., P. Maddon, R. Sekaly, M. A. Talle, M. Godfrey, E. Long, G. Goldstein, L. Chess, R. Axel, J. Kappler, and P. Marrack. 1987. Functional interaction between human T cell protein CD4 and the major histocompatibility complex HLA-DR antigen. Nature (London) 328:626–629.
15. Harbison, M. A., J. M. Gillis, P. Pinkston, R. A. Byrn, R. M. Rose, and S. M. Hammer. 1990. Effects of recombinant soluble CD4 (rCD4) on HIV-1 infection of monocyte/macrophages. J. Infect. Dis. 161:1–6.
16. Harris, R. J., K. L. Wagner, and M. W. Spellman. 1990. Structural characterization of a recombinant CD4-IgG hybrid molecule. Eur. J. Biochem. 194:611–620.
17. Hayashi, S., R. L. Fine, T.-C. Chou, M. J. Currens, S. Broder, and H. Mitsuya. 1990. In vitro inhibition of the infectivity and replication of human immunodeficiency virus type 1 by combination of antiretroviral 2',3'-dideoxynucleosides and virus-binding inhibitors. Antimicrob. Agents Chemother. 34:82–88.
18. Hussey, R. E., N. E. Richardson, M. Kowalski, N. R. Brown, H.-C. Chang, R. F. Siliciano, T. Dorfman, B. Walker, J. Sodroski, and E. L. Reinherz. 1988. A soluble CD4 protein selectively inhibits HIV replication and syncytium formation. Nature (London) 331:78–81.
19. Johnson, V. A., M. A. Barlow, D. P. Merrill, T.-C. Chou, and

M. S. Hirsch. 1990. Three-drug synergistic inhibition of HIV-1 replication in vitro by zidovudine, recombinant soluble CD4, and recombinant interferon-alpha A. J. Infect. Dis. 161:1059–1067.
20. Kahn, J. O., J. D. Allan, T. L. Hodges, L. D. Kaplan, C. J. Arri, H. F. Fitch, A. E. Izu, J. Mordenti, S. A. Sherwin, J. E. Groopman, and P. A. Volberding. 1990. The safety and pharmacokinetics of recombinant soluble CD4 (rCD4) in subjects with the acquired immunodeficiency syndrome (AIDS) and AIDS-related complex. Ann. Intern. Med. 112:254–261.
21. Klatzmann, D., E. Champagne, S. Chamaret, J. Gruest, D. Guetard, T. Hercend, J.-C. Gluckman, and L. Montagnier. 1984. T-lymphocyte T4 molecule behaves as the receptor for human retrovirus LAV. Nature (London) 312:767–768.
22. Lamarre, D., A. Ashkenazi, S. Fleury, D. H. Smith, R.-P. Sekaly, and D. J. Capon. 1989. The MHC-binding and gp120-binding functions of CD4 are separable. Science 245:743–746.
23. Lane, H. C., and A. S. Fauci. 1985. Immunologic abnormalities in the acquired immunodeficiency syndrome. Annu. Rev. Immunol. 3:477–500.
24. Lyerly, H. K., T. J. Matthews, A. J. Langlois, D. P. Bolognesi, and K. J. Weinhold. 1987. Human T-cell lymphotrophic virus III_B glycoprotein (gp 120) bound to CD4 determinants on normal lymphocytes and expressed by infected cells serves as target for immune attack. Proc. Natl. Acad. Sci. USA 84:4601–4605.
25. Maddon, P. J., A. G. Dalgleish, J. S. McDougal, P. R. Clapham, R. A. Weiss, and R. Axel. 1986. The T4 gene encodes the AIDS virus receptor and is expressed in the immune system and the brain. Cell 47:333–348.
26. McDougal, J. S., M. S. Kennedy, J. M. Sligh, S. P. Cort, A. Mawle, and J. K. A. Nicholson. 1986. Binding of HTLV-III/LAV to $T4^+$ T cells by a complex of the 110K viral protein and the T4 molecule. Science 231:382–385.
27. Sattentau, Q. J., P. R. Clapham, R. A. Weiss, P. C. L. Beverley, L. Montagnier, M. F. Alhalabi, J.-C. Gluckman, and D. Klatzmann. 1988. The human and simian immunodeficiency viruses HIV-1, HIV-2 and SIV interact with similar epitopes on their cellular receptor, the CD4 molecule. AIDS 2:101–105.
28. Schooley, R. T., T. C. Merigan, P. Gaut, M. S. Hirsch, M. Holodniy, T. Flynn, S. Liu, R. E. Byington, S. Henochowicz, E. Gubish, D. Spriggs, D. Kufe, J. Schindler, A. Dawson, D. Thomas, D. G. Hanson, B. Letwin, T. Liu, J. Gulinello, S. Kennedy, R. Fisher, and D. D. Ho. 1990. Recombinant soluble CD4 therapy in patients with the acquired immunodeficiency syndrome (AIDS) and AIDS-related complex. Ann. Intern. Med. 112:247–253.
29. Smith, D. H., R. A. Byrn, S. A. Marsters, T. Gregory, J. E. Groopman, and D. J. Capon. 1987. Blocking of HIV-1 infectivity by a soluble, secreted form of the CD4 antigen. Science 238: 1704–1707.
30. Traunecker, A., W. Luke, and K. Karjalainen. 1988. Soluble CD4 molecules neutralize human immunodeficiency virus type 1. Nature (London) 331:84–86.
31. Traunecker, A., J. Schneider, H. Kiefer, and K. Karjalainen. 1989. Highly efficient neutralization of HIV with recombinant CD4-immunoglobulin molecules. Nature (London) 339:68–70.
32. Ward, R. H. R., D. J. Capon, C. M. Jett, K. M. Murthy, J. Mordenti, C. Lucas, S. W. Frie, A. M. Prince, J. D. Green, and J. W. Eichberg. 1991. Prevention of HIV-1 III_B infection in chimpanzees by CD4 immunoadhesin. Nature (London) 352: 434–436.
33. Watanabe, M., K. A. Reimann, P. A. DeLong, T. Liu, R. A. Fisher, and N. L. Letvin. 1989. Effect of recombinant soluble CD4 in rhesus monkeys infected with simian immunodeficiency virus of macaques. Nature (London) 337:267–270.

18:150–156 © 1995 Lippincott-Raven Publishers, Philadelphia

Safety, Pharmacokinetics, and Antiviral Response of CD4–Immunoglobulin G by Intravenous Bolus in AIDS and AIDS-Related Complex

*Ann C. Collier, *†Robert W. Coombs, ‡David Katzenstein, ‡Mark Holodniy, †Joel Gibson, §Joyce Mordenti, §Allen E. Izu, §Anne Marie Duliege, §Arthur J. Ammann, ‡Thomas Merigan, and *†Lawrence Corey

*Departments of *Medicine and †Laboratory Medicine, University of Washington, Seattle, Washington; ‡Department of Medicine, Stanford University, Palo Alto, and §Genentech, South San Francisco, California, U.S.A.*

Summary: To assess the safety, pharmacokinetics, and antiviral effects of intravenous recombinant CD4 immunoglobulin G (CD4-IgG), a 12-week Phase One study with an optional maintenance phase was performed. Twenty-two subjects with advanced human immunodeficiency virus (HIV) infection were enrolled; 15 subjects completed the initial 12 weeks. CD4-IgG doses were 30, 100, or 300 μg/kg weekly; 1,000 μg/kg once, twice, or three times per week; or 3,000 μg/kg twice weekly. Serum concentrations of CD4-IgG increased linearly with dose, with average peak serum concentrations of 22 μg/ml with 1,000 μg/kg. CD4-IgG was well tolerated; one patient had self-limited tachycardia and flushing associated with CD4-IgG therapy. No changes were seen in CD4 cell counts, hematologic or coagulation studies, serum chemistries, HIV p24 antigen titers, or plasma HIV titers. No subject developed anti-CD4 antibodies. HIV isolates from five patients had IC_{90} values that were higher than the peak concentrations of CD4-IgG achieved in those patients. Additional studies that achieve higher CD4-IgG concentrations are necessary to evaluate the antiviral activity of this compound. Key Words: CD4 immunoglobulin—Antiretroviral therapy—HIV—Phase one—Recombinant CD4.

Therapies for human immunodeficiency virus type one (HIV) that inhibit viral reverse transcriptase delay progression of disease, but eventually are associated with clinical failure. New therapeutic strategies for the treatment of HIV are needed, and one potential strategy is based upon blocking viral entry into uninfected cells. The envelope glycoprotein of HIV (gp120) binds with high affinity to the human CD4 molecule (1–3). In vitro, recombinant soluble CD4 (rCD4) and derivatives of CD4 have been shown to inhibit HIV, although substantially higher concentrations are needed to inhibit primary clinical isolates of HIV than laboratory strains (4–9). Binding of CD4 also results in shedding of gp120 from virions (10). It appears that the differences seen between sensitivity to CD4 of clinical and laboratory strains of HIV may be related to structural changes in the HIV envelope glycoprotein, which effect both the binding of CD4 and gp120 shedding from virions (11).

In humans, rCD4 is well tolerated, but has a serum half-life of approximately 1 h, is associated with the development of anti-CD4 antibodies and Coombs positivity in some patients, and showed little antiviral or immunologic benefit at doses up to 30 mg/day, which were tested in two Phase One studies (12,13).

Address correspondence and reprint requests to Dr. Ann C. Collier at 1001 Broadway, Suite 218, Seattle, WA 98122, U.S.A.
Manuscript received July 13, 1994; accepted January 13, 1995.

Soluble CD4 was fused with a portion of the constant region of immunoglobulin G (IgG), resulting in CD4-IgG, a compound with a more favorable pharmacokinetic profile than soluble CD4 that could fix complement and bind to F_C receptors (14,15). One study demonstrated that high concentrations of CD4-IgG could prevent infection in chimpanzees challenged with HIV (16). A Phase one study of i.m. CD4-IgG using doses up to 1 mg/kg demonstrated that this agent was well tolerated, but that this mode of administration had less favorable pharmacokinetics than those seen with high-dose i.v. administration in two patients (17). We report the results of a Phase one study of intravenously administered CD4-IgG in humans, which achieved substantially higher serum concentrations of CD4 than had been achieved at the time the study was conducted, with no apparent toxicity. However, serum concentrations of CD4-IgG were still lower than the inhibitory concentrations of HIV isolates from the patients.

METHOD

Subjects

The subjects in this trial had confirmed antibody to HIV; and either acquired immune deficiency syndrome (AIDS) or AIDS-related complex as defined by the presence of one or more of the following symptoms for >30 days: unexplained fever, night sweats, weight loss >10% of body weight, fatigue, or diarrhea; or oral hairy leukoplakia, or oral candidiasis. All subjects had CD4 lymphocyte counts $<500/mm^3$, and failed to tolerate zidovudine therapy, or made a decision to decline or discontinue its use. Subjects did not take antiretroviral therapy for a minimum of 3 weeks prior to study entry. In addition, subjects had relatively preserved hematologic (granulocytes $\geq 1,000/mm^3$, platelets $\geq 75,000/mm^3$), hepatic (aspartate aminotransferase less than three times normal, prothrombin time less than or equal to one and one-half times normal), and renal (creatinine <2.0 mg/dl) function. Subjects were excluded if they had active opportunistic infections or malignancies other than Kaposi's sarcoma, or were taking chemotherapy, immunomodulators, other antiretrovirals, or other experimental therapies.

Study Design

This study, AIDS Clinical Trials Group Protocol 121, was a two-center, open-label trial of escalating doses of CD4-IgG (30, 100, 300 μg/kg once per week, 1000 μg/kg once, twice, or three times per week, and 3,000 μg/kg twice per week) given by i.v. bolus. For the initial 12 weeks of therapy, each subject received a fixed dose of CD4-IgG, and successive groups of subjects were enrolled at each dose level, with a plan to halt dose escalation if moderate or severe toxicities were noted. Subjects completing the initial 12 weeks were eligible to continue CD4-IgG at either the same dose (100, 300, 1,000, [illegible] μg/kg) given two or three times per week, or a higher dose (1,000 μg/kg for those initially treated with lower doses) given one to three times per week, depending upon how high the dose escalation had progressed when they finished the initial 12 weeks. During the extension phase of the study, subjects without a history of zidovudine intolerance could take concurrent zidovudine therapy at a dose of 300–600 mg/day.

Clinical and Laboratory Analyses

The subjects gave written informed consent, and the study protocol was approved by the institutional review boards of the participating institutions. Subjects were seen frequently for clinical and laboratory monitoring. Potential toxicities (symptoms and laboratory results) were graded as mild or minimally abnormal, moderate, or severe. Subjects receiving the first four dose levels had pharmacokinetic studies performed during Weeks 1 and 12, with blood collection prior to the CD4-IgG dose, and at 10 and 30 min, and 1, 2, 4, 6, 8, 10, and 12 hours, and once daily for 6 days postdosing. Selected subjects underwent voluntary lumbar puncture for collection of cerebrospinal fluid (CSF) for determination of CD4-IgG concentration; simultaneous serum was collected. The timing of these procedures relative to dosing of CD4-IgG was determined by the patient's convenience.

Serum and CSF specimens, frozen at −20°C were assayed for CD4-IgG concentrations, using an enzyme-linked immunosorbent assay (ELISA) (16). Serum samples were also assayed for anti-CD4 antibodies using a radioimmunoprecipitation assay (17). CD4 and CD8 cells from peripheral blood were counted with use of monoclonal antibodies and flow cytometry. Serum samples from each subject, frozen at −70°C, were assayed simultaneously for HIV p24 antigen by ELISA (Abbott Laboratories, North Chicago, IL, U.S.A.), and the findings were confirmed by neutralization assay. The cutoff for a positive result was ≥30 pg/ml. Plasma was drawn every 4 weeks for quantitative HIV cultures, which were performed as previously described, with serial fivefold dilutions to a maximum of 1:15,625 (18). The virology and immunology laboratories that performed the assays for this study followed quality control procedures established by the AIDS Clinical Trials Group.

Ex vivo determination of rCD4-IgG inhibitory concentration for plasma-associated HIV from patients was performed for CD4-IgG as follows for five subjects who had sufficient plasma available after the quantitative HIV cultures were performed (19). Undiluted plasma was obtained from heparinized whole blood following a low-speed centrifugation at 800 *g* for 20 min, and frozen at −70°C. After thawing, plasma was filtered (0.45 μ) to remove cellular or platelet debris, and a fivefold dilution series from 1:5 to 1:15,625 was prepared in 12 × 75-mm sterile screw-cap microtubes with sealing O-rings (Sarstedt, Princeton, NJ, U.S.A.), with use of 240-μl aliquots of plasma and 960 μl of tissue culture medium. A similar dilution series of rCD4-IgG was made over the range from 250 to 0 μg/ml. A matrix series comprising 12 × 75-mm polystyrene tubes each containing 850 μl of the respective plasma dilution and 850 μl of the respective rCD4-IgG dilution was prepared, mixed, and incubated at 37°C for 1 hour. An 800-μl aliquot from each dilution was added to duplicate wells (24-well plate; Costar, Cambridge, MA, U.S.A.), containing 2×10^6 2–3 day-old phytohemagglutinin-stimulated donor peripheral blood mononuclear cells in a final 2-ml volume of

culture medium per well. The plates were placed into low-density polyethylene bags (no. 6255-058, Nalgene, Rochester, NY, U.S.A.) and incubated for 14 days in a 5% CO_2 nonhumidified incubator. The culture wells were considered positive if the HIV p24 antigen increased by ≥30 pg/ml over the antigen concentration in each well at the time of initial setup. The concentration required to displace 50% (IC_{50}) and 90% (IC_{90}) of ligand binding per milliliter of plasma was calculated for logarithm-transformed data by the Reed-Muench method (20).

Statistical Analysis

Comparisons between baseline and on-therapy results were made with use of Wilcoxon's or *t* tests for continuous variables and the χ^2 test for discrete variables. All p values were two-tailed.

RESULTS

Study Population

Twenty-two subjects were enrolled between September 1989 and February 1991 at the University of Washington (n = 13) or at Stanford University (n = 9). During the first 12 weeks, subjects were assigned to receive the following doses and schedules of CD4-IgG: five to 30 μg/kg/week; four to 100 and 300 μg/kg/week; eight to 1,000 μg/kg, one once, three twice, and four three times per week; and one subject to receive 3,000 μg two times per week. The characteristics of the subjects are shown in Table 1. Nineteen (86%) of the subjects had CD4 cell counts of <200/mm^3. All 22 subjects had previously taken zidovudine, for a mean duration of 14 months (range, 1–31 months); 10 discontinued treatment because of toxicity, 7 refused additional use, and 5 discontinued for both reasons (toxicity at high dose and refusal of lower doses). Zidovudine had been discontinued a mean of 4 months (range, 1–24 months) prior to study entry. In addition, one subject each had received zalcitabine, didanosine, or foscarnet prior to enrollment. Among the subjects receiving prophylaxis for *Pneumocystis carinii* pneumonia (PCP) during the trial, 13 received pentamidine monthly by aerosol, three were taking trimethoprim-sulfamethoxazole, and two received dapsone. There were no significant differences in clinical characteristics among the various dosing groups.

TABLE 1. *Characteristics of the 22 subjects at entry*

Characteristic	Finding
Age (years, mean ± SD)	40.1 ± 7.5
No. of men	22/22
Diagnosis	
AIDS, no. (%)	12 (55)
AIDS-related complex	10 (45)
CD4 cells/mm^3, median (range)	
AIDS	12 (0–307)
AIDS-related complex	110 (8–240)
HIV p24 antigen detectable, no. (%)	17 (77)
Median, pg/ml (range)[a]	285 (45–8,612)
HIV plasma viremia,	
No. positive/no. tested (%)	14/18 (78)
Previous zidovudine	22/22
Pneumocystis carinii prophylaxis, no. (%)	18 (82)

AIDS, acquired immune deficiency syndrome; HIV, human immunodeficiency virus.
[a] Among those with detectable HIV p24 antigen.

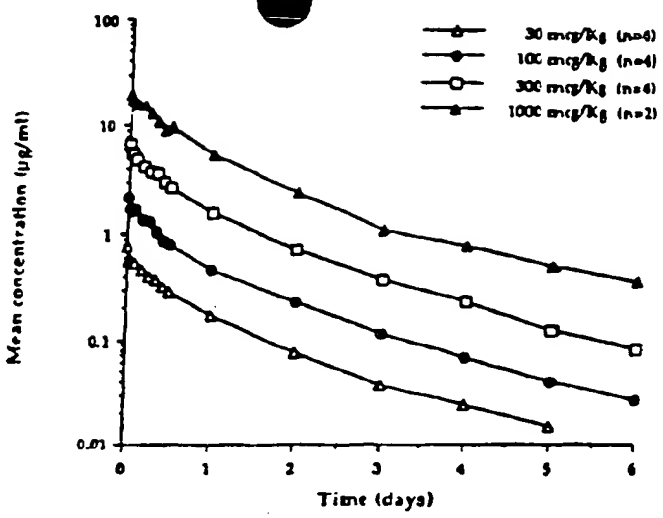

FIG. 1. Mean concentrations of recombinant CD4–immunoglobulin G following i.v. bolus administration of 30, 100, 300, and 1,000 μg/kg.

Pharmacokinetics

Serum concentrations of CD4-IgG increased linearly with dose, with average peak serum concentrations of 22 μg/ml following the first 1,000 μg/kg dose (Fig. 1 and Table 2). CD4-IgG was cleared slowly and the terminal half-lives ranged from 30.7 to 86.5 hours. There was no change in the pharmacokinetics during Week 12.

Twelve subjects underwent lumbar puncture during the study. CD4-IgG was undetectable (<0.013 μg/ml) in the CSF of eight subjects who had simultaneous serum concentrations ranging from undetectable to 0.103 μg/ml. Four subjects, each receiving 1,000 μg/kg, had CSF CD4-IgG concentrations of 0.018–0.042 μg/ml, with simultaneous serum concentrations of 9.8–11.4 μg/ml, indicating CSF:serum ratios of 0.2–0.4%.

TABLE 2. *Pharmacokinetic parameters after the first dose for subjects treated with varying doses of CD4–immunoglobulin G*

ose, μg/kg(n)	Concentration at 10 min (mean ± SD; μg/ml)	Initial half-life[a] (range; h)	Terminal half-life[a] (range; h)	Volume central compartment (mean ± SD; ml/kg)	Volume-steady state (mean ± SD; ml/kg)	Clearance (Mean ± SD; ml/h/kg)
30 (4)	0.77 ± 0.46	5.2–13.4	30.7–71	55.6 ± 23.8	91.3 ± 37.3	2.4 ± 0.7
100 (4)	2.15 ± 1.47	2.2–9.4	31.3–86.5	67.0 ± 39.0	110.8 ± 47.5	3.0 ± 1.5
300 (4)	6.75 ± 2.27	2.0–10.8	32.3–71.9	58.6 ± 25.2	95.1 ± 38.2	2.8 ± 1.4
1,000 (2)[b]	19.8 ± 0.11[c]	7.5–8.5	32.4–37.5	53.9 ± 4.0	85.6 ± 7.4	2.3 ± 0.0

[a] Described by bi- and tri-exponential equations so mean half-life not available.
[b] Pharmacokinetic analyses performed on the data from two patients who received 1,000 μg/kg once per week.
[c] The 10-min concentration (mean ± SD) for all nine patients receiving one of the three dosing regimens of 1,000 μg/kg was 22.0 ± .86 μg/ml.

Course During the Initial 12 Weeks

Fifteen subjects completed the initial 12 weeks of the study. Four subjects terminated early because of the progression of existing or development of new AIDS-related complications, disseminated *Mycobacterium avium* complex in three (one with new concurrent PCP), and new gastrointestinal Kaposi's sarcoma in one; two discontinued for other medical reasons (periappendiceal abscess and severe depression); and one patient withdrew consent.

CD4-IgG was well tolerated. The only event considered likely to be related to CD4-IgG therapy was transient mild-to-moderate tachycardia and flushing associated with the first five doses (1,000 μg/kg) in one subject; no specific therapy was required and the subject continued the study. The only severe symptom that occurred was transient dizziness and mild confusion during Week 5 in the subject who subsequently was diagnosed with AIDS–dementia complex; a relationship to CD4-IgG treatment was judged unlikely. A variety of mild, self-limited symptoms occurred in different subjects (vomiting, headache, fever, abdominal pain, fatigue), which were judged unrelated to CD4-IgG.

No significant changes were seen in weight, or CD4 and CD8 cells counts and percentages during treatment at any dose of CD4-IgG (Tables 3 and 4). Similarly, serum chemistries, hematologic or coagulation studies, renal function, liver function tests, serum immunoglobulins, serum complement, and urinalyses remained stable. All 17 subjects who had detectable HIV p24 antigen remained positive, with no significant change in titer (Tables 3 and 4). Among the 18 subjects who had quantitative plasma HIV titers performed, 14 (78%) had detectable plasma viremia. Among the subjects who completed the study, the median (range) titers at baseline and Week 12 were 139 mean tissue culture infective dose ($TCID_{50}$)/ml (0–3,493) and 139 $TCID_{50}$/ml (0–3,548), respectively (Table 4, Fig. 2).

No subject developed anti-CD4 antibodies (112 samples from 20 subjects were assayed).

Clinical Course During Maintenance

Eleven of the 15 subjects who completed 12 weeks of therapy continued treatment for a mean of 21 weeks (range, 3–34). One received 100 μg/kg twice weekly; two received 300 μg/kg twice weekly; eight received 1,000 μg/kg, four once, and four twice per week. During this phase, three subjects had progressive HIV disease; disseminated *M. avium* complex, PCP, and AIDS dementia complex occurred in one subject each.

CD4-IgG continued to be well tolerated, with no adverse experiences that were related to therapy. One subject who started the study with trace pro-

TABLE 3. *Hematologic and immunologic results at baseline and Week 12 of CD4–immunoglobulin G treatment*

Characteristic	Result (mean ± SD) Week 0	Week 12
Hemoglobin, g/dl	12.3 ± 2.4	12.3 ± 1.9
White blood count/mm³	3.8 ± 1.5	3.9 ± 1.6
Lymphocytes/mm³	1,134 ± 586	903 ± 432
Platelets × 10³/mm³	196 ± 85	204 ± 110
$CD4^+$ cells/mm³	71 ± 102	56 ± 80
$CD8^+$ cells/mm³	668 ± 406	489 ± 312
HIV p24 antigen, pg/ml; median (range)[a]	283 (45–8,612)	272 (36–10,855)
Weight, kg	75.3 ± 9.4	74.2 ± 9.6

[a] Among subjects who had detectable antigen prior to study entry.

TABLE 4. *CD4⁺ cell counts and quantitative virologic results at entry and Week 12*

Subject no.	CD4⁺ cells/mm³		Plasma HIV titer ($TCID_{50}$/ml)		HIV p24 antigen (pg/ml)	
	Entry	Week 12	Entry	Week 12	Entry	Week 12
1[a]	8	16	3,495	ND	249	224
2	20	13	3,493	699	171	205
3	0	0	699	699	Negative	Negative
4	6	6	139	139	Negative	Negative
5	67	31	631	631	341	414
6[a]	144	131	699	139	285	768
7	8	13	139	139	328	447
8[a]	12	9	6	ND	Negative	Negative
9[a]	24	30	699	ND	50	36[b]
10	15	10	139	139	125	238
11[a]	159	180	0	689	67	170
12	54	19	0	0	426	432
13	171	138	ND	ND	Negative	Negative
14[a]	3	7[c]	ND	ND	Negative	Negative
15	307	335	0	0	717	455
16	178	63	139	0	922	273
17	240	99	0	699	45	120
18	74	20	5	28	149	150
19[a]	5	10[d]	ND	ND	921	2,668[d]
20[a]	78	75	ND	ND	280	179
21	15	19	141	3,548	8,612	10,855
22	68	0	3,548	ND	408	399

HIV, human immunodeficiency virus; $TCID_{50}$, mean tissue culture infective dose; ND, not done.
[a] Terminated study therapy early. [b]Week 2. [c]Week 1. [d]Week 3.

teinuria developed 2+ proteinuria during Week 32, but had stable renal function; and one subject developed moderate but self-limited dizziness and ataxia for 4 days during Week 15. Laboratory results for CD4 and CD8 counts, immunoglobulins, hematologic and coagulation tests, renal function, liver function, complement, and serum chemistries continued to be stable. Absolute CD4 cell counts/mm³ were (mean ± 1 SD) 67 ± 105 and 64 ± 103 at the beginning and end of maintenance therapy, respectively. Among the seven HIV p24 antigen subjects participating in this phase of the study, antigen levels were stable, with median (range) values in pg/ml of 454 (55–10,855) and 150 (64–12,386), respectively, at the start and end of this treatment phase. Similarly, titers of quantitative plasma cultures were stable in five patients for whom data are available over a median of 12 weeks (Fig. 2).

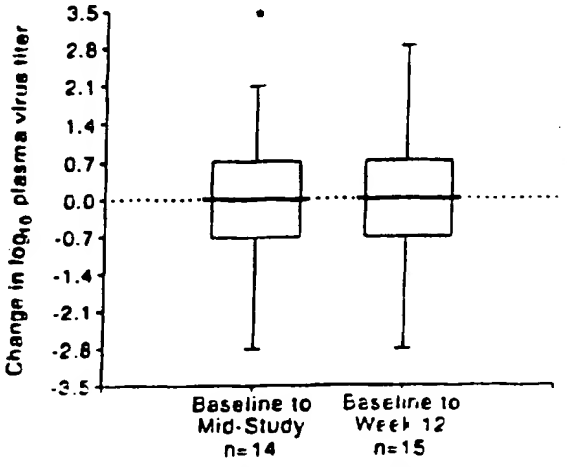

FIG. 2. Change in quantitative human immunodeficiency virus plasma virus titers from baseline during i.v. recombinant CD4–immunoglobulin G therapy. Horizontal lines show the median and range of titers; the boxes represent the interquartile (25–75%) range. The star represents data from one outlier. Mid-study samples were drawn at Weeks 2 (n = 9), 3 (n = 1), 5 (n = 2), and 6 (n = 2).

HIV Susceptibility Results

Because of the unimpressive in vivo antiviral effects of these doses of CD4-IgG, eight isolates from five subjects who had sufficient plasma available were tested for their in vitro susceptibility to CD4-IgG. All five HIV isolates from baseline had IC_{90} values that were above peak serum concentrations of CD4-IgG that were achieved in that patient, and four of five had IC_{50} values that were above peak serum concentrations (Table 5). The susceptibilities of three isolates tested prior to and after 12 weeks of CD4-IgG therapy were unchanged.

TABLE 5. *Inhibitory concentrations of CD4–immunoglobulin G (IgG) for clinical human immunodeficiency virus (HIV) isolates from plasma before and after therapy*

Subject	Study week	rCD4-IgG dose (μg/kg)	Plasma HIV titer ($TCID_{50}$/ml)[a]	Inhibitory concentration of rCD4-IgG (μg/ml)		Peak serum rCD4-IgG (μg/ml)
				IC_{50}	IC_{90}	
1	Entry	30	3,495	10	36	1.3
2	Entry	300	3,495	78	2,540	3.5
3	Entry	300	699	38	774	4.2
	12		699	15	130	
4	Entry	1,000	139	13	193	19
	12		139	11	88	
5	Entry	1,000	699	>250	—	27.5
	12		699	>250	—	23.3

Subject numbers are the same as in Table 3. $TCID_{50}$, mean tissue culture infective dose; IC_{50}, concentration required to displace 50% of ligand binding per ml plasma; IC_{90}, concentration required to displace 90% of ligand binding per ml plasma.
[a] Plasma was obtained for culture prior to the infusion.

DISCUSSION

This study demonstrates the critical important for clinical studies of antiretroviral therapies of understanding the biology of HIV and the potential for differences in laboratory strains and patient isolates of HIV. Although the serum concentrations of CD4-IgG achieved in this study were 1,000 times greater than the IC_{50} of laboratory strains of HIV, they were still less than the IC_{90} of HIV strains isolated from subjects in this study. Thus, the lack of effect of CD4-IgG on the virologic and immunologic parameters in this study is likely explained by the failure to achieve sufficiently high concentrations of this agent rather than because of its intrinsic lack of antiviral efficacy. This study was designed and conducted prior to the recognition that clinical isolates of HIV have a markedly lower susceptibility to CD4-IgG than do laboratory strains of HIV (9). Further support for this hypothesis comes from animal studies, in which high concentrations of CD4-IgG were demonstrated to prevent infection in chimpanzees challenged with HIV (16), and from a simian immunodeficiency virus model in Rhesus monkeys where high dose soluble CD4 therapy was associated with clinical improvement (21). These studies both achieved peak serum concentrations of CD4 greater then 190 mcg/ml, almost 9-fold greater than we achieved in this study with our 1,000 μg/kg dose. In addition, we have subsequently shown that sufficiently high concentrations of recombinant soluble CD4 can be achieved in vivo to neutralize the HIV infectivity of plasma virus (22).

CD4-IgG has a more favorable pharmacokinetic profile for chronic intermittent administration than does soluble CD4, which has a half-life of ~1 hour (12,13). Bioavailability of CD4-IgG administered i.m. is 9–47%, resulting in peak serum concentrations substantially less than that achieved with i.v. dosing (17).

This study provided an opportunity to measure HIV plasma virus titers in patients with advanced HIV infection over time. The median titer remained unchanged, and most patients appeared to have stable titers during the study, suggesting that this assay may be a useful, albeit labor intensive, way to measure the antiviral efficacy of higher concentrations of CD4-based agents.

Although designed as a dose-escalation study, economic limits in the potential cost of a therapy that would require chronic administration of high doses (grams) of recombinant protein precluded escalation to a maximum tolerated dose. At the doses studied, CD4-IgG was well tolerated, with no dose-limiting toxicity identified, and no evidence of development of anti-CD4 antibodies. In addition, others have demonstrated that continuous infusion CD4-IgG therapy was associated with improved T helper cell function (23). In order to further characterize the activity of CD4 therapy, additional studies using higher doses, especially in populations such as pediatric patients, where higher concentrations could be more easily achieved, would be of interest and are warranted.

In addition, further investigation of the use of CD4-IgG in combination with other antiretroviral agents would be of interest. Lower doses of CD4-IgG in conjunction with other therapies might provide additive or synergistic antiviral activity in vivo, as has been demonstrated in vitro for recombinant soluble CD4 (24,25).

Acknowledgment: This work was supported by grants AI-27664 from the AIDS Clinical Trials Group of the National Institute of Allergy and Infectious Diseases and RR-37 from the National Institutes of Health. The authors thank Douglas Arditti, Kathryn Berger, and Charles Cooper for clinical assistance; Paul Boutin and Ellen Gilkerson for statistical assistance; J. Groopman, Kim Chaloupka, and James Stamateou for laboratory assistance; and Nancy Coomer for manuscript preparation.

REFERENCES

1. Dalgleish AG, Beverley PC, Clapham PR, Crawford DH, Greaven MF, Weiss RA. The CD4 (T4) antigen is an essential component of the receptor for the AIDS retrovirus. *Nature* 1984;312:763–7.
2. Klatzmann D, Champagne E, Chamaret S, et al. T-lymphocyte T4 molecule behaves as the receptor for human retrovirus LAV. *Nature* 1984;312:767–8.
3. McDougal JS, Kennedy MS, Sligh JM, Cort SP, Mawle A, Nicholson JK. Binding of HTLV-III/LAV to T4+ T cells by a complex of the 110K viral protein and the T4 molecule. *Science* 1986;231:382–5.
4. Smith DH, Byrn RA, Marsters SA, Gregory T, Groopman JE, Capon DJ. Blocking of HIV-1 infectivity by a soluble, secreted form of the CD4 antigen. *Science* 1987;238:1704–7.
5. Fisher RA, Bertonis JM, Meier W, et al. HIV infection is blocked in vitro by recombinant soluble CD4. *Nature* 1988; 331:76–8.
6. Hussey RE, Richardson NE, Kowalski M, et al. A soluble CD4 protein selectively inhibits HIV replication and syncytium formation. *Nature* 1988;331:78–81.
7. Deen KC, McDougal JS, Inacker R, et al. A soluble form of CD4 (T4) protein inhibits AIDS virus infection. *Nature* 1988; 331:82–4.
8. Traunecker A, Luke W, Karjalainen K. Soluble CD4 molecules neutralize human immunodeficiency virus type 1. *Nature* 1988;331:84–6.
9. Daar ES, Li VL, Moudgil T, Ho DD. High concentrations of recombinant soluble CD4 are required to neutralize primary human immunodeficiency virus type 1 isolates. *Proc Natl Acad Sci USA* 1999;87:6474–8.
10. Moore JP, McKeating JA, Weiss RA, Sattentau QJ. Dissociation of gp120 from HIV-1 virions induced by soluble CD4. *Science* 1990;250:1139–42.
11. Moore JP, McKeating JA, Huang Y, Ashkenazi A, Ho DD. Virions of primary human immunodeficiency virus type 1 isolates resistant to soluble CD4 (sCD4) neutralization differ in sCD4 binding and glycoprotein gp120 retention from sCD4-sensitive isolates. *J Virol* 1992;66:235–43.
12. Schooley RT, Merigan [illegible] Gaut P, et al. Recombinant soluble CD4 therapy in patients with the acquired immunodeficiency syndrome (AIDS) and AIDS-related complex. *Ann Intern Med* 1990;112:247–53.
13. Kahn JO, Allan JD, Hodges TL, et al. The safety and pharmacokinetics of recombinant soluble CD4 (rCD4) in subjects with the acquired immunodeficiency syndrome (AIDS) and AIDS-related complex. *Ann Intern Med* 1990;112:254–61.
14. Capon DJ, Chamow SM, Mordenti J, et al. Designing CD4 immunoadhesins for AIDS therapy. *Nature* 1989;337:525–31.
15. Byrn RA, Mordenti J, Lucas C, et al. Biological properties of a CD4 immunoadhesin. *Nature* 1990;344:667–70.
16. Ward RHR, Capon DJ, Jett CM, et al. Prevention of HIV-1 IIIB infection in chimpanzees by CD4 immunoadhesin. *Nature* 1991;352:434–6.
17. Hodges TL, Kahn JO, Kaplan LD, et al. Phase I study of the recombinant human CD4-immunoglobulin G therapy of patients with AIDS and AIDS-related complex. *Antimicrob Agents Chemother* 1991;35:2580–6.
18. Coombs RW, Collier AC, Allain J-P, et al. Plasma viremia in human immunodeficiency virus infection. *N Engl J Med* 1989;321:1626–31.
19. Coombs RW, Collier AC, Gibson JW, Nelson KE, Chaloupka K, Ammann A, Corey L. Relationship between the in vitro HIV-1 inhibitory dose of rCD4-IgG and the ex vivo plasma-associated HIV-1 titer. Twenty-first Annual Keystone Symposia, March 27–31, 1992. [Abstract Q512]. *J Clin Biochem* 1992;suppl 16E:77.
20. Ballew HC. Neutralization. In: Spector S, Lancz GJ, eds. *Clinical virology manual*. New York: Elsevier, 1986:187–99.
21. Matanabe M, Reimann KA, DeLong PA, Liu T, Fisher RA, Letvin NL. Effect of recombinant soluble CD4 in rhesus monkeys infected with simian immunodeficiency virus of macaques. *Nature* 1989;337:267–70.
22. Schacker T, Coombs RW, Collier AC, et al. The effects of high-dose recombinant soluble CD4 on human immunodeficiency virus type 1 viremia. *J Infect Dis* 1994;169:37–40.
23. Clerici M, Yarchoan R, Blatt S, Hendrix CW, Ammann AJ, Broder S, Shearer GM. Effect of a recombinant CD4-IgG on in vitro T helper cell function: data from a phase I/II study of patients with AIDS. *J Infect Dis* 1993;168:1012–6.
24. Johnson VA, Barton MA, Chou T-C, et al. Synergistic inhibition of human immunodeficiency virus type 1 (HIV-1) replication in vitro by recombinant soluble CD4 and 3'azido-3'deoxythymidine. *J Infect Dis* 1989;159:837–44.
25. Johnson VA, Barlow MA, Merrill DP, Chou T-C, Hirsch MA. Three-drug synergistic inhibition of HIV-1 replication in vitro by zidovudine, recombinant soluble CD4 and recombinant interferon-alpha A. *J Infect Dis* 1990;161:1059–67.

CONCISE COMMUNICATION

Single-Dose Safety, Pharmacology, and Antiviral Activity of the Human Immunodeficiency Virus (HIV) Type 1 Entry Inhibitor PRO 542 in HIV-Infected Adults

Jeffrey M. Jacobson,[1] Israel Lowy,[1] Courtney V. Fletcher,[4] Tobias J. O'Neill,[3] Diep N. H. Tran,[3] Thomas J. Ketas,[2] Alexandra Trkola,[2] Mary E. Klotman,[1] Paul J. Maddon,[3] William C. Olson,[3] and Robert J. Israel[3]

[1]*Mount Sinai Medical Center and* [2]*Aaron Diamond AIDS Research Center, New York, and* [3]*Progenics Pharmaceuticals, Inc., Tarrytown, New York;* [4]*University of Minnesota, Minneapolis*

PRO 542 (CD4-IgG2) is a recombinant antibody-like fusion protein wherein the Fv portions of both the heavy and light chains of human IgG2 have been replaced with the D1D2 domains of human CD4. Unlike monovalent and divalent CD4–based proteins, tetravalent PRO 542 potently neutralizes diverse primary human immunodeficiency virus (HIV) type 1 isolates. In this phase 1 study, the first evaluation of this compound in humans, HIV-infected adults were treated with a single intravenous infusion of PRO 542 at doses of 0.2–10 mg/kg. PRO 542 was well tolerated, and no dose-limiting toxicities were identified. Area under the concentration-time curve, and peak serum concentrations increased linearly with dose, and a terminal serum half-life of 3–4 days was observed. No patient developed antibodies to PRO 542. Preliminary evidence of antiviral activity was observed as reductions in both plasma HIV RNA and plasma viremia. Sustained antiviral effects may be achieved with repeat dosing with PRO 542.

There is an urgent need for new human immunodeficiency virus (HIV) therapies that target additional stages of the viral replicative cycle. PRO 542 (tetravalent CD4-IgG2 fusion protein) [1] is a novel HIV-1 entry inhibitor that incorporates 4 copies of the virus-binding domains of CD4, the primary receptor for HIV-1. PRO 542 binds the HIV-1 envelope (env) glycoprotein gp120 with nanomolar affinity and neutralizes primary HIV-1 regardless of genotype or phenotype [2, 3]. The concentration required to achieve a 90% reduction in viral infectivity in vitro (IC_{90}) is ~20 μg/mL and is readily achieved in vivo. In ex vivo assays, PRO 542 is similarly effective at neutralizing the infectivity of plasma obtained from HIV-1–infected persons, which indicates that this agent is active against the diverse viral quasi species that are encountered clinically [4]. PRO 542 also protects against infection by primary isolates in the human peripheral blood lymphocyte (hu-PBL)–SCID mouse model of HIV-1 infection [5].

Compared with monovalent or divalent CD4–based proteins, PRO 542 has consistently demonstrated as much as 100-fold greater activity against primary HIV-1 isolates [1, 2, 4, 6]. PRO 542's antiviral activity compares favorably with that of the rare human monoclonal antibodies (MAbs) that broadly and potently neutralize primary viruses [1–3, 6]. In addition, PRO 542 therapy is, in principle, less susceptible to the development of drug-resistant viruses than are therapies that employ anti-env MAbs or portions of the highly mutable HIV-1 env glycoproteins. Thus, PRO 542 may have clinical utility as a therapeutic or prophylactic agent that neutralizes cell-free virus before it can establish new rounds of infection.

This report describes the results of the first clinical investigation of PRO 542. The phase 1 trial was conducted to evaluate the tolerability, pharmacokinetics, and immunogenicity of this compound in HIV-infected adults. Additional analyses examined the antiviral effects of PRO 542 when administered as a single intravenous infusion.

Methods

PRO 542. PRO 542 (Progenics Pharmaceuticals, Tarrytown, NY) was expressed in recombinant Chinese hamster ovary cells, was purified via column chromatography, and was supplied at 5 mg/mL in PBS [1].

Study design. This was an open-label, dose-escalation study

Received 16 December 1999; revised 23 March 2000; electronically published 30 June 2000.

Presented in part: 39th Interscience Conference on Antimicrobial Agents and Chemotherapy, San Francisco, 26 September 1999 (abstract 323).

All study participants provided written informed consent. The study protocol was approved by the Institutional Review Board, Mount Sinai Medical Center.

Financial support: National Institutes of Health (AI-43084).

Reprints or correspondence: Dr. Jeffrey M. Jacobson, Mount Sinai Medical Center, 1 Gustave L. Levy Plaza, New York, NY 10029-6574 (jeffrey.jacobson@mssm.edu).

The Journal of Infectious Diseases 2000; 182:326–9

0022-1899/2000/18201-0044$02.00

of PRO 542 in HIV-infected adults. Cohorts of 3–6 patients were treated successively with a single 15–30-min intravenous infusion of PRO 542 at doses of 0.2, 1.0, 5.0, and 10 mg/kg. Inclusion criteria included stable or no anti-HIV therapy for ≥4 weeks prior to the study, >3000 copies of viral RNA/mL, >50 CD4 cells/μL, and normal hematologic and serum chemistry values.

Patient evaluation. Vital signs were recorded at frequent intervals on the day of treatment and on follow-up visits. Blood samples were collected ~2 weeks before treatment, immediately before dosing, and at specified time points ≤4 weeks after infusion. Complete blood counts, serum chemistries, and urine analyses were done 1 week after treatment. Samples were processed in the clinical laboratories of Mount Sinai Medical Center for routine hematology and chemistry. Plasma and serum fractions were stored at −70°C prior to virologic and immunologic evaluations.

Pharmacokinetic analysis. Cryopreserved serum samples were analyzed for PRO 542 by ELISA. In brief, patient serum containing PRO 542 was used to inhibit binding of the anti-CD4 antibody Leu-3a (Becton Dickinson, Franklin Lakes, NJ) to microtiter plates coated with recombinant soluble CD4 (Bartels, Issaquah, WA). Bound Leu-3a was detected by enzyme-conjugated goat antibody to mouse IgG. The lower limit of detection is 50 ng/mL. The terminal serum half-life was calculated by regression analysis of the terminal portion of the concentration-time curve. Area under the concentration-time curve, from time 0 to infinity ($AUC_{0-\infty}$), was calculated by using the linear trapezoidal rule [7].

Immunogenicity analysis. Predose and 4-week serum samples were analyzed for the presence of antibodies to PRO 542. In the ELISA, microtiter plates were coated with PRO 542, contacted with patient serum or anti–PRO 542 antibody standards, and incubated with biotinylated PRO 542, which was detected by using streptavidin-horseradish peroxidase. With Leu-3a as a standard anti-CD4 antibody, assay sensitivity was 15 ng/mL.

Virologic analyses. Plasma HIV RNA levels were measured by reverse transcription–polymerase chain reaction (RT-PCR) by the Amplicor Monitor assay (Roche Diagnostic Systems, Branchburg, NJ). The changes in log-transformed HIV RNA levels were evaluated for statistical significance by the 2-tailed Wilcoxon signed-rank tests. Additional assays measured plasma levels of infectious HIV. In brief, CD4 lymphocytes were purified from activated peripheral blood mononuclear cells and cultured as described elsewhere [8]. We combined 2×10^6 CD4 lymphocytes with serially diluted patient plasma for 16–20 h at 37°C. Cultures then were washed and combined with an additional 5×10^5 cells. At weekly intervals thereafter, culture supernatant was collected for analysis and replaced with an equal volume of fresh medium containing 2.5×10^5 cells. The extent of HIV replication was determined by p24 ELISA as described elsewhere [2]. Samples were analyzed in 2 or 3 separate assays and were scored as positive if replication-competent HIV was detected in any analysis.

Results

Demographics. The median virus loads for the 0.2-, 1.0-, 5.0-, and 10-mg/kg cohorts were 5310, 207,000, 11,800, and 35,500 copies/mL, respectively, whereas the corresponding median numbers of CD4 lymphocytes were 310, 100, 390, and 314/μL, respectively. Seven patients were on stable combination antiretroviral therapy, and 8 were treatment naive. The latter group included subject 125, who received zidovudine and lamivudine therapy for ~2 months ~1 year before enrollment but who was otherwise treatment naive. All patients received a full infusion of PRO 542 and were available for follow-up.

Safety evaluation. PRO 542 was well tolerated, and no dose-limiting toxicities were identified. One patient in the lowest dose cohort presented 1 week after treatment with a grade 2 neutropenia that worsened to grade 3 at week 4 and then resolved without intervention by week 6. No other patient experienced neutropenia. One patient in the 1-mg/kg dose cohort experienced mild and transient headache. While these events could not be attributed directly to the study drug, a possible relationship could not be excluded. All other adverse events were mild and/or unlikely to be related to the study drug. There was no significant change in the number of CD4 lymphocytes (data not shown).

Pharmacokinetics and immunogenicity. Mean serum concentrations of PRO 542 observed for the different dose cohorts are plotted in figure 1. Serum concentrations of PRO 542 increased linearly with dose as did the mean $AUC_{0-\infty}$ values ($r^2 = .99$), which were 13,500 ± 3500 and 23,800 ± 7800 hr × μg/mL for the 2 highest dose cohorts. A mean peak serum concentration of 564 ± 110 μg/mL was observed for the 10-mg/kg cohort. Mean terminal serum half-lives of 4.2 ± 0.9 and 3.3 ± 0.7 days were observed in the 5.0- and 10-mg/kg dose cohorts, respectively. About 2-fold shorter half-lives were observed for the lower dose cohorts, for which the 28-day time point was not evaluable. No patient developed measurable levels of antibodies to PRO 542.

Plasma HIV RNA. As indicated in figure 2*A*, a significant decline in plasma HIV RNA was observed after a single 10-mg/kg dose of PRO 542. The most consistent decreases were observed 4 h after treatment, when the mean reduction was

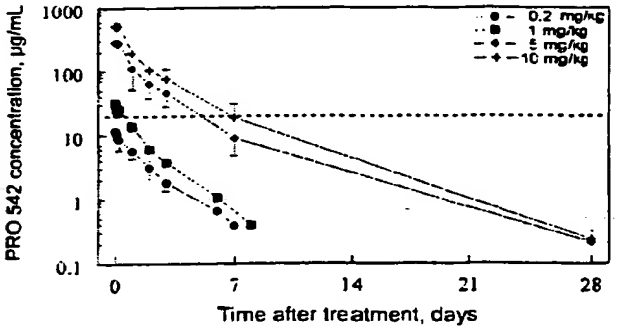

Figure 1. Pharmacokinetics of PRO 542. Mean serum concentrations (± SD) are plotted for each dose cohort. *Dashed line*, approximate in vitro IC_{90} value (20 μg/mL) of PRO 542 for primary human immunodeficiency virus–1 isolates [3].

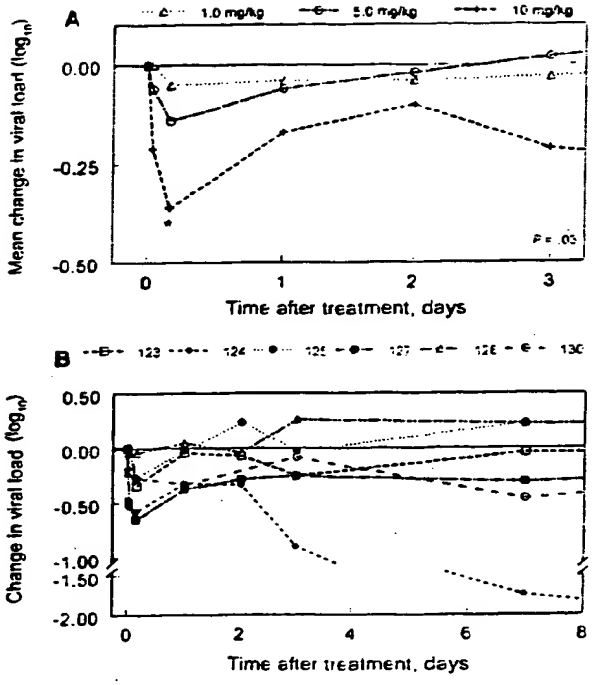

Figure 2. Virologic evaluations. *A*, Mean change in plasma human immunodeficiency virus RNA for patients in 3 highest dose cohorts. Virus load changes for lowest dose cohort were −0.09 to +0.07 log_{10} and have been omitted for clarity. *B*, Individual antiviral responses of subjects in 10-mg/kg cohort. Their predose virus loads were 8210, 498,000, 21,300, 3220, 23,000, and 413,000 copies/mL. Treatment-naive and -experienced patients are indicated by open and filled symbols, respectively.

0.36 log_{10} copies/mL ($P = .03$, 2-tailed Wilcoxon signed-rank test). Smaller and statistically nonsignificant reductions were observed at 1 and 24 h after injection. A similar trend was observed in the 5-mg/kg cohort. Spiking studies showed that assay performance was not affected significantly by the PRO 542 concentrations achieved in this study (data not shown).

Antiviral responses of individual patients in the 10-mg/kg cohort are plotted in figure 2*B*. Virus load reductions were observed in most patients at all posttreatment time points. Patient 124 experienced a 2-log reduction in virus load 7–14 days after treatment. The 10-mg/kg cohort comprised 3 treatment-naive individuals (subjects 123, 128, and 130) and 3 subjects who were receiving stable antiretroviral therapy at entry (subjects 124, 125, and 127). The 3 subjects on therapy experienced greater reductions in mean virus load at all postinfusion time points, including a 0.50 log_{10} mean reduction at 4 h, but the differences between the 2 groups did not reach statistical significance.

Plasma viremia. Plasma from patients 124 and 130 also was analyzed for levels of infectious HIV. These patients were in the 10-mg/kg cohort and had the highest baseline virus loads (498,000 and 413,000 copies/mL, respectively). Culturable virus was isolated from both patients at screening (1–2 weeks before treatment) and immediately before dosing. For subject 130, infectious virus could not be detected in plasma drawn at 1, 4, 24, 48, and 72 h and at 1 and 2 weeks after infusion but was detected at 4 weeks. Subject 124's plasma was culture negative at 1, 4, and 24 h and then was positive intermittently thereafter (i.e., positive at 72 h and 2 weeks but negative at 1 and 4 weeks). Of the subjects treated with 10-mg/kg PRO 542, subject 124 experienced the greatest sustained reduction in virus load, whereas subject 130 experienced a fairly typical pattern of response (figure 2*B*).

Discussion

PRO 542 was extremely well tolerated at all doses tested. This favorable safety profile is consistent with the compound's design to have minimal reactivities with molecules other than the HIV-1 surface glycoprotein. Serum concentrations of >500 μg/mL were attained after administration of a single 10-mg/kg dose, and serum concentrations remained above the in vitro IC_{90} for ~1 week. The terminal serum half-life of PRO 542 was 3–4 days in the high-dose cohorts. No subject developed measurable amounts of antibodies to PRO 542. Thus, any potential neoepitopes formed at the juncture of the CD4 and IgG domains were nonimmunogenic in this study. The pharmacologic and safety data support higher and/or repeat dosing of PRO 542.

Preliminary evidence of antiviral activity was observed as reductions in both plasma HIV RNA and plasma viremia. A statistically significant acute reduction in plasma virus load was observed after administration of a single 10-mg/kg dose of PRO 542, and 1 subject experienced a >2 log reduction in HIV RNA at 1–2 weeks after injection. Smaller virus load reductions were observed at lower doses. Since the in vivo half-life of virus-producing cells is ~2 days [9, 10], the rapid reduction in plasma HIV RNA is striking. One possible mechanism is active clearance of PRO 542–coated virus by the reticuloendothelial system. Although PRO 542 incorporates an IgG2 heavy chain constant region so as to minimize effector functions and does not measurably bind human Fc receptors in vitro [1], IgG2 molecules retain residual effector functions that may mediate clearance [11]. In addition, PRO 542 has the potential to cross-link virions and thereby form large complexes with heightened clearance rates. Conceivably, PRO 542 may also affect the budding of new viruses.

Numerous preclinical studies have established PRO 542's ability to neutralize primary HIV-1 isolates regardless of organ-based clearance mechanisms. Since RT-PCR measurements of

CONCISE COMMUNICATION

Recombinant CD4-IgG2 in Human Immunodeficiency Virus Type 1–Infected Children: Phase 1/2 Study

William T. Shearer,[1] Robert J. Israel,[2] Stuart Starr,[3] Courtney V. Fletcher,[4] Diane Wara,[5] Mobeen Rathore,[6] Joseph Church,[6] Jaime DeVille,[7] Terence Fenton,[8] Bobbie Graham,[10] Pearl Samson,[11] Silvija Staprans,[12] James McNamara,[13] John Moye,[14] Paul J. Maddon,[2] and William C. Olson[2] for the Pediatric AIDS Clinical Trials Group Protocol 351 Study Team*

[1]*Departments of Pediatrics and Immunology, Baylor College of Medicine, Houston, Texas;* [2]*Progenics Pharmaceuticals, Inc., Tarrytown, New York;* [3]*Division of Immunologic and Infectious Diseases, Children's Hospital of Philadelphia, Philadelphia, Pennsylvania;* [4]*Division of Clinical Pharmacology, University of Minnesota, Minneapolis;* [5]*Department of Pediatrics, University of California at San Francisco;* [6]*Children's AIDS Center, Children's Hospital of Los Angeles and* [7]*Department of Pediatrics, University of California at Los Angeles;* [8]*Division of Infectious Diseases/Immunology, University of Florida Health Science Center at Jacksonville; Frontier Science and Technology Research Foundation, Inc. at* [9]*Brookline, Massachusetts (Statistical and Data Analysis Center), and* [10]*Amherst, New York (Statistical and Data Management Center);* [11]*Statistical and Data Analysis Center, Harvard School of Public Health, Boston, Massachusetts;* [12]*Department of Microbiology and Immunology, Emory University School of Medicine, Atlanta, Georgia;* [13]*Pediatric Medicine Branch, Division of AIDS, National Institute of Allergy and Infectious Diseases and* [14]*Pediatric, Adolescent, and Maternal AIDS Branch, Center for Research for Mothers and Children, National Institute of Child Health and Human Development, Bethesda, Maryland*

The use of recombinant CD4-IgG2 in pediatric human immunodeficiency virus type 1 (HIV-1) infection was evaluated by single and multidose intravenous infusions in 18 children in a phase 1/2 study. The study drug was well tolerated, and dose proportionality was observed in terms of area under time-concentration curve and peak serum concentration. Acute decreases of >0.7 $\log_{10}$ copies/mL in serum HIV-1 RNA concentration were seen in 4 of the 6 children treated with 4 weekly 10 mg/kg doses. At 14 days after treatment, 3 children had sustained reductions in serum HIV-1 RNA; the other children had rebounded to baseline levels or above. By 28 days after therapy, the peak HIV-1 cellular infectious units was reduced in all 6 children, including the 2 who had experienced an earlier transient increase in values. Thus, recombinant CD4-IgG2 treatment of HIV-1–infected children appears to be well tolerated and capable of reducing HIV-1 burden.

Despite recent advances in the treatment of human immunodeficiency virus type 1 (HIV-1) with highly active antiretroviral therapy (HAART), long-lived reservoirs of virus, the increasing prevalence of drug-resistant viruses, and significant toxicities mandate the search for new therapies. Virtually all persons with HIV-1 infection have disease progression and eventually die of complications of HIV-1 disease. Since the early discovery that the CD4 molecule on cellular targets was actually a receptor for the HIV-1 surface glycoprotein 120 (gp120) [1], the concept of using CD4 as a soluble competitor molecule to treat HIV-1 infection and prevent perinatal HIV-1 transmission has been raised [2–7]. The recent discoveries of a second cognate receptor, such as CCR5 and CXCR4 (reviewed in [8]), have increased the enthusiasm for using receptor-based therapies.

In this pediatric phase 1/2 clinical trial, we used the CD4-

Received 20 June 2000; revised 29 August 2000; electronically published 27 October 2000.

Presented in part: 7th Conference on Retroviruses and Opportunistic Infections, San Francisco, 2 February 2000 (abstract 701).

Reprints or correspondence: Dr. William T. Shearer, Dept. of Pediatrics–Allergy/Immunology, Baylor College of Medicine, 6621 Fannin St. (MC 1-3291), Houston, TX 77030 (wshearer@bcm.tmc.edu).

The Journal of Infectious Diseases 2000; 182:1774–9

0022-1899/2000/18206-0027$02.00

Informed consent was obtained from parents or caretakers, and assent was obtained from children ≥ 7 years old. Human experimentation guidelines of the US Department of Health and Human Services and of the authors' institutions were followed in the conduct of this research.

R.J.I., W.C.O., and P.J.M. are employees of Progenics Pharmaceuticals.

Financial support: National Institutes of Health (grants AI-27550, AI-27551, AI-32921, AI-41089, AI-41110, AI-43084, RR-00043, RR-00071, RR-00188, RR-00240, RR-00533, RR-00645, RR-00885, and RR-02172; contract HD-3-3162).

* PACTG Protocol 351 Study Team Coordinators are listed after the text.

based molecule recombinant (r) CD4-IgG2 (PRO 542; Progenics Pharmaceuticals, Tarryt wn, NY) [9]. This protein is an antibody-like molecule consisting of 4 copies of the D1D2 immunoglobulin super family domains of human CD4 that have been genetically fused to the highly conserved heavy and light chain constant regions of human IgG2. rCD4-IgG2 has several distinct advantages over earlier CD4-based molecules, including an extended peripheral blood half-life, multiple (tetrameric) binding to HIV-1 gp120, and potent neutralization of primary isolates in a variety of preclinical models of HIV-1 infection [9–13]. Phase 1/2 studies of this fusion protein in HIV-1–infected adults have shown excellent safety, tolerability, and pharmacokinetic properties, plus promising evidence for an antiviral effect on HIV-1 [14].

Methods

Study design and patient evaluation. Thirteen children were enrolled in single-dose studies of 0.2 (n = 4), 1.0 (n = 3), 5.0 (n = 3), and 10 (n = 3) mg/kg; 6 children were enrolled in multidose studies in which 10 mg/kg of rCD4-IgG2 was given as 4 weekly doses. Children in the multidose studies were required to have a stable HIV-1 RNA copy number ≥10,000/mL. No children who were taking immunomodulating drugs, vaccines, or IgG were included.

The study drug, stored at −70°C in 5-, 20-, and 100-mg vials in PBS, was thawed, filtered through 0.20-μm filters, and infused intravenously for 15–30 min. For 2 h after infusion, vital signs were measured, and local and systemic reactions were monitored at 15- and 30-min intervals. The children were observed for side effects in the clinic at least hourly for ≤12 h.

At intervals before and after infusion of rCD4-IgG2 into study subjects in the single-dose (≤28 days later) and multidose study (≤19 weeks later), blood specimens were obtained for complete blood counts and routine serum chemistry and lymphocyte subset determination. Standard Pediatric AIDS Clinical Trials Group (PACTG) toxicity tables were used to grade adverse events on a scale of 1–4 (grade 1, mild; grade 4, life-threatening adverse events). Adverse events were scored as not related, possibly related, and probably related to study drug.

Pharmacokinetic studies. Cryopreserved serum specimens were obtained at fixed time points before and after rCD4-IgG2 infusion for pharmacokinetic analysis, as described elsewhere [14]. Area under the concentration-time curve (AUC) from time 0 to the last measured concentration (C_{last}) was calculated according to the linear trapezoidal rule [15]. AUC from time 0 to infinity (AUC_{∞}) was calculated as AUC from time 0 to C_{last} + C_{last}/ke, where ke is the elimination rate constant determined by regression analysis of the terminal portion of the concentration-time curve. The half-life was calculated as the natural logarithm of $2/ke$. The steady-state AUC was calculated from the concentration-time data of subjects who participated in the multiple dose study as that within the 7-day interval following infusion 4.

Quantitative virology. Blood samples were obtained at fixed time points before and after rCD4-IgG2 infusion for HIV-1 RNA plasma levels, HIV-1 quantitative plasma cultures, and HIV-1 quantitative peripheral blood mononuclear cell (PBMC) cultures. Plasma HIV-1 RNA was measured by a quantitative polymerase chain reaction assay (Amplicor HIV Monitor assay; Roche Diagnostic Systems, Basel, Switzerland), as recommended in [16] and by the manufacturer. This assay has a lower limit of detection f 400 copies/mL. Because of the availability of frequently collected serum specimens from the pharmacokinetic studies, remaining serum specimens were also used to quantify HIV-1 RNA by the Amplicor assay. rCD4-IgG2 does not significantly affect this assay at the concentrations reached in this study [14].

Quantitative microcultures of PBMC and plasma were done by standard methods [16]. The titer of HIV-1 was expressed as the number of infectious units per million cells (IUPM) or per milliliter of plasma. The P value for the goodness-of-fit (PGOF) of the observed distribution of positive wells, given the estimated titer, was calculated for each assay. Assay results with PGOF < .05 were considered unreliable and were excluded.

Statistical analysis. Because of the small sample sizes for each treatment group, the study lacks the statistical power for tests f significance. Thus, the findings are presented as descriptive statistics and graphical displays.

Results

Patient cohort. Thirteen and 6 children were enrolled in the single- and multidose studies, respectively (1 child was in both). Of the 18 children, 56% were girls. The race/ethnicity breakdown was 17% white, 44% black, 33% Hispanic, and 6% other ethnic groups; the median age was 7 years (range, 2–13 years); the median CD4 cell count was 433/μL (range, 36–1849 cells/μL); the median CD4 cell percentage was 20 (range, 4–58); and the median $\log_{10}$ HIV-1 RNA level was 4.03 copies/mL (range, 2.6–5.04 copies/mL).

Safety, toxicity, and tolerability. In the single-dose study, there were no adverse experiences above grade 2 and no study drug–related events of any severity, as assessed by standard PACTG toxicity tables. In the multidose study, 1 child with a history of flu-like reactions to intravenous immunoglobulin experienced similar flu-like symptoms after the second of 4 doses. The grade 3 symptoms were easily controlled with an antipyretic/analgesic compound and were considered to be possibly related to the study product.

Pharmacokinetic measurements. Figure 1 illustrates the concentration-time profiles for single and multidose rCD4-IgG2, respectively. The AUC increased linearly (r^2 = 0.997; P = .0016) with dose. The median AUC after the fourth 10 mg/kg infusion in the multidose studies was 11,361 μg × h/mL, which was in excellent agreement with that (12,335 μg × h/mL) observed for a single 10-mg/kg dose. The elimination half-life of rCD4-IgG2 was >2 days (median, 2.27 days; range, 2.06–2.41 days) for the single-dose cohorts and 2.13 days for the multidose cohort. Peak serum concentrations were achieved shortly after infusion, and median values of 6.67, 57.4, 215, and 360 μg/mL were observed for the 0.2, 1.0, 5.0, and 10 mg/kg single-dose cohorts, whereas the corresponding median serum concentrations 7 days after infusion were 0.23, 1.01, 5.06, and 4.74 μg/mL. Median peak and

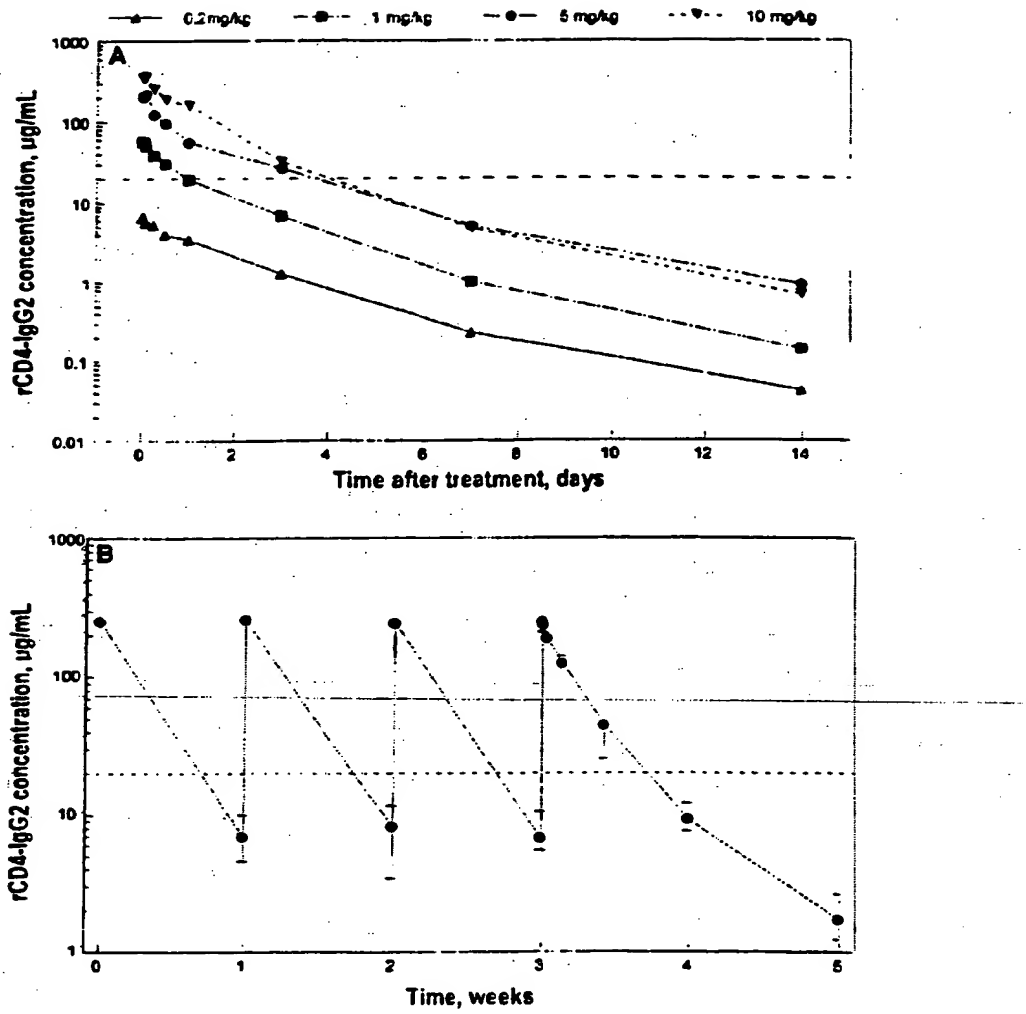

Figure 1. Pharmacokinetic data of recombinant CD4-IgG2 (rCD4-IgG2). *A*, Single-dose concentrations. *B*, Multiple-dose concentrations. Concentration-time profiles for 6 children who received 10 mg/kg of rCD4-IgG2 weekly for 4 doses. 95% Confidence intervals are shown where possible *(brackets)*.

7-day serum concentrations of 274 and 6.95 µg/mL were observed for the multidose cohort.

HIV-1 RNA levels. In the single-dose studies, there were modest acute reductions (~0.50 $\log_{10}$) in plasma HIV-1 RNA levels in some patients and acute increases (≤1.50 $\log_{10}$) in others. In the multidose studies, 4 subjects (nos. 1–4) experienced decreases in serum HIV-1 RNA concentration >0.70 $\log_{10}$ (figure 2). One subject (no. 2) was noncompliant with her HAART program at the time of the second rCD4-IgG2 infusion, and a full adherence program was initiated by medical personnel at a camp (days 7–18); the patient's HIV-1 RNA level rose after she returned home (days 18–39), underscoring the importance of strict adherence to antiretroviral therapy in clinical trials with agents such as rCD4-IgG2. Rebound of HIV-1 RNA serum concentrations occurred in some subjects (e.g., patient 3 had a 2.61 $\log_{10}$ increase between the first and second rCD4-IgG2 infusions; figure 2). Overall, the median $\log_{10}$ RNA value for the 6 children given multidoses was 4.26 on day 0, with a nadir of 3.96 $\log_{10}$ 1 h after treatment at day 14 and an increase to near baseline levels (4.22 $\log_{10}$) at day 35, 14 days after the last infusion (data not shown).

Quantitative HIV-1 PBMC and plasma cultures. In the single-dose study arm in the 3 subjects with undetectable HIV-1 RNA at baseline, quantitative IUPM results remained below

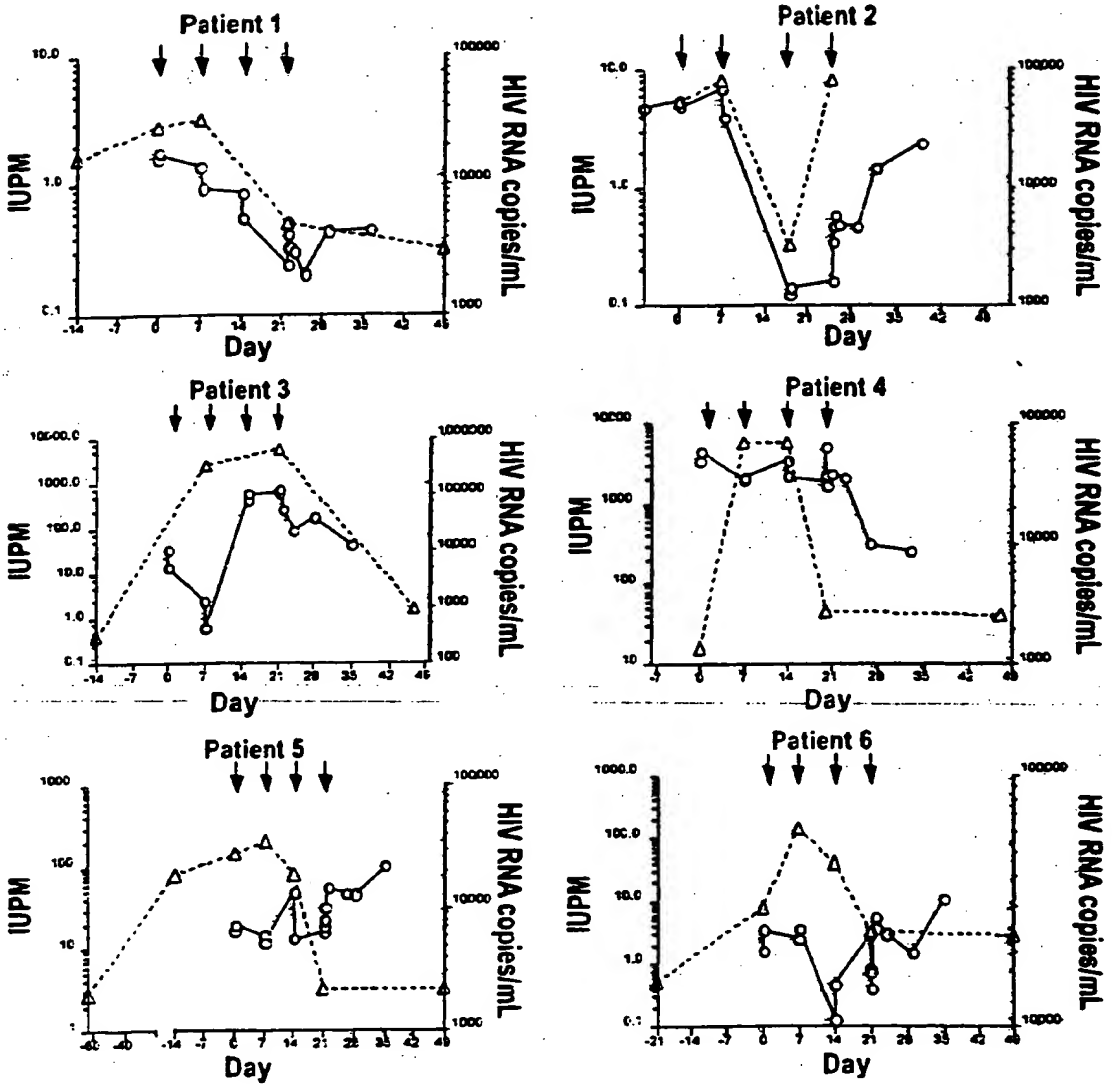

Figure 2. Comparison of serum human immunodeficiency virus (HIV)–1 RNA levels (copies/mL) and quantitative (peripheral blood mononuclear cell [PBMC]) microcultures (infectious units/million cells [IUPM]) in 6 children receiving 10 mg/kg of recombinant CD4-IgG2 (rCD4-IgG2) in multidose studies. Day 0 is beginning of study. Arrows indicate times of rCD4-IgG2 infusion. ○, HIV-1 RNA values (copies/mL). △, PBMC IUPM no. Screening test data (before day 0) are shown for most subjects.

the limit of detection. In subjects with detectable HIV-1 RNA levels at baseline, the IUPM generally reflected changes in plasma HIV-1 RNA levels (data not shown).

In the multidose study arm, there was a general lowering trend in IUPM values after treatment with rCD4-IgG2 (figure 2). The IUPM values decreased to near or below baseline in patients 4 and 6 after a transient increase from days 0 to 7. Patients 1, 5, and 6 experienced an increase in IUPM in the week(s) before drug infusion. Patients 1 and 5 experienced an ~10-fold decline in IUPM relative to that measured just before infusion (day 0), whereas patient 6 had an ~4-fold fall in IUPM from days 0 to 21. Patient 3 (baseline assessment not available) had a change from 2503 IUPM (day 7) to 5607 IUPM at day 21 (day 15 culture results were invalid) to 2 IUPM at day 49. Patient 4 went from 16 IUPM at day 0 to 5608 IUPM at days 7 and 14, a 350-fold increase, followed by a decline to ~45

IUPM thereafter. Patient 2 had an insignificant change from 5.4 IUPM at day 0 to 8.1 IUPM at day 7, followed by a decrease to 0.32 IUPM at day 18. Subsequently, the IUPM returned to 8.1 at day 25, which was concordant with an increase in HIV-1 RNA level after the child's removal from supervised antiretroviral drug therapy. Similarly, the IUPM values in patients 1, 3, and 5 fell to low levels after therapy. With the exception of patient 2 (likely to have been noncompliant with antiretroviral therapy), the IUPM levels after completion of the 4 doses of rCD4-IgG2 stayed depressed for at least 28 days. The IUPM decreases in all the children after infusion of rCD4-IgG2 appeared to be unrelated to CD4 cell count (data not shown). Most assessments of infectious titers in the plasma were at or below the level of assay detection at baseline and did not appear to change significantly with treatment.

Discussion

This new agent appeared to be well tolerated in HIV-1–infected children. Its pharmacokinetic properties also appeared to be excellent, and high concentrations of product were achieved shortly after infusion. At a dose of 10 mg/kg, rCD4-IgG2 produced a median peak level of 274 μg/mL and a trough level of 6.95 μg/mL 7 days later; the first of these values was well above that of 15–20 μg/mL, which was shown in laboratory and animal model systems to inhibit many wild-type HIV-1 strains [10, 11]. The AUC analysis suggests that this fusion protein at 10 mg/kg might be highly effective in binding HIV-1 virions for ≥5 days.

rCD4-IgG2 appeared to produce acute, sometimes sustained, decreases in serum HIV-1 RNA concentrations and cellular IUPM in individual pediatric patients. This is consistent with the findings of a phase 1 study of the molecule in HIV-infected adults, in which a statistically significant acute reduction in plasma HIV RNA was observed after administration of a single 10 mg/kg dose of rCD4-IgG2; reductions to 2 logs were observed 1–2 weeks after injection [14]. In 2 of 6 patients, an apparent early and substantial transient increase in circulating infected PBMC, but not in serum HIV-1 RNA level, was observed. Numerous possible explanations could account for the increases in circulating infected cells, including altered trafficking of HIV-1 in lymphoid tissue and formation of HIV-1 virion rCD4-IgG2 complexes by virtue of multimeric binding, but additional clinical trials will be necessary to better characterize their existence.

In summary, this first clinical trial of rCD4-IgG2 in children has established, in single and multidose studies, that the product is safe and well tolerated. This new product has excellent pharmacokinetic properties, and serum concentrations in excess of the in vitro inhibitory concentration were maintained for about 5 days after infusion. The trial results also suggest that rCD4-IgG2 may be effective in lowering the HIV-1 burden in children and clearly point the way toward additional pediatric clinical trials in which drug dosage and frequency of administration can be optimized.

Pediatric AIDS Clinical Trials Group Protocol 351 Study Team Study Coordinators

Pediatric AIDS Clinical Trials Group Protocol 351 Study Team study coordinators are Deborah Trevithick (University of California, San Francisco), Melissa Scites (University of Florida Health Science Center, Jacksonville), Sarah Fox (Children's Hospital of Los Angeles), Carol Vincent (Children's Hospital of Philadelphia), and Pegg Dobmeier (Baylor College of Medicine, Houston).

Acknowledgments

We thank the investigators, study staff, and the families who participated in this study; Elizabeth Hawkins and Wende Levy (Social and Scientific Systems, Bethesda, MD) for assistance with protocol development and management; Karen Hsia for virologic assays in the Pediatric Virology Core Laboratory, University of California, San Diego (Steven A. Spector, director); and Marlene Cooper, Frontier Science and Technology Research Foundation, Amherst, New York.

References

1. Maddon PJ, Dalgleish AG, McDougal JS, Clapham PR, Weiss RA, Axel R. The T4 gene encodes the AIDS virus receptor and is expressed in the immune system and the brain. Cell 1986;47:333–48.
2. Kahn JO, Allan JD, Hodges TL, et al. The safety and pharmacokinetics of recombinant soluble CD4 (rCD4) in subjects with the acquired immunodeficiency syndrome (AIDS) and AIDS-related complex: a phase 1 study. Ann Intern Med 1990;112:254–61.
3. Schooley RT, Merigan TC, Gaut P, et al. Recombinant soluble CD4 therapy in patients with the acquired immunodeficiency syndrome (AIDS) and AIDS-related complex: a phase I–II escalating dosage trial. Ann Intern Med 1990;112:247–53.
4. Schacker T, Coombs RW, Collier AC, et al. The effects of high-dose recombinant soluble CD4 on human immunodeficiency virus type 1 viremia. J Infect Dis 1994;169:37–40.
5. Schacker T, Collier AC, Coombs R, et al. Phase I study of high-dose, intravenous rsCD4 in subjects with advanced HIV-1 infection. J Acquir Immune Defic Syndr Hum Retrovirol 1995;9:145–52.
6. Collier AC, Coombs RW, Katzenstein D, et al. Safety, pharmacokinetics, and antiviral response of CD4-immunoglobulin G by intravenous bolus in AIDS and AIDS-related complex. J Acquir Immune Defic Syndr Hum Retrovirol 1995;10:150–6.
7. Shearer WT, Duliege AM, Kline MW, et al. Transport of recombinant human CD4-immunoglobulin G across the human placenta: pharmacokinetics and safety in six mother-infant pairs in AIDS clinical trial group protocol 146. Clin Diagn Lab Immunol 1995;2:281–5.
8. Berger EA, Murphy PM, Farber JM. Chemokine receptors as HIV-1 coreceptors: roles in viral entry, tropism, and disease. Annu Rev Immunol 1999;17:657–700.
9. Allaway GP, Davis-Bruno KL, Beaudry GA, et al. Expression and characterization of CD4-IgG2, a novel heterotetramer which neutralizes primary HIV-1 isolates. AIDS Res Hum Retroviruses 1995;11:533–9.
10. Trkola A, Pomales AP, Yuan H, et al. Cross-clade neutralization of primary isolates of human immunodeficiency virus type 1 by human monoclonal

antibodies and tetrameric CD4-IgG2. J Virol 1995; 69:6609–17.
11. Gauduin MC, Allaway GP, Maddon PJ, Barbas CF 3rd, Burton DR, Koup RA. Effective ex vivo neutralization of plasma HIV-1 by recombinant immunoglobulin molecules. J Virol 1996; 70:2586–92.
12. Gauduin MC, Allaway GP, Olson WC, Weir R, Maddon PJ, Koup RA. CD4-immunoglobulin G2 protects Hu-PBL-SCID mice against challenge by primary human immunodeficiency virus type 1 isolates. J Virol 1998; 72:3475–8.
13. Trkola A, Ketas T, Kewalramani VN, et al. Neutralization sensitivity of human immunodeficiency virus type 1 primary isolates to antibodies and CD4-based reagents is independent of coreceptor usage. J Virol 1998; 72:1876–85.
14. Jacobson JM, Lowy I, Fletcher CV, et al. Single-dose safety, pharmacology and antiviral activity of the human immunodeficiency virus (HIV) type 1 entry inhibitor PRO 542 in HIV-infected adults. J Infect Dis 2000; 182:326–9.
15. Gibaldi M, Perrier D. Pharmacokinetics. 2d ed. Vol 15. New York: Marcel Dekker, 1982.
16. Division of AIDS, National Institute of Allergy and Infectious Diseases. DAIDS virology manual for HIV laboratories. Washington, DC: US Department of Health and Human Services (NIH publication 97-3828), 1997.

(E)

BIOGRAPHICAL SKETCH

NAME	TITLE	BIRTH DATE
Paul J. Maddon, M.D., Ph.D.	Chief Science Officer	09/15/59

EDUCATION

INSTITUTION	DEGREE	YEAR	FIELD OF STUDY
Columbia College of Columbia University	B.A.	1981	Biochemistry/Mathematics
College of Physicians and Surgeons, Columbia University	M.D.	1988	Medicine
Graduate School of Arts and Sciences, Columbia University	Ph.D.	1988	Biochemistry/Biophysics

P sitions: Chief Science Officer (1988-present), Progenics Pharmaceuticals, Inc., Old Saw Mill River Road, Tarrytown, NY 10591
Adjunct Assistant Professor (1989-present), Department of Medicine, Columbia University, New York, NY 10032

Honors: Westinghouse Science Talent Search National Winner (1977); International Science and Engineering Fair Finalist (1977) New York State Regents Scholarship (1977-81); Phi Beta Kappa, Summa Cum Laude, Columbia University (1981) Medical Scientist Training Program (MSTP) NIH Grant Recipient (1981-87); Dr. Alfred Steiner Award for Biomedical Research, Columbia Univerisity (1985); Dr. Harold Lamport Biomedical Research Prize, Columbia University (1989) ICAAC/Merck Young Investigator Award, American Society for Microbiology (1990)

Pr fessional Activities: Editorial Board, *AIDS Research and Human Retroviruses* (1990-present); *Journal of Virology* (1994-2002)

Reviewer: *AIDS Research and Human Retroviruses* (1990-present); *Journal of Acquired Immune Deficiency Syndromes* (1991-present); *Journal of Clinical Investigation* (1990-present); *Journal of Immunology* (1990-present); *Journal of Virology* (1989-present); *Molecular and Cellular Biology* (1992-present); *Proceedings of the National Academy of Sciences USA* (1989-present); *Science* (1992-present)

NIH Study Section Member: National Cooperative Drug Discovery Group for HIV, NIAID, 1993; HIV Vaccine Preclinical Development, 1994; Biological and Physiological Sciences, SBIR/STTR, 1996-present; AIDS and Related Research 1 (ARRA), NIAID, 1997-1998; Microbiological and Immunological Sciences, SBIR/STTR, 1997-1998; Novel HIV Therapies: Integrated Preclinical/Clinical Program, NIAID, 1999 & 2001; Vaccine Study Section, NIAID, 1999-present; AIDS Vaccine Program Site Visit Team, NCI, 1999; HIV Special Emphasis Panel, NINDS, 1999; HIV Vaccine Trials Network Units (HVTU), NIAID, 2000

Section Chairman, V International Conference on AIDS, Montreal, 1989; Chairman, AIDS Research Symposium, Columbia University, Arden House, NY, 1991; Section Chairman, Annual Meeting of the Laboratory of Tumor Cell Biology, 1993; Member. NYS Science and Technology Foundation Review Committee, Centers for Advanced Technology, 1994; Reviewer, International Human Frontier Science Program, 1995-present; Director, New York Biotechnology Association, 1999-2002; Consultant, Health Sciences Division, The Rockefeller Foundation, 1999-present

Selected Scientific Publications:

Madd n, P.J., Littman, D.R., Godfrey, M., Maddon, D.E., Chess, L., and Axel, R. (1985). The isolation and nucleotide sequence of a cDNA encoding the T cell surface protein T4: a new member of the immunoglobulin gene family. Cell 42, 93-104.

Littman, D.R., Thomas, Y., **Maddon, P.J.**, Chess, L. and Axel, R. (1985). The isolation and sequence of the gene encoding T8: a molecule defining functional classes of T lymphocytes. Cell 40, 237-246.

Madd n, P.J., Dalgleish, A.G., McDougal, J.S., Clapham, P.R., Weiss, R.A., and Axel, R. (1986). The T4 gene encodes the AIDS virus receptor and is expressed in the immune system and the brain. Cell 47, 333-348.

Isobe, M., Huebner, K., **Maddon, P.J.**, Littman, D.R., Axel, R., and Croce, C.M. (1986). The gene encoding the T-cell surface protein T4 is located of human chromosome 12. Proc. Natl. Acad. Sci. USA 83, 4399-4402.

Maddon, P.J., Molineaux, S.M., Maddon, D.E., Zimmerman, K.A., Godfrey, M., Alt, F.W., Chess, L., and Axel, R. (1987). Structure and expression of the human and mouse T4 genes. Proc. Natl. Acad. Sci. USA 84, 9155-9159.

Gay, D., **Maddon, P.J.**, Sekaly, R., Talle, M.A., Godfrey, M., Long, E., Goldstein, G., Chess, L., Axel, R., Kappler, J., and Marrack P. (1987). Functional interaction between human T-cell protein CD4 and the major histocompatiblity complex HLA-DR antigen Nature 328, 626-628.

Maddon, P.J., McDougal, J.S., Clapham, P.R., Dalgleish, A.G., Jamal, S., Weiss, R.A., and Axel, R. (1988). HIV infection does no require endocytosis of its receptor, CD4. Cell 54, 865-874.

Deen, K.C., McDougal, J.S., Inacker, R., Folena-Wasserman, G., Arthos, J., Rosenberg, J., **Maddon, P.J.**, Axel, R., and Sweet, R (1988). A soluble form of CD4 (T4) inhibits AIDS virus infection. Nature 331, 82-84.

Malkovsky, M., Philpott, K., Dalgleish, A.G., Mellor, A.L., Patterson, S., Webster, A.D.B., Edwards, A.J., and **Maddon, P.J.** (1988) Infection of B lymphocytes by the human immunodeficiency virus and their susceptibility to cytotoxic cells. Eur. J. Immunol. 18 1315-1321.

Arthos, J., Deen, K.C., Chaikin, M.A., Fornwald, J.A., Sathe, G., Sattentau, Q.J., Clapham, P.R., Weiss, R.A., McDougal, J.S Pietropaolo, C., Axel, R., Truneh, A., **Maddon, P.J.**, and Sweet, R.W. (1989). Identification of the residues in human CD critical for the binding of HIV. Cell 57, 469-481.

Ibegbu, C.C., Kennedy, M.S., **Madd n, P.J.**, Deen, K.C., Hicks, D., Sweet, R.W., and McDougal, J.S. (1989). Structural features CD4 required for binding to human immunodeficiency virus (HIV). J. Immunol. 142, 2250-2256.

Clapham, P.R., Weber, J.N., Whitby, D., McIntosh, K., Dalgleish, A.G., **Madd n, P.J.**, Deen, K.C., Sweet, R.W., and Weiss, R.A. (1989). Soluble CD4 blocks the infectivity of diverse strains of HIV and SIV for T cells and monocytes but not for brain and muscle cells. Nature 337, 368-370.

Orloff, G.M., Orloff, S.L., Kennedy, M.S., **Maddon, P.J.**, and McDougal, J.S. (1991). Penetration of $CD4^+$ T cells by HIV-1. The CD4 receptor does not internalize with HIV, and CD4-related signal transduction events are not required for entry. J. Immunol. 146, 2578-2587.

Kennedy, M.S., Orloff, S., Ibegbu, C.C., Odell, C.D., **Maddon, P.J.**, and McDougal, J.S. (1991). Analysis of synergism/antagonism between HIV-1 antibody-positive human sera and soluble CD4 in blocking HIV-1 binding and infectivity. AIDS Res. Hum. Retroviruses 7, 975-981.

Orloff, S.L., Kennedy, M.S., Belperron, A.A., **Maddon, P.J.**, and McDougal, J.S. (1993). Two mechanisms of soluble CD4 (sCD4)-mediated inhibition of human immunodeficiency virus (HIV-1) infectivity and their relation to primary HIV-1 isolates with reduced sensitivity to sCD4. J. Virol. 67, 1461-1471.

Allaway, G.P., Ryder, A.M., Beaudry, G.A., and **Maddon, P.J.** (1993). Synergistic inhibition of HIV-1 envelope-mediated cell fusion by CD4-based molecules in combination with antibodies to HIV gp120 or gp41. AIDS Res. Hum. Retroviruses 9, 581-587.

Orloff, S.L., Bandea, C.I., Kennedy, M.S., Allaway, G.P., **Maddon, P.J.**, and McDougal, J.S. (1995). Increase in sensitivity to soluble CD4 (sCD4) by primary HIV-1 isolates after passage through C8166 cells: association with sequence differences in the first constant (C1) region of gp120. AIDS Res. Hum. Retroviruses 11, 335-342.

Allaway, G.P., Davis-Bruno, K.L., Beaudry, G.A., Garcia, E.B., Wong, E.L., Ryder, A.M., Hasel, K.W., Gauduin, M.-C., Koup, R.A., McDougal, J.S., and **Maddon, P.J.** (1995). Expression and characterization of CD4-IgG2, a novel heterotetramer which neutralizes primary HIV-1 isolates. AIDS Res. Hum. Retroviruses 11, 533-539.

Trkola, A., Pomales, A.P., Yuan, H., Korber, B., **Maddon, P.J.**, Allaway, G.P., Katinger, H., Barbas III, C., Burton, D.R., Ho, D.D., and Moore, J.P. (1995). Cross-clade neutralization of primary isolates of human immunodeficiency virus type 1 by human monoclonal antibodies and tetrameric CD4-IgG2. J. Virol. 69, 6609-6617.

Gauduin, M.-C., Allaway, G.P., **Maddon, P.J.**, Barbas, C.F., Burton, D.R., and Koup, R.A. (1996). Effective *ex vivo* neutralization of plasma HIV-1 by recombinant immunoglobulin molecules. J. Virol. 70, 2586-2592.

Dragic, T., Litwin, V., Allaway, G.P., Martin, S., Huang, Y., Nagashima, K.A., Cayanan, C., **Maddon, P.J.**, Koup, R.A., Moore, J.P., and Paxton, W.A. (1996). HIV-1 entry into CD4+ cells is mediated by the chemokine receptor CC-CKR-5. Nature 381, 667-673.

Litwin, V., Nagashima, K.A., Ryder, A.M., Chang, C-H., Carver, J.M., Olson, W.C., Alizon, M., Hasel, K.W., **Maddon, P.J.**, and Allaway, G.P. (1996). Human immunodeficiency virus type 1 membrane fusion mediated by a laboratory-adapted strain and a primary isolate analyzed by resonance energy transfer. J. Virol. 70, 6437-6441.

Trkola, A., Dragic, T., Arthos, J., Binley, J., Olson, W.C., Allaway, G.P., Cheng-Mayer, C., Robinson, J., **Maddon, P.J.**, and Moore, J.P. (1996). CD4-dependent, neturalizing antibody-sensitive interactions between HIV-1 and its co-receptor CCR-5. Nature 384, 184-187.

Dragic, T., Trkola, A., Lin, S.W., Nagashima, K.A., Kajumo, F., Zhao, L., Olson, W.C., Wu, L., Mackay, C.R., Allaway, G.P., Sakmar, T.P., Moore, J.P., and **Maddon, P.J.** (1998). N-terminal substitutions in the CCR5 co-receptor impair gp120 binding and HIV-1 entry. J. Virol. 72, 279-285.

Donzella, G.A., Schols, D., Lin, S.W., Este, J.A., Nagashima, K.A., **Maddon, P.J.**, Allaway, G.P., Sakmar, T.P., Henson, G., De Clercq, E., and Moore, J.P. (1998). AMD3100, a small molecule inhibitor of HIV-1 entry via the CXCR4 co-receptor. Nature Medicine 4, 72-77.

Gauduin, M.-C., Allaway, G.P., Olson, W.C., Weir, R., **Maddon, P.J.**, and Koup, R.A. (1998). CD4-IgG2 protects hu-PBL-SCID mice against challenge by primary HIV type 1 isolates. J. Virol. 72, 3475-3478.

Olson, W.C., Rabut, G.E.E., Nagashima, K.A., Tran, D.N.H., Anselma, D.J., Monard, S., Segal, J.P., Thompson, D.A.D., Kajumo, F., Guo, Y., Moore, J.P., **Maddon, P.J.**, and Dragic, T. (1999). Differential inhibition of human immunodeficiency virus type 1 fusion, gp120 binding, and CC-chemokine activity by monoclonal antibodies to CCR5. J. Virol. 73, 4145-4155.

Binley, J.M., Sanders, R.W., Clas, B., Schuelke, N., Master, A., Guo, Y., Kajumo, F., **Maddon, P.J.**, Olson, W.C., and Moore, J.P. (2000). A recombinant human immunodeficiency virus type 1 envelope glycoprotein complex stablized by an intermolecular disulfide bond between the gp120 and gp41 structure is an antigenic mimic of the trimeric virion-associated structure. J. Virol. 74(2), 627-643.

Jacobson, J.M., Lowy, I., Fletcher, C.V., O'Neill, T.J., Tran, D.N.H., Ketas, T.J., Trkola, A., Klotman, M.E., **Maddon, P.J.**, Olson, W.C., and Israel, R.J. (2000). Single-dose safety, pharmacology and antiviral activity of the human immunodeficiency virus (HIV) type 1 entry inhibitor PRO 542 in HIV-infected adults. J. Inf. Dis. 182, 326-329.

Shearer, W.T., Israel, R.J., Starr, S., Fletcher, C.V., Wara, D., Rathore, M., Church, J., DeVille, J., Fenton, T., Graham, B., Samson, P., Staprans, S., McNamara, J., Moye, J., **Maddon, P.J.**, and Olson, W.C. for the Pediatric AIDS Clinical Trials Group Protocol 351 Study Team (2000). Recombinant CD4-IgG2 in HIV-1 infected children: Phase I/II study. J. Inf. Dis. 182, 174-179.

Trkola, A., Ketas. T.J., Nagashima, K.A., Zhao, L., Cilliers, T., Morris, L., Moore, J.P., **Madd n, P.J.**, and Olson, W.C. (2001). Potent, broad-spectrum inhibition of human immunodeficiency type 1 virus (HIV-1) by the CCR5 monoclonal antibody PR 140. J. Virol. 75(2), 579-588.

0022-1767/85/1355-3564$02.00/0
The Journal of Immunology

Vol. 135, No. 5, November 1985
Printed in U.S.A.

A HUMAN-MOUSE CHIMERIC IMMUNOGLOBULIN GENE WITH A HUMAN VARIABLE REGION IS EXPRESSED IN MOUSE MYELOMA CELLS[1]

LEE K. TAN,* VERNON T. OI,† AND SHERIE L. MORRISON[2]*

*From the *Department of Microbiology and the Cancer Center/Institute for Cancer Research, Columbia University College of Physicians and Surgeons, New York, NY 10032; and the †Becton-Dickinson Monoclonal Center, Mountain View, CA 94040*

We have constructed and obtained expression of a chimeric human-mouse immunoglobulin gene after transfection into mouse myeloma cells. A human VDJ_H gene segment was joined to a mouse C_γ gene in the plasmid vector pSV2-gpt, and the construct was transfected into J558L cells by protoplast fusion. Analyses of six transformants by RIA and SDS-PAGE indicated that the chimeric protein was synthesized in large amounts in five. A κ-specific transcript was observed by Northern blot analysis. Four out of five clones were stable producers of this chimeric chain over a period of 10 mo.

The technique of introducing cloned genes into eukaryotic cells has been widely used as a tool to study gene regulation and expression. Such studies on eukaryotic gene expression were initially conducted in heterologous host cells, particularly in human HeLa cells and mouse L cells that normally do not express the gene of interest (1–4). More recently, with the understanding that normal expression of specialized genes probably requires tissue-specific factors and regulatory elements, and with the availability of appropriate cell lines, immunoglobulin (Ig) genes have been transfected into the cell types that normally express them (5–9). Homologous cell types should, in addition, provide the appropriate protein modification systems necessary to make biologically functional products.

With the availability of appropriate expression systems, it is now feasible to produce novel Ig molecules. These molecules may consist either of a heavy and light chain combination not normally synthesized within the same cell or of Ig chains with a novel structure produced in vitro. In initial studies by Oi et al. (10), a novel chain combination resulted when a transfected light chain assembled with the endogenous heavy chain. Transfection of both heavy and light chain genes into the same cell was shown to result in the production of an anti-TNP Ig molecule (11). In previous studies, we constructed a chimeric gene with V_H from an anti-azophenylarsonate myeloma joined to C_γ. When introduced into a light chain-producing variant of the same myeloma, this hybrid chain was synthesized and assembled with the endogenous light chain to produce a heterodimer that bound antigen (12). In additional studies, we constructed chimeric genes where V_L from mouse was joined to C_γ of human and V_H from mouse was joined to $C_{\gamma 1}$ or $C_{\gamma 2}$ of human (13). When the heavy and light chain were expressed together in the same cell, a chimeric Ig was produced with the specificity of mouse origin and the constant regions, and hence effector function, of human origin.

In all of these constructions described above, the Ig genes were introduced into mouse cells, and the promoter region that directed the synthesis of the Ig was of mouse origin. Potter et al. (9) recently reported the expression of a cloned human κ Ig gene transfected into mouse pre-B lymphocytes. Their studies demonstrate that a human Ig L chain promoter can function in a mouse lymphocyte. In this paper, we describe the expression in mouse cells of a hybrid gene that utilizes the human heavy chain promoter. A V_H of human origin was joined to C_γ from mouse. When the chimeric gene was introduced into a mouse myeloma, it resulted in the high level production of a chimeric protein of about 25,000 daltons. These experiments show that during mRNA processing V_H of human is spliced to C_γ of mouse so that the correct reading frame is preserved. Even more importantly, they demonstrate that the human Ig heavy chain promoter functions in the mouse myeloma cells and show the feasibility of expressing human Ig genes in mouse cells. Thus, it should be possible to use mouse myeloma cells to produce Ig molecules with the V region of human origin; potentially it should also be possible to use the mouse myeloma cells to rescue Ig genes from human lymphoblastoid cells where they are expressed at low levels, and achieve a high level of expression of the genes by introducing them into mouse myeloma cells.

MATERIALS AND METHODS

Construction of the chimeric gene with V_H from human and C_γ from mouse. The plasmid vector pSV2-gpt has been described (14). The vector contains the simian virus 40 origin of DNA replication (SV40 ori) and the early promoter located 5′ of the *E. coli* xanthine-guanine phosphoribosyl transferase (Eco-gpt)[3] gene. This gene confers resistance to mycophenolic acid on mammalian cells when xanthine is present in the medium. The plasmid pSV2-S107-21 has the rearranged phosphorylcholine-specific κ-chain gene from the S107 cell line cloned into the Bam HI site in pSV2-gpt (10). To construct the chimeric light chain, the EcoR1-Hind III fragment from pSV2-S107-21 containing the S107 V_γ gene was replaced by a

Received for publication February 25, 1985.
Accepted for publication August 2, 1985.
The costs of publication of this article were defrayed in part by the payment of page charges. This article must therefore be hereby marked *advertisement* in accordance with 18 U.S.C. Section 1734 solely to indicate this fact.
[1] This work was supported in part by Grants KO4 AI 00408, AI 19042, CA 16858, CA 22736, and CA 13696 from the National Institutes of Health and Grant IMS-360 from the American Cancer Society.
[2] Address correspondence to: Dr. Sherie L. Morrison, Department of Microbiology, Columbia University College of Physicians and Surgeons, 701 West 168th St., New York, NY 10032.

[3] Abbreviations used in this paper: DME, Dulbecco's modified Eagle's medium; Eco-gpt, xanthine-guanine phosphoribosyl transferase; IMD, Iscove's modified Dulbecco's medium; VTL, valine, threonine, leucine.

EcoR1-Hind III fragment containing a productively rearranged human VDJ_H gene (15) producing phV-mC$_\kappa$, shown in Figure 1. The mouse κ gene enhancer sequences 3' of the Hind III site are intact (16, 17). The chimeric gene is oriented so that the direction of transcription is opposite to that from the SV40 promoter. The V_H clone was a gift from T. Honjo, Osaka University, Japan.

Cell lines. The S107 BALB/c myeloma line synthesizing an IgA, κ protein specific for phosphorylcholine was acquired from M. D. Scharff, Albert Einstein College of Medicine, Bronx, NY. J558, a BALB/c mouse myeloma cell line synthesizing IgA, λ with specificity for $\alpha(1 \rightarrow 3)$-dextran was adapted to continuous growth in tissue culture in our laboratory (18). J558L is a spontaneous heavy chain-loss-variant of J558, which synthesizes and secretes only the λ light chain (10). Cell lines were maintained in Iscove's modified Dulbecco's (IMD) medium (GIBCO Laboratories, Grand Island, NY) supplemented with 10 to 20% horse serum. Before fusion, cells were grown in Dulbecco's modified Eagle's (DME) medium (GIBCO) supplemented with 10% horse serum. Cells were grown in suspension cultures in petri dishes at 37°C in a water-saturated atmosphere of 5% CO_2 and 95% air.

Protoplast fusion. The plasmid phV-mC$_\kappa$ was transfected into *Escherichia coli* K12 strain HB101. Bacteria harboring this plasmid were converted to protoplasts and fused to J558L cells according to the procedure described by Oi et al. (10) with the following modifications. We used 3×10^8 cells and supplemented DME growth medium with 10% horse serum. After protoplast fusion, cells were resuspended in IMD medium containing 20% horse serum and garamycin (100 μg/ml) and plated in 96-well microtiter plates at a density of 2×10^4 cells/well. After 48 hr, transformants were selected in IMD medium containing xanthine at 250 μg/ml, hypoxanthine at 15 μg/ml, and mycophenolic acid at 3 μg/ml. Eleven transformants were recovered and were designated TAF 1 through 11.

Biosynthetic radiolabeling. Transfected J558L cells (3×10^6) were labeled for 3 hr in the presence of 5 to 10 μCi/ml of [^{14}C]-valine, threonine, leucine (VTL) as described (19). Ig were precipitated with specific rabbit antiserum directed against mouse κ or λ light chains. Hyperimmune rabbit anti-mouse κ antiserum was the gift of M. D. Scharff, Albert Einstein College of Medicine, Bronx, NY, and the rabbit antiserum to mouse λ myeloma protein was prepared in our laboratory by Letitia A. Wims. The soluble rabbit anti-mouse Ig complexes were absorbed to inactivated and formalin-fixed *Staphylococcus aureus* (75 μl/2.5 μl of antiserum) (IgG sorb: Enzyme Center, Malden, MA). The precipitated material was prepared for analysis by electrophoresis in 5% SDS-polyacrylamide gel containing phosphate, under nonreducing conditions, as described (18).

Competitive radioimmunoassay (RIA). Cells (1×10^7) were washed once with ice-cold phosphate-buffered saline (PBS: 0.15 M NaCl, 0.01 M sodium phosphate, pH 7.6) and centrifuged; the pellet was resuspended in 100 μl of PBS in an Eppendorf tube. The cells were lysed by twice freezing in liquid nitrogen and subsequent thawing at 37°C. The suspension was spun at 13,000 × G for 15 min at 4°C, and the supernatant was obtained.

Two rat hybridomas, 187.1 (20) and 226.3.5 (20), producing monoclonal antibodies to mouse κ protein were biosynthetically labeled with ^{14}C-VTL as described above. Freeze-thaw lysates from the transfectants as well as J558L and S107 were analyzed to determine if they could compete out the binding of a mixture of the two labeled rat anti-mouse κ monoclonal antibodies (1:1) to mouse myeloma $\gamma_{3\kappa}$ protein adsorbed onto the wells of polystyrene hemagglutination plates. The $\gamma_{3\kappa}$ protein was from a mouse hybridoma P51.2 made by C. Desaymard. The two rat hybridomas 187.1 and 226.3.5 and the $\gamma_{3\kappa}$ protein were the gifts of M. D. Scharff, Albert Einstein College of Medicine, Bronx, NY.

RNA isolation and gel analysis. Total cytoplasmic RNA was isolated from 5×10^7 cells and fractionated by electrophoresis on formaldehyde-agarose gels as described (21). RNA was blotted to nitrocellulose filters and hybridized at 42°C to a nick-translated mouse κ cDNA probe by following the procedure of Thomas (22).

DNA isolation and analysis. High m.w. DNA was isolated from the myeloma cells essentially as described by Wigler et al. (23) except that lysates were treated with RNase (50 μg/ml, 30 min at 37°C) before the pronase treatment. Ten micrograms of each DNA were digested with various restriction endonucleases under the conditions specified by the supplier (New England Biolabs, Beverly, MA). Digestions were performed at an enzyme to DNA ratio of 4 U/μg at 37°C for 5 hr. The DNA was then electrophoresed on horizontal 0.5% agarose slab gels in 40 mM Tris-acetate and 2 mM EDTA (pH 8.0), with either Hind III-digested λCI857 or pTKB$_{25}$ DNA as size markers. The plasmid pTKB$_{25}$ was the generous gift of Saul Silverstein. DNA fragments were transferred to nitrocellulose filters, hybridized, and washed according to the protocol described by Maniatis et al. (24) but with the following modifications. SDS and Denhardt's were omitted from the hybridization solution. We used 2×10^6 cpm of denatured probe per 10 μg of DNA, and hybridization was performed at 65°C for 16 hr. The filters were washed twice in 2× SSC/0.1% SDS followed by another two times in 1× SSC/0.1% SDS, at 65°C, allowing 20 to 30 min per wash. The EcoR1-Hind III fragment isolated from phV-mC$_\kappa$ (Fig. 1) was nick translated as described (25) except that 2 μM each of cold dGTP, dATP, dTTP, and ^{32}P-labeled dCTP were used. This labeled fragment served as a V region-specific probe.

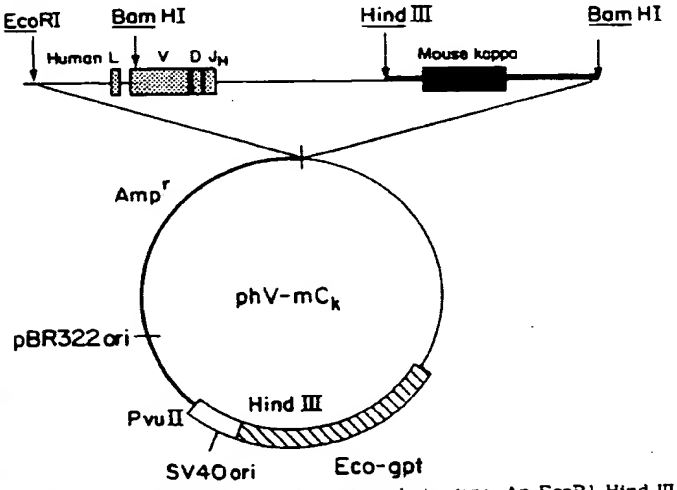

Figure 1. Structure of the chimeric κ chain gene. An EcoR1-Hind III fragment containing a rearranged human heavy chain variable region gene (VDJ_H) was joined to a mouse κ constant region gene from the S107 myeloma cell line. The hybrid chain is cloned in the plasmid vector pSV2-gpt. The human gene segment is represented by stippled boxes and thin lines; the mouse κ exon, intron, and flanking 3' sequences are represented by the solid box and thick lines. The entire insert from EcoR1 to Bam H1 is 7.4 kilobases (kb). The vector sequences total 4.3 kb.

RESULTS

Protoplast fusion yielded 11 independent gpt transformants that survived mycophenolic acid selection. Six of these clones were analyzed for the expression of the chimeric κ gene by competitive RIA. Cytoplasmic lysates from five out of six clones were able to inhibit the binding of [^{14}C]-VTL labeled rat anti-mouse κ monoclonal antibodies to $\gamma_{3\kappa}$ bound to polystyrene plates (results not shown). Lysates from transfectant TAF 6 and from J558L were not inhibitory. The level of inhibition was between 33 and 66% of that obtained with the lysate from the S107 cell line from which the κ gene was derived. Thus, the transfected cell lines contain approximately half as much cytoplasmic κ chain as does the myeloma, as determined by this assay.

Figure 2 shows the results of a 3-hr labeling of cytoplasmic proteins from the six transformants. The anti-mouse κ antiserum precipitated a protein that co-migrated with the S107 κ chain. A similar band was absent from TAF 6 (lane 5) which showed no competition for binding to anti-κ antibodies by RIA. The level of κ expression from the five positive transformants, as estimated by band intensity, ranged from 8 to 20% of that seen in the S107 cell line. The chimeric κ protein was not immunoprecipitated from the culture medium in which the cells were grown, indicating that the protein accumulates in the cytoplasm but is not secreted. The κ chain does not associate with the endogenous λ light chain either covalently or noncovalently, because anti-mouse λ antiserum failed to precipitate the chimeric protein.

To determine the stability of expression of the transfected Ig genes, clones frozen in liquid nitrogen were

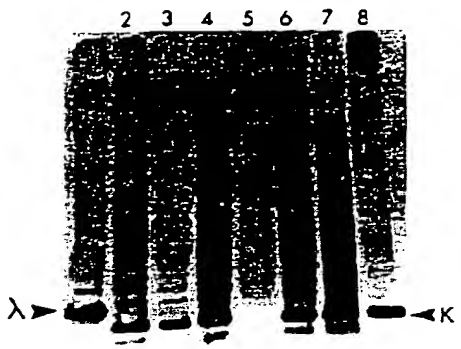

Figure 2. SDS-PAGE analysis of immunoprecipitates obtained from the cytoplasm of 3 × 10^6 cells labeled for 3 hr with [^{14}C]-VTL. The immunoprecipitated material was suspended in 50 μl of sample buffer, and the volumes indicated were applied to a 5% SDS-polyacrylamide gel. Cells transfected with phV-mC$_\kappa$ are designated TAF. Lane 1: 10 μl from J558L (λ) cells immunoprecipitated with rabbit anti-mouse λ antiserum; lanes 2–7: 25 μl each from TAF 2, 3, 4, 6, 9, 10; lane 8: 10 μl from S107 (α, κ). The transfectants and the S107 cells were immunoprecipitated with rabbit anti-mouse κ antiserum. The positions of the J558L λ and S107 κ light chains are indicated.

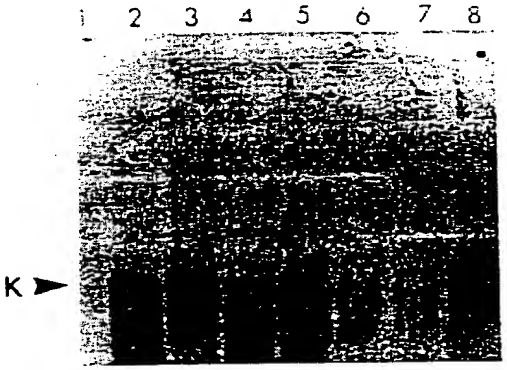

Figure 3. Northern gel analysis of transfected cell RNA. Total cell cytoplasmic RNA was electrophoresed on a formaldehyde-agarose gel, transferred onto nitrocellulose filter, and hybridized to nick-translated C$_\kappa$ probe. Lane 1: J558L (4 μg of RNA); lane 2: S107 (4 μg of RNA); lanes 3–8: TAF 2, 3, 4$^+$, 4$^-$, 6, 10 (10 μg of RNA each). The position of the κ mRNA is indicated.

thawed and the labeling experiment was repeated 4 mo later. Only one clone, TAF 4, ceased to synthesize the chimeric κ chain (results not shown). TAF 4$^+$ designates the clone that initially synthesized the chimeric protein; TAF 4$^-$ designates the nonproducer derivative.

To determine the size of the κ-specific mRNA in the transfectants, Northern blot analysis of total cytoplasmic RNA was performed as described in *Materials and Methods*, and the results are shown in Figure 3. TAF 2, 3, 4$^+$, and 10 (lanes 3–5, 8) show a band that hybridized with ^{32}P-labeled C$_\kappa$ probe. This κ transcript is of the same size as the κ mRNA in the S107 myeloma. The κ transcript is missing from the control untransformed J558L RNA (lane 1), TAF 4$^-$, and TAF 6 (lanes 6, 7). TAF 4$^-$ RNA was prepared 4 mo after the TAF 4$^+$ batch (from the same clone), when it was noted that the clone had lost synthesis of the chimeric protein. To confirm that the RNA in lanes 6 and 7 were not degraded, the κ probe was eluted from the blot, which was then rehybridized with a ^{32}P-λ cDNA fragment. J558L and all six transformants were positive for a λ-specific transcript (results not shown).

Southern blot analyses of genomic DNA from the transformants show that each transfectant has a different pattern of integration (Fig. 4). In TAF 10 (lane 6) the

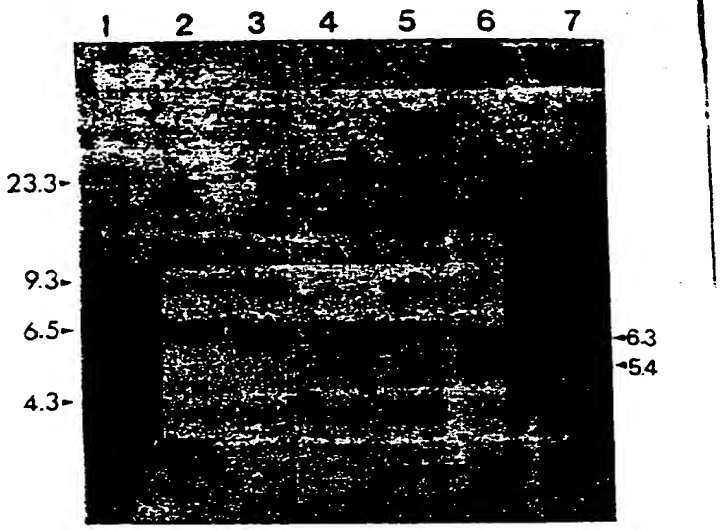

Figure 4. High m.w. DNA (10 μg per lane) was digested to completion with Bam HI, fractionated on a 0.5% agarose gel, transferred onto nitrocellulose membrane filter, and hybridized to the nick-translated EcoR1-Hind III fragment containing the human V region gene (Fig. 1). Lanes 1–6: TAF 2, 3, 4$^+$, 4$^-$, 6, 10; lane 7: 22 pg phV-mC$_\kappa$. The positions of the Hind III-digested λCI857 DNA size markers are shown on the left. The two fragments obtained by Bam H1 digestion of pHV-mC$_\kappa$ are indicated on the right. The 5.4-kb fragment contains the pSV2-gpt sequences.

transfected gene appears present as multiple concatameric copies. Integrated gene copies were lost when TAF 4 ceased production of the chimeric Ig (compare lanes 3 and 4). Under the hybridization conditions used, no hybridization was seen with J558L genomic DNA.

DISCUSSION

In this paper we show that it is possible to obtain high level expression from a human heavy chain promoter of a human-mouse chimeric κ chain gene after transfection of mouse myeloma cells. Expression was stable up to at least 10 mo. Unlike the previously described V$_H$C$_\kappa$ chimeric protein where V$_H$ was of mouse origin, the hybrid protein was not secreted. This difference is not unexpected: many mouse κ chains are not secreted in the absence of heavy chains (10, 26, 27). The hybrid protein also failed to assemble either covalently or noncovalently with the endogenous λ chain produced by the recipient myeloma.

Several groups of investigators have reported successful expression of κ genes transfected into myelomas or hybridomas (10, 28–30), but the level of expression is generally low, about 1/15 of that observed in the parent cell line from which the gene was derived. This is in contrast to transfection experiments with heavy chain (H) genes like γ2b (31), α (32), and μ (11), where large quantities of heavy chain protein can be produced. Several explanations for this difference are possible, among which is that the L and H chain promoters have different strengths, or that the H and L chain enhancer regions are more or less effective. Studies have suggested that the L chain enhancer is less effective than the H chain enhancer (16, 33). It is not yet possible to define which elements of the chimeric gene described here are necessary for its efficient expression. The promoter is from a heavy chain. The genes are fused so that an enhancer from the mouse κ chain is included. However, because th human heavy chain enhancer has not been identi-

fied, it is possible that it is also present in the construction.

In their studies, Potter et al. (9) recently demonstrated that human Ig L chain promoter can function in mouse lymphocytes. Our current studies demonstrate that the human Ig heavy chain promoter is also functional in a mouse myeloma cell, and so is not species specific. In addition, our studies demonstrate that it is possible to construct a chimeric gene where V_H from human is joined to C_κ of mouse. Furthermore, the chimeric intron is spliced out to yield an appropriate κ size mature mRNA molecule. The splicing is carried out by using the human splice donor sequences at J_H and the mouse splice acceptor site and recognition sequences in C_κ to yield a mature mRNA with an in-phase reading frame.

The ability to express Ig molecules after gene transfection has many potential applications. Because human promoters will effectively function in mouse cells, it is potentially possible to transfer human genes from cell lines, where they are poorly expressed, to mouse myeloma cells, where they are efficiently expressed. Gene transfection may be a feasible alternative to hybridoma methodology for the production of human monoclonal antibodies. In addition, the ability to create novel Ig molecules by reassortment of V and C regions and in vitro exon shuffling should facilitate studies on the requirements for antibody function.

REFERENCES

1. Mantei, N., W. Ball, and C. Weissman. 1979. Rabbit β-globin mRNA production in mouse L cells transformed with cloned rabbit β-globin chromosomal DNA. *Nature 281:40.*
2. Wold, B., M. Wigler, E. Lacy, T. Maniatis, S. Silverstein, and R. Axel. 1979. Introduction and expression of a rabbit β-globin gene in mouse fibroblasts. *Proc. Natl. Acad. Sci. USA 76:5684.*
3. Mellon, P., V. Parker, Y. Gluzman, and T. Maniatis. 1981. Identification of DNA sequences required for transcription of the human α1-globin gene in a new SV40 host-vector system. *Cell 27:279.*
4. Mantei, N., and C. Weissman. 1982. Controlled transcription of a human α-interferon gene introduced into mouse L cells. *Nature 297:128.*
5. Falkner, F. G., and H. G. Zachau. 1982. Expression of mouse immunoglobulin genes in monkey cells. *Nature 298:286.*
6. Picard, D., and W. Schaffner. 1983. Correct transcription of a cloned mouse immunoglobulin gene *in vivo*. *Proc. Natl. Acad. Sci. USA 80:417.*
7. Stafford, J., and C. Queen. 1983. Cell-type specific expression of a transfected immunoglobulin gene. *Nature 306:77.*
8. Brinster, R. L., K. A. Ritchie, R. E. Hammer, R. L. O'Brien, B. Arp, and U. Storb. 1984. Expression of a microinjected immunoglobulin gene in the spleen of transgenic mice. *Nature 306:322.*
9. Potter, H., L. Weir, and P. Leder. 1984. Enhancer-dependent expression of human κ immunoglobulin genes introduced into mouse pre-B lymphocytes by electroporation. *Proc. Natl. Acad. Sci. USA 81:7161.*
10. Oi, V. T., S. L. Morrison, L. A. Herzenberg, and P. Berg. 1983. Immunoglobulin gene expression in transformed lymphoid cells. *Proc. Natl. Acad. Sci. USA 80:825.*
11. Ochi, A., R. G. Hawley, T. Hawley, M. J. Schulman, A. Traunecker, G. Kohler, and N. Hozumi. 1983. Functional immunoglobulin M production after transfection of cloned immunoglobulin heavy and light chain genes into lymphoid cells. *Proc. Natl. Acad. Sci. USA 80:6351.*
12. Sharon, J., M. L. Gefter, T. Manser, S. L. Morrison, V. T. Oi, and M. Ptashne. 1984. Expression of a V_HC_κ chimeric protein in mouse myeloma cells. *Nature 309:364.*
13. Morrison, S. L., M. J. Johnson, L. A. Herzenberg, and V. T. Oi. 1984. Chimeric human antibody molecules: mouse antigen-binding domains with human constant region domains. *Proc. Natl. Acad. Sci. USA 81:6851.*
14. Mulligan, R. C., and P. Berg. 1981. Selection for animal cells that express the *Escherichia coli* gene coding for xanthine-guanine phosphoribosyl transferase. *Proc. Natl. Acad. Sci. USA 78:2072.*
15. Johnson, M. J., A. M. Natali, H. M. Cann, T. Honjo, and L. L. Covalli-Sforza. 1984. Polymorphisms of a human variable heavy chain gene show linkage with constant heavy chain genes. *Proc. Natl. Acad. Sci. USA 81:7840.*
16. Picard, D., and W. Schaffner. 1984. A lymphocyte-specific enhancer in the mouse immunoglobulin κ gene. *Nature 307:80.*
17. Queen, C., and J. Stafford. 1984. Fine mapping of an immunoglobulin gene activator. *Mol. Cell. Biol. 4:1042.*
18. Matsuuchi, L., L. A. Wims, and S. L. Morrison. 1981. A variant of the dextran-binding mouse plasmacytoma J558 with altered glycosylation of its heavy chain and decreased reactivity with polymeric dextran. *Biochemistry 20:4827.*
19. Morrison, S. L. 1979. Sequentially derived mutants of the constant region of the heavy chain of murine immunoglobulins. *J. Immunol. 123:793.*
20. Yelton, D. E., C. Desaymard, and M. D. Scharff. 1981. Use of monoclonal anti-mouse immunoglobulin to detect mouse antibodies. *Hybridoma 1:5.*
21. Matsuuchi, L., and S. L. Morrison. 1982. Isolation and characterization of a variant of mouse plasmacytoma J558 synthesizing a 110,000 dalton immunoglobulin heavy chain and of secondary variants synthesizing either a 55,000 dalton or an 80,000 dalton immunoglobulin heavy chain: possible implications. *Mol. Cell. Biol. 2:1134.*
22. Thomas, P. S. 1980. Hybridization of denatured RNA and small DNA fragments transferred to nitrocellulose. *Proc. Natl. Acad. Sci. USA 77:5201.*
23. Wigler, M., R. Sweet, G. K. Sim, B. Wold, A. Pellicer, E. Lacy, T. Maniatis, S. Silverstein, and R. Axel. 1979. Transformation of mammalian cells with genes from procaryotes and eukaryotes. *Cell 16:777.*
24. Maniatis, T., E. Fritsch, and J. Sambrook. 1982. Southern transfer. In *Molecular Cloning. A Laboratory Manual.* Cold Spring Harbor Laboratory, Cold Spring Harbor, NY. P. 382.
25. Weinstock, R., R. Sweet, M. Weiss, H. Cedar, and R. Axel. 1978. Intragenic DNA spacers interrupt the ovalbumin gene. *Proc. Natl. Acad. Sci. USA 75:1299.*
26. Margulies, D. H., W. M. Kuehl, and M. D. Scharff. 1976. Somatic cell hybridization of mouse myeloma cells. *Cell 8:405.*
27. Köhler, G., S. L. Howe, and C. Milstein. 1976. Fusion between immunoglobulin secreting and nonsecretory myeloma cell lines. *Eur. J. Immunol. 6:292.*
28. Rice, D., and D. Baltimore. 1982. Regulated expression of an immunoglobulin κ gene introduced into a mouse lymphoid cell line. *Proc. Natl. Acad. Sci. USA 79:7862.*
29. Stafford, J., and C. Queen. 1983. Cell type specific expression of a transfected immunoglobulin gene. *Nature 306:77.*
30. Ochi, A., R. G. Hawley, M. J. Schulman, and N. Hozumi. 1983. Transfer of a cloned immunoglobulin light-chain gene to mutant hybridoma cells restores specific antibody production. *Nature 302:340.*
31. Gillies, S. D., S. L. Morrison, V. T. Oi, and S. Tonegawa. 1983. A tissue-specific transcription enhancer element is located in the major intron of a rearranged immunoglobulin heavy chain gene. *Cell 33:717.*
32. Deans, R. J., K. A. Denis, A. Taylor, and R. Wall. 1984. Expression of an immunoglobulin heavy chain gene transfected into lymphocytes. *Proc. Natl. Acad. Sci. USA 81:1292.*
33. Bergman, Y., D. Rice, R. Grosschedl, and D. Baltimore. 1984. Two regulatory elements for κ immunoglobulin gene expression. *Proc. Natl. Acad. Sci. USA 81:7041.*

Proc. Natl. Acad. Sci. USA
Vol. 80, pp. 825–829, February 1983
Immunology

Immunoglobulin gene expression in transformed lymphoid cells

(*gpt*/transformation)

VERNON T. OI*, SHERIE L. MORRISON†, LEONARD A. HERZENBERG*, AND PAUL BERG‡

Departments of *Genetics and †Biochemistry Stanford University School of Medicine, Stanford, California 94305; and ‡Department of Microbiology and the Cancer Center, Institute of Cancer Research, College of Physicians and Surgeons of Columbia University, New York, New York 10032

Contributed by Leonard A. Herzenberg, October 15, 1982

ABSTRACT Myeloma, hybridoma, and thymoma cell lines have been successfully transfected for the *Escherichia coli* xanthine-guanine phosphoribosyltransferase gene (*gpt*) by using the plasmid vector pSV2-gpt. The transformed cells synthesize the bacterial enzyme 5-phospho-α-D-ribose-1-diphosphate:xanthine phosphoribosyltransferase (XGPRT; EC 2.4.2.22) and have been maintained in selective medium for over 4 months. Lymphoid cell lines expressing a κ immunoglobulin light chain were obtained by transfecting cells with pSV2-gpt containing a rearranged κ light chain genomic segment from the S107 myeloma cell line. The S107 light chain is synthesized in gpt-transformed J558L myeloma cells and is identical to the light chain synthesized by the S107 myeloma cell line, as judged by immunoprecipitation and two-dimensional gel electrophoresis. Furthermore, this light chain is synthesized and secreted as part of an intact antibody molecule by transformed hybridoma cells that normally secrete an IgG1 (γ,κ) antibody molecule. No light chain synthesis was detected in a similarly transformed rat myeloma or a mouse thymoma line.

Techniques to introduce novel genes into eukaryotic cells provide a powerful tool to study mechanisms of gene regulation and expression. Most studies on eukaryotic gene expression have been conducted in heterologous host cells—i.e., genes have been transfected into cell types (particularly human HeLa and mouse L cells) that normally do not express the gene of interest (1–3). Though a great deal has been learned about eukaryotic regulator sequences with these gene transfer experiments, it would be preferable to transfer genes encoding proteins expressed during differentiation back into the cell type that normally expresses the genes of interest. The appropriate cell type provides protein modification systems, such as glycosyltransferases, necessary to make fully biological functional products. In addition, the appropriate cell type may be used to study tissue-specific regulation of gene expression.

To undertake studies of (*i*) the regulation and expression of immunoglobulin genes, (*ii*) the biosynthesis, chain-assembly, and secretion of immunoglobulin heavy and light chains, and (*iii*) structure–function correlates of antibody molecules, we have explored techniques for transfection of lymphoid cells using the pSV2-gpt vector (4, 5). This DNA can express the *Eco gpt* gene encoding xanthine-guanine phosphoribosyltransferase (XGPRT; 5-phospho-α-D-ribose-1-diphosphate:xanthine phosphoribosyltransferase, EC 2.4.2.22). Cells synthesizing XGPRT can be grown with xanthine as the sole precursor of guanine nucleotide formation (4, 5). Successfully transformed cells can be isolated by their ability to grow in medium containing xanthine and mycophenolic acid, an inhibitor of guanine nucleotide synthesis; if the transformed cell line is hypoxanthine phosphoribosyltransferase-negative (HPRT⁻; IMP pyrophosphate phosphoribosyltransferase, EC 2.4.2.8), transformants can be selected in hypoxanthine/aminopterin/thymidine (HAT) medium (6). In the present experiments both calcium phosphate precipitation (7, 8) and protoplast fusion (9) techniques have been used to transfect cells.

pSV2-gpt containing a rearranged κ light chain gene (10) was used to transform several cultured lymphoid cell lines. Among the gpt transformants were clones that produce a new immunoglobulin light chain. The light chain produced by these transformed cell lines appears to be identical to the light chain synthesized by the myeloma cell from which the rearranged gene was isolated. Furthermore, in transformed hybridoma cells, this light chain is assembled with an immunoglobulin heavy chain and secreted as a complete antibody molecule.

MATERIALS AND METHODS

Cell Lines. J558L is a spontaneous heavy chain-loss-variant myeloma cell line obtained from the J558 cell line [α,λ; anti-α1-3 dextran (11)] that synthesizes and secretes a λ light chain. Y3-Ag1.2.3 is a HPRT⁻ rat myeloma cell line originally described by Galfre *et al.* (12) that synthesizes and secretes a rat κ light chain. 27-44 is a HPRT⁻ mouse IgG1 anti-dansyl hybridoma cell line (13); and BW5147 is a HPRT⁻, ouabain^r AKR thymoma originally described by Hyman and Stallings (14). Cell lines were maintained in either 10% newborn calf serum in Dulbecco's modified minimal essential medium (DME medium) or 10% fetal calf serum in alpha modified minimal essential medium.

Recombinant DNA Vectors. The plasmid vector pSV2-gpt has been described (4, 5). Fig. 1 shows a partial restriction enzyme map of this vector. A second vector, which is derived from pSV2-gpt, but contains the herpes simplex thymidine kinase promoter inserted 5′ of the *gpt* gene, was constructed by J.-F. Nicolas (unpublished data). pSV2-S107 was constructed by inserting a *Bam*HI fragment containing the entire rearranged phosphocholine-specific κ chain gene from the S107 myeloma cell line (10) into the unique *Bam*HI site in pSV2-gpt. The light chain gene is oriented so that the direction of transcription is opposite to the *gpt* gene (Fig. 1). The genomic rearranged S107 κ light chain DNA was a gift from M. Scharff.

Transfection by Protoplast Fusion. Protoplasts were prepared essentially as described by Sandri-Goldin *et al.* (9). *Escherichia coli* K-12 strain HB101, containing the appropriate plasmid, was grown at 37°C in Luria broth containing 1% glucose to an absorbance at 600 nm of 0.6–0.8. Chloramphenicol was added to 125 μg/ml, the culture was incubated at 37°C for 12–16 hr to amplify the plasmid copy number, and the cells were harvested by centrifugation. For every 25 ml of culture, 1.25 ml of chilled 20% sucrose/0.05 M Tris·HCl (pH 8) was added;

The publication costs of this article were defrayed in part by page charge payment. This article must therefore be hereby marked "*advertisement*" in accordance with 18 U. S. C. §1734 solely to indicate this fact.

Abbreviations: XGPRT, xanthine-guanine phosphoribosyltransferase; HPRT, hypoxanthine phosphoribosyltransferase; HAT, hypoxanthine/aminopterin/thymidine; DME medium, Dulbecco's modified minimal essential medium.

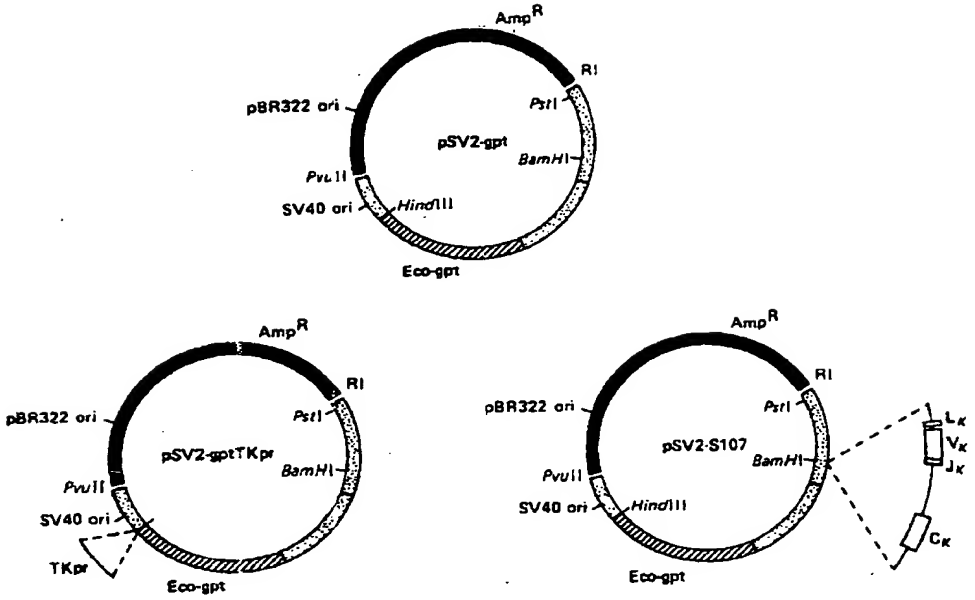

FIG. 1. Structure of the vectors used for lymphoid cell transformations. The diagram of the parental pSV2-gpt plasmid vector was taken from Mulligan and Berg (4, 5): pBR322 DNA is represented by the solid black lines and the plasmid's DNA replication origin and β-lactamase gene are indicated; the *gpt* gene sequence is represented by the hatched segments; simian virus 40 (SV40) sequences are the stippled segments. The SV40 origin of DNA replication (ori) and early promoter are located 5′ of the *gpt* sequences. pSV2-gptTKpr has an insertion of 250 base pairs, containing the herpes simplex thymidine kinase promoter, between the *gpt* gene and the SV40 early promoter (unpublished data). pSV2-S107 has a 7-kilobase *Bam*HI fragment, containing the entire genomic S107 light chain gene, inserted into the unique *Bam*HI site of pSV2-gpt. This rearranged light chain gene is oriented in the opposite direction to *gpt* and contains the leader, V, and κ constant region exons as well as flanking 5′ and 3′ sequences.

the bacteria were suspended and 0.25 ml of lysozyme [a freshly prepared solution of 5 mg/ml in 0.25 M Tris·HCl (pH 8)] was added. After 5 min of incubation on ice, 0.5 ml of 0.25 M EDTA (pH 8) was added and incubation on ice was continued for an additional 5 min. After addition of 0.5 ml of 0.05 M Tris·HCl (pH 8), the bacteria were transferred to a 37°C water bath and were incubated for 10 min. At this time examination of the bacteria with a phase-contrast microscope showed that the vast majority had been converted to protoplasts. The bacteria were diluted with 10 ml of DME medium containing 10% sucrose and 10 mM $MgCl_2$ that was warmed to 37°C. After further incubation for 10 min at room temperature the protoplasts were ready for fusion.

Fusion of protoplasts with suspension cells was effected with a procedure normally used in the production of hybridomas (15). Cell lines were grown to a density of $0.3–1 \times 10^6$ cells per ml in DME medium supplemented with 10% newborn calf serum. Five milliliters of the protoplast suspension was added to 2×10^6 cells in growth medium. The mixture was centrifuged for 5 min at room temperature at approximately 500 × g. The supernate was aspirated and the pellet was resuspended gently in 2 ml of a polyethylene glycol solution [50 g of polyethylene glycol 1,500 (BDH) in 50 ml of DME medium] adjusted to pH 8 with CO_2. After 3 min of centrifugation at 500 × g the polyethylene glycol was diluted with 7 ml of DME medium while resuspending the pellet. After 5 min of centrifugation at 500 × g, the supernate was removed carefully and the cells were resuspended in DME medium containing 10% newborn calf serum and garamycin at 100 μg/ml and were plated either in 96-well or 24-well plates. After 48 hr, cells were diluted with an equal volume of DME medium containing xanthine at 250 μg/ml, hypoxanthine at 15 μg/ml, mycophenolic acid at 6 μg/ml, and 10% newborn calf serum. Every several days, as required, spent medium was aspirated carefully and was replaced with fresh medium containing the same supplements. Colonies of transformants were visible by 10 days. Transformants were maintained in selective medium.

Transfection by Calcium Phosphate Precipitation. Lymphoid cell lines grown in suspension were transfected by calcium phosphate precipitation as described by Chu and Sharp (7). Ten times concentrated HeBS buffer was stored at −20°C until used, whereupon it was diluted to two times concentrated and adjusted to pH 7.05. Plasmid DNA (80 μg/ml) was made up in 125 mM $CaCl_2$ which was stored as a 2 M stock solution at −20°C. DNA-calcium phosphate precipitates were formed by dropwise addition of the DNA into the HeBS solution. The precipitate formed in 30 min at room temperature. The final DNA concentration was 40 μg/ml.

Cells were washed once in serum-free medium and were suspended directly in the DNA-calcium phosphate precipitate (10^6 cells per 20 μg of DNA per 0.5 ml). This suspension was incubated at 37°C for 30 min and then was diluted 1:10 in serum-containing medium. The cells were plated either into 24-well plates (2×10^5 cells per well) or 96-well plates (2×10^4 cells per well). Transfection of Y3 cells was done as described by Graham and Van der Eb (8) for adherent cell lines. The DNA-calcium phosphate precipitate was put directly onto the cell monolayer. After 30 min at 37°C, serum-containing medium was added. After 24 hr, half of the medium volume from each culture was removed and was replaced with fresh medium. On days 3, 4, 5, 8, 11, and 14, half the medium volume was removed and HAT medium was added. Transformed colonies were visible between 10 and 21 days.

Immunoprecipitations and Gel Electrophoresis. Immunoprecipitations were done with [^{35}S]methionine-labeled cell lysates and supernates. Biosynthetic labeling procedures have been described (16). Rabbit anti-mouse light chains, rabbit anti-mouse κ light chains, rabbit anti-mouse immunoglobulin, and a hybridoma anti-mouse IgG1 allotype antibody were used for immunoprecipitations. *Staphylococcus aureus*, Cowan strain I (IgGsorb; Enzyme Center, Boston) was used to coprecipitate the antigen–antibody complexes (16).

One-dimensional $NaDodSO_4$/polyacrylamide slab electrophoresis and two-dimensional nonequilibrium gradient gel electrophoresis were done as described (17). Autoradiography of polyacrylamide gels was with preflashed XAR-5 film and fluorography by using sodium salicylate (18).

RESULTS

Transfection Frequencies. The frequency at which stable transformed lymphoid cell lines were generated was influenced

by every parameter tested. Different cell lines and different vectors produced different transformation frequencies. Moreover, the two DNA delivery procedures, protoplast fusion and calcium phosphate precipitation, yielded different transformation frequencies. Tables 1 and 2 summarize the results by using protoplast fusion and calcium phosphate precipitation, respectively.

Under the present experimental conditions, BW5147 appears to be the least competent recipient of the cell lines tested, having a transformation frequency of approximately 10^{-6}. Y3 and 27-44 yielded frequencies in the range of 0.3 to $>5 \times 10^{-6}$. In the present experiments, J558L yielded the highest frequency with the range of 3×10^{-6} to $>10^{-4}$. Protoplast fusion appears on balance to be a more efficient delivery system than calcium phosphate precipitation.

A striking feature of these results is the enhanced transformation frequency for *gpt* obtained with the light chain-containing vector, pSV2-S107. This dramatic increase is evident when the pSV2-S107 vector was used with the J558L and Y3 myeloma cell lines; transformation with this recombinant was 5- to at least 10-fold greater than that obtained with the other vectors. Transformation of the hybridoma 27-44 cell line was increased only about 2-fold with pSV2-S107. The sequence(s) in the pSV2-S107 insert that is responsible for the enhanced transformation frequency must yet be mapped. Transformation of the Y3 cell line was occasionally greater with pSV2-gptTKpr than with pSV2-gpt (Table 2). Regardless of which vector was used, BW5147 transformants were detected only at very low frequencies. The amount of XGPRT activity in cell lines stably transformed by the three recombinant plasmids was not significantly different (Fig. 2 and data not shown).

XGPRT Activity. The transformed cell lines expressed the *Eco gpt* gene, as measured by the presence of XGPRT activity in the cell lysates. *E. coli* XGPRT can be distinguished from mammalian HPRT activity by its different electrophoretic mobility (4, 5). In cells selected for resistance to mycophenolic acid, both the cellular HPRT and bacterial XGPRT activities were detectable (Fig. 2). Cells lacking their own HPRT activity and selected for *gpt* in HAT medium had only the bacterial enzyme activity (Fig. 2).

Immunoglobulin Light Chain Expression. The organization of exons in the S107 genomic light chain gene is shown in Fig. 1. To produce the S107 light chain protein from this gene, two introns must be processed from the primary mRNA transcripts and the leader polypeptide removed by post-translational cleavage. For secretion of the light chain as part of an intact antibody molecule, the newly synthesized light chain must fold and assemble with an immunoglobulin heavy chain to form an H_2L_2 tetramer. This also involves the formation of interchain disulfide bonds.

Table 1. Transformation of lymphoid cell lines with the pSV2-gpt vectors by using protoplast fusion

Vector	Cell line J558L		Cell line BW5147	
pSV2-gpt	21/288*	27/36†	0/76*	1/48†
pSV2-gptTKpr	10/190*	24/36†	0/80*	1/48†
pSV2-S107	186/192*	36/36†	4/96*	8/48†
	149/192‡			

Results are from three experiments and are expressed as the number of culture wells having stable transformants.
* After protoplast fusion cells were plated in 96-well culture dishes at 10^4 cells per well.
† Cells were plated at 10^5 cells per 2.0 ml of culture in 24-well dishes.
‡ Cells were plated at $5 > 10^3$ cells per well in 96-well culture dishes.

Table 2. Transformation of lymphoid cell lines with the pSV2-gpt vectors by using calcium phosphate precipitation

Vector	Cell line Y3	Cell line 27-44	Cell line BW5147
pSV2-gpt	3/48*	10/192†	1/192†
pSV2-gptTKpr	19/48*	10/192†	1/192†
pSV2-S107	47/48*	43/288†	0/192†

Results are from three experiments with the Y3 cell line and two experiments with 27-44 and BW5147 cell lines.
* Cells were plated in 24-well culture dishes at 2×10^5 cells per well.
† Cells were plated in 96-well culture dishes at 4×10^4 cells per well.

Of the four cell lines stably transformed with pSV2-S107, the J558L cell line synthesized, but did not secrete, the S107 κ light chain. However, this cell line was not expected to secrete the newly made light chains because heavy chain-loss-variants of the S107 myeloma cell line also do not secrete endogenous light chains (M. Scharff, personal communication). Transformants of the 27-44 hybridoma cell line synthesized and secreted the S107 light chain. Moreover, the S107 light chain was assembled into tetrameric H_2L_2 immunoglobulin molecules with the endogenous γ1 heavy chain and was secreted. Twelve independently transformed Y3 and seven BW5147 cell lines did not produce detectable amounts of the S107 light chain, as judged by immunoprecipitation and gel analyses. XGPRT analyses verified that these cells were, indeed, transformants.

Autoradiograms of two-dimensional polyacrylamide gels showing the apparent M_r and charge of the light chains produced by J558L and 27-44 transformants are shown in Figs. 3 and 4. The two-dimensional gel pattern of the S107 light chain synthesized by S107 myeloma cells is included to show that the transformed cell lines produced a light chain that is identical in apparent M_r and charge. The two-dimensional gel patterns also show that the leader polypeptide was removed in transformed cell lines that expressed the light chain. This indicates that proper transcription, mRNA, and protein processing occur in the transformants. Transcription of the S107 light chain gene probably occurs from its own promoter, because the light chain gene is oriented opposite to the direction of the SV40 early promoter (see Fig. 1).

The antibodies secreted by 27-44 transformants were immunoprecipitated with both hybridoma anti-IgG1 allotypic antibody and rabbit anti-mouse light chain antisera. Both reagents precipitated the S107 light chain (data not shown). Sequential precipitation, first with the hybridoma anti-IgG1 antibody and

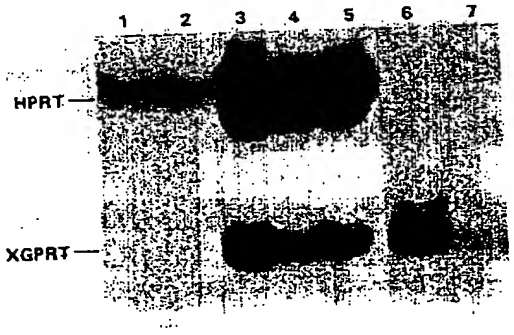

FIG. 2. XGPRT and HPRT production in transformed lymphoid cell lines. Enzyme analyses were done as described by Mulligan and Berg (4, 5). Lanes: 1 and 2, electrophoretic mobility of mammalian HPRT; 3–5, J558L cell transformants; and 6 and 7, transformants of the 27-44 cell line. Because 27-44 is a HPRT⁻ cell line, only XGPRT is present.

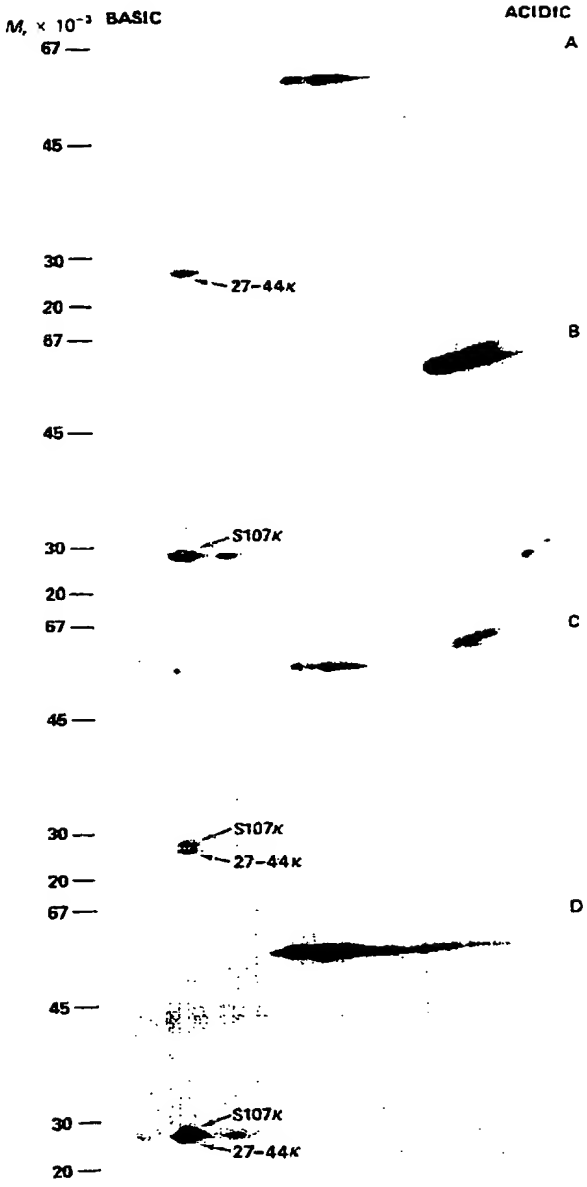

FIG. 3. S107 light chain produced by transformed 27-44 cells. Autoradiograms of two-dimensional gels of the light and heavy chains produced by parental and transformed cell lines are shown. (*A*) Parental 27-44 IgG1 anti-dansyl antibody immunoprecipitated with an anti-IgG1-specific hybridoma antibody. Both the γ1 heavy and κ light chains can be seen. (*B*) S107 IgA antibody immunoprecipitated with a rabbit anti-IgA antiserum. The α heavy chain was distinguished clearly by charge and apparent M_r from the γ1 heavy chain in *A*. (*C*) A mixture of the immunoprecipitates of *A* and *B*. The two κ light chains can be seen as distinct spots (indicated by arrows) having nearly identical charge but different apparent M_r. (*D*) Immunoprecipitate of a transformed 27-44 cell line. Only the γ1 heavy chain was present, but two light chains can be seen. In this case the amount of S107 light chain was considerably lower than in the artificial mixture shown in *C*.

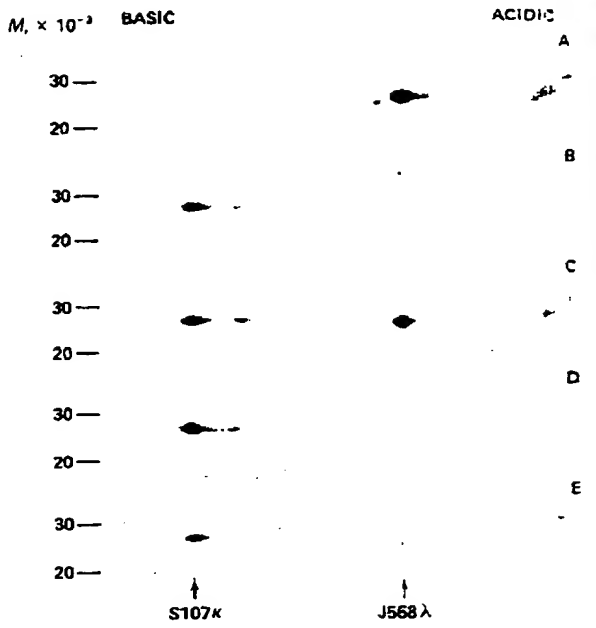

FIG. 4. S107 light chain produced by transformed J558L cells. Autoradiograms of two-dimensional gels of light chains immunoprecipitated from cell lysates of J558L transformed with pSV2-S107 DNA are shown. Because J558L does not produce a heavy chain, only the light chain portions of the two-dimensional gels are shown. (*A*) λ light chain produced by the parental J558L cell line. (*B*) S107 κ light chain. (*C*) A mixture of the two light chains. The κ and λ light chains are distinguished on the basis of both charge and apparent M_r. (*D* and *E*) Two independently derived J558L cell lines transformed with pSV2-S107 DNA. The transformant examined in *D* only appears to produce larger quantities of the S107 κ light chain than the endogenous J558 λ light chain, because the S107 κ chain is synthesized and remains in the cytoplasm, while the J558 λ chain is synthesized and secreted.

then with the rabbit anti-κ antisera, indicated that little, if any, free S107 light chain was secreted by these cells. This shows that the S107 light chain is assembled with the γ1 heavy chain into an intact antibody molecule.

Different amounts of S107 light chains were produced when a number of independent J558L and 27-44 transformants were compared. Amounts varied from barely detectable to quantities equal to endogenous light chain. This variation may be due to the chromosomal region where the light chain has integrated. It also could result from different copy number of the light chain gene in different transformants. Quite possibly, mutations or deletions of sequences needed for the expression of this gene could have occurred during transformation or subsequent to integration of the light chain sequence. Further studies are needed to determine the cause of this variation and why light chain expression does not occur in Y3 or BW5147 cell lines transformed with the same light chain gene vector.

DISCUSSION

These experiments show that it is possible to use two methods, calcium phosphate precipitation and protoplast fusion, to introduce genes into lymphoid cells. With pSV2-gpt containing the gene for an immunoglobulin light chain (pSV2-S107) both methods give rise to transformants that synthesize bacterial XGPRT and the murine light chain. Higher transformation frequencies are seen following protoplast fusion. Indeed, by using protoplast fusion and the pSV2-S107 plasmid, transformants can be obtained at a frequency of greater than 10^{-4}. Transformation frequencies are lower when using the other plasmids or calcium phosphate precipitation. Because mycophenolic acid resistance or reversion of the $HPRT^-$ phenotype do not occur spontaneously in the cell lines used, stable transformation, at even low frequencies, can be detected.

A surprising result is the increased frequency of *gpt* transformation when the S107 light chain is incorporated into the

pSV2-gpt vector. This enhancing effect occurs with both the rat and mouse myelomas. A similar increased transformation frequency has been observed with a bovine papillomavirus vector containing the human β-globin region sequences (19). At present, the mechanism for the increased transformation frequency in both cases is obscure. Possibly, the chromosomal DNA provides an origin of DNA replication, which permits the plasmid to replicate within the transformed cell and increases the transformation frequency. Transcription from the immunoglobulin promoter cannot be essential for the increased transformation frequencies because deletion of the fragments that are presumed to contain the immunoglobulin promoter region does not abolish the enhancement of transformation. It also is possible that pSV2-S107 is more efficient for transformation because of increased XGPRT production; this seems unlikely because there are no consistent differences in enzyme levels in the stable transformants obtained with either vector.

DNA-mediated gene transfer into lymphoid cells may permit a study of the regulation and expression of immunoglobulin genes in cells in which they normally are synthesized. It may be possible to examine the basis for differential immunoglobulin gene expression at different stages of lymphocyte differentiation. Cell lines in which immunoglobulin synthesis can be induced (20–22) are suitable hosts to determine if the transduced immunoglobulin genes also are responsive to those signals. Studies with cells transformed with genetic elements that are inducible by steroid hormones demonstrate that transduced DNA can respond, if the cell contains the appropriate receptors (23).

A question of central importance is what determines the utilization of various promoters and thus the synthesis of defined proteins in certain cell lines. In our experiments light chains are efficiently produced in both transformed mouse myeloma and hybridoma cell lines. However, light chain production did not occur in either a rat myeloma or a mouse thymoma. The inability of the immunoglobulin promoter to function in a different species has been reported by Falkner and Zachau (24). The lack of production of mouse immunoglobulin in a rat myeloma is surprising because mouse myelomas have been used to fuse to rat myelomas to produce hybrid cells that synthesize both rat and mouse immunoglobulin molecules (25). The possibility that the S107 light chain is synthesized but rapidly degraded in the Y3 myeloma has not been excluded.

There is evidence that differentiated cell types express immunoglobulin genes to varying levels. For example, somatic cell hybridization of myelomas yields hybridomas that produce antibodies, whereas thymomas yield hybrid cells with T-cell phenotypes (26). Furthermore, hybridization of myelomas with non-B cells results in cessation of immunoglobulin production (26, 27). The lack of light chain expression in the transformed thymoma may reflect tissue-specific gene regulation. It is important to determine if immunoglobulin gene expression in the nonexpressing mouse thymoma and rat myeloma cell lines is regulated at the level of transcription, RNA processing, translation, or rapid protein turnover.

The study of the structure and function of the immunoglobulin molecule has been of great interest, both because of the ability of immunoglobulin to react with a diverse family of ligands and also because of the biologic importance of antibody molecules. Initially, the study of immunoglobulins was limited to the study of heterogeneous serum pools after immunization. The advent of myelomas, and more recently hybridomas, has permitted the study of homogeneous populations of antibodies. DNA-mediated transfection and immunoglobulin gene expression is an important tool to permit the study of immunoglobulin molecules. By using this technique, it should be possible to study the function of both novel chain combinations and novel chain structures. *In vitro* site-specific mutagenesis techniques can be used to construct specific mutations in immunoglobulin genes that can be expressed after transfection. Because significant quantities of immunoglobulin are produced in the transformants, sufficient quantities of protein necessary for detailed analyses should be obtained.

Note Added in Proof. After this paper was submitted for publication, we learned that Douglas Rice and David Baltimore have reported similar results with a different κ light chain gene and different lymphoid cell recipients (28).

We thank Dr. P. Jones for assistance with two-dimensional gel electrophoresis. This work was supported in part by National Institutes of Health Grants GM-13235, CA-15513 (P.B.), AI-08917 (L.A.H.), CA-16858 (S.L.M.), CA-22736 (S.L.M.), and CA-13696 to The Cancer Center of Columbia University and by a grant from the Becton Dickinson FACS Systems (L.A.H.). S.L.M. is a recipient of Research Career Development Award AI-00408.

1. Mantei, N., Boll, W. & Weissmann, C. (1979) *Nature (London)* 281, 40–46.
2. Mellon, P., Parker, V., Gluzman, Y. & Maniatis, T. (1981) *Cell* 27, 279–288.
3. Mantei, N. & Weissmann, C. (1982) *Nature (London)* 297, 128–132.
4. Mulligan, R. C. & Berg, P. (1980) *Science* 209, 1422–1427.
5. Mulligan, R. C. & Berg, P. (1981) *Proc. Natl. Acad. Sci. USA* 78, 2072–2076.
6. Littlefield, J. W. (1964) *Science* 145, 709–710.
7. Chu, G. & Sharp, P. A. (1981) *Gene* 13, 197–202.
8. Graham, F. L. & Van der Eb, A. J. (1973) *J. Virol.* 52, 455–456.
9. Sandri-Goldin, R. M., Goldin, A. L., Levine, M. & Glorioso, J. C. (1981) *Mol. Cell. Biol.* 1, 743–752.
10. Kwan, S.-P., Rudikoff, S., Seidman, J. G., Leder, P. & Scharff, M. D. (1981) *J. Exp. Med.* 153, 1366–1370.
11. Lundblad, A., Steller, R., Kabat, E. A., Hirst, J. W., Weigert, M. G. & Cohn, M. (1972) *Immunochemistry* 9, 535–544.
12. Galfre, G., Milstein, C. & Wright, B. (1979) *Nature (London)* 277, 131–133.
13. Dangl, J. L., Parks, D. R., Oi, V. T. & Herzenberg, L. A. (1982) *Cytometry* 2, 395–401.
14. Hyman, R. & Stallings, V. (1974) *J. Natl. Cancer Inst.* 52, 429–436.
15. Sharon, J., Morrison, S. L. & Kabat, E. A. (1979) *Proc. Natl. Acad. Sci. USA* 76, 1420–1424.
16. Oi, V. T., Bryan, V. M., Herzenberg, L. A. & Herzenberg, L. A. (1980) *J. Exp. Med.* 151, 1260–1274.
17. Oi, V. T., Jones, P. P., Goding, J. W., Herzenberg, L. A. & Herzenberg, L. A. (1978) *Curr. Top. Microbiol. Immunol.* 81, 115–129.
18. Moosic, J. P., Sung, E., Nilson, A., Jones, P. & McKean, D. J. (1982) *J. Biol. Chem.* 257, 9684–9691.
19. Di Maio, O., Treisman, R. & Maniatis, T. (1982) *Proc. Natl. Acad. Sci. USA* 79, 4030–4034.
20. Paige, C. J., Kincade, P. W. & Ralph, P. (1978) *J. Immunol.* 121, 641–647.
21. Knapp, M. R., Severinson-Gronowicz, E., Schroder, J. & Strober, S. (1979) *J. Immunol.* 123, 1000–1006.
22. Boyd, A. W., Goding, J. W. & Schrader, J. W. (1981) *J. Immunol.* 126, 1261–1265.
23. Lee, F., Mulligan, R., Berg, P. & Ringold, G. (1981) *Nature (London)* 294, 228–232.
24. Falkner, F. G. & Zachau, H. G. (1982) *Nature (London)* 298, 286–288.
25. Cotton, R. G. H. & Milstein, C. (1973) *Nature (London)* 244, 42–43.
26. Goldsby, R. A., Osborne, B. A., Simpson, E. & Herzenberg, L. A. (1977) *Nature (London)* 267, 707–708.
27. Coffino, P., Knowles, B., Nathenson, S. G. & Scharff, M. D. (1971) *Nature (London)* 231, 87–90.
28. Rice, D. & Baltimore, D. (1982) *Proc. Natl. Acad. Sci. USA* 79, 7862–7865.

0022-1767/87/1381-0324$02.00/0
THE JOURNAL OF IMMUNOLOGY
Vol. 138, 324–329, No. 1, January 1, 1987
Printed in U.S.A.

EXPRESSION OF A RECOMBINANT MURINE IgE IN TRANSFECTED MYELOMA CELLS[1]

CHRISTINE A. GRITZMACHER[2] AND FU-TONG LIU[3]

From the Division of Molecular Biology, Medical Biology Institute, La Jolla, CA 92037

We constructed a recombinant gene encoding an immunoglobulin (Ig) heavy chain consisting of the variable region from the phosphorylcholine (PC)-specific secreting myeloma MOPC167 and the ε constant region from SJL mice. This gene, cloned into the shuttle vector pSV2*gpt*, was transfected into J558L myeloma cells, and stable transformants that expressed the ε gene were cloned. The IgE heavy chain in these transformants is associated with the endogenous λ light chain and is secreted as an intact IgE molecule. However, the secreted IgE does not bind to PC conjugated to bovine serum albumin (PC-BSA). The MOPC167 κ chain gene was cloned into the shuttle vector pSV2*neo* and was transfected into the ε heavy-chain transformant. Stable transformants were cloned that expressed both the ε heavy chain and the κ light chain. IgE secreted from such a transformant was shown to bind to PC-BSA. Both types of secreted recombinant IgE bound to rat basophilic leukemia (RBL) cells, but only the IgE produced by the cell line transformed with the MOPC167 κ gene could be cross-linked with PC-BSA to cause serotonin release.

Immunoglobulin E (IgE) is an important molecule in the allergic response. It is involved in antigen and cell recognition that leads to a series of events that culminate in the release of vasoactive substances and an allergic reaction (1, 2). The availability of hybridomas that produce monoclonal IgE (3, 4) has aided in the study of the structure of IgE molecules and the functions associated with the Fc portion of the antibody (5). By using the techniques of molecular cloning, mutagenesis, and expression of Ig in transformed cells, one should be able to additionally define the structure-function relationships of IgE molecules (6–8). Furthermore, by constructing IgE genes that include the variable (V) regions from existing myelomas and hybridomas with the heavy chain ε constant region (C_ϵ), one should be able to produce IgE of predetermined specificity and affinity for a wide variety of antigens and haptens. Finally, the regulation of IgE expression by both T cell soluble factors (1, 2) and by *cis*-acting genetic elements should be aided by the use of defined recombinant IgE genes expressed in transformed myeloma cells.

To initiate such studies, we constructed a murine recombinant IgE gene consisting of the heavy chain variable region (V_{H167}) from the myeloma MOPC167 (9) with the C_ϵ region from a genomic clone of SJL mouse DNA. These two components, consisting of exons and introns along with the Ig expression control regions, were cloned into a pSV2*gpt* vector (10) and were introduced by protoplast fusion into a myeloma that produces only λ light chains. Stable transformants expressing the IgE heavy chain were isolated, and one was additionally transformed with another pSV2 vector, pSV2*neo* (11), containing the complete κ light chain gene from the MOPC167 myeloma (9). Stable transformants were obtained that expressed both the ε heavy chain and the κ light chain genes and secreted a functional IgE molecule. The secreted IgE binds to phosphorylcholine-bovine serum albumin (PC-BSA).[4] Furthermore, the secreted IgE molecule binds to IgE receptors ($Fc\epsilon R$) on rat basophilic leukemia (RBL) cells and can cause those cells to release serotonin after cross-linking with either PC-BSA or an anti-IgE antibody. Collectively, the experiments presented herein show that the gene for a functional murine IgE molecule of predetermined specificity can be constructed and expressed by transformed cells.

MATERIALS AND METHODS

Plasmids and their construction. Plasmids $pV_{167}\Delta5'E$ *and* $pV_{167}C_\epsilon$. A plasmid, $pV_{167}\Delta5'E$ (9), containing the V_H gene from the MOPC167 myeloma and the corresponding regulatory regions (promoter and enhancer) and a plasmid, $pV_{167}C_\kappa$ (9), containing the κ light chain gene from MOPC167 cells (diagrammed in Fig. 1 *A* and *B*) were gifts from Dr. Ursula Storb (University of Washington, Seattle, WA).

Isolation of C_ϵ *gene.* Genomic DNA of SJL mice was digested with restriction enzyme EcoRI and was cloned into the bacteriophage λ vector L47.1 (12). The genomic library was screened by hybridization (13) with a radioactively labeled IgE cDNA probe (14). A clone containing a 20 kb EcoRI insert (diagrammed in Fig. 1*C*), called L47-SJL(E20), was isolated, and a 4.6 kb BamHI restriction fragment containing the IgE constant region gene was identified by Southern blotting (13, 15) by using the IgE cDNA probe.

Plasmid pSV-C_ϵ*, construction.* The 4.6 kb BamHI C_ϵ fragment was isolated and was ligated into the unique BamHI site of the vector pSV2*gpt* (10), to make plasmid pSV-C_ϵ (diagrammed in Fig. 2); orientation of the C_ϵ insert was determined by digestion with PstI.

Construction of plasmids pSV-V_{H167}-C_ϵ *and* pSV-$_{H167}$V-C_ϵ. A 4.5 kb EcoRI-SmaI restriction fragment containing the IgH promoter, the rearranged V_{H167} exons, and the IgH enhancer was constructed as follows. Plasmid $pV_{H167}\Delta5'E$ was digested with EcoRI, SacI, and XbaI to generate a 3.8 kb SacI-XbaI V_{H167} fragment and a 0.7 kb XbaI-EcoRI enhancer fragment. The two purified fragments were ligated into the multiple cloning site of plasmid pUC12 that had been cut with EcoRI and XbaI. This plasmid was then cut with EcoRI and SmaI (in the multiple cloning site of pUC12) to generate a single 4.5 kb V_{H167} gene fragment that was inserted in the unique EcoRI site of the plasmid pSV-C_ϵ, by ligation but using EcoRI recognition sites, followed by polymerase I Klenow fragment filling-in (13) of the

Received for publication July 19, 1986.
Accepted for publication September 18, 1986.
The costs of publication of this article were defrayed in part by the payment of page charges. This article must therefore be hereby marked *advertisement* in accordance with 18 U.S.C. Section 1734 solely to indicate this fact.
[1] This work was supported by National Institutes of Health Grant AI-20958. This is publication number 97 from the Medical Biology Institute, La Jolla, CA.
[2] To whom correspondence should be addressed. Phone: (619) 450-3033.
[3] Recipient of a Leukemia Society of America Scholar Award.

[4] Abbreviation used in this paper: PC, phosphorylcholine.

remaining EcoRI site to create a blunt end and a second ligation of the blunt ends. The orientation of the EcoRI-SmaI/EcoRI insert was determined by digestions with BamHI and BamHI plus EcoRI. One plasmid with each orientation of the V_{H167}-enhancer fragment relative to C_ϵ was retained: the plasmid in which the inserts have the same orientation as V_H and C_ϵ would have on a normal rearranged chromosome was called pSV-V_{H167}-C_ϵ, whereas the other with the V_H fragment in the opposite orientation was called pSV-$_{H167}$V-C_ϵ (diagrammed in Fig. 2).

Plasmid pSV-V_{167}-C_ϵ. A 17.4 kb EcoRI-KpnI fragment containing the V_{167}-C_ϵ region was excised from p$V_{167}C_\epsilon$ (see Fig. 1*B*) and was inserted into the unique EcoRI site of vector pSV2*neo* by EcoRI and blunt-end ligation as above. A plasmid in which the κ gene is transcribed in the opposite orientation as the *neo* gene (as determined by HindIII digestion) was called pSV-V_{167}-C_ϵ (diagrammed in Fig. 2). All plasmids were maintained in *Escherichia coli* strain HB101 after $CaCl_2$ transformation (13).

Cell lines and tissue culture. The myeloma cell line J558L, which is a spontaneous heavy-chain-loss derivative of myeloma J558 (6), was a gift from Dr. S. L. Morrison (Columbia University, New York, NY) and was maintained in Dulbecco's modified minimal essential medium (DME) containing 10 mM HEPES buffer, 2 mM glutamine, penicillin (50 U/ml), streptomycin (50 μg/ml) (all from Whittaker M.A. Bioproducts), and 10% (v/v) fetal calf serum (from HyClone Laboratories), called complete-DME.

RBL cells, strain 2H3, were a gift from Dr. D. Holowka (Cornell University, Ithaca, NY) and were grown in RPMI medium supplemented with nonessential amino acids, penicillin, streptomycin, and fetal calf serum as above.

Transformation of myeloma cells. Plasmids were introduced into J558L cells by protoplast fusion (6); cells were grown in complete-DME containing 100 μg kanamycin/ml for 48 hr after fusion. Selection for expression of the *gpt* and *neo* genes was initiated 48 hr after fusion by growing the cells in complete-DME containing xanthine (250 μg/ml), hypoxanthine (15 μg/ml), and mycophenolic acid (6 μg/ml) for *gpt* expression, and in complete-DME containing an effective concentration of 1 mg/ml of the antibiotic G418 sulfate (from GIBCO) for *neo* expression. Transformed cells were maintained in the selective media for 2 to 3 wk, and clones were usually visible after 10 to 14 days. Individual clones were selected by limiting dilution.

Detection of gene expression in transformed cells. RNA dot blots (16). Cytoplasmic RNA was isolated after detergent lysis of approximately 10^6 cells and was spotted at various dilutions on nitrocellulose membrane, was heat fixed, and then was probed with ^{32}P-labeled nick-translated DNA specific for C_ϵ (14), *gpt* (10), *neo* (11), and C_γ (9). Probed membranes were washed at high stringency (1X SSC, 65°C) and were exposed to Kodak X-AR5 film.

Polyacrylamide gel electrophoresis (PAGE) and Western blotting of proteins. Proteins were separated by PAGE on sodium dodecyl sulfate (SDS)-10% acrylamide gels (17) and were transferred to nitrocellulose membrane (18). After blocking the membrane with 2% BSA in phosphate-buffered saline (PBS) for 3 hr at 25°C, the transferred proteins were detected by binding with ^{125}I-labeled goat anti-mouse IgE antibody (GAME: affinity purified) (3) (approximately 10^7 cpm). Filters were washed with PBS containing 1% Triton X-100 for 1 hr at 25°C and were exposed to x-ray film.

Radioimmunoassay (RIA). IgE was detected by solid-phase RIA (3, 19) in which either PC conjugated to BSA at 8.3 PC per BSA (provided by Dr. J. Marcelletti, Medical Biology Institute, La Jolla, CA) or GAME was immobilized on polyvinyl wells by coating the wells with 100 μl of PC-BSA (at 20 μg/ml) or GAME (at 1 μg/ml) in PBS and drying at 37°C. After blocking with 5% BSA-PBS for 1 hr at 25°C, 100 μl of complete-DME containing IgE or purified IgE diluted in 0.5% BSA-PBS were added to each well and were incubated for 3 to 12 hr at 5°C. The wells were washed, and 50 μl of ^{125}I-labeled GAME (approximately 2×10^5 cpm) were added to each well, and were incubated for 1 hr at 25°C. The wells were washed five times with borate-buffered saline and were individually counted in a gamma counter. All samples were assayed in duplicate. A monoclonal anti-PC IgE from hybridoma 3B12, used as a positive control, was a gift from Dr. A. Feeney (Medical Biology Institute, La Jolla, CA).

RIA was also used to determine whether a secreted IgE contained a κ or a λ light chain. Antibodies to be tested were coated on the wells and were blocked with 1% BSA. Then 100 μl of rabbit anti-mouse κ chain (from Bethyl Laboratories) or rabbit anti-mouse λ chain antibodies (from Tago Laboratories) were added to each well at 1/4000 dilution and were incubated 3 hr at 37°C. After washing the wells, 50 μl of ^{125}I-goat anti-rabbit antibody (approximately 10^5 cpm) were added to each well as above and were incubated 1 hr at 37°C. Wells were washed and were counted as above. Reagents were standardized for optimal response with monoclonal antibodies (mAb): anti-DNP IgE 26.82 (ϵ, κ) (3), mAb 62 (γ1, κ) (19), and mAb 18.1.16 (γ1, λ) (20). The latter two were a gift from Dr. M. Zanetti (Medical Biology Institute, La Jolla, CA).

Serotonin-release by RBL cells (3, 21, 22). Approximately 3×10^5 RBL cells were incubated with 20 μCi of [^{3}H]serotonin ([^{3}H]hydroxytryptamine binoxalate; from DuPont NEN at 29 Ci/mMol) in the presence of complete-DME containing IgE (monoclonal at 3 μg/ml or recombinant from cell supernatants at the dilutions indicated in the text) for 1 hr. After incubation, cells were washed to remove unincorporated [^{3}H]serotonin and were incubated in the presence of a cross-linking agent, either GAME or PC-BSA. Serotonin release was measured by counting duplicate aliquots of supernatants in scintillation fluid. Total serotonin uptake was measured by counting an aliquot of washed cells lysed in 10% trichloroacetic acid.

Purification of IgE by affinity chromatography. Recombinant IgE were purified from supernatants of transformed cells by affinity chromatography by using columns of GAME coupled to Sepharose (3, 23). A column (0.5 x 15 cm) containing 0.5 to 1 ml packed vol of GAME-Sepharose was loaded three successive times with cell supernatant, was washed with 100 vol of PBS containing 1 mM phenylmethylsulfonyl fluoride (PMSF), and was eluted successively with 2 vol of 0.2, 0.4, 0.6, and 0.8 M acetic acid containing 1 mM PMSF. The eluted fractions were immediately neutralized with 4 M ammonium hydroxide, were assayed for IgE by RIA, and were lyophilized. All fractions that contained IgE were solubilized in PBS.

RESULTS

Construction and transfection of recombinant mouse ϵ heavy chain and κ light chain genes. To express an IgE antibody with known specificity, we constructed a complete IgE gene consisting of the heavy chain variable region (V_{H167}) from the MOPC167 myeloma (9) and the constant region for IgE (C_ϵ) in a selectable shuttle vector, pSV2*gpt* (10). This was done in a stepwise manner in which the unrearranged C_ϵ gene of the SJL mouse (Fig. 1) was inserted into the unique BamHI site in the vector. A clone where the C_ϵ gene is transcribed in the opposite orientation as the *gpt* gene on the vector was used subsequently and was called pSV-C_ϵ. The V_{H167} region (Fig. 1), containing the heavy chain promoter, the rearranged VDJ region, and the IgH enhancer was then cloned into the unique EcoRI site of the pSV-C_ϵ plasmid. Plasmids with both orientations of the V_{H167} fragment were used subsequently in transformation experiments. The plasmid with the V_{H167} insert in the normal chromosomal orientation relative to the C_ϵ gene was called pSV-V_{H167}-C_ϵ, and the plasmid with the opposite orientation of V_{H167} was called pSV-$_{H167}$V-C_ϵ. These constructs are diagrammed in Figure 2.

The C_ϵ insert was cut with BamHI and consists of the four Fc exons with their intervening sequences. Previous mapping of the IgE gene in BALB/c mice (24) indicates that BamHI cuts between the two membrane exons (M1

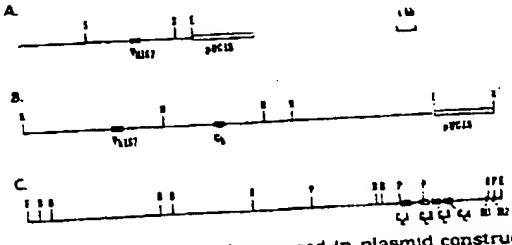

Figure 1. MOPC167 and C_ϵ clones used in plasmid constructions. In *Panel A*, p$V_{H167}\Delta$5'E contains a 7.4 kb insert in vector pUC18 (9). The 4.5 kb SacI-EcoRI fragment contains the V_{H167} region used in constructing pSV-V_{H167}-C_ϵ and pSV-$_{H167}$V-C_ϵ. In *Panel B*, p$V_{167}C_\epsilon$ contains a 17.4 kb KpnI-EcoRI fragment in vector pUC18 (9). The entire fragment was used to construct pSV-V_{167}-C_ϵ. In *Panel C*, the 20 kb EcoRI insert from L47-SJL(E20) is shown (the L47 vector is not shown). The 4.6 kb BamHI fragment containing the four C_ϵ exons and the M1 exon was used to construct pSV-C_ϵ. Restriction enzyme abbreviations are: B, BamHI; E, EcoRI; H, HindIII; K, KpnI; P, PstI; S, SacI; and X, XbaI. Exons are shown as *solid boxes*.

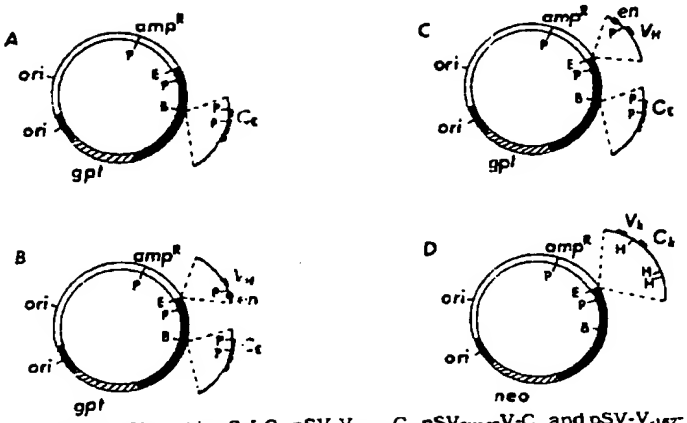

Figure 2. Plasmids pSV-C$_\epsilon$, pSV-V$_{H167}$-C$_\epsilon$, pSV-$_{H167}$V-C$_\epsilon$, and pSV-V$_{\epsilon 167}$-C$_\epsilon$. The parental vector, pSV2*gpt* (10) (shown as a *circle*) was used in the first three constructs and consists of DNA from pBR322 (*unshaded*) where the positions of the origin of replication (*ori*) and β-lactamase gene (*amp^R*); SV40 DNA (*solid black*) with its origin of replication; and the *E. coli gpt* gene (*cross-hatched*) are indicated. The SV40 early promoter is located 5′ to the *gpt* gene. In *Circle A*, pSV-C$_\epsilon$ is a plasmid in which the C$_\epsilon$ region (shown as an *arc*) was subcloned into the unique BamHI site of pSV2*gpt*. In *Circle B*, pSV-V$_{H167}$-C$_\epsilon$ is a plasmid in which the V$_{H167}$ and IgH enhancer (*en*) region (shown as an *arc*) was subcloned into the unique EcoRI site of pSV-C$_\epsilon$ so that the V$_{H167}$ fragment is in the normal chromosomal orientation relative to the C$_\epsilon$ fragment and so that its transcription is in the opposite direction to that of the *gpt* gene. In *Circle C*, pSV-$_{H167}$V-C$_\epsilon$ is a vector similar to pSV-V$_{H167}$-C$_\epsilon$ except that the V$_{H167}$-IgH enhancer fragment is in the opposite orientation. In *Circle D*, pSV-V$_{\epsilon 167}$-C$_\epsilon$ consists of the complete κ gene (shown as an *arc*) cloned into pSV2*neo* (11) shown as a *circle* and labeled as above. Abbreviations are as in Figure 1: exons are denoted by *boxes* and the enhancer as a *closed circle*.

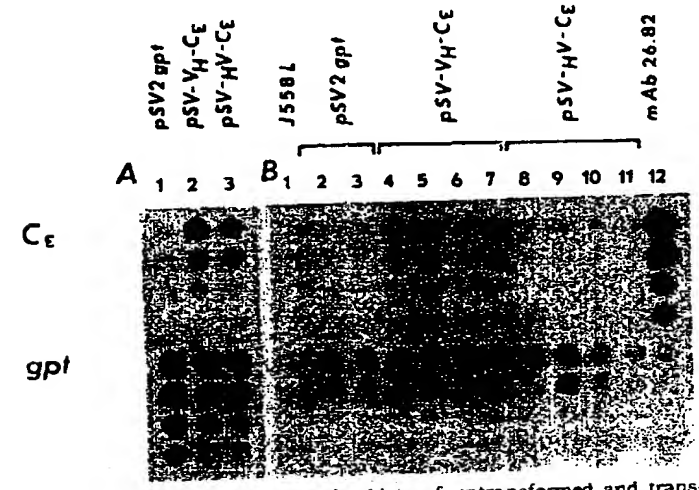

Figure 3. Cytoplasmic RNA dot blots of untransformed and transformed J558L cells. The *upper panel* is probed with a C$_\epsilon$ DNA and the *lower panel* with a *gpt* probe. *Panel A* shows transient expression of J558L cells transformed with: *Lane 1*, pSV2*gpt*; *Lane 2*, pSV-V$_{H167}$-C$_\epsilon$; and *Lane 3*, pSV-$_{H167}$V-C$_\epsilon$. *Panel B* shows RNA from clones of *Lane 1*, untransformed J558L cells; and stable transformants of J558L for: *Lanes 2* and *3*, pSV2*gpt*; *Lanes 4* through *7*, pSV-V$_{H167}$-C$_\epsilon$; and *Lanes 8* through *11*, pSV-$_{H167}$V-C$_\epsilon$. *Lane 12* is RNA from hybridoma mAb 26.82. Four dilutions of RNA extracts were spotted *from top to bottom* for each *panel*: 1/4, 1/16, 1/64, and 1/256. Exposure time: 20 hr.

and M2 in Fig. 1). This region has not been sequenced in SJL mice, but we assume that the BamHI site occurs in the same position, because the genomic restriction map for BamHI and other restriction enzymes in this region is identical for both BALB/c and SJL mice (C.A.G. and F.-T.L., manuscript in preparation).

Protoplast fusion was used to introduce the plasmids pSV2*gpt*, PSV-V$_{H167}$-C$_\epsilon$, and pSV-$_{H167}$V-C$_\epsilon$ into J558L cells (6). Some of the cells were harvested 48 hr after fusion, and RNA dot blotting (16) was used to assay for transcription of the transfected *gpt* and C$_\epsilon$ genes. As shown in Figure 3*A*, all of the transfected populations showed transient *gpt* expression, but only those transformed with pSV-V$_{H167}$-C$_\epsilon$ and pSV-$_{H167}$V-C$_\epsilon$ showed transcription of the C$_\epsilon$ region. Stable transformants were selected, and four independent clones for each transformation were assayed for transcription of the *gpt* and C$_\epsilon$ genes by cytoplasmic RNA dot blotting. Figure 3*B* shows that all of the clones transcribed *gpt* as expected, but only two of the four clones transformed with pSV-V$_{H167}$-C$_\epsilon$ transcribed the C$_\epsilon$ gene. The stable clones transformed with pSV2*gpt* do not produce RNA that hybridizes with the C$_\epsilon$ probe. In contrast to the transient expression results, none of the clones from cells transformed with pSV-$_{H167}$V-C$_\epsilon$ showed C$_\epsilon$ transcription.

The entire light chain gene from MOPC167 (9) in plasmid pSV-V$_{\epsilon 167}$-C$_\epsilon$, was introduced into one of the stable transformants for each of the above fusions. Again the transformed populations were assayed for transient expression of the vector selectable marker (*neo*) and C$_\epsilon$ 48 hr after fusion, and all cell lines showed that fusion had been successful (data not shown). Stable transformants were selected, and clones were isolated.

Analysis of Ig produced by transformed cells. Protein expression in all of the transformed cell lines was assayed for production of IgE antibodies by Western blotting by using a radiolabeled anti-IgE antibody to detect both cellular (data not shown) and secreted IgE. As shown in Figure 4, only clones transfected with the plasmid pSV-V$_{H167}$-C$_\epsilon$ with or without pSV-V$_{\epsilon 167}$-C$_\epsilon$ secreted a molecule recognized by anti-IgE that co-migrates with IgE heavy chain from mAb 26.82. As expected, cells that did not show transcription of the C$_\epsilon$ gene did not produce any IgE heavy chain. The cells transformed with the heavy chain gene alone produced an IgE that was secreted. This is probably due to pairing of the ε heavy chain with the endogenous λ light chain produced by the J558L cells.

To additionally characterize the secreted IgE, we tested cell supernatants from two IgE secreting clones by RIA. Two RIA experiments were used: one to detect binding of IgE to anti-IgE and one to detect binding of IgE to PC-BSA. The results of such assays are shown in Figure 5.

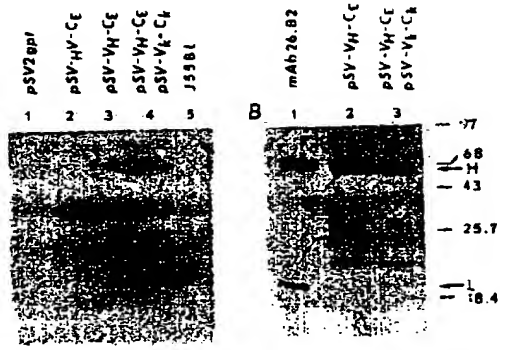

Figure 4. Panel A shows a Western blot of supernatants of transformed and untransformed J558L cells probed with ^{125}I-GAME. Cell supernatants (50 μl from approximately 10^6 cells/ml) for J558L cells transformed with: *Lane 1*, pSV2*gpt*; *Lane 2*, pSV-$_{H167}$V-C$_\epsilon$; *Lane 3*, pSV-V$_{H167}$-C$_\epsilon$; *Lane 4*, pSV-V$_{H167}$-C$_\epsilon$ and pSV-V$_{\epsilon 167}$-C$_\epsilon$; and *Lane 5*, for untransformed J558L cells were used. *Panel B* shows a Western blot of affinity-purified IgE from *Lane 1*, mAb 26.82; J558L transformants of: *Lane 2*, pSV-V$_{H167}$-C$_\epsilon$; and *Lane 3*, pSV-V$_{H167}$-C$_\epsilon$ and pSV-V$_{\epsilon 167}$-C$_\epsilon$. Positions of m.w. standards (×10^{-3}) are shown *at the right*; *arrows* indicate the positions of the heavy (H) and light (L) chains. Two additional bands present in *lanes 2* and *3* may be degradation products of the H chain.

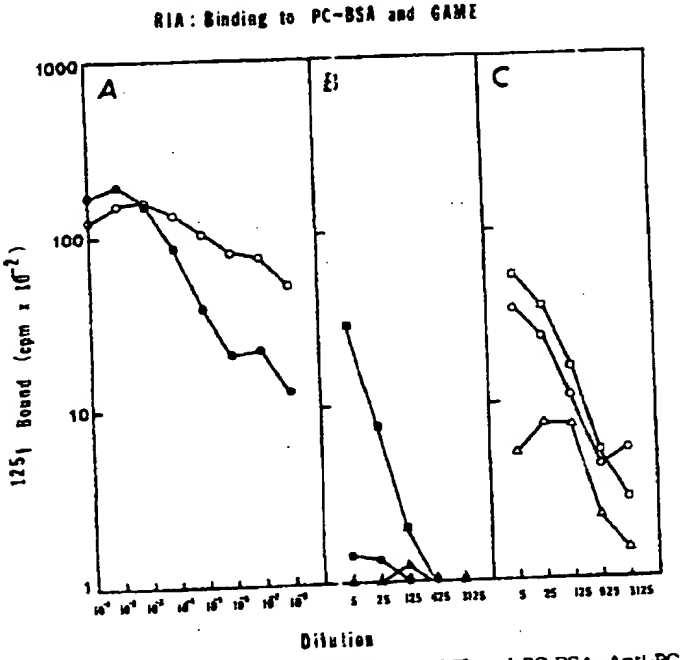

Figure 5. RIA results of IgE binding to GAME and PC-BSA. Anti-PC IgE (ascites fluid of hybridoma mAb 3B12) and cell supernatants from clones of untransformed and stably transformed J558L cells (grown to approximately 10^6/ml) were used. *Closed symbols* (*Panels A* and *B*) indicate binding to PC-BSA and *open symbols* (*Panels A* and *C*) indicate binding to GAME. *Panel A* is for mAb 3B12. *Panels B* and *C* are for cell supernatants from: *triangles*, untransformed J558L cells; *circles*, a J558L pSV-V_{H167}-C_γ clone; and *squares*, a J558L pSV-V_{H167}-C, and pSV-$V_{\lambda167}$-C_γ transformant. For *Panels B* and *C* the reciprocal of the dilution factor is shown.

Cells stably transformed with pSV-V_{H167}-C_γ, called J558L (ϵ, λ), produced an IgE that was detected by binding to anti-IgE only. In contrast, a stable transformant of both pSV-V_{H167}C, and pSV-$V_{\kappa167}$-C_κ, called J558L (ϵ, λ, κ), produced IgE that bound to both anti-IgE and PC-BSA. These results indicate that both the heavy and light chains with V_{167} specificity are required for PC-BSA recognition; the V_{H167}-C, heavy chain paired with the endogenous J558L light chain is not sufficient for PC-BSA binding. In addition, a clone of J558L stably transformed with pSV-$V_{\kappa167}$-C, showed no PC-BSA binding activity in the cell supernatant (data not shown). For both assays supernatants from untransformed J558L cells were used as a negative control, and an anti-PC IgE (mAb 3B12) was used as a positive control. From RIA results obtained with known concentrations of a standard IgE (affinity-purified anti-DNP mAb 26.82) we calculated that the transformed clones produce IgE to a final concentration of approximately 250 to 500 ng/ml of supernatant from cells grown to 1 to 3 × 10^6 cells/ml.

IgE was purified from cell supernatants from both stable IgE-secreting transformants, J558L (ϵ, λ) and J558L (ϵ, λ, κ), by affinity chromatography. The purified IgE gave RIA results qualitatively identical to those obtained with the unpurified supernatants. Furthermore, purified IgE from both transformed clones could successfully compete with monoclonal anti-DNP IgE for GAME on a solid phase RIA (data not shown). We used purified IgE from both clones in RIA to confirm that cells transformed with pSV-V_{H167}-C, produced IgE with a λ light chain, whereas the clone transformed with both pSV-V_{H167}-C, and pSV-$V_{\kappa167}$-C, produced IgE molecules with κ and/or λ light chains. These results are presented in Table I.

TABLE I

RIA analysis of the light chain isotypes of secreted IgE

IgE Coating Wells	Source of IgE	^{125}I-Goat Anti-Rabbit Binding (cpm ± SD)	
		Rabbit anti-λ	Rabbit anti-κ
IgE(λ)	J558L/ pSV-V_{H167}-C_γ	537 ± 0	9245 ± 480
IgE(λ,κ)	J558L/ pSV-V_{H167}-C_γ pSV-$V_{\kappa167}$-C_κ	1266 ± 29	5517 ± 10
IgE(κ)	mAb 26.82	1987 ± 45	647 ± 15
None (background)	—	558 ± 7	638 ± 18

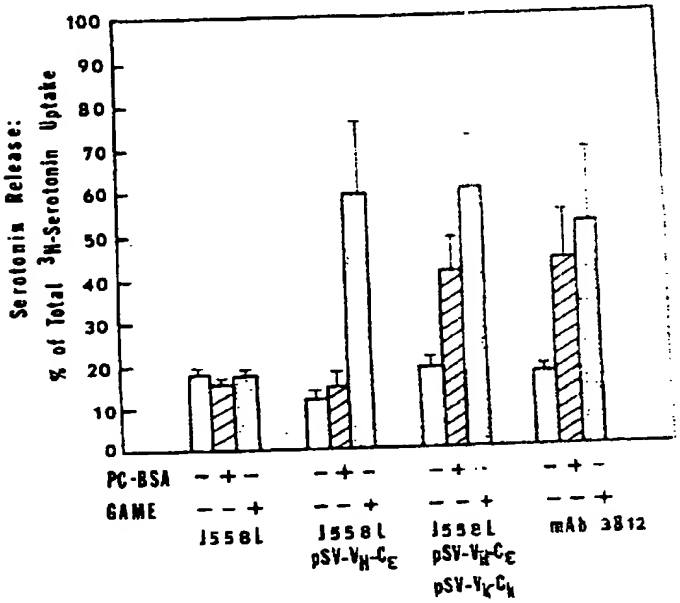

Figure 6. [^{3}H]Serotonin release from RBL cells. RBL cells were incubated with cell supernatants from untransformed J558L cells; a J558L pSV-V_{H167}-C, clone; and a J558L pSV-V_{H167}-C, and pSV-$V_{\kappa167}$-C_κ transformant; and with mAb 3B12 (indicated *below the bars*). *Bars* represent the mean of duplicate samples from two separate experiments measured under optimal conditions (mAb 3B12 at 3 μg/ml cell supernatants at 1/25 dilutions; PC-BSA at 100 μg/ml and GAME at 1 μg/ml); SD are shown *above the bars*; *open bars* are for no cross-linking agent, *cross hatched bars* for PC-BSA, and *stippled bars* for GAME.

Effector functions of the recombinant IgE molecules. To determine whether the recombinant IgE molecules exhibited biological functions, we used cell supernatants in a serotonin-release assay with RBL cells. In this assay, the IgE first binds to the FcRϵ on the RBL cells while the cells simultaneously take up [^{3}H]serotonin. Subsequently, the bound IgE are cross-linked with either anti-IgE antibody or PC-BSA, which causes the cells to release [^{3}H]serotonin. As expected from the RIA results, the supernatants from the cells transformed only with the heavy chain clone caused serotonin release only when cross-linked with anti-IgE antibody. The cell supernatants from a clone transformed with both the recombinant heavy chain clone and the $V_{\lambda167}$-C_κ clone caused serotonin release when cross-linked with either the anti-IgE antibody or PC-BSA. Neither cross-linking agent caused increased serotonin release from cells incubated in medium alone or in supernatants from untransformed J558L cells. The results obtained from these experiments by using optimal concentrations of both cell supernatants and cross-linking agents are shown in Figure 6.

DISCUSSION

In this paper we have shown that a complete murine IgE gene can be constructed, transfected, and expressed in myeloma cells to produce a functional IgE with known specificity. This method should allow one to produce IgE with a variety of specificities by cloning the appropriate V-regions available from known myelomas and hybridomas with the C$_\epsilon$ gene.

In the IgE heavy chain gene construction presented here, the V_{H167} region including the promoter and enhancer was separated from the C$_\epsilon$ region by 751 base pairs of vector DNA (10). This artificial separation of the two expressed regions did not appear to affect transcription of the final constructed gene or translation of the resulting mRNA. However, because we have not varied the spacing of the two regions, we cannot determine whether greater expression of the cloned gene could be achieved with different placement of the V_H and C$_\epsilon$ inserts.

The orientation of the V_{H167} region relative to the C$_\epsilon$ region is critical for transcription of the C$_\epsilon$ exons in stable transformants. The C$_\epsilon$ gene is transcribed and ϵ heavy chain is produced only when the two regions are in the orientation as they would appear in a normal rearranged chromosome. This is probably not due to any position effect on the enhancer because the IgH enhancer has been shown to function in either direction (25, 26). Therefore the orientation of the IgH promoter relative to C$_\epsilon$ is implicated: transcripts initiating in the "opposite" orientation would probably terminate before transcribing the C$_\epsilon$ region. Thus the ϵ gene cannot be transcribed, at least under the conditions presented here, without proper linkage to the IgH promoter.

Although C$_\epsilon$ transcription was not seen in stable clones when the promoter-V_{H167} fragment was in the opposite orientation, transient expression was observed in uncloned transformed cells. This transient expression probably represents "sterile" C$_\epsilon$ transcripts initiating within the intron located 5′ of the C$_\epsilon$ region. Such "sterile" transcripts have been observed for C$_\mu$ genes in a variety of cells (27–30). Because we have not looked at a larger number of stable clones of pSV-$_{H167}$V-C$_\epsilon$ transformed cells, we do not know whether this discrepancy between expression of C$_\epsilon$ in transient and stably transformed cells is due to the position of integration, to different levels of transcription for integrated and unintegrated vectors, or to a copy number effect. In addition, the transcription initiation site used may be determined by the state of the transformant: transient expression may originate at the 5′ intron initiation site, whereas stable transformants may preferentially use the IgH promoter initiation site. Additional characterization of the C$_\epsilon$ transcripts from transiently and stably transformed cells would be required to differentiate between these possibilities.

Only some of the stably transformed clones that were selected on the basis of expression of the *E. coli gpt* gene of the vector expressed the cloned C$_\epsilon$ gene. The phenomenon has been noted by other investigators (6, 31–33) and is probably due to the position of the recombination site used when the transfected plasmid enters a chromosome. If recombination occurred between the IgH promoter and the C$_\epsilon$ gene, then the promoter would become unlinked from the ϵ gene and transcription would not occur. Alternatively, expression of the integrated plasmid may be negatively regulated by some component of the chromosome at or near the site of integration of the plasmid. This also suggests that some integrated plasmids may be positively regulated by the chromosome integration position, allowing for selection of transformed cells that express the foreign genes at high levels. In addition, it cannot be ruled out that portions of the cloned genes may be selectively lost during stable integration.

It is interesting to note that the myeloma cells stably transformed with our constructs produced less IgE than any of the IgE-secreting hybridomas tested (3, 4) (unpublished results). This could be due to many reasons including the position of integration of the introduced IgE gene. However, the C$_\epsilon$ gene used in the constructions presented here came from a genomic unrearranged IgE gene of the SJL strain of mice. SJL mice exhibit a very low IgE response but a normal IgG response to immunogens (34). Although this is probably due to differences in regulation by suppressor T cells in these mice (35, 36), regulatory signals near the IgE locus itself could influence the level of this isotype response. By constructing recombinant Ig genes in which the constant region genes are derived from either high or low IgE responder mice and expressing these in transfected cells, one could directly test whether the origin of the C$_\epsilon$ gene affects the level of IgE expression, independent of T and B cell interaction.

Cells transformed with the complete V_{H167}-C$_\epsilon$ gene produced and secreted IgE heavy chain associated with a λ light chain, presumably the endogenous light chain. This molecule would have a hybrid variable region (V_{H167} anti-PC and $V_{\lambda 1}$ anti-dextran) and did not bind PC-BSA in either an RIA or antigen cross-linking assay. The cells stably transformed with both the heavy chain gene and MOPC167 κ light chain gene secreted IgE associated with both λ and κ light chains. The secreted molecules could be of three types: IgE(λ^2), IgE(λ^1, κ^1), and IgE(κ^2). Given the previous result, only the latter two could be contributing to the PC-BSA binding seen by the secreted IgE from this clone. Because the third type would represent simply a different isotype of the Ig produced by MOPC167 cells, this IgE must certainly bind PC-BSA. Whether the second type of IgE is produced and binds PC-BSA has not been determined. Both types of stably transformed cells produced IgE molecules that could bind the RBL cells and cause serotonin release from these cells when the bound IgE was cross-linked by GAME. Thus the hybrid variable regions did not interfere with binding to FcR$_\epsilon$. As expected, cross-linking by PC-BSA only occurred with IgE produced by the κ chain transformed clone. Similar inability to bind to PC was seen with a mouse-human chimeric IgG when the chimeric heavy chain gene, with a variable region derived from anti-PC myeloma S107, was expressed in J558L cells (37).

In contrast with our results in which both the V_H and V_κ regions from MOPC167 were required for PC-BSA binding, a hapten-binding chimeric IgE antibody the heavy chain of which is composed of a human C$_\epsilon$ region fused to a mouse V_H region was produced and was expressed in J558L cells (7). The mouse V_H region in this chimeric IgE came from a myeloma with specificity for the hapten 4-hydroxy-3-nitrophenacetyl (NP). Like most anti-NP myelomas, it made use of a $\lambda 1$ light chain, the same light chain isotype expressed by J558L cells, and therefore the combination of the chimeric heavy chain with the J558L light chain was capable of recognizing

the hapten NP. Thus binding of recombinant Ig molecules to hapten may or may not require the V_H and V_L regions from the same myeloma or hybridoma, and many situations will have to be experimentally determined. The chimeric IgE could compete with human IgE and also bind to FcRϵ on mononuclear cells, causing histamine release in the presence of NP. A similar but more highly refined mouse-human chimeric IgE was recently constructed in which the mouse complementarity-determining regions (CDR) were used to replace the human CDR (8). This molecule in combination with the corresponding mouse light chain acquired the hapten affinity of the mouse antibody.

From our results and those of others working with chimeric IgE it can be seen that functional IgE of predetermined specificity can be produced by using the techniques described here. This same approach should be useful in determining a possible role of the C_ϵ region in regulation of IgE expression and in defining the regulatory functions of soluble T cell factors (1, 2) that affect IgE-expressing B lymphocytes. Genetic manipulation of the genes before transfection and analysis of the molecules produced by the transformed cells should help to define the regions of the C_ϵ gene involved in IgE biological functions.

Acknowledgments. We thank Dr. M. W. Robertson and J. Rogers for help with immunologic methods; Dr. M. W. Robertson for iodinating reagents; and all those mentioned for supplying plasmids, cells, and reagents. We appreciate Drs. M. Zanetti's and A. Feeney's criticisms of the manuscript; and B. Burgess' and J. Czarnecki's aid in manuscript preparation.

REFERENCES

1. Katz, D. H. 1982. IgE antibody responses *in vitro*: from rodents to man. *Prog. Allergy 32:105.*
2. Ishizaka, K. 1984. Regulation of IgE synthesis. *Ann. Rev. Immunol. 2:159.*
3. Liu, F.-T., J. W. Bohn, E. L. Ferry, H. Yamamoto, C. A. Molinaro, L. A. Sherman, N. R. Klinman, and D. H. Katz. 1980. Monoclonal dinitrophenyl-specific murine IgE antibody: preparation, isolation and characterization. *J. Immunol. 124:2728.*
4. Rudolf, A. K., P. D. Burrows, and M. R. Wabl. 1981. Thirteen hybridomas secreting hapten-specific immunoglobulin E from mice with Ig^a or Ig^b heavy chain haplotype. *Eur. J. Immunol. 11:527.*
5. Liu, F.-T. 1986. Gene expression and structure of immunoglobulin ϵ chains. *CRC Crit. Rev. Immunol. 6:47.*
6. Oi, V. T., S. L. Morrison, L. A. Herzenberg, and P. Berg. 1983. Immunoglobulin gene expression in transformed lymphoid cells. *Proc. Natl. Acad. Sci. USA 80:825.*
7. Neuberger, M. S., G. T. Williams, E. B. Mitchell, S. S. Jouhal, J. G. Flanagan, and T. H. Rabbitts. 1985. A hapten-specific chimeric IgE antibody with human physiological effector function. *Nature 314:268.*
8. Jones, P. T., P. H. Dear, J. Foote, M. S. Neuberger, and G. Winter. 1986. Replacing the complimentarity determining regions in a human antibody with those from a mouse. *Nature 321:522.*
9. Storb, U., C. Pinkert, B. Arp, P. Engler, K. Gollahon, J. Manz, W. Brady, and R. L. Brinster. 1986. Transgenic mice with μ and ϵ genes encoding antiphosphocholine antibodies. *J. Exp. Med. 164:627.*
10. Mulligan, R. C., and P. Berg. 1981. Selection for animal cells that express the *Escherichia coli* gene coding for xanthine-guanine phosphoribosyltransferase. *Proc. Natl. Acad. Sci. USA 78:2072.*
11. Southern, P. J., and P. Berg. 1982. Transformation of mammalian cells to antibiotic resistance with a bacterial gene under control of the SV40 early region promoter. *J. Mol. Appl. Genet. 1:327.*
12. Loenen, W. A., and W. J. Brammer. 1980. A bacteriophage λ vector for cloning large DNA fragments made with several restriction enzymes. *Gene 10:249.*
13. Maniatis, T., E. F. Fritsch, and J. Sambrook. 1982. *Molecular cloning.* Cold Spring Harbor Laboratory, Cold Spring Harbor, NY
14. Liu, F.-T., K. Albrandt, J. G. Sutcliffe, and D. H. Katz. 1982. Cloning and nucleotide sequence of mouse immunoglobulin ϵ chain DNA. *Proc. Natl. Acad. Sci. USA 79:7852.*
15. Southern, E. 1975. Detection of specific sequences among DNA fragments separated by gel electrophoresis. *J. Mol. Biol. 98:503.*
16. White, B. A., and F. C. Bancroft. 1982. Cytoplasmic dot hybridization, simple analysis of relative mRNA levels in multiple small cell or tissue samples. *J. Biol. Chem. 257:8569.*
17. Laemmli, U. K. 1970. Cleavage of structural proteins during the assembly of the head of the bacteriophage T4. *Nature 227:680.*
18. Towbin, H., T. Staehelin, and J. Gordon. 1979. Electrophoretic transfer of proteins from polyacrylamide gels to nitrocellulose sheets: procedure and some applications. *Proc. Natl. Acad. Sci. USA 79:4350.*
19. Zanetti, M., M. De Baets, and J. Rogers. 1983. High degree of idiotypic cross-reactivity among murine monoclonal antibodies to thyroglobulin. *J. Immunol. 131:2452.*
20. White-Scharf, M. E., and T. Imanishi-Kari. 1982. Cross-reactivity of the NP^a and NP^b idiotypic responses of BALB/c and C57BL/6 mice to (4-hydroxy-3-nitrophenyl)acetyl (NP). *Eur. J. Immunol. 12:935.*
21. Morrison, D. C., J. F. Rosen, P. M. Henson, and C. G. Cochrane. 1974. Activation of rat mast cells by low molecular weight stimuli. *J. Immunol. 112:573.*
22. Taurog, J. D., G. R. Mendoza, W. A. Hood, R. P. Siraganian, and H. Metzger. 1977. Noncytotoxic IgE-mediated release of histamine and serotonin from murine mastocytoma cells. *J. Immunol. 119:1757.*
23. Ikeyama, S., S. Nakagawa, M. Arakawa, H. Sugino, and A. Kakinuma. 1986. Purification and characterization of IgE produced by human myeloma cell line, U266. *Mol. Immunol. 23:159.*
24. Ishida, N., S. Ueda, H. Hayashida, T. Miyata, and T. Honjo. 1982. The nucleotide sequence of the mouse immunoglobulin ϵ gene: comparison with the human ϵ gene sequence. *Embo J. 1:1117.*
25. Banerji, T., L. Olson, and W. Schaffner. 1983. A lymphocyte-specific cellular enhancer is located downstream of the joining region in immunoglobulin heavy chain genes. *Cell 33:729.*
26. Gillies, S. D., S. L. Morrison, V. T. Oi, and S. Tonegawa. 1983. A tissue-specific transcription enhancer element is located in the major intron of a rearranged immunoglobulin heavy chain gene. *Cell 33:717.*
27. Kemp, D. J., A. W. Harris, S. Cory, and J. M. Adams. 1980. Expression of the immunoglobulin Cμ gene in mouse T and B lymphoid and myeloid cell lines. *Proc. Natl. Acad. Sci. USA 77:2876.*
28. Kemp, D. J., A. W. Harris, and J. M. Adams. 1980. Transcripts of the immunoglobulin Cμ gene vary in structure and splicing during lymphoid development. *Proc. Natl. Acad. Sci. USA 77:7400.*
29. Alt, F. W., N. Rosenberg, V. Enea, E. Siden, and D. Baltimore. 1982. Multiple immunoglobulin heavy-chain gene transcripts in Abelson murine leukemia virus-transformed lymphoid cell lines. *Mol. Cell Biol. 2:386.*
30. Nelson, K. J., J. Haimovich, and R. P. Perry. 1983. Characterization of productive and sterile transcripts from the immunoglobulin heavy-chain locus: processing of μ_m and μ_s mRNA. *Mol. Cell. Biol. 3:1317.*
31. Neuberger, M. S. 1983. Expression and regulation of immunoglobulin heavy chain gene transfected into lymphoid cells. *Embo J. 2:1373.*
32. Ochi, A., R. G. Hawley, M. J. Shulman, and N. Hozumi. 1983. Transfer of a cloned immunoglobulin light-chain gene to mutant hybridoma cells restores specific antibody production. *Nature 302:340.*
33. Kobrin, B. J., C. Milcarek, and S. L. Morrison. 1986. Sequences near the 3' secretion-specific polyadenylation site influence levels of secretion-specific and membrane-specific IgG2b mRNA in myeloma cells. *Mol. Cell. Biol. 6:1687.*
34. Levine, B. B., and N. M. Vaz. 1970. Effect of combinations of inbred strain, antigen, and antigen dose on immune responsiveness and reagin production in the mouse. *Int. Arch. Allergy 39:156.*
35. Watanabe, N., S. Kojima, and Z. Ovary. 1976. Suppression of IgE antibody production in SJL mice. I. Nonspecific suppressor T cells. *J. Exp. Med. 143:833.*
36. Chiorazzi, N., D. A. Fox, and D. H. Katz. 1977. Hapten-specific IgE antibody responses in mice. VII. Conversion of IgE "non-responder" strains to IgE "responders" by elimination of suppressor T cell activity. *J. Immunol. 118:48.*
37. Morrison, S. L., M. J. Johnson, L. A. Herzenberg, and V. T. Oi. 1984. Chimeric human antibody molecules: mouse antigen-binding domains with human constant region domains. *Proc. Natl. Acad. Sci. USA 81:6851.*

Transfectomas Provide Novel Chimeric Antibodies

Sherie L. Morrison

Summary. Methods have been developed to transfect immunoglobulin genes into lymphoid cells. The transfected genes are faithfully expressed, and ass mbly can occur both between the transfected and endogenous chains and betw en two transfected chains. Gene transfection can be used to reconstitute immunoglobulin molecules and to produce novel immunoglobulin molecules. These novel molecules can represent unique combinations of heavy and light chains; alternatively, by means of recombinant DNA technology, genes can be assembled in vitro, transfected, and expressed. The end products of such manipulations include chimeric molecules with variable regions joined to different isotypic constant regions; this is possible both within and between species. It is also possible to synthesize altered immunoglobulin molecules, as well as molecules having immunoglobulin sequences fused with nonimmunoglobulin sequences (for example, enzyme sequences).

Nearly 100 years ago it was shown that the antibodies circulating in the serum provided the basis for the immune response. With the development of serum electrophoresis it was possible to demonstrate that these antibodies were protein molecules (*1*). Many years of research have revealed that antibodies are responsible for specific protection against bacterial and viral diseases and are involved in normal and disease-related immune reactions, including inflammation, autoimmunity, graft rejection, and idiotype-mediated network regulation. Antibodies have also proven to be invaluable, exquisitely sensitive reagents for the location, identification, and quantification of antigens in many different assay systems.

The advent of hybridoma technology in 1975 made it possible to obtain antibodies of a defined specificity in large quantities (*2*). However, limitations persisted, and it was not always possible to generate antibodies with the precise specificity desired or with the appropriate combination of specificity and effector functions. In addition, hybridomas cannot be produced with equal ease from all species; in particular, human hybridoma antibodies have been difficult to obtain. Thus, an exciting recent advance has been the development of transfectomas, in which a combination of recombinant DNA techniques and gene transfection can be used to create novel, chimeric immunoglobulin molecules.

Structural Basis of Antibody Function

Two functions are characteristic of every antibody molecule: (i) specific binding to an antigenic determinant, and (ii) participation in effector functions, such as binding and activation of complement, stimulation of phagocytosis by macrophages, and triggering of granule release by mast cells. The specific binding of antigen by antibodies is determined by the structure of the variable regions of both heavy (V_H) and light (V_L) chains (see Fig. 1). The effector functions are determined by the structure of the constant region (C) of the heavy chains. Immunoglobulins (Ig's) with different constant regions—that is, Ig's of differing isotypes (in the human IgM, IgD, IgG_1, IgG_2, IgG_3, IgG_4, IgA_1, IgA_2, and IgE)—therefore exhibit different biologic properties. Antibodies are glycoproteins, and the presence of carbohydrate on the antibody molecule is essential for some of the effector functions of antibodies (*3*). Cleavage with the enzyme papain splits the Ig molecule into an Fab region that can bind antigen and into an Fc region containing the effector functions (Fig. 1).

Both the heavy and light chains are encoded by multiple DNA segments. A functional Ig gene is generated only after somatic rearrangement of distinct DNA segments (*4*). In the functional Ig gene, intervening sequences separate the hydrophobic leader sequence from the variable region and also the variable-region gene segment from the constant region; in addition, intervening sequences separate the different domains of the constant region in heavy chains so that each functional region of the heavy chain constant region is on a separate exon (Fig. 1).

In the past, structural and functional studies of Ig molecules were complicated by the heterogeneity of the molecules. Because antibodies present in an antiserum are a mixture of specificities, antisera of defined specificities were difficult to obtain in large quantities. These problems were solved to a certain degree when it was realized that the disease multiple myeloma represents a mon clonal proliferation of plasma cells and that large quantities of homogeneous antibodies could be obtained. The majority of what is known about the structure of antibody molecules and the organization of Ig genes has come from the study of these myeloma proteins and cells. Unfortunately, only a few of the myeloma proteins can be demonstrated to bind known antigens, so their usefulness as specific reagents is severely limited.

Monoclonal antibodies of defined specificity became available when Köhler and Milstein demonstrated that cultured mouse myeloma cells could be fused to spleen cells from immunized mice (*2*). The hybrid cells (hybridomas) grow continuously in culture (property acquired from the myeloma cell) and continue to produce in large quantities the Ig that had been synthesized by the spleen cell partner. These antibody molecules are monoclonal; hence, they have an advantage over classical antisera in that their combining sites are homogeneous. However, the fact that the Ig produced by one hybridoma is of only one isotype can be a problem if the isotype expressed does not have the effector function, such as complement fixation or binding of staphylococcal protein A, required for a certain assay.

The large quantities of chemically defined antibodies produced by hybridomas have been invaluable tools for immunologists, but they do have certain limitations. Although hybridoma proteins that bind defined antigen can be identified, the affinity of the binding cannot be determined by the researcher.

Sherie L. Morrison is a professor of microbiology at the Cancer Center/Institute for Cancer Research, Columbia University College of Physicians and Surgeons, New York 10032.

Furthermore, the isotype of the antibody is determined by the constant region gene being used by the normal cell at the time of fusion.

An additional problem associated with hybridomas is their species limitations. While it is relatively easy to produce mouse or rat monoclonal antibodies, it is difficult to produce human monoclonal antibodies, which would be desirable for certain studies and in vivo use. Many human hybridomas produce only limited quantities of Ig and are unstable in their production.

The isolation of somatic mutants of hybridoma cells has provided investigators with additional capabilities. Cell lines with both decreased and increased affinity for antigen can be isolated (*5*). In addition, it is possible to isolate somatic mutants with alterations in their Fc regions (*6*). These mutations may be either structural changes in the Fc region or may represent isotype switch mutants. Switch variants have permitted an assessment of the contribution of the hinge region to the segmental flexibility of Ig molecules (*7*).

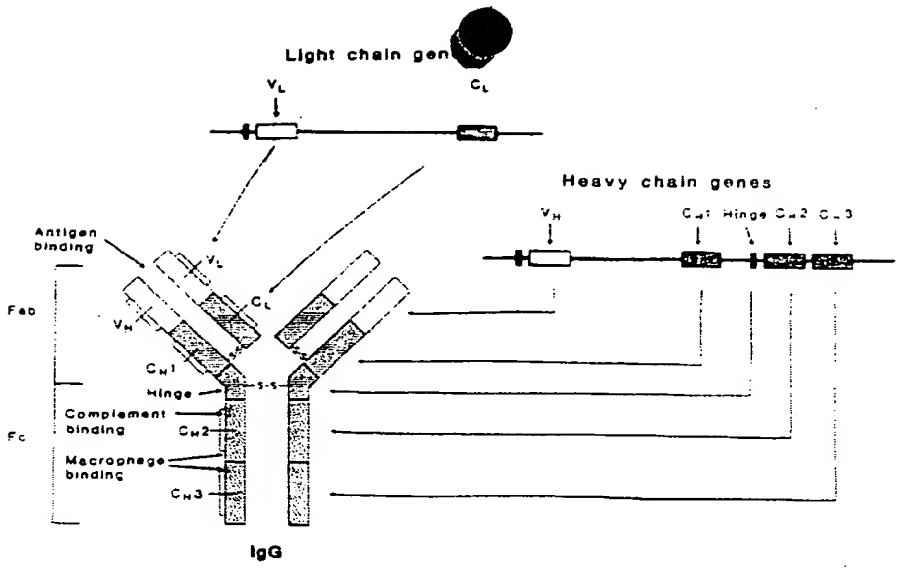

Fig. 1. Structure of an Ig molecule and the genes that encode it. The regions of the molecule that participate in antigen binding (Fab) or different effector functions (Fc) are indicated. Arrows indicate the correspondence between the DNA segments and the different domains of the Ig polypeptide chain that they encode. The hydrophobic leader sequence of both heavy and light chains is removed immediately after synthesis and is not present in the mature immunoglobulin molecule.

Ig Gene Transfection into Lymphoid Cells

Gene transfection provides a method for making novel Ig molecules (Fig. 2). Ig genes, either wild-type or altered in vitro, can be transfected and expressed (*8, 9*). The transfected cells (transfectomas) grow continuously in culture and produce the Ig specified by the transfected gene. This approach has the advantage over the isolation of mutants that alteration can be predetermined and does not depend on the chance occurrence of the desired changes.

The expression of transfected genes can be studied transiently (a few days after transfection) or stable transfectants in which the transfected gene has integrated into the chromosome can be isolated. If the objective is to produce a new protein, stable transfectants need to be isolated to provide a continuous source of the protein. Because only a small percentage (10^{-3} to 10^{-6}) of the cells exposed to foreign DNA go on to become stably transformed, selective techniques are required that permit the isolation of rare, stably transformed cells from among the many nontransformed cells. Initial experiments used the thymidine kinase gene from herpes simplex virus as the selective marker (*10*). However, this required that the recipient cells be deficient in endogenous thymidine kinase (TK^-); consequently, only a few available cell lines lacking thymidine kinase could be used as recipients.

To overcome these limitations, vectors with dominant selectable markers have been developed (*11–13*). Dominant-acting genetic markers produce a selectable change in the phenotype of normal cells; such markers have been produced by placing bacterial genes within mammalian transcription units. The most commonly used vectors have been the pSV2 vectors (*11*), in which the selectable marker is placed under the control of the SV40 early promoter; SV40 sequences provide splice signals and a polyadenylation site.

Two selectable bacterial genes have been used: (i) the xanthine-guanine phosphoribosyltransferase gene (*gpt*) (*12*), and (ii) the phosphotransferase gene from Tn5 (designated *neo*) (*13*). Selection with *gpt* is based on the fact that the enzyme encoded by this gene can use xanthine as a substrate for purine nucleotide synthesis, whereas the analogous endogenous enzyme cannot. Thus, for cells provided with xanthine and in which the conversion of inosine monophosphate to xanthine monophosphate is blocked by mycophenolic acid (*14*), only cells expressing the bacterial gene can survive. The product of the *neo* gene inactivates the antibiotic G418 (*15, 16*), which interferes with the function of 80*S* ribosomes and blocks protein synthesis in eukaryotic cells. The two selection procedures depend on two entirely different mechanisms; therefore, they can be used simultaneously to select for the expression of genes introduced on two different DNA segments. Alternatively, they can be used to select for the expression of different genes introduced sequentially into cells.

The recipient cell type of choice for the production of Ig molecules would appear to be myeloma cells. Myelomas represent malignancies of plasma cells, and they are capable of producing large quantities of Ig. Expression of transfected heavy chain genes by myelomas approaches the level seen for the endogenous myeloma protein (*17, 18*). Expression of light chain genes after transfection has been more of a problem, and frequently it is only 5 to 10 percent of that seen in myeloma cells expressing the same gene (*19*). However, it has been possible to identify transfectants in which the synthesis of both the light and heavy chain of the functional Ig molecule has been directed by a transfected gene (*20–22*).

Several methods exist for introducing DNA into eukaryotic cells. Calcium phosphate precipitation is routinely used to introduce DNA into many cell types (*10, 23, 24*). However, this technique results in a low frequency of recovery of transfectants from myeloma cells (*9*). A more efficient way of introducing DNA into lymphoid cells is by protoplast fusion (*9, 24*). In this method, lysozyme is used to remove the bacterial cell walls from *Escherichia coli* bearing the plasmids of interest (*9, 24*), and the resulting spheroplasts are fused with myeloma cells by means of polyethylene glycol. After protoplast fusion, stable transfectants have been isolated at frequencies

ranging from 10^{-4} to 10^{-3} (*9*, *17*, *20*). Recent results have suggested that electroporation may also be an efficient method for introducing DNA into lymphoid cells (*25*). For electroporation, a high-voltage pulse is applied to cells in suspension in the presence of DNA. Stable transfectants have been isolated from many different cell types at frequencies as high as 3×10^{-4}.

Variations in transfectability have been observed among the different myeloma cell lines and among different clones of the same myeloma cell line. The cause of the variations in unknown. The myeloma J558L, which produces λ light chains and no heavy chains, is among the best recipient cell lines. With the appropriate vectors, it can be transfected with efficiencies approaching 10^{-3} (*9*, *17*, *26*, *27*). However, J558L has the disadvantage that it continues to synthesize its own λ light chain; it has been impossible to isolate nonproducing variants of J558L. Although some nonproducing myelomas, such as SP2/0, have been transfected, the transfection frequencies are 10^{-1} to 10^{-2} of that seen with J558L.

Expression of Transfected Genes

It is necessary to prove that the proteins synthesized after gene transfection are the same as those synthesized in myeloma cell lines. When the MOPC-41 κ light chain was introduced into a cell line that had been transformed with Abelson murine leukemia virus, the cells directed the synthesis of a κ chain that could assemble with the endogenous γ_{2b} heavy chain to produce molecules containing two heavy and two light chains (H_2L_2) (*8*). The light chain produced after the transfection of the S107A κ chain was identical, by two-dimensional gel analysis, to the S107A myeloma κ chain (*9*). The S107A light chain is not secreted by light chain–producing variants of this myeloma; a transfected S107A light chain was also not secreted when introduced into a myeloma that did not produce any heavy chain. However, when the S107A κ chain was introduced into a hybridoma cell line that synthesized a heavy chain, it assembled with the endogenous heavy chain to produce H_2L_2 molecules; these H_2L_2 molecules were secreted.

By means of genes isolated from a trinitrophenyl (TNP)-binding hybridoma, the faithful expression of transfected genes with the retention of the original antigen-binding specificity was seen (*20*, *28*). Transfection of the light chain from this hybridoma into a cell line that synthesized the TNP-specific heavy chain, but that had lost the abiiity to synthesize the TNP-specific light chain, resulted in the synthesis of a complete H_2L_2 molecule with the ability to bind antigen. This TNP-specific IgM was secreted by the transfected cells, and the hemagglutination titer of antibody to TNP (anti-TNP) in some transformants was comparable to that of the parental anti-TNP–producing hybridoma. Conversely, by transferring a μ heavy chain gene from an anti-TNP–specific myeloma into a light chain–producing variant of that myeloma, it was also possible to express a pentameric IgM molecule with anti-TNP activity. Simultaneous transfer of specific light and heavy chains into a nonproducing myeloma also resulted in the production of pentameric, antigen-binding antibody, although in this case the amount of antibody synthesized was less than that seen in the parental myeloma.

Gene transfection can be used to identify tissue-specific regulatory elements.

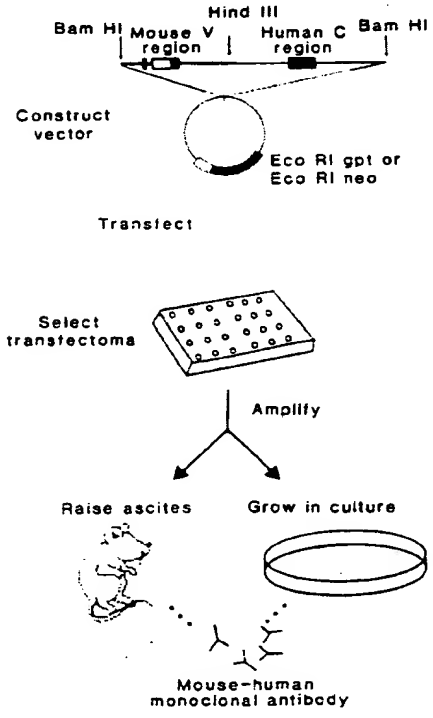

Fig. 2. Steps in production of chimeric Ig molecules. First, a chimeric gene containing the sequences of interest is ligated into an expression vector containing a selectable marker. Then, this vector is transfected into the appropriate recipient cell line, and stable transfectants synthesizing the genes of interest are identified; if vectors are used with independent selectable markers, transfectants synthesizing more than one novel chain can be isolated. Finally, the chimeric proteins are isolated either from tissue culture or from the ascitic fluid of tumor-bearing mice.

A segment of DNA located between J_4 and the switch region in the major intervening sequence of a heavy chain gene is necessary for the expression of heavy chain genes transfected in lymphoid cells of the B lineage (*17*); this region does not influence the expression of Ig genes transfected into L cells (*29*). The location of this DNA segment 5′ of the switch site guarantees that the segment will remain associated with the expressed variable region gene during isotype switching and is consistent with the segment having a regulatory role. However, cell lines have been reported in which deletion of this segment does not abolish heavy chain synthesis (*30*). Therefore, a question remains as to relationship between the sequences needed for the expression of transfected genes and those needed for the expression of endogenous genes.

Controlling regions have been identified in the major intervening sequence of κ light chains. A mouse sequence lying approximately 600 base pairs 5′ of C_κ enhanced production of κ chain genes transfected into lymphoid cells (*19*, *31*). Like the heavy chain controlling region, it does not function in nonlymphoid cells. This sequence corresponds to a DNA segment (*32*) that is highly conserved among rabbit, mouse, and man and that becomes sensitive to deoxyribonuclease when Ig is expressed (*33*). In addition, a second DNA segment from the 5′ half of the κ intervening sequence has been identified that facilitates expression of κ genes transfected into mouse myeloma but not into hamster lymphoma cells (*19*, *34*).

Production of Novel Ig Molecules by Gene Transfection

With the demonstration that transfected Ig genes faithfully exhibited the expected properties, it became possible to produce novel Ig molecules. These novel Ig's can be divided into two categories: (i) those synthesizing wild-type Ig chains but in a combination not normally expressed and (ii) those synthesizing molecules with a novel gene structure that has been produced by recombinant DNA techniques (Table 1).

Novel combinations of wild-type heavy and light chains. In vitro reassembly of Ig heavy and light chain polypeptides has been used to create novel heavy-light chain combinations and to study chain interactions (*35*–*37*). This method, however, requires that the original interchain disulfide bonds in the Ig be broken and that heavy and light chains be separated in the presence of denatur-

ing agents. As a result, only a small percentage of the chains renature to produce functional molecules (*36*). On the other hand, chain assembly between transfected gene products occurs within the cell by normal pathways of assembly. Because the assembled molecules have never been subjected to a denaturing step, their structure and function should more accurately reflect those of native molecules.

Experiments either with cell lines transformed by Abelson murine leukemia virus or with hybridomas have indicated that assembly can occur between the transfected and the endogenous Ig chains (Fig. 3) (*8*, *9*), and this has been found to be generally true. When the γ_{2b} heavy chain of the myeloma MPC-11 was transfected into the λ myeloma J558, it was expressed (Fig. 3, lane 3), assembled with the endogenous λ chain, and secreted as H_2L_2 molecules (Fig. 3, lane 4). These novel molecules, in which the MPC-11 heavy chains are associated with λ light chains, have been useful in exploring the relative contribution of V_H and V_L to idiotypic determinants (*38*).

Novel combinations of variable and constant regions. By means of standard recombinant DNA techniques, it is possible to attach any variable region to any heavy chain constant region. The existence of the large intervening sequence between the two regions (see Fig. 1) makes such joining easier. Because the reading frame does not have to be maintained and the intervening sequence will be removed by splicing, many different joints will lead to functional molecules. This approach can be used to produce isotype switch variants of mouse hybridoma proteins.

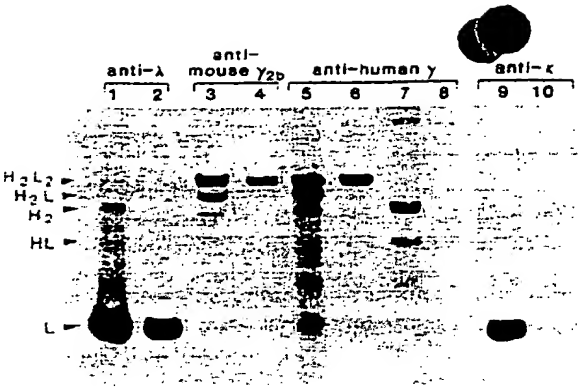

Fig. 3. Synthesis of Ig chains in transfectomas. Cells were labeled with [^{14}C]valine, [^{14}C]threonine, and [^{14}C]leucine for 3 hours, and cytoplasmic lysates and secreted material were immunoprecipitated with the antibodies shown at the top of the figure. (Lanes 1 and 2) J558L; (lanes 3 and 4) J558L containing a transfected MPC-11 γ_{2b} heavy chain; (lanes 5 and 6) J558L containing a chimeric mouse-human heavy chain; (lanes 7 and 8) nonproducing myeloma cells containing a chimeric mouse-human heavy chain; and (lanes 9 and 10) V_HC_κ in light chain–producing variant of anti-phosphocholine myeloma S107. Lanes 1, 3, 5, 7, and 9 represent cytoplasmic extracts; lanes 2, 4, 6, 8, and 10 represent secreted material.

Another family of molecules can be created in which the variable regions from the heavy and light chains of a mouse myeloma are joined to human constant regions (Fig. 2). These molecules have the antigen-binding specificity of the mouse hybridoma, but they should exhibit the effector function associated with the human constant regions and should be less antigenic in humans than are totally mouse antibodies.

Initially, the variable region from the heavy chain of the anti-phosphocholine myeloma S107 was joined to either human γ_1 or γ_2 heavy chain (*21*). After transfection into J558L, the chimeric gene was expressed (Fig. 3, lane 5), the chimeric heavy chain was assembled with the endogenous λ chain, and H_2L_2 molecules were secreted. The chimeric heavy chain was also expressed by myeloma cells not synthesizing any light chains (nonproducing) (Fig. 3, lane 7); however, these heavy chains were not secreted (Fig. 3, lane 8).

Subsequently, the antigen-specific light chain of S107 was joined to human C_κ and ligated into the pSV2neo vector, and transfectants synthesizing both chimeric heavy and light chains were identified (*21*). The chimeric heavy and light chains of the expected molecular weight were assembled and secreted as H_2L_2

Table 1. Creation of novel molecules by gene transfection.

Genes used for transfection	Objective	Potential uses
	Wild-type Ig chains	
Wild-type heavy or light chains (or both)	To create new heavy and light chain combinations, both within a species and between species	Explore the nature of heavy and light chain interactions
		Define the relative contributions of each chain to idiotype expression and antigen-binding specificity
		Determine if all chain combinations and thus combinational diversity are possible
	Novel Ig chains	
V_H attached to new C_H; V_L attached to new C_L	To create chains with the same variable region associated with a new isotype	Produce isotype switch variants within one species
		Create cross-species chimerics, with a variable region from one species and a constant region from another
V_H attached to C_L; V_L attached to C_H	To create chains with a variable region attached to an isotype with which it is never associated in vivo	Evaluate contributions of constant regions to functions
		Create molecules with altered effector functions
V_H or V_L attached to a non-Ig sequence	To create fusion proteins	Attach antibody specificity to enzymes for use in assays
		Isolate non-Ig proteins by antigen columns
		Specifically deliver toxic agents

molecules. Comparison of the apparent molecular weights of heavy chains synthesized in the presence and absence of tunicamycin showed that the mouse myeloma cell attaches *N*-linked carbohydrate to the human heavy chain. The chimeric H_2L_2 molecules bound the antigen phosphoch line and were recognized both by monoclonal antibodies specific for human κ chain antibodies and by monoclonal antibodies specific for the idiotype prepared against the mouse myeloma protein. The cells from the transfectoma produced an ascites after being injected into a mouse, and the chimeric proteins were found to be present in the ascitic fluid.

Chimeric human-mouse molecules have also been produced in which the variable regions of the heavy and light chains from an anti-TNP mouse myeloma were linked to human μ and κ genes, respectively, and were transfected into myeloma cells (*22*). The chimeric genes were expressed and assembled such that pentameric IgM was present in the secretions; however, both the chimeric μ and κ chains migrated more slowly than was expected on gels containing sodium dodecyl sulfate. There was no significant difference in affinity for TNP between the mouse and the chimeric IgM's. The chimeric IgM, however, was about one-fourth as effective as the mouse IgM in hemolysis of TNP-coupled sheep red blood cells and showed a displaced binding curve in hapten inhibition assays. The molecular basis for these apparent binding differences remains unclear.

Another chimeric molecule has been produced in which a heavy chain with the variable region of a mouse antibody to 4-hydroxy-3-nitro-phenacetyl (NP) was joined to human ε heavy chain (*27*). This fused segment was transfected into the J558L cell line, which synthesizes a mouse λ light chain identical to that used by mouse antibody to NP. The J558L λ chain assembled with the chimeric heavy chain to produce H_2L_2 molecules, which were secreted and, like human ε, were heavily glycosylated. The chimeric IgE bound NP efficiently and, when the chimeric antibodies were bound to the appropriate receptors on human basophils, antigen was able to stimulate a dose-dependent release of histamine.

Variable regions can also be placed on constant regions with which they would not normally be associated. When the V_H from an anti-azophenylarsonate hybridoma was joined to mouse C_κ and introduced into a mouse myeloma cell, a 25,000-dalton chimeric protein was produced (*39*). When the chimeric V_H-C_κ gene was transfected into a light chain–producing variant of the anti-azophenylarsonate hybridoma from which the gene was isolated, the V_H-C_κ protein was synthesized and assembled with the endogenous V_L-C_κ to yield a secreted light chain heterodimer that bound antigen with the same affinity as the original H_2L_2 hybridoma protein. The light chain heterodimer represents, in essence, an antibody-combining site with no associated effector functions, as light chains by themselves have no known effector function. In a second case in which V_H from the S107 myeloma was joined to Cκ and introduced in a light chain–producing variant of S107, a 25,000-dalton chimeric protein was produced, but heterodimers were not secreted (Fig. 3, lanes 9 and 10).

The V_H from a human myeloma can be joined to mouse C_κ (*40*). Although this human-mouse chimeric protein was produced, it did not assemble with the endogenous λ light chain of the recipient mouse myeloma and remained cytoplasmic. These experiments demonstrated that the human heavy chain promoter can function in mouse myelomas. Additional studies have shown that the human light chain promoter also can function in mouse myeloma cells (*25*). It is thus possible to consider using gene transfection techniques for gene rescue; that is, genes could be cloned from human myelomas or lymphoblastoid lines where they are expressed at low levels and then introduced by gene transfection into mouse myeloma lines. These initial studies suggest that such transfected genes will effectively function to produce high levels of protein.

Gene transfection has also been used to create cell lines synthesizing $F(ab')_2$-like antibody (*26*). [$F(ab')_2$ is two Fab's joined by disulfide bonds (see Fig. 1)]. A chimeric gene was constructed in which the variable region of a mouse NP-binding heavy chain was joined to the C_H1 and hinge regions of mouse γ_{2b}. The fifth exon from the δ heavy chain provided translation termination and polyadenylation signals at the end of the heavy chain. This chimeric gene was transfected into λ_1-producing J558L cells; the λ_1 light chain associated with the NP-specific heavy chains to produce an antigen-binding protein that could be isolated from culture supernatants of transfected cells. The protein had a molecular weight of approximately 110,000 daltons and, on reduction, yielded one band that comigrated with λ light chain and several other bands of higher molecular weight; the predominant species was approximately 31,000 daltons in size. It thus appeared that an $F(ab')_2$-like antibody to NP was synthesized and secreted in large quantities.

Chimeric molecules with Ig sequences joined to non-Ig sequences. Finally, chimeric molecules can be produced in which Ig and non-Ig sequences are joined. The gene for *Staphylococcus aureus* nuclease was inserted into the C_H2 exon of a mouse γ_2 heavy chain specific for NP, and the construction was transfected into J558L cells (*26*). The chimeric heavy chain was produced and assembled with the λ light chain to form an NP-binding protein. Molecules of the appropriate size to be H_2L_2 were isolated from the secretions; these molecules bound the antigen NP and also had nuclease activity that, like the activity of authentic *S. aureus* nuclease, was dependent on Ca^{2+} but not Mg^{2+} ions. On a molar basis, the catalytic activity of the constructed nuclease was about 10 percent of that of authentic *S. aureus* nuclease. Similarly, in another study, the C_H2 and C_H3 domains of the heavy chain were replaced with the third exon of c-*myc*. After transfection into J558L cells, a secreted protein was produced that retained its ability to bind antigen and that was recognized by a monoclonal antibody to c-*myc*. These molecules show the feasibility of making unique combinations of antibody and protein functions that are secreted in large quantities by myeloma cells and retain their ability to bind antigen; hence, they can be rapidly purified on antigen columns.

Expression of Ig Genes in Nonlymphoid Cells

Expression of Ig genes and synthesis of Ig molecules in bacteria provide an alternative to expression in lymphoid cells. Bacteria have been used to make fragments of ε heavy chain that were at least partially biologically active in that they bound to the IgE receptor on basophils (*41–43*). However, heavy chains, light chains, and light chain fragments made in bacteria became insoluble components of inclusion bodies (*42–44*)
er than functionally intact
Assembly did not occur even when
forts were made to promote heavy and light chain assembly by including them within the same bacterium on two different plasmids. Antigen-binding Ig molecules that bound antigen could be produced only by in vitro assembly and at very low yields (*44*). In addition, bacteria have the inherent limitation that they do not glycosylate proteins; therefore, any biologic function of Ig's that depends on carbohydrate would be missing.

Yeast can glycosylate proteins and hence may be preferred over bacteria for Ig expression. Recently, the synthesis in yeast of both λ light chains and μ heavy chains has been reported (*45*); a portion of the μ chains was *N*-glycosylated. Both the λ and μ chains were secreted, and, when μ and λ chains were expressed together, some assembly into antibody molecules that bound antigen occurred. However, the specific activity of antibody molecules isolated from a soluble extract of yeast cells was only about 0.5 percent, indicating that the efficiency of heavy and light chain assembly into functional molecules was low.

Future Perspectives and Applications

The initial experiments demonstrated the feasibility of producing novel Ig molecules by gene transfection. Myeloma cells appear to be the best recipient for the Ig genes because the transfected Ig genes are faithfully transcribed, translated, and glycosylated in them. The antibody components are synthesized in large amounts and can be assembled either with endogenous Ig chains or with other transfected chains to produce functional molecules. Nonlymphoid cells synthesize only small amounts of Ig, and both bacteria and yeast have proved to be inefficient in assembling functional Ig molecules.

Chimeric Ig molecules should provide a new family of reagents of wide potential application. Changing the Fc portion of the Ig can alter its ability to bind staphylococcal protein A, to be multivalent, or to fix complement and, therefore, would affect the usefulness of the Ig for many in vitro assays. Molecules with increased or decreased binding affinity can be useful in creating detection assays that have different levels of sensitivity and stringency.

The ability to produce antibody-protein chimeras permits the construction of a molecule with the Fab of an Ig molecule covalently bound to a non-Ig protein. When the Fab is bound to an enzyme, the binding of the Fab to its antigen can be detected by addition of the appropriate substrate. If the Fab is bound to a toxin, it can potentially be used as a specific cytotoxic agent. In addition, chimeric Ig molecules can function to facilitate protein isolation in that the non-Ig protein attached to a functional antibody-combining site can be purified on an antigen column.

In vitro mutagenesis may provide an additional way to generate molecules of altered function. It should be possible to generate molecules lacking only one specific effector function, with the remainder of the molecule intact; to eliminate or generate glycosylation sites; and through small changes in the variable region, to increase or decrease affinity for antigen. In turn, analysis of the exact structure of the mutated region is expected to reveal those areas of the Ig molecules required for effector function or antigen binding.

Human antibodies would clearly be optimal for use in man, but it has been difficult to produce human hybridoma that synthesize large quantities of antibodies with the desired specificities. Mouse antibodies have been used in trial studies for the treatment of certain human diseases. However, on continued use, they frequently elicit an immune response that renders them noneffective (*46*). Chimeric molecules may help solve this problem because molecules in which only the variable region is of nonhuman origin should be much less antigenic than completely foreign molecules. Chimeric molecules may prove useful in antibody-mediated cancer therapy and in the treatment of certain autoimmune diseases (*47*).

Even in the diagnosis or treatment of diseases in which chronic exposure to the treatment agent is not necessary (resulting in fewer anticipated problems with the agent's antigenicity), the use of chimeric molecules would appear to be preferable to the use of totally foreign Ig. Such chimeric antibodies are potentially useful, for example, for the treatment of immunosuppressed individuals who are subject to fatal viremias and of nonimmunized individuals exposed to tetanus who would be treated with horse antitoxin. Use of chimeric molecules also provides a choice of Ig's with the desired effector functions; alternatively, if no effector function is wanted, use of light chain heterodimers of IgA or Fab-type molecules should permit antigen clearing without complement activation. The application of these molecules to many clinical problems should be quite rewarding.

References and Notes

1. A. Tiselius and E. A. Kabat, *J. Exp. Med.* 69, 119 (1939).
2. G. Köhler and C. Milstein, *Nature (London)* 256, 495 (1975).
3. M. Nose and H. Wigzell, *Proc. Natl. Acad. Sci. U.S.A.* 80, 6632 (1983).
4. S. Tonegawa, *Nature (London)* 302, 575 (1983).
5. W. D. Cook and M. D. Scharff, *Proc. Natl. Acad. Sci. U.S.A.* 74, 5687 (1977); W. D. Cook, S. Rudikoff, A. Giusti, M. D. Scharff, *ibid.* 79, 1240 (1982).
6. J.-L. Preud'homme, B. K. Birshtein, M. D. Scharff, *Proc. Natl. Acad. Sci. U.S.A.* 72, 1427 (1975); B. Liesegang, A. Radbruch, K. Rajewsky, *ibid.* 75, 3901 (1978); D. E. Yelton and M. D. Scharff, *J. Exp. Med.* 156, 1131 (1982); C. Muller and K. Rajewsky, *J. Immunol.* 131, 977 (1983).
7. V. T. Oi *et al.*, *Nature (London)* 307, 136 (1984).
8. D. Rice and D. Baltimore, *Proc. Natl. Acad. Sci. U.S.A.* 79, 7862 (1982).
9. V. T. Oi, S. L. Morrison, L. A. Herzenberg, P. Berg, *ibid.* 80, 825 (1983).
10. M. Wigler *et al.*, *Cell* 11, 223 (1977); A. Pellicer, M. Wigler, R. Axel, S. Silverstein, *ibid.* 14, 133 (1978).
11. R. C. Mulligan and P. Berg, *Science* 209, 1422 (1980).
12. R. C. Mulligan and P. Berg, *Proc. Natl. Acad. Sci. U.S.A.* 78, 2072 (1981).
13. P. J. Southern and P. Berg, *J. Mol. Appl. Genet.* 1, 327 (1982).
14. T. J. Franklin and J. M. Cook, *Biochem. J.* 113, 515 (1969).
15. J. Davies and A. Jiminez, *Am. J. Trop. Med. Hyg.* 29 (5) (suppl.), 1089 (1980).
16. J. Davies and D. I. Smith, *Annu. Rev. Microbiol.* 32, 469 (1978).
17. S. D. Gillies, S. L. Morrison, V. T. Oi, S. Tonegawa, *Cell* 33, 717 (1983).
18. S. L. Morrison, L. A. Wims, B. Kobrin, V. T. Oi, *Mt. Sinai J. Med.*, in press.
19. S. L. Morrison and V. T. Oi, in *Transfer and Expression of Eukaryotic Genes*, H. Ginsberg and H. Vogel, Eds. (Academic Press, New York, 1984), p. 93.
20. A. Ochi, R. G. Hawley, M. Shulman, N. Hozumi, *Nature (London)* 302, 340 (1983).
21. S. L. Morrison, M. J. Johnson, L. A. Herzenberg, V. T. Oi, *Proc. Natl. Acad. Sci. U.S.A.* 81, 6851 (1984).
22. G. L. Boulianne, N. Hozumi, M. J. Shulman, *Nature (London)* 312, 643 (1984).
23. F. L. Graham and A. J. van der Erb, *Virology* 52, 456 (1973); G. Chu and P. A. Sharp, *Gene* 13, 197 (1981).
24. R. M. Sandri-Goldin, A. L. Goldin, M. Levine, J. C. Glorioso, *Mol. Cell. Biol.* 1, 743 (1981).
25. H. Potter, L. Weir, P. Leder, *Proc. Natl. Acad. Sci. U.S.A.* 81, 7161 (1984).
26. M. S. Neuberger, G. T. Williams, R. O. Fox, *Nature (London)* 312, 604 (1984).
27. M. S. Neuberger *et al.*, *ibid.* 314, 268 (1985).
28. A. Ochi *et al.*, *Proc. Natl. Acad. Sci. U.S.A.* 80, 6351 (1983).
29. S. D. Gillies and S. Tonegawa, *Nucleic Acids Res.* 11, 7981 (1983).
30. M. Wabl and P. D. Burrows, *Proc. Natl. Acad. Sci. U.S.A.* 81, 2452 (1984); D. M. Zeller and L. A. Eckhardt, *ibid.* 82, 508 (1985).
31. C. Queen and D. Baltimore, *Cell* 33, 741 (1983).
32. L. Emorine, M. Kuehl, L. Weir, P. Leder, E. E. Max, *Nature (London)* 304, 447 (1983).
33. T. G. Parslow and D. K. Granner, *ibid.* 299, 449 (1982); S.-Y. Chung, V. Folsom, J. Wooley, *Proc. Natl. Acad. Sci. U.S.A.* 80, 2427 (1983); T. G. Parslow and D. K. Granner, *Nucleic Acids Res.* 11, 4775 (1983).
34. S. L. Morrison, K. P. Sun, V. T. Oi, unpublished observations.
35. B. N. Majula, C. P. J. Glaudemans, E. B. Mushinski, M. Potter, *Proc. Natl. Acad. Sci. U.S.A.* 73, 932 (1976).
36. D. M. Kranz and E. W. Voss, Jr., *ibid.* 78, 5807 (1981).
37. C. Horne, M. Klein, I. Polidonlis, K. J. Dorrington, *J. Immunol.* 129, 660 (1982).
38. C. Victor-Kobrin and C. Bona, unpublished observations.
39. J. Sharon *et al.*, *Nature (London)* 309, 364 (1984).
40. L. K. Tan, V. T. Oi, S. L. Morrison, *J. Immunol.*, in press.
41. T. Kurokawa *et al.*, *Nucleic Acids Res.* 11, 3077 (1983).
42. J. Kenten, B. Helm, T. Ishizaka, P. Cattini, H. Gould, *Proc. Natl. Acad. Sci. U.S.A.* 81, 2955 (1984).
43. F.-T. Lui, K. A. Albrandt, C. G. Bry, T. Ishizaka, *ibid.*, p. 5369.
44. M. A. Boss, J. H. Kenten, C. R. Wood, J. S. Emtage, *Nucleic Acids Res.* 12, 3791 (1984).
45. C. R. Wood *et al.*, *Nature (London)* 314, 446 (1985).
46. R. L. Levy and R. A. Miller, *Annu. Rev. Med.* 34, 107 (1983).
47. M. K. Waldor *et al.*, *Science* 227, 415 (1985).

48. I would like to acknowledge the invaluable contribution of V. T. Oi to the collaborative experiments on the production of chimeric human-mouse antibody molecules, of L. Wims for assistance in performing many experiments discussed here, and of B. Newman for assistance with and critical comments on the manuscript. Supported by grants from the National Institutes of Health (CA 16858, CA 22736, CA 13696, and AI 19042) and the American Cancer Society (IMS-360) and a research career development award (AI 00408).

COS cell transfection V_1C_K + $V_1\delta_2$

purpose: To cotransfect COS cells with the light chain & δ_2 heavy chain to see if a fully assembled antibody will be produced.

procedure:

1. 6 - 6cm dishes seeded with 5×10^5 COS cells each

1. cells ~ 70-80% confluent + appear healthy
   media changed to 4ml (DMEM + 10% gFCS + pen/strep)

2. Transfection mixes:

	DNA (20 ug)	dH_2O	Ca^{++} (2.5M)
mock	—	225 ul	25 ul
G CD4	20 ul	205	
$HCD\delta_2$	44 ul	181	
V_1C_K	61 ul	164	
$V_1\delta_2$	26 ul	199	
$V_1C_K + V_1\delta_2$	61 ul + 26 ul	138	

- Ca^{++} dropped in slowly to DNA containing tube & tapping
- each DNA/Ca^{++} soln dropped slowly in 450ul 2XBS + bubbled
- RT x 30'
- dropped onto appropriate dish of cells - ½ of even media (450ul)
- 3% CO_2 incubated O.N.

1. media D+ by c.odell → 5% CO_2 incubator

1. Cond media collected and saved at -20°C
2. 2cc of the following put on cells: 10.8cc DMEM met-
   1.2cc 66F FCS
   10 ul pen/strep
   300 ul (3 mCi) ^{35}S met
3. 37°C 5% CO_2 incubator O.N.

JTO

DBrenstein

1. 35S labelled media removed, cell spun out in microfuge, sup saved.
2. 1cc detergent (1% DOC, 1% NP40, 20mM Tris pH 7.4, 20mM NaCl, 2mM MgCl2) added to each, cells scraped c cell scraper → microfuge tube spun x 3', sup → clean tube, 1cc dH2O added, 2ul 100mM AMF 5ul 1mg/ml Tras X added to each stored at -20°c
3. media aliquoted as follows

		ab (2ul)	300ul TNS
1	300ul mock	αT4	↓
2	"	αH	
3	"	αL	
4	300ul vT4	αT4	
5	"	αH	
6	"	αL	
7	~~[illegible]~~ "	OKT4a	
8	300ul HCDT2	αT4	
9	"	αH	
10	"	αL	
11	300ul V.Ce	αT4	
12	"	αH	
13	"	αL	
14	300 ul V.T2	αT4	
15	"	αH	
16	"	αL	
17	300ul V.Ce + V.T2	αT4	
18	"	αH	
19	"	αL	

4. 4°c rotating O.N.

1. 5ul packed PAS beads in 50ul total vol added to each
2. incubated 4°c rotating x 4°
3. washed in 500ul TNS x 3
4. resuspended in 50 ul 1X loading buffer, 2ul BME added boiled x 3' loaded on gels - run at 80mV x 2°
5. gels fixed x 60' enlightning x 30' film exposed.

[signature]

D Bush

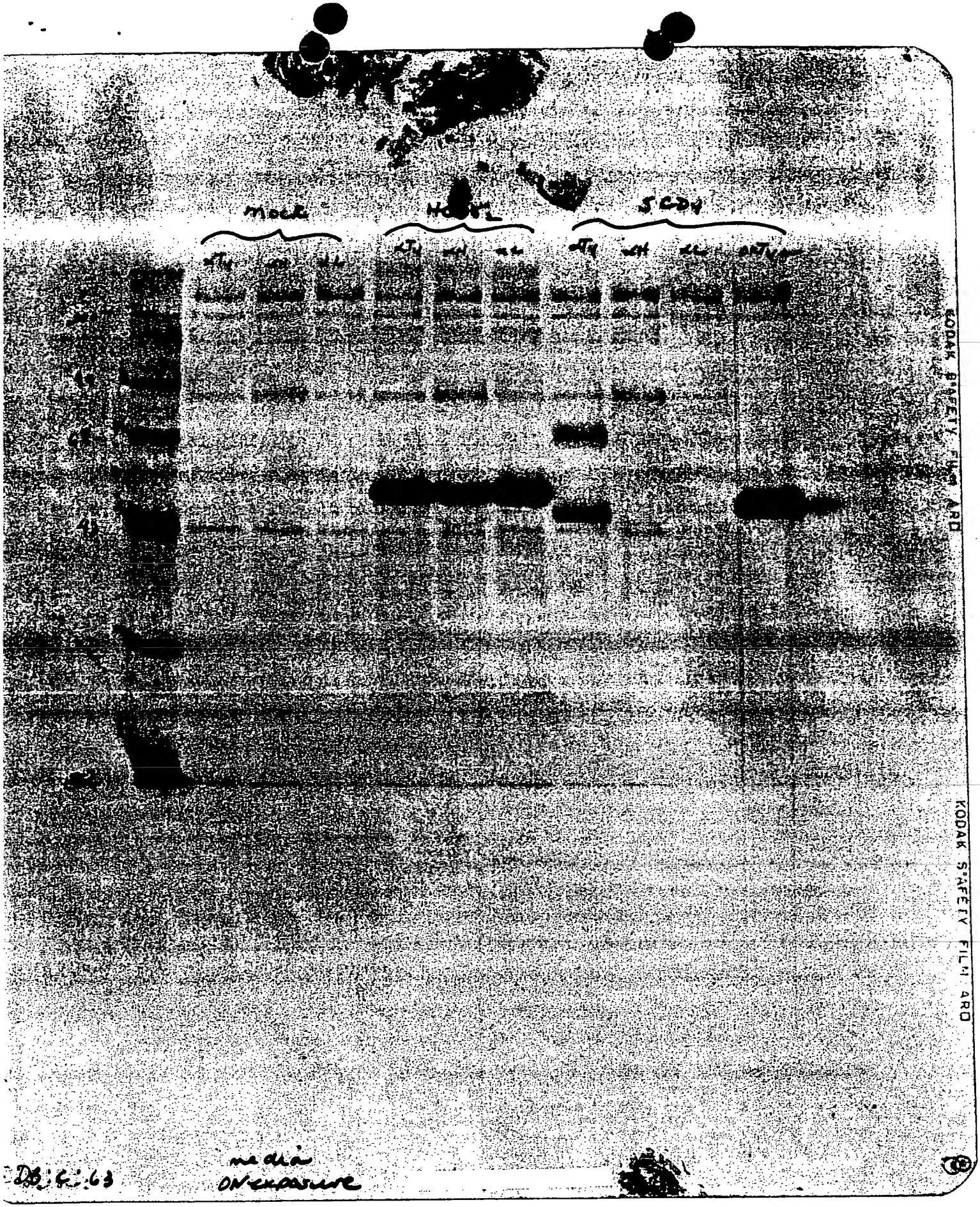

DB: 6-6-3

media
ON exposure

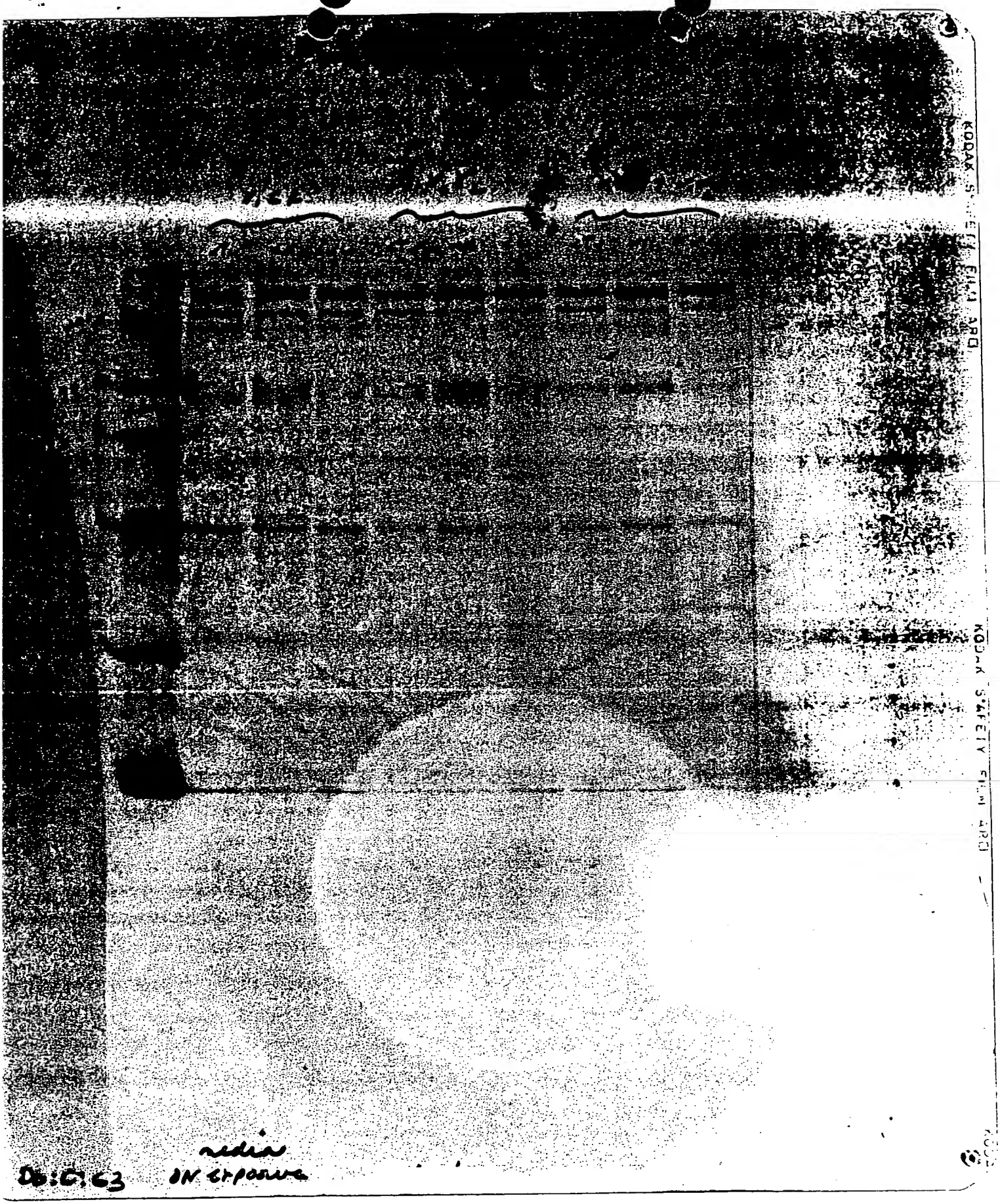

Proc. Natl. Acad. Sci. USA
Vol. 84, pp. 3886–3890, June 1987
Medical Sciences

Expression f functionally active human antithrombin III

ANDREW W. STEPHENS*, ALEEM SIDDIQUI†, AND C. H. W. HIRS*

Departments of *Biochemistry, Biophysics, and Genetics and †Microbiology and Immunology, University of Colorado Health Sciences Center, 4200 East Ninth Avenue, Denver, CO 80262

Communicated by David W. Talmage, February 27 1987 (received for review February 2, 1987)

ABSTRACT **Human antithrombin III cDNA was cloned into an expression vector suitable for transient expression in COS cells. Upon transfection COS cells secreted a single immunoreactive 58-kDa protein. Quantitation of secretion levels by ELISA indicated that at 44 hr posttransfection cells were secreting 48 ± 5 ng of antithrombin III per 10^6 cells per 24 hr. Heparin-agarose chromatography resulted in the elution of the COS-derived protein as a broad band between 0.3 and 1.0 M NaCl. ^{35}S-labeled medium from transfected cells reacted with human thrombin (1.5 ng/ml) in the absence of heparin. In 40 min, >80% of the immunoreactive material was found as a higher molecular weight species, consistent with stoichiometric covalent complex formation. In a two-stage chromogenic thrombin inactivation assay, under pseudo-first-order conditions, at 16 nM antithrombin III the $t_{1/2}$ was 74 min and 50 min for plasma and COS cell-derived antithrombin III, respectively, in the absence of heparin. In the presence of 17.4 nM high-affinity heparin, the $t_{1/2}$ was 5.2 min and 2.2 min, respectively.**

Antithrombin III (AT-III) is one of the primary inhibitors of hemostasis (1–3). It is a plasma glycoprotein of 432 residues and four N-linked carbohydrate moieties comprising 9% of the molecule by weight (1, 4–7). AT-III forms a stoichiometric covalent complex with all the serine proteases of the intrinsic coagulation pathway, including factors XII_a (8), XI_a (9), IX_a (3), X_a (3), and thrombin (10). This complex formation has been shown to take place in a two-step process, presumably through an acyl enzyme intermediate (11). A unique feature of AT-III is that the rate of protease inactivation is greatly accelerated by heparin. It has been shown that there are distinct binding domains on both heparin and AT-III required for activation (12–15) and that heparin induces a conformational change in the inhibitor, detectable by intrinsic fluorescence enhancement and circular dichroism (16, 17), responsible for increasing the affinity of the inhibitor for the protease by nearly 3 orders of magnitude (11).

Human AT-III (hAT-III) has been almost completely sequenced by protein sequencing methods (4), and three groups have cloned and sequenced the human cDNA (5–7). The protein is a member of a superfamily with considerable homology to α_1-proteinase inhibitor and ovalbumin (7, 18, 19). Recently, sequence similarity has been found to thyroxin-binding protein (20) and a 38-kDa protein from cowpox virus (21). hAT-III is synthesized primarily in the liver, with smaller amounts produced in kidney and vascular endothelial cells (22, 23). Functionally active hAT-III is secreted in large quantities by the human hepatoma line Hep-G2 (23). Bock *et al.* have expressed an antigenically reactive polypeptide in *Escherichia coli* (5). Prochownik and Orkin reported the appearance of mRNA in COS and mouse C127 cells transfected with a "minigene" construct (24). However, no synthetic protein was detected. Here we report the expression and secretion of an antigenically reactive protein that is functionally active by three criteria: ability to bind heparin, formation of a stable complex with thrombin, and enhancement of thrombin inactivation rate by heparin.

MATERIALS AND METHODS

Enzymes. Restriction endonucleases, T4 DNA polymerase, and T4 DNA ligase were purchased from Boehringer Mannheim. All enzymes were used under conditions stipulated by the manufacturer. Human thrombin, 99% active as determined by active-site titration, was a generous gift of J. W. Fenton II (New York State Department of Health, Albany, NY).

Heparin-Agarose. Crude porcine mucosal heparin (Diosynth) was purified by repeated cetylpyridinium chloride precipitation (25) and attached to CNBr-activated Sepharose 4B (Pharmacia) at pH 10.5 by the method of Porath (26).

hAT-III. hAT-III was prepared in homogeneous form by chromatography on heparin-Sepharose and DEAE-cellulose (9, 27). The protein was determined spectrophotometrically at 280 nm using $E^{1\%}$ per cm of 6.5 (28).

hAT-III Agarose. Highly purified hAT-III was attached to CNBr-activated Sepharose-4B as described above at pH 7.5 to a concentration of 3 mg per ml of packed gel.

ELISA. Goat anti-hAT-III IgG was purified from antiserum (Atlantic Antibodies, Westbrook, ME) by sodium sulfate precipitation and DE-52 chromatography (29). Up to 40 mg of the IgG fraction was applied to a 5-ml hAT-III-agarose column equilibrated with 0.01 M NaP_i, pH 7.5/0.5 M NaCl. The column was washed with the same buffer until baseline A_{280} was reached, followed by elution with 0.1 M glycine hydrochloride (pH 2.5). Fractions were collected into tubes containing 2 vol of 1.0 M NaP_i (pH 8.0). Those containing specific IgG were pooled, dialyzed at 4°C into NaCl/P_i, and concentrated. The column was immediately returned to its equilibration buffer. The crude IgG contained 10–12% anti-hAT-III-specific antibodies. Two milligrams of the specific IgG underwent reaction for 16 hr at 4°C with 4 mg of horseradish peroxidase (Sigma) previously activated by overnight incubation with 1.25% glutaraldehyde (30). Enzyme conjugate was dialyzed into NaCl/P_i/50% (vol/vol) glycerol and stored at −20°C.

ELISA was performed by standard procedures. Goat anti-hAT-III IgG was applied to each well of a 96-well microtiter plate (Nunclon; Scientific Resource Associates, Bellevue, WA) at 1 μg/ml for 16 hr followed by at least a 3-hr block with bovine serum albumin (0.5 mg/ml)/ovalbumin (0.5 mg/ml). After the initial antibody attachment, all steps except the color reaction were carried out in NaCl/P_i/0.5% Tween 20. After blocking, antigen standards or samples were added and incubated from 1 to 16 hr, followed by extensive washing. A predetermined 1:50,000 dilution of anti-hAT-III-peroxidase conjugate was incubated for 1–3 hr, again followed by extensive washing. *o*-Phenylenediamine (20 μg/ml)

The publication costs of this article were defrayed in part by page charge payment. This article must therefore be hereby marked "*advertisement*" in accordance with 18 U.S.C. §1734 solely to indicate this fact.

Abbreviations: AT-III, antithrombin III; hAT-III, human antithrombin III; SV40, simian virus 40.

(Sigma) containing 0.006% hydrogen peroxide was used as the substrate. The reaction was quenched after 15 min with 2 M H_2SO_4. A_{492} was read in an automated plate reader [Dynatech (Alexandria, VA), MR600]. The standard plot was linear from 10 to 500 pg of antigen per ml.

Immunoblot Transfer Analysis. NaDodSO$_4$/7% polyacrylamide gels were electrotransferred onto Nylon sheets (ICN) at 1 A for 1.5 hr. Bands were visualized using the Promega Biotec (Madison, WI) gt11 system (Protoblot) substituting the anti-β-galactosidase–antibody conjugate with goat anti-hAT-III–alkaline phosphatase conjugate (Atlantic Antibodies) at a 1:1000 dilution.

Construction of pAd-AT-III. The mammalian expression vector was derived from pQ3 [p91023, through the courtesy of R. Kaufman, Genetics Institute, Boston (31)]. pMLAd contains the *Eco*RI/*Sal* I fragment of pQ3 including the adenovirus-associated (*VA*) genes [shown to enhance the translational efficiency of viral as well as nonviral mRNAs in a transient expression assay (32)], the simian virus 40 (SV40) origin of replication and enhancer elements, the adenovirus major late promoter, and the tripartite leader sequences with a 5′ and 3′ splice site derived from an immunoglobulin gene. It does not contain the dihydrofolate reductase cDNA, the tetracycline-resistance gene, or the *E. coli* origin of replication of pQ3. Instead, the latter two are replaced by the ampicillin-resistance gene and origin of replication from pML [kindly provided by M. Botchan, University of California, Berkel y (33)]. This modified expression vector has been used extensively in our laboratory and shows increased prokaryotic transformation efficiency compared to the parent plasmid while maintaining comparable eukaryotic transfectability.

pH.ATIII, generously provided by S. Woo (Baylor University, Houston), contains the completely sequenced hAT-III cDNA, including the signal sequence, in a pBR322 background (6). The 1.5-kilobase cDNA was removed by *Mst* I/*Pst* I digestion and directionally inserted into the polylinker of pSP65 (Bethesda Research Laboratories) opened at *Hinc*II/*Pst* I sites. The hepatitis B surface antigen polyadenylylation signal sequences (nucleotides 1809–1991) were subcloned into the *Pst* I (blunt-ended with T4 polymerase) and *Hin*dIII sites of pSP-AT-III. The newly formed plasmid was linearized with *Hin*dIII, blunt-ended as before, and *Eco*RI linkers were added. This fragment with *Eco*RI linkers, which contains the hAT-III cDNA and the poly(A) signal of hepatitis B surface antigen, was cloned into the unique *Eco*RI site of pMLAd to produce pAd-AT-III (Fig. 1). Correct orientation and confirmation of intact cDNA was determined by diagnostic restriction digestions.

Cell Culture and Transfection. COS cells were grown in Dulbecco's minimal essential medium (GIBCO) supplemented with 7% calf serum containing penicillin and streptomycin. COS cells were transfected at 40% confluency with 1–2 μg of supercoiled plasmid DNA (twice purified by CsCl ultracentrifugation) per 100-mm plate, by the method of Luthman and Magnusson (34) using DEAE-dextran/chloroquine.

Protein Analysis and Purification. COS cells were radiolabeled with 150–200 μCi of [^{35}S]methionine (800 Ci/mmol; 1 Ci = 37 GBq; Translabel, ICN) per 2.5 ml of serum-free medium. Cells (44 hr posttransfection) were starved for methionine for 30 min followed by addition of radiolabel. After 3 hr, media were brought to normal methionine concentration with unlabeled amino acid. Media were harvested 3 hr later and brought to 1 mM diisopropylphosphorofluoridate (Sigma), clarified by centrifugation at 12,000 × *g* for 10 min, and concentrated 10- to 100-fold over an Amicon PM-30 membrane. Immunoprecipitation was performed by addition of 1% rabbit anti-hAT-III antiserum (Calbiochem or a gift of William Hathaway, Department of Pediatrics, University of Colorado) for 16 hr followed by additi n of formalin-fixed protein A-positive *Staphylococcus aureus* at a predetermined dilution, typically 10- to 20-fold over antiserum volume. After 1 hr at 25°C, the bacterial pellet was washed three times with RIPA buffer (0.1 M NaCl/0.05 M Tris·HCl, pH 7.5/1% Nonidet P-40/1% deoxycholate) and boiled in phosphate-buffered NaDodSO$_4$ reducing sample solution. Alternatively, medium was precipitated with 20% trichloroacetic acid and the precipitate was washed with cold ethanol/ether (1:1) prior to boiling in NaDodSO$_4$-containing sample buffer for gel electrophoresis or applied directly to a heparin-agarose column.

AT-III Activity Assay. The ability of hAT-III to inactivate thrombin was assayed in a two-stage assay using the chromogenic thrombin substrate S-2238 (D-phenylalanylpipecolylarginyl-*p*-nitroanilide) (Kabi-Vitrum). Thrombin, diluted in 0.15 M NaCl/0.1% PEG 6000, was added to a concentration of 1.4 nM to a 16 nM solution in NaCl/P$_i$ of purified hAT-III derived from either plasma or medium from transfected COS cells. Reactions contained either 17.6 nM low molecular weight affinity-fractionated heparin (a gift of S. Olson, Henry Ford Hospital, Detroit) or Polybrene (5 μg/ml) (Aldrich). At various times 50-μl aliquots were removed and added to 1.0 ml of S-2238 (300 μg/ml)/Polybrene (50 μg/ml). The rate of *p*-nitroaniline formation was monitored on a Gilford recording spectrophotometer.

RESULTS

Expression of hAT-III. The construction of the expression vector pAd-AT-III is shown in Fig. 1. In vector pAd-AT-III, the AT-III cDNA is under the transcriptional control elements of the adenovirus major late promoter, the SV40 enhancer sequences and the hepatitis B surface antigen polyadenylylation signal. COS cells are derived from the green monkey kidney cell line CV-1 constitutively expressing SV40 large tumor antigen. Transfected vectors containing a SV40 origin of replication are able to replicate efficiently, resulting in an amplification of cDNA template to drive transcription. Initially, COS cells were transiently transfected with plasmid pAd-AT-III and the parent plasmid pMLAd. Culture medium was immunoprecipitated and analyzed by NaDodSO$_4$/PAGE (36). A 58-kDa protein clearly appeared from pAd-AT-III-transfected COS cells (Fig. 2, lane 2). No corresponding band appeared in samples from culture medium of pMLAd-transfected cells (lane 1). This protein comi-

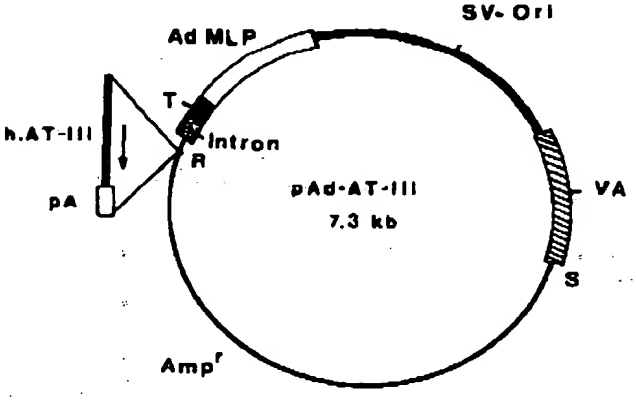

FIG. 1. Construction of expression vector pAd-AT-III (see *Materials and Methods* and *ref.* 35). AdMLP, adenovirus major late promoter; T, tripartite leader; Intron, first intron of mouse immunoglobulin gene with 5′ and 3′ splice sites; SV-Ori, SV-40 origin of replication and enhancer; VA, adenovirus *VA* gene; Amp^r, ampicillin-resistance gene within pML; R, *Eco*RI site; S, *Sal* I site; kb, kilobases.

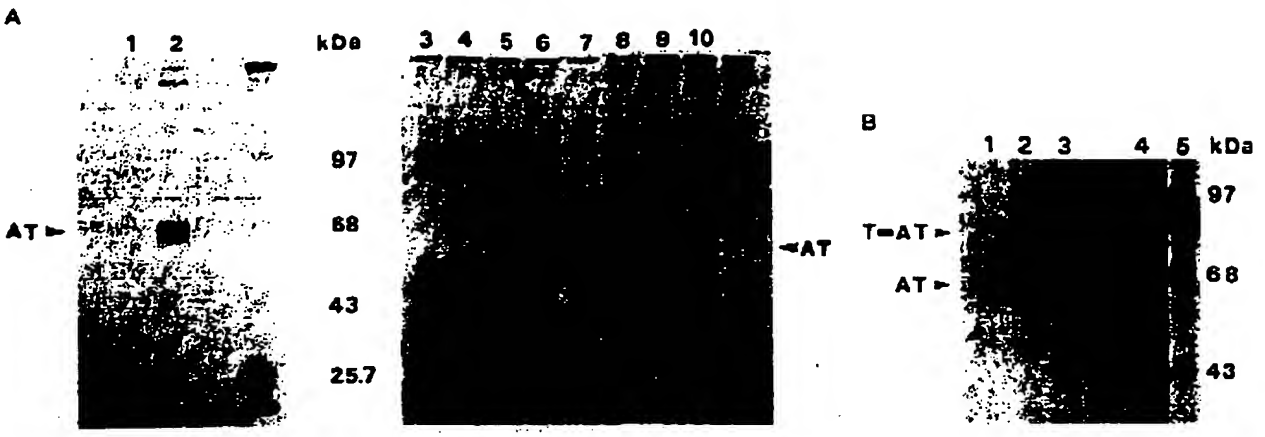

FIG. 2. NaDodSO$_4$/PAGE analysis of hAT-III gene expression in COS cells. (*A*) Immunoprecipitation of culture medium of [^{35}S]methionine-labeled COS cells transfected with pMLAd (lane 1) and with pAd-AT-III (lane 2). Heparin-Sepharose chromatography of ^{35}S-labeled culture medium transfected with either pMLAd (lanes 3, 5, 7, and 9), or pAd-AT-III (lanes 2, 4, 6, 8, and 10). Medium after heparin-Sepharose absorption (lanes 3 and 4); elution from heparin-Sepharose with 0.01 M Tris·HCl, pH 8.1/0.15 M NaCl (lanes 5 and 6); 0.3 M NaCl (lanes 7 and 8); 1.4 M NaCl (lanes 9 and 10). Lanes 3–10 are from trichloroacetic acid precipitates, not immunoprecipitates. (*B*) Immunoprecipitation of medium from ^{35}S-labeled COS/pAd-AT-III (lane 4); medium reacted with thrombin (1.5 μg/ml) at 37°C for 0 min (lane 1) or 40 min (lane 3). Lane 2 represents a 1:1 mixture of lane 1 and lane 3.

grated with plasma-derived AT-III (data not shown). An unidentified high molecular weight doublet was often detected near the origin. Much longer exposure failed to reveal any bands in the control, indicating that COS cells synthesize undetectable amounts of immunocrossreactive protein.

COS cells were labeled and cell lysates were examined by immunoprecipitation (data not shown). Gel electrophoresis indicated that a 46-kDa protein was precipitated in the lysates within 1 hr and that a considerable amount of this presumably unglycosylated hAT-III remained after 3 hr of labeling. This is consistent with a previous report (5) dealing with AT-III expression in a prokaryotic system. In addition, a 3-hr chase with unlabeled methionine completely removed this species with the concomitant increase of the larger 58-kDa protein seen in the medium.

For quantitation of AT-III expression and secretion, unlabeled transfected media were obtained by aspiration from cells at 44 hr posttransfection, washing cells three times with Tris-buffered saline, and culturing the cells in serum-free Dulbecco's minimal essential medium. At various times, media were harvested as described above. Media from three independent transfections assayed by ELISA indicated that under these conditions cells were secreting 48 ± 5 ng of hAT-III per 10^6 cells per 24 hr.

The protein was then examined for functional activity. ^{35}S-labeled media from three plates of COS cells transfected in parallel with either pAd-AT-III or its parent pMLAd were admixed with 1 ml of heparin-agarose equilibrated in Tris-buffered saline. The slurry was held at 25°C for 45 min and loaded into a small column. The heparin-agarose was washed with 10 ml of Tris-buffered saline (0.15 M salt) followed by tw 1-ml washes of 0.3 M NaCl and two 1-ml washes of 1.4 M NaCl (these salt solutions were each buffered to pH 7.5 with 0.01 M Tris·HCl). Flow-through 0.15, 0.3, and 1.4 M NaCl cuts of both pAd-AT-III and pMLAd were precipitated with trichloroacetic acid and subjected to 10% NaDodSO$_4$/PAGE analysis. As shown in Fig. 2, the distinctive 58-kDa protein is absent in all pMLAd lanes (lanes 3, 5, 7, and 9). It is also absent in lanes 4 and 6, representing pAd-AT-III flow-through and 0.15 M NaCl salt cuts, respectively. A small amount of AT-III is observed in the 0.3 M cut (lane 8), while the bulk of the protein elutes in the high-salt cut (lane 10). This experiment clearly shows that there is a protein produced specifically in the pAd-AT-III-transfected cells that comigrates with fully glycosylated hAT-III from plasma. Moreover, this material binds heparin and is eluted from an affinity column at >0.3 M NaCl.

To further investigate this phenomenon, forty 100-mm plates of COS cells were transfected with pAd-AT-III. Forty hours posttransfection cells were washed three times with Tris saline and overlaid with 8 ml of Dulbecco's minimal essential medium per plate without calf serum. This medium was harvested 48 hr later (96 hr posttransfection) and concentrated 10-fold on an Amicon PM-30 membrane. Concentrate was applied to a 5-ml heparin-agarose column equilibrated with 0.02 M NaPO$_4$, pH 7.5/0.05 M NaCl. hAT-III was eluted over 12 hr with a linear 40-ml gradient from 0.05 to 1.0 M NaCl (pH 7.5). Fractions were diluted and assayed by ELISA (Fig. 3). The immunoactive protein eluting at >0.7 M NaCl was pooled, concentrated, dialyzed into NaCl/P$_i$, and subjected to immunoblot analysis (Fig. 3 *Inset*). hAT-III elutes as a broad band on heparin-agarose compared to plasma-derived hAT-III, indicating heterogeneity with respect to heparin binding. The majority of the inhibitor elutes at >0.7 M NaCl. By immunoblot analysis, a single band is observed on NaDodSO$_4$/PAGE and comigrates with plasma-derived hAT-III.

Transfected COS cell-derived hAT-III was then investigated for its ability to form a stable complex with thrombin. To this end, ^{35}S-labeled medium underwent reaction with 1.5 μg of thrombin per ml in the absence of heparin for 0 and 60 min. Reactions were quenched by addition of benzamidine hydrochloride to 10 mM and diisopropylphosphorofluoridate to 1 mM. Samples were immunoprecipitated and fractionated by Weber–Osborn NaDodSO$_4$/PAGE (37). In Fig. 2*B*, lanes 1 and 3 represent the 0- and 60-min time points, respectively. Lane 2 is a 1:1 mixture of the samples from lanes 1 and 3, while lane 4 is a control in the absence of thrombin. This experiment indicates that heterologously produced hAT-III is capable of forming a covalent bond stoichiometrically with thrombin. Gels were run with more time points, indicating that the complex formation was time dependent and accelerated by heparin (data not shown). Quantitation in these studies was complicated in that, for the reaction to occur under pseudo-first-order conditi ns, excess thrombin over AT-III had to be used. Under such conditions, modification

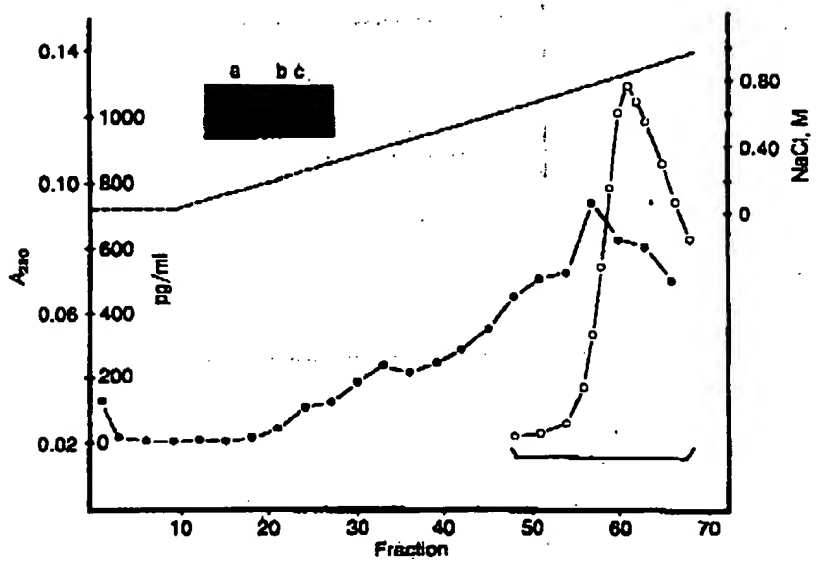

FIG. 3. Heparin-Sepharose chromatography of medium from COS/pAd-AT-III. Serum-free medium from forty 100-mm plates, applied 40 hr posttransfection and harvested at 96 hr posttransfection, was applied to a 5-ml heparin-Sepharose column. Linear gradient elution was from 0.05 M NaCl to 1.0 M NaCl (—), in 0.02 M $NaPO_4$ (pH 7.5). ●, Data from ELISA (in pg/ml). ○, A_{280} from plasma-derived hAT-III (control). (*Inset*) Lane a, immunoblot analysis of pooled fractions 48–68 (bar); lane b, 250 ng of standard hAT-III; lane c, 2.5 μg of standard hAT-III.

of the complexed inhibitor is promoted by virtue of an apparent increase in the reaction stoichiometry, a process aggravated by the presence of excess thrombin and heparin (38, 39).

To circumvent this problem, the ability of hAT-III to inactivate thrombin was investigated in a two-stage chromogenic assay. In this assay, excess AT-III (with or without heparin) is incubated with thrombin under pseudo-first-order conditions. At given times, an aliquot is removed and added to the substrate S-2238 in a cuvette, and the rate of change in A_{405} is measured. COS-derived hAT-III eluting from heparin-agarose at >0.7 M NaCl was quantitated by ELISA. Plasma-derived hAT-III was diluted to the same concentration. Fig. 4 shows a semi-logarithmic plot of the results. In the absence of heparin, thrombin is slowly inactivated with a $t_{1/2}$ of 74 and

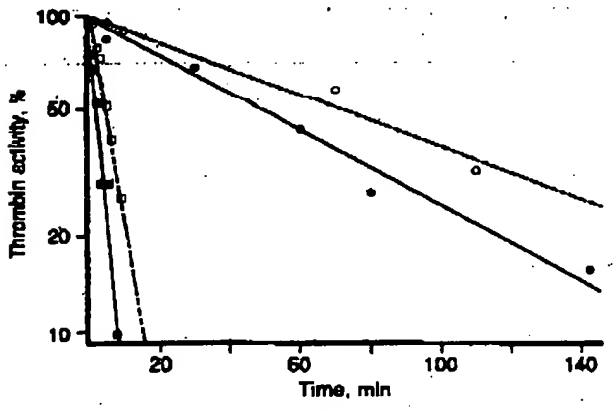

FIG. 4. Inactivation of thrombin by COS-derived hAT-III. hAT-III from serum-free medium of COS/pMLAd-AT-III eluting at >0.7 M NaCl was compared in parallel to a similar concentration (16 nM) of standard plasma-derived hAT-III under pseudo-first-order conditions. ●, COS hAT-III in the absence of heparin; ○, plasma hAT-III in the absence of heparin; ■, COS hAT-III in the presence of 17.6 nM high-affinity heparin; □, plasma hAT-III in the presence of high-affinity heparin.

50 min for plasma and COS-derived hAT-III, respectively. When a 1.1:1 molar equivalent of high-affinity heparin with respect to AT-III is added, the rate of thrombin inactivation is greatly increased. The $t_{1/2}$ in this instance is 5.2 and 2.2 min for the two preparations. This represents a 14- and 23-fold enhancement of the thrombin inactivation rate in the presence of heparin for the plasma and COS-derived hAT-III, respectively. Although this rate enhancement is lower than previously reported by a factor of 6 (11), within our system the rates of inactivation of plasma and COS-derived hAT-III are comparable in both the absence and presence of heparin. The slower rates of inactivation by plasma-derived AT-III can be explained by an underestimation of the concentration of COS-derived AT-III in the ELISA.

DISCUSSION

In this study, we report on the synthesis of hAT-III in COS cells transfected with the cDNA for the inhibitor. Expression was achieved by the use of the expression vector pMLAd, which has the eukaryotic replication and transcription controlling sequences from pQ3 and the prokaryotic replication and drug-resistance sequences from pML. With this hybrid vector, we have achieved a high level of AT-III expression in a transient scheme. The hAT-III produced is secreted into the medium and appears, by molecular weight, to have its carbohydrate moieties intact. Moreover, its comigration with plasma-derived AT-III suggests that the 32-residue signal peptide (6) has been removed. The protein appears in cells 44 hr posttransfection within 1 hr of labeling and is intracellularly turned over within 3 hr. Hep-G2 cells secrete AT-III in quantities that may be estimated from the data of Fair and Bahnak (23) at ≈300 ng per 10^6 cells per 24 hr. The pAd-AT-III-transfected cells in the present study produce AT-III at a rate of 50 ng per 10^6 cells per 24 hr. This rate is constant between 44 and 92 hr posttransfection and would suggest that the transfection efficiency attained is of the order of 15–20%. Secreted hAT-III displays heterogeneity when assayed with respect to heparin binding. While all of the protein binds heparin-agarose at 0.15 M NaCl, it elutes as a broad peak between 0.3 and 1.0 M NaCl. While plasma-

derived AT-III characteristically elutes as an asymmetric band in such gradient elutions (Fig. 3), the COS-derived protein does n t elute with as pronounced an ascending limb as plasma-derived AT-III.

Transfected COS cell-produced hAT-III was also capable of forming a stable covalent complex with thrombin in the absence of heparin. Forty-minute incubations of thrombin with [^{35}S]methionine-labeled medium showed that >80% of the hAT-III was capable of complex formation in that time frame (Fig. 2*B*). This is more than the percentage of the protein that has submaximal heparin binding (Fig. 3), indicating that there is a subpopulation that has thrombin inactivating capacity and reduced heparin binding. The remaining low molecular weight band in Fig. 2*B* could be due to incomplete reaction, an inactive subpopulation, or formati n of an indistinguishable proteolytically modified AT-III. That COS-derived AT-III is capable of protease complex formation yet has variable heparin binding indicates that the heparin- and protease-binding domains are in some way functionally separable. Either the heparin-binding domain is less stable than the protease-binding domain and there is a subpopulation that is not folding correctly in COS cells, or minor alterations in glycosylation are preferentially affecting the heparin-binding domain. Analysis of thrombin inactivation in a chromogenic assay substantiated that COS-derived hAT-III is capable of inactivating thrombin. Moreover, it extends our data by showing that this AT-III is activated by heparin and that the reaction in the presence and absence of heparin occurs on the same time scale as that with plasma-derived hAT-III.

Two previous reports (5, 24) have described the heterologous expression of hAT-III. Bock *et al.* (5) cloned the cDNA and expressed it in *E. coli*. They observed a band in $NaDodSO_4$/PAGE immunoblot analysis of ≈50 kDa and attributed the size to the absence of glycosylation in the prokaryotic system they used. They did not report on any functional activity despite abundant production. Prochownik and Orkin (24) have also examined expression of a cloned hAT-III transiently in COS cells and in stable transformants of the mouse fibroblast line C127. They constructed a "mini-gene" consisting of 300 base pairs of 5′ untranslated sequences including the endogenous promoter, the first intron and corresponding 5′ and 3′ splice sites, the remainder of the cDNA, and 175 base pairs of 3′ noncoding sequences presumably containing a polyadenylylation signal. They dem nstrated production of mRNA and correct splicing in both cell lines. Furthermore, they were able to show the existence of an alternative splice site that may result in a truncated protein.

The data presented here provide a baseline for the examination of hAT-III synthesis in other heterologous systems, the investigation of signals required for secretion, and the basis for the generation of site-specific mutants to probe the importance of various implicated amino acid residues in the function of this important inhibitor.

We express our appreciation to Drs. M. Botchan, J. W. Fenton II, William Hathaway, Randolph Kaufman, Stephen Olson, and Savio Woo for providing materials and information that greatly facilitated the present research. Their individual contributions are identified in the text. This work was supported by a grant from the Colorado Heart Association.

1. Heimburger, N., Haupt, H. & Schwick, H. G. (1971) in *Proceedings of the International Research Conference on Proteinase Inhibitors*, eds. Fritz, H. & Tschesche, H. (de Gruyter, Berlin), pp. 1–22.
2. Osterud, B., Miller-Andersson, M., Abildgaard, U. & Prydz, H. (1976) *Thromb. Haemostasis* 35, 295–305.
3. Kurachi, K., Fujikawa, K., Schmer, G. & Davie, E. W. (1976) *Biochemistry* 15, 373–377.
4. Petersen, T. E., Dudek-Wojciechowska, G., Sottrup-Jensen, L. & Magnusson, S. (1979) in *The Physiological Inhibitors of Blood Coagulation and Fibrinolysis*, eds. Collen, D., Wiman, B. & Verstraete, M. (Elsevier/North Holland, Amsterdam), pp. 43–54.
5. Bock, S. C., Wion, K. L., Vehar, G. A. & Lawn, R. M. (1982) *Nucleic Acids Res.* 10, 8113–8125.
6. Chandra, T., Stackhouse, R., Kidd, V. J. & Woo, S. L. C. (1983) *Proc. Natl. Acad. Sci. USA* 80, 1845–1848.
7. Prochownik, E. V., Markham, A. F. & Orkin, S. H. (1983) *J. Biol. Chem.* 258, 8389–8394.
8. Stead, N., Kaplan, A. P. & Rosenberg, R. D. (1976) *J. Biol. Chem.* 251, 6481–6488.
9. Damus, P. S., Hicks, M. & Rosenberg, R. D. (1973) *Nature (London)* 246, 355–357.
10. Rosenberg, R. D. & Damus, P. S. (1973) *J. Biol. Chem.* 248, 6490–6505.
11. Olson, S. T. & Shore, J. D. (1982) *J. Biol. Chem.* 257, 14891–14895.
12. Lam, L. H., Silbert, J. E. & Rosenberg, R. D. (1976) *Biochem. Biophys. Res. Commun.* 69, 570–577.
13. Blackburn, N. M., Smith, R. L., Carson, J. & Sibley, C. C. (1984) *J. Biol. Chem.* 259, 939–941.
14. Koide, T., Takahashi, K., Odani, S., Ono, T. & Sakuragawa, N. (1984) *Proc. Natl. Acad. Sci. USA* 81, 289–293.
15. Chang, J. & Tran, T. H. (1986) *J. Biol. Chem.* 261, 1174–1176.
16. Olson, S. T. & Shore, J. D. (1981) *J. Biol. Chem.* 256, 11065–11072.
17. Stone, A. L., Beeler, D., Oosta, G. & Rosenberg, R. D. (1982) *Proc. Natl. Acad. Sci. USA* 79, 7190–7194.
18. Carrell, R. W., Boswell, D. R., Brennan, S. O. & Owen, M. C. (1980) *Biochem. Biophys. Res. Commun.* 93, 399–402.
19. Hunt, L. T. & Dayhoff, M. O. (1980) *Biochem. Biophys. Res. Commun.* 95, 864–871.
20. Flink, I. L., Bailey, T. J., Gustafson, T. A., Markam, B. E. & Morkin, E. (1986) *Proc. Natl. Acad. Sci. USA* 83, 7708–7712.
21. Pickup, D. J., Ink, B. S., Hu, W., Ray, C. A. & Joklik, W. K. (1986) *Proc. Natl. Acad. Sci. USA* 83, 7698–7702.
22. Lee, A. K. Y., Chan, V. & Chan, T. K. (1979) *Thromb. Res.* 14, 209–217.
23. Fair, D. S. & Bahnak, B. R. (1984) *Blood* 64, 194–204.
24. Prochownik, E. V. & Orkin, S. H. (1984) *J. Biol. Chem.* 259, 15386–14392.
25. Lindahl, U., Cifonelli, J. A., Lindahl, B. & Roden, L. (1965) *J. Biol. Chem.* 240, 2817–2820.
26. Porath, J. (1968) *Nature (London)* 218, 834–838.
27. Jordan, R. E., Zuffi, T. & Schroeder, D. D. (1982) in *Affinity Chromatography and Related Techniques*, eds. Bribnau, T. C., Visser, J. & Nivard, R. J. F. (Elsevier, Amsterdam), pp. 275–282.
28. Nordenmann, B., Nystrom, C. & Bjork, I. (1971) *Eur. J. Biochem.* 78, 195–203.
29. Johnstone, H. & Thorpe, R. (1982) *Immunochemistry in Practice* (Blackwell Scientific, Boston).
30. Evan, E. (1980) *Methods Enzymol.* 70, 419–439.
31. Kaufman, R. (1985) *Proc. Natl. Acad. Sci. USA* 82, 689–693.
32. Svensson, C. & Akusjarvi, G. (1986) *Proc. Natl. Acad. Sci. USA* 83, 4690–4694.
33. Luskey, M. & Botchan, M. (1981) *Nature (London)* 293, 79–81.
34. Luthman, H. & Magnusson, G. (1983) *Nucleic Acids Res.* 5, 1295–1308.
35. Jameel, S. & Siddiqui, A. (1986) *Mol. Cell. Biol.* 6, 710–715.
36. Laemmli, U. K. (1970) *Nature (London)* 227, 680–685.
37. Weber, K. & Osborn, M. (1969) *J. Biol. Chem.* 244, 4406–4411.
38. Jesty, J. (1978) *J. Biol. Chem.* 254, 1044–1049.
39. Olson, S. T. (1985) *J. Biol. Chem.* 260, 10153–10160.

Mol Gen Genet (1982) 187:384

DNA-Mediated Gene Transfer in Chinese Hamster Ovary Cells: Clonal Variation in Transfer Efficiency*

Rodney S. Nairn, Gerald M. Adair, and Ronald M. Humphrey
The University of Texas System Cancer Center, Science Park, Research Division, P.O. Box 389, Smithville, Texas 78957, USA

Summary. Thymidine kinase-deficient Chinese hamster ovary (CHO) cells were genetically transformed with the *Bam*HI restriction fragment encoding the thymidine kinase gene of herpes simplex virus (HSV-tk). We have observed considerable clonal variation among independent CHO sublines with respect to transformation competence for the DNA-mediated gene transfer of HSV-tk. Transformation frequencies $\geq 3 \times 10^{-4}$ were observed consistently in one subline, with a transformation efficiency of approximately 1 transformant per ng viral gene. The frequency and efficiency of transformation we observed in this system are at least 10-fold greater than those previously reported for DNA-mediated transformation of CHO cells by HSV-tk. All of the CHO HSV-tk$^+$ transformants examined were stable for the transferred genotype in the absence of selection, and all showed evidence of co-transformation by unselected plasmid pBR322 sequences.

Introduction

Genetic transformation of cultured mammalian cells by DNA-mediated gene transfer (DMGT) is a promising approach to the study of gene expression and its regulation in mammalian cells (Pellicer et al. 1980; Scangos and Ruddle 1981; Weinberg 1981). To date, most studies using DMGT methods have used mouse L or 3T3 cells as gene transfer recipients (Wigler et al. 1977; Pellicer et al. 1978; Weinberg 1981). This is because mouse L cells exhibit high transformation frequencies (Pellicer et al. 1980). Comparable transformation frequencies have not been obtained in most other cultured cell lines (Graf et al. 1979; Lewis et al. 1980; Robins et al. 1981).

The desirability of extending DMGT methods to other cell lines has been pointed out (Pellicer et al. 1980). In particular, the advantages of using Chinese hamster ovary (CHO) cells as gene transfer recipients have long been recognized (Srinivasan and Lewis 1980). These advantages include a stable, near-diploid karyotype, a characteristic that facilitates genetic analysis of somatic cell hybrids and which is in contrast to the pronounced aneuploidy observed in mouse L cells. In addition, there is a large and growing number of recessive mutant phenotypes available in CHO cell lines (Siminovitch 1979; Adair et al. 1979; Siciliano et al. 1982). Furthermore, linkage data in CHO are rapidly being generated, with 23 of 25 gene mapping assignments to date having been made in the last 2 years (Stallings and Siciliano 1981; Stallings et al. 1982; Siciliano et al. 1982). Unfortunately, however, CHO cells have been reported to be difficult to transform, with transformation frequencies 50 to 100-fold lower than Ltk-Cl. 1D cells (Graf et al. 1979; Lewis et al. 1980; Abraham et al. 1982).

We have used the cloned herpes simplex virus thymidine kinase (HSV-tk) gene to transform CHO cells in a DMGT system. Recently, Abraham et al. (1982) and Linsley and Siminovitch (1982) have also reported DMGT in CHO cells with the HSV-tk gene. Our DMGT system in CHO is substantially more efficient than those previously described. We have also observed considerable clonal variation for HSV-tk DMGT in independently selected CHO thymidine kinase-deficient (tk$^-$) sublines using this system. One subline showed consistently higher transformation frequencies with the HSV-tk gene and extremely high transformation efficiency (1 transformant/ng HSV-tk gene). W report here details of our DMGT system in CHO and the characteristics of HSV-tk$^+$ transformants derived from the high efficiency transforming subline.

Materials and Methods

Cell Culture. Table 1 describes the mammalian cell lines used in this study. Cells were cultured routinely in a α-modified Eagle's minimal essential medium (αMEM) without $NaHCO_3$, containing 2 mM glutamine and 10% fetal calf serum (FCS). Sources of FCS over the course of this study were KC Biologicals, Flow Laboratories, and GIBCO. Bromodeoxyuridine-resistant (BrdU^R) sublines were selected and maintained in αMEM containing 10% dialyzed FCS, bromodeoxyuridine at 150 μg/ml, and deoxycytidine at 10 μg/ml. BrdU^R sublines were selected by seeding CHO-AT3-2 cells at 25–50 cells per 25 cm^2 T-flask, expanding each population independently, and replating at 4×10^4 cells per 10 cm dish in 15 ml selective medium. Individual colonies were picked after 18–21 days and expanded. Each independent BrdU^R subline was cloned from one original, independent population of CHO-AT3-2 cells.

HAT selective medium was αMEM with 10% FCS containing 0.1 mM hypoxanthine, 0.002 mM amethopterin, and 0.05 mM thymidine. All media contained streptomycin (50 μg/ml), penicillin (50 units/ml), and where indicated, kanamycin (100 μg/ml).

Preparation of Plasmid DNA. Escherichia coli K-12 strain LE578, containing plasmid pX1, a recombinant molecule of pBR322 and the 3.5 kilobase pair (kb) *Bam*HI HSV-1

Offprint requests to: Rodney S. Nairn

* A preliminary account of these results was given at the ICN-UCLA Symposia, March 21–28, 1982

0026-8925/82/0187/0384/$01.40

able 1. Cell lines

esignation	Parental strain	Relevant genotype	Ploidy	Source	Reference
HO-AT3-2	CHO-SBU'-3	tk +/−	2n	G.M. Adair	Adair et al. (1980)
HO-3-25	CHO-AT3-2	tk −/−	4n	This work	–
HO-2E5	CHO-AT3-2	tk −/−	2n	This work	–
HO-3B10	CHO-AT3-2	tk −/−	2n	This work	–
HO-3G3	CHO-AT3-2	tk −/−	4n	This work	–
HO-6E10	CHO-AT3-2	tk −/−	4n	This work	–
tk⁻ Clone 1D	Mouse L Cell	tk −/−	aneuploid	M.J. Siciliano	Kit et al. (1963)

ugment encoding thymidine kinase (Enquist et al. 1979) as the generous gift of Lynn Enquist, Laboratory of umor Virology, NCI. Plasmid DNA was prepared by a eared-lysate method (Humphreys et al. 1975) and isolated / isopycnic dye-buoyant density centrifugation in CsCl-hidium bromide gradients. Ethidium bromide was moved by repeated extractions with saline-saturated opropanol, and DNA preparations were extensively dia-zed at 4° C against TES (0.03 M Tris·HCl, 0.05 M NaCl, 005 M EDTA, pH 8.0) and stored at −20° C.

eparation of Mammalian DNA. Mouse Ltk⁻ Cl. 1D cells ere used as the source for carrier nucleic acid in transfor-ation experiments. Confluent monolayer cultures were sed on plates by adding 10 ml per 15 cm plate of a lysing lution (0.01 M Tris·HCl, 0.01 M NaCl, 0.01 M EDTA, l 8.0, containing 0.5% sodium dodecyl sulfate and pro-nase K to 0.2 mg/ml) after rinsing plates twice with ick's S lution A. Plates were incubated for 3 h at 37° C d the viscous lysate was recovered by scraping with a bber policeman. Sequential organic extractions with ffer-saturated, redistilled phenol, phenol-chloroform-amyl alcohol (25:24:1), and chloroform-isoamyl alcohol):1) were performed on the lysate. Interfaces were pooled d re-extracted in the same fashion. Nucleic acid was col-ted from pooled aqueous phases by adding 3 volumes freezer-temperature ethanol and spooling on a glass rod.

For DNA samples used in restriction analysis, nucleic d was isolated as described above, redissolved in TE ffer (0.01 M Tris·HCl, 0.001 M EDTA, pH 8.0), and in-bated with previously boiled pancreatic ribonuclease A NAase) at 50 µg/ml for 1 h at 37° C. DNA was then rified by sequential organic extractions and spooled on lass rod as described above.

lA-Mediated Transformation. Prior to an experiment, l DNA was dissolved to 38 µg/ml in a buffer consisting 0.1 M Tris·HCl, 0.01 M $MgCl_2$, 0.02 M KCl, 0.006 M niothreitol, 5% glycerol, pH 7.5, and digested with *n*HI (3 units/µg DNA) for 3 h at 37° C. Carrier nucleic d dissolved in TE buffer to OD_{260} of 12 was added the digest (0.625 ml carrier nucleic acid per ml digest) l the material was ethanol-precipitated and collected by trifugation. For use in transformations, the ethanol pre-itates were dissolved in sterile, 0.1 × TE to OD_{260} of

Digested pXl DNA was delivered at 2 µg per plate nost experiments, and at 0.5 or 1.0 µg per plate in some eriments, as indicated.

BrdU^R CHO sublines or Ltk⁻ Cl. 1D cells were plated 5 ml αMEM + 10% FCS at 7×10^5 cells per 10 cm plate the afternoon prior to an experiment. Plates were refed the next morning with 12.5 ml αMEM + 10% FCS. After 2–4 h, one ml of calcium phosphate-DNA precipitate was added per plate. Calcium phosphate-DNA precipitates were formed in sterile polypropylene tubes over 35–40 min essentially as described by Wigler et al. (1977). After 3.5 h, DNA-treated monolayers were exposed to dimethyl sulfoxide (DMSO) by adding 1.5 ml DMSO dropwise to each plate, while swirling gently. Exposure to DMSO was for exactly 25 min, medium was then withdrawn and plates were refed with αMEM + 10% FCS containing kanamycin. After 40 h, cells were harvested by trypsin-EDTA treatment, counted, and replated at 1:5 ratio into HAT. On the fourth day after replating, the plates were replenished with fresh HAT medium and left undisturbed until HAT^R colonies were evident 8–10 days later.

Southern Blot Analysis of Transformant DNA. The 3.5 kb HSV-1 *Bam*HI fragment was purified by electroelution (Yang et al. 1979) after *Bam*HI digestion of pX1 and then dissolved in water after phenol extraction and ethanol precipitation. Nick translation reactions were conducted essentially as described by Weinstock et al. (1978). Southern blot analysis was performed using dextran sulfate to accelerate hybridization as described by Wahl et al. (1979). Hybridization was performed with 5×10^6 cpm per cm^2 of nitrocellulose transfer for 72 h at 42° C. Hybridized blots were washed as described by Smith and Summers (1980), air-dried, and exposed to Kodak X-Omat AR film at −70° C for 1–3 days, using an intensifying screen.

Cytogenetic Analysis. Modal chromosome nubmers were determined from airdried chromosome spreads. Chromosome spreads were prepared and stained using standard G-banding methods, as described by Worton and Duff (1979). The parental cell line used in these studies, CHO-AT3-2, has a modal chromosome number of 21, with a karyotype closely resembling that previously described for CHO by Deaven and Peterson (1973).

Stability Tests of Transformant Clones. Individual, independent transformant colonies (only one colony from each plate originally exposed to calcium phosphate-DNA precipitate) were picked and expanded in HAT in 25 cm^2 T-flasks. Cultures (4–6 days) were trypsinized and plated to both HAT and non-selective media. Cultures in HAT were expanded for DNA isolation and cultures in non-selective αMEM + 10% FCS were maintained for up to 34 days, during which time cells were trypsinized and replated at intervals at 200 cells per 6 cm plate to 6 plates each of selective and non-selective media. After 8–9 days, colonies were stained with crystal violet and scored.

Results

Influence of Carrier Nucleic Acid on DMGT of the HSV-tk Gene into CHO Cells

Using the calcium phosphate-DNA co-precipitation protocol as described in "Materials and Methods", we investigated to what extent the presence of carrier nucleic acid influenced transformation frequency in subline CHO-2E5. From preliminary experiments in line CHO-3-25, we determined that it was unnecessary to digest carrier nucleic acid with RNAase. Figure 1 represents results of experiments at constant inputs of *Bam*HI-digested pX1 (2 μg/plate) with differing amounts of carrier nucleic acid added per plate. By colorimetric analysis (Burton 1956) we determined that Ltk$^-$ carrier nucleic acid, isolated as described and not RNAase-treated, was approximately 40% DNA. Assuming that an OD_{260} of 1 represents 50 μg/ml (Humphreys et al. 1975), an input of 0.6 OD_{260} units carrier nucleic acid per plate corresponds to 12 μg DNA, and is shown by these data to be optimal for DMGT of the HSV-tk gene into CHO-2E5.

In addition, we transformed CHO-2E5 cells successfully without any added carrier nucleic acid, at an input of 4 μg pX1 digest per plate. The transformation frequency was significantly diminished in this case, to less than 5×10^{-6}. Some of these transformant clones were expanded and analyzed for stability. Presence of the HSV-tk transforming gene was verified by Southern blot analysis of DNA from these transformants.

Frequency and Efficiency of HSV-tk Gene Transfer in CHO Cells

Table 2 presents data from a large number of experiments conducted in BrdU[a] derivatives of CHO-AT3-2. Several

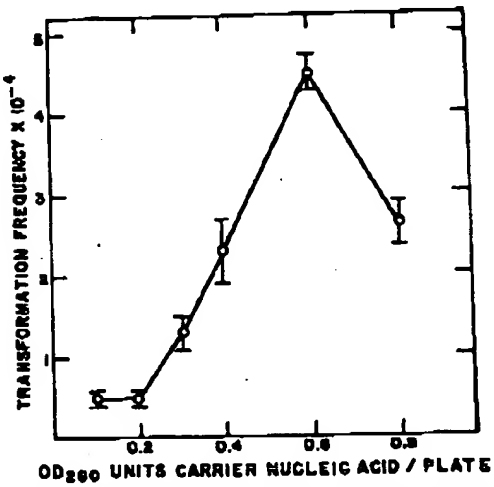

Fig. 1. Dependence of transformation frequency on input of carrier nucleic acid. CHO-2E5 cells were transformed with 2 μg *Bam*HI-digested pX1 per plate, at the carrier nucleic acid inputs indicated. Transformation frequencies were calculated on the basis of HAT[a] colonies arising on plates after cells were counted and replated into HAT 40 h post-pX1 exposure. Each point represents calculated frequencies from results of 4 plates

Table 2. Results of transformation experiments

Cell line	Experiment	DNA exposed cells plated	HAT[a] colonies	Transformation frequency[a]	Transformation efficiency[b]
CHO-2E5	1	1.47×10^7 (24 plates)	4,408	3.0×10^{-4}	1.05
	2	6.38×10^6 (16 plates)	2,840	4.5×10^{-4}	1.01
	3	7.01×10^6 (24 plates)	3,548	5.0×10^{-4}	0.85
	4[c]	4.59×10^6 (16 plates)	1,070	2.3×10^{-4}	0.76
	5[d]	1.38×10^6 (16 plates)	326	2.4×10^{-4}	0.47
	6 (control)	2.49×10^6 (4 plates)	0	$<4.0 \times 10^{-7}$	–
	7 (control)	3.28×10^6 (4 plates)	0	$<3.0 \times 10^{-7}$	–
CHO-3B10	1	7.82×10^6 (24 plates)	1,543	2.0×10^{-4}	0.37
	2	5.08×10^6 (12 plates)	1,026	2.0×10^{-4}	0.49
	3 (control)	4.83×10^6 (8 plates)	0	$<2.1 \times 10^{-7}$	–
CHO-3G3	1	8.63×10^6 (24 plates)	842	9.8×10^{-5}	0.20
	2	6.97×10^6 (19 plates)	281	4.0×10^{-5}	0.17
	3 (control)	2.82×10^6 (8 plates)	0	$<3.6 \times 10^{-7}$	–
CHO-3-25	1	1.15×10^7 (23 plates)	595	5.2×10^{-5}	0.15
	2	5.31×10^6 (32 plates)	384	7.2×10^{-5}	ND
	3 (control)	4.79×10^6 (8 plates)	0	$<2.1 \times 10^{-7}$	–
CHO-6E10	1	7.16×10^6 (14 plates)	59	8.0×10^{-6}	0.05
	2 (control)	4.98×10^6 (8 plates)	0	$<2.0 \times 10^{-7}$	–
Ltk$^-$ Clone 1D	1	1.13×10^7 (24 plates)	2,458	2.2×10^{-4}	0.59
	2 (control)	5.69×10^6 (8 plates)	0	$<1.8 \times 10^{-7}$	–

[a] Transformation frequency was calculated on the basis of HAT[a] colonies arising from the number of DNA-exposed cells plated into HAT

[b] Transformation efficiency was calculated on the basis of HAT[a] colonies arising per ng 3.5 kb *Bam*HI HSV fragment

[c] This experiment differed from the standard protocol described in the text in that 1.0 μg pXl *Bam*HI-digest per plate was used

[d] This experiment differed from the standard protocol described in the text in that 0.5 μg pXl *Bam*HI-digest per plate was used

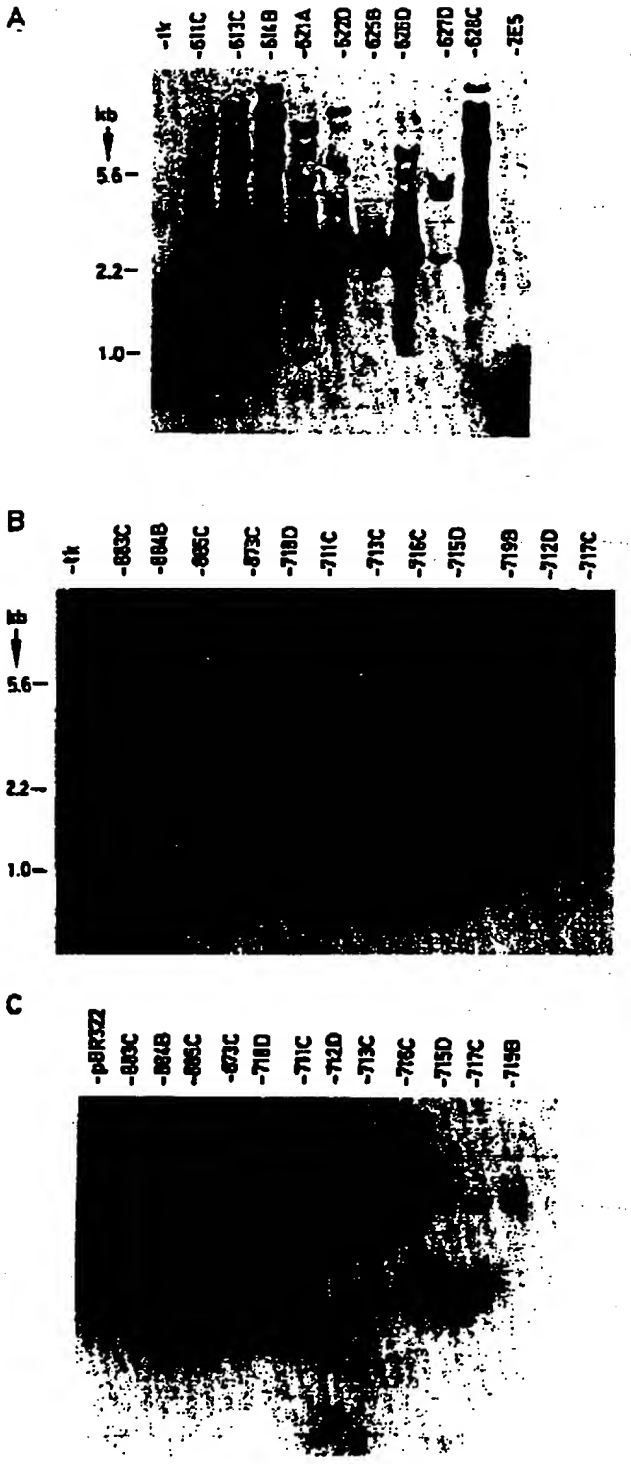

Fig. 2A–C. Southern blot analysis of independent HSV-tk$^+$ CHO-2P5 transformants. HAT^R colonies were picked at random, only one colony from each plate originally exposed to transforming DNA, and expanded. DNA was isolated and RNAase-treated as described in the text, then digested to completion with *Eco*RI. Southern blots, nick-translation of probes, and hybridizations were performed as described in the text. A Restriction digests of DNA from independent transformant clones (611C, 613C, 614B, 621A, 622D, 625B, 626D, 627D, and 628C), and the parental tk$^-$ line (2E5) were probed with the nick-translated 3.5 kb HSV-tk fragment, also represented on the transfer in lane at far left (tk). B Restriction digests of DNA from four transformant clones isolated in the absence of carrier DNA (883C, 884B, 885C, 873C) and of eight transformant clones isolated in presence of carrier DNA (718D, 711C, 713C, 716C, 715D, 719B, 712D, 717C) probed with the 3.5 kb HSV-tk fragment. C The same restriction digests as represented in B, probed with nick-translated pBR322

points concerning the frequency and efficiency of DMGT f HSV-tk into CHO cells can be made from these data. First of all, there is clonal variation in the observed frequencies of HSV-tk$^+$ transformation among these sublines. Frequencies shown in Table 2 were calculated on the basis of scored HAT^R colonies appearing on plates after replating cells that had been exposed to calcium phosphate-DNA precipitates 40 h earlier. Therefore, any differences in rates of expansion of different cell populations during the 40-h expression period are negated, since cells were counted at the time of plating into HAT. Secondly, subline CHO-2E5 consistently exhibits both higher transformation frequency and efficiency than other, independently selected BrdU^R CHO-AT3-2 sublines (experiments 4 and 5 in CHO-2E5 were conducted with 1 and 0.5 μg pX1 per plate, respectively). Transformation efficiency is defined on the basis of the ratio of total HAT^R colonies to the total mass of the HSV-tk gene introduced to cells as calcium phosphate-DNA precipitate. Third, most of the CHO-AT3-2 BrdU^R sublines exhibit transformation frequencies with the HSV-tk gene of the same order of magnitude as mouse Ltk$^-$ Cl. 1D cells in the conditions described for our protocol. This finding is in marked contrast to reports of DMGT in other CHO cell systems (Abraham et al. 1982; Linsley and Siminovitch 1982). Finally, stable tetraploid cell lines (CHO-3G3, CHO-3-25, and CHO-6E10) exhibit lower frequencies and efficiencies of DMGT than do stable pseudodiploid lines (CHO-2E5 and CHO-3B10).

Presence of HSV-tk and pBR322 Sequences in DNA of Transformants

High molecular weight DNA was isolated from independent HSV-tk$^+$ CHO-2E5 transformants and analyzed by Southern blotting for the presence of transforming and co-transformed DNA sequences. Each transformant analyzed originated from a different 10 cm plate originally exposed to calcium phosphate-DNA precipitate. Figure 2 shows results of this analysis for *Eco*RI-digested transformant DNA samples. Panel A shows that the HSV-tk gene is present in multiple copies in 9 independent HSV-tk$^+$ transformants, but not in DNA of CHO-2E5 (lane at far right). The 3.5 kb HSV-tk fragment is present at 40 pg in lane 1 (far left), approximating single-copy gene presence in the amount of DNA (15 μg) loaded to gels (Ketner and Kelly 1976). Panels B and C display results for other independent transformants probed with nick-translated 3.5 kb *Bam*HI fragment (B) and pBR322 (C).

Digestion with *Eco*RI reveals the presence of the 2.3 kb *Eco*RI HSV fragment within the 3.5 kb cloned HSV-1 *Bam*HI sequence in all HSV-tk$^+$ transformants probed with the 3.5 kb fragment, except clone 873C (panel B). It is ap-

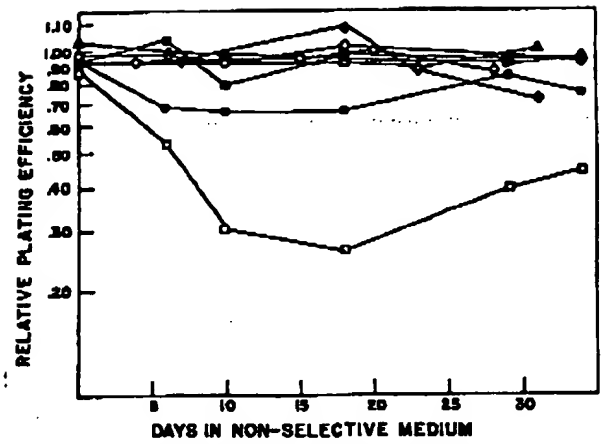

Fig. 3. Stability analysis of transformant clones. Independent CHO-2E5 transformants were isolated and maintained in non-selective medium for the lengths of time indicated. At intervals, cultures were replated into HAT and non-selective media (6 plates each) and scored after 8–9 days. Transformant clones so analyzed were 711 C (●), 716C (○), 715D (■), 719B (□), 717C (▲), 885C (△), 883C (◆) and 873C (◇). Each transformant was derived originally from a different transforming DNA-exposed plate. Clones 885C, 883C and 873C were isolated in a protocol in which carrier DNA was absent from the transforming DNA precipitate

parent from the restriction patterns that multiple integrations of the HSV-tk gene have occurred and that the pattern and extent of integration differ among the different cell lines. Panel C shows the presence of pBR322 sequences in the same transformants probed for HSV-tk sequences in Panel B. The linear pBR322 sequence is present in *Eco*RI-digested high molecular weight DNA of all transformants examined, and the presence of other bands indicates differences in integration of pBR322 sequences as well among these transformants.

Stability of CHO-2E5 Transformants

Figure 3 shows results of monitoring the stability of the tk^+ phenotype over 30 or more days in eight of the CHO-2E5 sublines analyzed in Fig. 2 (panel B). A total of 19 independent transformants were tested for stability, and the results shown in Fig. 3 are representative of the stability exhibited by CHO-2E5 transformants. With the exceptions of clone 719B (open squares) and one other transformant (not shown), the relative plating efficiencies (ratio of plating efficiency in HAT selective medium to plating efficiency in non-selective medium) were uniformly high. This result indicates that the tk^+ phenotype is extremely stable in CHO-2E5 HSV-tk^+ transformants, in agreement with the results reported by Abraham et al. (1982) for another DMGT system in CHO, and in marked contrast to the instability observed in Ltk^- Cl. 1D HSV-tk^+ transformants (Scangos et al. 1981).

Discussion

Genetic transformation of CHO cells by efficient DMGT offers avenues for gene cloning and investigation of gene expression in mammalian cells that are of considerably wider scope than offered by DMGT in other cultured cel lines, simply because there are so many more mutant pheno types available in CHO (Siminovitch 1979; Adair et al 1979). It was important to us, therefore, to establish DMGT system in CHO of high efficiency, with transforma tion frequencies comparable to those obtainable for mous Ltk^- Cl. 1D cells. We used the HSV-tk gene for transfe because of the readily selectable phenotype it offers, it availability as a cloned gene, and the extensive data bas accumulated for its DMGT in mouse Ltk^- Cl. 1D cell including data regarding the co-transformation and stabili ty characteristics of mouse Ltk^- HSV-tk^+ transformant (Wigler et al. 1979; Scangos et al. 1981).

There have been two other recent reports f DMG of the HSV-tk gene into CHO cells. Abraham et al. (198 were able to achieve maximal transformation frequenci of 5×10^{-5} with the HSV-tk gene, at an input of 10 µ pX1 per plate. Linsley and Siminovitch (1982) reporte transformation frequencies of 8×10^{-5} at the same DN input, and 3×10^{-5} at 2 µg pX1 added per plate, the inpu level used in this study. From data presented in Table we report transformation frequencies of 3×10^{-4} at 2 µ pX1 per plate in $BrdU^R$ line CHO-2E5, a significantly high frequency than reported elsewhere, representing a transfo matiqn efficiency (transformant colonies per ng HSV-t gene) of approximately 1.0. This frequency is comparab to that observed in Ltk^- Cl. 1D cells in our hands, usin DMGT conditions identical to those used for CHO lin (Table 2). Abraham et al. (1982) observed essentially th same frequency of transfer for Ltk^- cells as we have r ported here. DMGT frequencies 10 to 50-fold higher f Ltk^- cells with the HSV-tk gene have been reported (C merini-Otero and Zasloff 1980; Robins et al. 1981), b in these instances, pBR322 sequences were absent from th transforming DNA precipitate. Plasmid pBR322 was pre ent in precipitates used in our DMGT protocol, as w as in those of Abraham et al. (1982) and Linsley a Siminovitch (1982). Excess pBR322 sequences have be found to inhibit DMGT transformation in mouse L ce (Perucho et al. 1980; Lusky and Botchan 1981), and th may explain the transformation frequencies that Abraha et al. (1982) and we observed for Ltk^- cells.

Whether the higher transformation frequencies we ha observed in $BrdU^R$ subline CHO-2E5 result from diffe ences in DMGT protocol or from factors intrinsic to t cells used as recipients is not completely clear, since the are differences among the three DMGT protocols. In t protocol we describe, cells are exposed for 3.5 h to calciu DNA precipitate, shocked with 10% DMSO f r 25 mi allowed 40 h of expression time, then trypsinized and re lated into HAT. Both of the other two DMGT procedu use long exposure times to calcium-DNA precipitate (ov night to 26 h). This protocol is suggested f r Ltk^- ce by data of Lewis et al. (1980) and Corsaro and Pears (1981a). However, in one experiment with CHO-2E5 (da not shown), we used overnight exposure without DMS treatment, 48 h expression, and then replated cells by try sinizing into HAT. We found that the number of HA colonies ultimately obtained was greater by 2.5-fold; ho ever, since the cell population had also numerically creased by about 3-fold at the time of replating, there w no significant increase in transformation frequency as calculate it. By trypsinizing and replating cells (with plati efficiencies determined), we know precisely the number

viable cells that serve as the population on which selecti n is performed, and transformation frequencies are calculated on the basis of the number of cells plated into HAT after expressi n time. If we were to calculate transformation frequency on the basis of the number f cells originally exposed to calcium-DNA precipitate (Linsley and Siminovitch 1982), our calculated DMGT HSV-tk$^+$ frequencies would be approximately double what we have reported, since each original 10 cm dish gives rise to about 2×10^6 cells.

We have used Ltk$^-$ nucleic acid as carrier for the pX1 transforming precipitate, as did Linsley and Siminovitch (1982). Abraham et al. (1982) used commercial calf thymus DNA which they further purified. Since comparable results for CHO line 2F3 were obtained in both laboratories, the source of carrier DNA probably did not affect these results. However, as Fig. 1 shows, the amount of carrier nucleic acid added per plate has a significant influence on the transformation frequency. Abraham et al. (1982) also observed this effect using calf thymus DNA over a range of considerably greater carrier DNA input (up to 80 μg per plate). The optimal quantity of carrier DNA suggested by our data (12 μg per plate) and by data of Abraham et al. (1982) are in cl se agreement. The presence of RNA in our carrier nucleic acid seemed to have no effect on the optimal carrier DNA input.

The data from Table 2 suggest that intrinsic cellular factors may be more responsible than differences in DMGT protocol for the higher transformation frequencies we observed in BrdU^R CHO sublines. The apparent clonal variation we observed among independently selected BrdU^R CHO sublines suggests a cellular basis for the differences in DMGT frequencies and efficiencies we report, and perhaps most reasonably explains the differences in frequency we observe between BrdU^R derivatives of CHO-AT3-2 and line CHO-2F3 used by both Abraham et al. (1982) and Linsley and Siminovitch (1982). This conclusion is reinforced when one considers that Abraham et al. (1982) observed transformation frequencies approaching 10^{-4} using the pSV2-gpt vector to transfer the bacterial hypoxanthine guanine phosphoribosyltransferase gene (*Eco*gpt) to another CHO cell line, and that Linsley and Siminovitch (1982) observed high transformation frequencies with pSV2-gpt in DR-21, a CHO-KI hprt$^-$ derivative. Of course, since these genes are under the control of the early SV40 promoter in pSV2, higher frequencies might be anticipated. Nevertheless, the facts that a) there is variation in DMGT of different genes in different CHO sublines and b) we observe a pronounced difference in DMGT of HSV-tk among our CHO-AT3-2 derived tk$^-$ sublines and between these and the CHO-Toronto derived tk$^-$ line (2F3) indicate that the determinants of DMGT are probably cellular rather than procedural in nature.

Clonal variation in competence for DMGT has been reported f r sublines of mouse Ltk$^-$ Cl. 1D (Corsaro and Pearson 1981 b). Furthermore, Abraham et al. (1982) point out that their results for DMGT of HSV-tk, using two tk$^-$ CHO lines, suggest preliminary evidence of clonal variation for DMGT competence. We believe we have sufficient data (Table 2) to extend this suggestion to the conclusion that there is in fact clonal variation in CHO for DMGT competence. We interpret this observation in the same context as did Corsaro and Pearson (1981 b) for Ltk$^-$ Cl. 1D cells; that is, there are *genetic* factors that contribute t transformation competence. It is of interest to note that, in our hands, stable tetraploid BrdU^R CHO-AT3-2 derivative sublines consistently transform more poorly than do BrdU^R sublines of CHO-AT3-2 with a modal chromosome number of 21. Stable tetraploidy occurs in CHO-AT3-2 sublines at a somewhat higher frequency in BrdU^R selecti n than it otherwise occurs during routine maintenance of cell lines in culture. We have no explanation at present for this observation.

Two other points brought out in this study warrant discussion. One point is that co-transformation of unselected nucleotide sequences in CHO-2E5 cells is very high. Of twelve, randomly selected, independent HSV-tk$^+$ transformants, isolated by DMGT at equimolar pBR322 and HSV *Bam*HI fragment concentrations, all show evidence of co-transformation by pBR322 sequences (Fig. 2C) Abraham et al. (1982) also observed pBR322 and pSR1 cotransformation in the two transformants they examined. Thus, CHO cells, like mouse Ltk$^-$ Cl. 1D cells, are capable of integrating and maintaining unselected DNA sequences when these are presented in a transforming calcium-DNA precipitate. The second point concerns the stability of CHO HSV-tk transformants. Abraham et al. (1982) observed that all five transformants they tested for stability of the HAT^R phenotype were very stable. We have examined a total of 19 HSV-tk$^+$ CHO-2E5 transformants, data for eight of which are shown in Fig. 3, and our data convincingly support the conclusion that CHO transformants exhibit pronounced stability of the transformed gene. This finding contrasts with the finding in mouse Ltk$^-$ Cl. 1D cells that the ability of transformant populations maintained in non-selective media to clone in HAT is rapidly lost, at the rate of 10% per day (Scangos et al. 1981). One final point regarding the contrasting, marked stability of transferred genotype exhibited by CHO transformants seems pertinent. In context of the transgenome model for DMGT proposed on the basis of stability studies in Ltk$^-$ cells (Scangos et al. 1981), the physical association of the transforming gene with carrier or other high molecular weight DNA (transgenomes) is a prerequisite for stable genetic transformation. Stable transformants ultimately show physical association of the transforming gene with the host chromosomal DNA (Robins et al. 1981). If transgenomes are formed during DMGT in CHO cells, they must be stably maintained from the beginning or very soon thereafter, perhaps by very early, stable association with recipient chromosomal DNA. Since Ltk$^-$ cells are highly aneuploid, whereas CHO is known for its balanced ploidy, perhaps this characteristic of CHO is important in its stable genetic transformation. Further DMGT studies in CHO cell lines may provide a clearer answer to this question.

The DMGT system we have described in CHO, and those described by Abraham et al. (1982) and Linsley and Siminovitch (1982), should be important for extending the usefulness of this powerful technology. Because of the stability of the transformed genotype in CHO, and because there are now available DMGT systems for CHO which are efficient and provide high transformation frequencies, investigations of expression, maintenance, and isolation of transferred genes in CHO mutants will become an increasingly important approach in cell and molecular biology.

Acknowledgements. This work was supported in part by NCI Grant CA-04484. RSN was supported by NCI Training Grant CA-09191. We thank Megan Phillips for excellent technical assistance.

References

Abraham I, Sivaswami T, Gottesman MM (1982) Transfer of genes to Chinese hamster ovary cells by DNA-mediated transformation. Somat Cell Genet 8:23–39

Adair GM, Carver JH, Wandres DL (1980) Mutagenicity testing in mammalian cells. I. Derivation of a Chinese hamster ovary cell line heterozygous for the adenine phosphoribosyltransferase and thymidine kinase loci. Mutat Res 72:187–205

Adair GM, Thompson LH, Fong S (1979) 3H-amino acid selection of aminoacyl-tRNA synthetase mutants of CHO cells: evidence of homo- vs. hemizygosity at specific loci. Somat Cell Genet 5:329–344

Burton K (1956) A study of the conditions and mechanisms of the diphenylamine reaction for the colorimetric estimation of deoxyribonucleic acid. Biochem J 62:315–323

Camerini-Otero RD, Zasloff MA (1980) Nucleosomal packaging of the thymidine kinase gene of herpes simplex virus transferred into mouse cells: an actively expressed single-copy gene. Proc Natl Acad Sci USA 77:5079–5083

Corsaro CM, Pearson ML (1981a) Enhancing the efficiency of DNA-mediated gene transfer in mammalian cells. Somat Cell Genet 7:603–616

Corsaro CM, Pearson ML (1981b) Competence for DNA transfer of ouabain resistance and thymidine kinase: clonal variation in mouse L-cell recipients. Somat Cell Genet 7:617–630

Deaven LL, Peterson DF (1973) The chromosomes of CHO, an aneuploid Chinese hamster cell line: G-band, C-band, and autoradiographic analysis. Chromosoma 41:129–144

Enquist LW, VandeWoude GF, Wagner M, Smiley JR, Summers WC (1979) Construction and characterization of a recombinant plasmid encoding the gene for the thymidine kinase of herpes simplex type 1 virus. Gene 7:335–342

Graf LH, Urlaub G, Chasin LA (1979) Transformation of the gene for hypoxanthine phosphoribosyltransferase. Somat Cell Genet 5:1031–1044

Humphreys GO, Willshaw GA, Anderson ES (1975) A simple method for the preparation of large quantities of pure plasmid DNA. Biochim Biophys Acta 383:457–463

Ketner G, Kelly TJ (1976) Integrated simian virus 40 sequences in transformed cell DNA: analysis using restriction endonucleases. Proc Natl Acad Sci USA 73:1102–1106

Kit S, Dubbs DR, Piekarski LJ, Hsu T (1963) Deletion of thymidine kinase activity from L cells resistant to bromodeoxyuridine. Exp Cell Res 31:297–312

Lewis WH, Srinivasan PR, Stokoe N, Siminovitch L (1980) Parameters governing the transfer of the genes for thymidine kinase and dihydrofolate reductase into mouse cells using metaphase chromosomes or DNA. Somat Cell Genet 67:333–347

Linsley PS, Siminovitch L (1982) Comparison of phenotypic expression with genotypic transformation by using cloned, selectable markers. Mol Cell Biol 2:593–597

Lusky M, Botchan M (1981) Inhibition of SV40 replication in simian cells by specific pBR322 DNA sequences. Nature 293:79–81

Pellicer A, Robins D, Wold B, Sweet R, Jackson J, Lowy I, Roberts JM, Sim GK, Silverstein S, Axel R (1980) Altering genotype and phenotype by DNA-mediated gene transfer. Science 209:1414–1422

Pellicer A, Wigler M, Axel R, Silverstein S (1978) The transfer and stable integration of the HSV thymidine kinase gene into mouse cells. Cell 14:133–141

Perucho M, Hanahan D, Lipsich L, Wigler M (1980) Isolation of the chicken thymidine kinase gene by plasmid rescue. Nature 285:207–210

Robins DM, Ripley S, Henderson AS, Axel R (1981) Transforming DNA integrates into the host chromosome. Cell 23:29–39

Scangos GA, Huttner KM, Juricek DK, Ruddle FH (1981) DNA-mediated gene transfer in mammalian cells: molecular analysis of unstable transformants and their progression to stability. Mol Cell Biol 1:111–120

Scangos G, Ruddle FH (1981) Mechanisms and applications of DNA-mediated gene transfer in mammalian cells – a review. Gene 14:1–10

Siciliano MJ, Stallings RL, Adair GM, Humphrey RM (1982) Provisional assignment of TP1 and GPI/PEPD to Chinese hamster autosomes 8 and 9: a cytogenetic basis for functional haploidy of an autosmal linkage group in CHO cells. Cytogenet Cell Genet (in press)

Siminovitch L (1979) On the origin of mutants in somatic cells. In: Axel R, Maniatis T, Fox CF (eds) Eucaryotic gene regulation. Academic Press, New York, pp 433–443

Smith GE, Summers MD (1980) The bidirectional transfer of DNA and RNA to nitrocellulose or diazobenzyloxymethyl-paper. Anal Biochem 109:123–129

Srinivasan PR, Lewis WH (1980) Transfer of the dihydrofolate reductase gene into mammalian cells using metaphase chromosomes or purified DNA. In: Baserga R, Croce C, Rovera G (eds) Wistar Symposium Series, vol 1, Introduction of macromolecules into viable mammalian cells. Alan R Liss, Inc New York, pp 27–45

Stallings RL, Siciliano MJ (1981) Conformational, provisional, and/or regional assignment of 15 enzyme loci onto Chinese hamster autosomes 1, 2 and 7. Somat Cell Genet 7:683–698

Stallings RL, Siciliano MJ, Adair GM, Humphrey RM (1982) Structural and functional hemi- and dizygous Chinese hamster chromosome 2 gene loci in CHO cells. Somat Cell Genet 8:413–422

Wahl GM, Stern M, Stark GR (1979) Efficient transfer of large DNA fragments from agarose gels to diazobenzyloxymethyl paper and rapid hybridization by using dextran sulfate. Proc Natl Acad Sci USA 76:3683–3687

Weinberg RA (1981) Use of transfection to analyze genetic information and malignant transformation. Biochim Biophys Acta 651:25–35

Weinstock R, Sweet R, Weiss M, Cedar H, Axel R (1978) Intervening DNA spacers interrupt the ovalbumin gene. Proc Natl Acad Sci USA 75:1299–1303

Wigler M, Silverstein S, Lee LS, Pellicer A, Cheng Y, Axel R (1977) Transfer of purified herpes virus thymidine kinase gene to cultured mouse cells. Cell 11:237

Wigler M, Sweet R, Sim GK, Wold B, Pellicer A, Lacy E, Maniatis T, Silverstein S, Axel R (1979) Transformation of mammalian cells with genes from procaryotes and eucaryotes. Cell 16:777–785

Worton RG, Duff C (1979) Karyotyping. In: Jakoby WG and Pastan IH (eds) Methods in enzymology, vol 58. Academic Press, New York, pp 322–344

Yang RC, Lis J, Wu R (1979) Elution of DNA from agarose gels after electrophoresis. In: Wu R (ed) Methods in enzymology, vol 65. Academic Press, New York, pp 176–182

Communicated by G. O'Donovan

Received July 2, 1982

Human GM-CSF: Molecular Cloning of the Complementary DNA and Purification f the Natural and Recombinant Proteins

Gordon G. Wong, JoAnn S. Witek, Patricia A. Temple
Kathleen M. Wilkens, Anne C. Leary, Deborah P. Luxenberg
Simon S. Jones, Eugene L. Brown, Robert M. Kay
Elizabeth C. Orr, Charles Shoemaker, David W. Golde
Randal J. Kaufman, Rodney M. Hewick
Elizabeth A. Wang, Steven C. Clark

Abstract. *Clones of complementary DNA encoding the human lymphokine known as granulocyte-macrophage colony-stimulating factor (GM-CSF) were isolated by means of a mammalian cell (monkey COS cell) expression screening system. One of these clones was used to produce recombinant GM-CSF in mammalian cells. The recombinant hematopoietin was similar to the natural product that was purified to apparent homogeneity from medium conditioned by a human T-cell line. The human T-cell GM-CSF was found to be 60 percent homologous with the GM-CSF recently cloned from murine lung messenger RNA.*

Proteins necessary for the survival, proliferation, and differentiation of hematopoietic progenitor cells are produced by a variety of murine and human cell types (*1*). The biological activity of these factors, known as colony-stimulating factors or CSF's, is measured by their ability to stimulate hematopoietic progenitor cells to form colonies in semisolid medium. The CSF's are classified by the types of mature blood cells found in the resulting colonies. Thus multi-CSF, also known as interleukin-3 (IL-3) (*2*), stimulates the progenitor cells for most of the hematopoietic cell lineages. Other CSF's have been identified which specifically stimulate committed progenitor cells of the granulocyte-monocyte lineage: macrophage-CSF (M-CSF; also known as CSF-1) (*3*) and granulocyte-CSF (G-CSF) (*4*) stimulate the proliferation of progenitors committed to the macrophage or granulocyte lineages, respectively, while granulocyte-macrophage CSF (GM-CSF; also known as CSF-2) (*1*, *5*) stimulates the proliferation of cells of both lineages.

Results of experiments in vitro suggest a primary role for the various CSF's in the regulation of hematopoiesis (*1*, *6*), but the paucity of highly purified material has impeded their study and virtually precluded analysis of their functions in vivo. Thus it has not been possible to evaluate the potential clinical utility of natural CSF in the treatment or prevention of human disease. The ability of GM-CSF to stimulate both neutrophilic granulocyte and macrophage production implies that this factor could be clinically useful in situations where increased production of these cells may be desirable, for example, in immuno-compromised patients or those about to undergo irradiation or chemotherapeutic treatment of cancer (*7*).

We now report the isolation of complementary DNA (cDNA) clones that express biologically active human GM-CSF. The cloning was accomplished by a novel direct method involving the construction of cDNA libraries in an expression vector and the screening of plasmid pools by transient expression in COS monkey cells. We also describe the purification of natural human GM-CSF to homogeneity. This protein served as a standard to demonstrate the authenticity of the CSF we further purified from medium conditioned by monkey cells expressing the cloned sequence. The recent publication (*8*) of the nucleotide sequence of a murine lung GM-CSF cDNA has allowed us to compare the sequences of the human and murine proteins.

Identification and isolation of a human GM-CSF cDNA clone. A number of human cell lines that produce GM-CSF have been described (*9*). The development of methods for transforming normal human T cells in vitro with the use of human T-cell leukemia virus (HTLV) has provided a routine means of generating continuous T-cell lines (*10*), many of which could serve as useful sources of the hematopoietin. We have used a naturally arising HTLV-transformed T-lymphoblast cell line designated Mo (*11*) as a starting point both for the purification of analytical amounts of the GM-CSF protein and for the isolation of GM-CSF cDNA clones. Like other HTLV transformed T-cell lines, the Mo cell line produces several regulatory factors including GM-CSF (*9*, *12*). GM-CSF protein has been partially purified from the Mo-conditioned medium (*13*) and the GM-CSF mRNA has been identified by translation of Mo cell messenger RNA (mRNA) in *Xenopus* oocytes (*14*). However, the difficulty we encountered in obtaining sufficient sequence information from the very small quantities of GM-CSF that could be purified to homogeneity and the unreliability of the oocyte assay for the GM-CSF mRNA prompted us to develop a novel strategy to directly identify lymphokine cDNA clones by transient expression in COS-1 (*15*) cells.

Our cloning procedure exploits the efficient protein expression obtained after transfection of COS-1 monkey cells with the cDNA cloning vector (*16*) illustrated in Fig. 1. Control experiments demonstrated that p91203(B)-derived constructs synthesized proteins such as γ-interferon or interleukin-2 (IL-2) sufficiently well to allow detection after 500- to 1000-fold dilution with other plasmid DNA. It was therefore possible to construct cDNA libraries directly in p91203(B) and to screen pools of 300 or more recombinants for the ability to induce GM-CSF secretion by transfected COS-1 cells (see Table 1). The library, derived from membrane-bound mRNA of lectin-stimulated Mo cells, consisted of 60,000 independent clones. Two hundred pools, each containing 200 to 500 colonies, were screened initially, colony formation with the KG-1 human myeloid

All but one of the authors are members of the Genetics Institute, 225 Longwood Avenue, Boston, Massachusetts 02115. David W. Golde is in the Division of Hematology-Oncology, Department of Medicine, UCLA School of Medicine, Los Angeles 90024.

leukemia cell line being used as an indicator of CSF activity (*17*). Six pools induced the transfected COS cells to secrete GM-CSF activity; the same six pools were also positive when reassayed with fresh human b ne marrow in the colony assay (Table 1). Standard subselection methods were used to identify one single GM-CSF cDNA clone present in each of three of the original six positive pools (Table 1). Hybridization and DNA sequence analysis proved that the three independent plasmids pCSF-1, -2, and -3 contain the same cDNA sequence. We subsequently identified, by colony hybridization, the same cDNA sequence in each of the three remaining positive plasmid pools. To confirm that this sequence encoded a GM-CSF, we examined several colonies from the bone marrow CSF assay of the transfected COS cell–conditioned medium and found that the majority of the cells were either granulocytes or macrophages (Fig. 2).

Sequence of human GM-CSF. The DNA sequence of the first GM-CSF cDNA (pCSF-1), shown in Fig. 3, contains a single long open reading frame of 432 nucleotides encoding 144 amino acids. Comparison of this sequence with the NH_2-terminal sequence from the purified Mo protein suggested that GM-CSF, like other secreted proteins, is synthesized as a precursor that is cleaved after residue 17 to yield a mature protein of 127 residues. Two potential NH_2-glyc sylation sites (Asn-X-Thr/Ser) (*18*) were noted in the sequence (residues 44 to 46 and 54 to 56; Fig. 3). The complete nucleotide sequence of pCSF-1 consists of 754 nucleotides (exclusive of the polyadenylated stretch) including eight nucleotides of 5′ and 314 nucleotides of 3′ untranslated sequence.

Determination of the DNA sequence of four other, independently isolated, GM-CSF clones confirmed the sequence of pCSF-1. All of the clones contain the complete coding region identified in Fig. 3. In three of the clones, however, a single base substitution (thymine for cytosine) was noted at the nucleotide numbered 358. This was the only base change detected among all of the clones. As multiple independent clones were obtained having either sequence, we believe this difference probably results from a polymorphism among the GM-CSF genes in Mo cell DNA. Restriction enzyme analysis of the CSF genomic sequences in Mo cell DNA and in human liver DNA suggested that there is a single human gene encoding GM-CSF that has one or more introns (Fig. 4B). The sequence polymorphism found in Mo cell cDNA's was not detected at the le[redacted] restriction endonuclease mapping of the genomic DNA. We infer therefore that Mo has two different alleles of a common GM-CSF gene. Our results imply that there are no other genes with [redacted]A sequence very closely related to [redacted]ell GM-CSF, but do not rule out the possibility that there are other CSF genes that have little or no sequence homol gy.

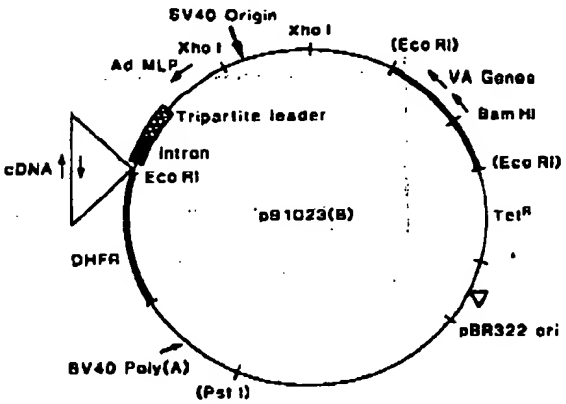

Fig. 1. Structure of expression vector p91023(B). The basic features of the expression system used have been described (*16*). The expression vector p91023(B) was derived from pQ2 (*16*) by standard DNA manipulations. The plasmid has the pBR322 origin of replication and tetracycline resistance gene for propagation in *Escherichia coli*, and lacks the bacterial sequences which inhibit DNA replication in COS monkey cells (*32*). It contains, in addition, eukaryotic regulatory elements from several different sources: (i) an SV40 origin and SV40 enhancer segment, which together allow the plasmid to replicate to a very high copy number in COS cells (*15*) and to efficiently transcribe inserted cDNA genes (*33*); (ii) the adenovirus major late promoter (*34*) coupled to a cDNA copy of the adenovirus tripartite leader (*16*); (iii) a hybrid intron consisting of a 5′ splice site from the first exon of the tripartite leader and a 3′ splice site from a mouse immunoglobulin gene (*16*); (iv) the SV40 early polyadenylation signal; and (v) the adenovirus VA I and VA II gene region (*35*). Plasmid p91023(B) also contains the mouse dihydrofolate reductase (DHFR) coding sequence downstream from the unique Eco RI cloning site which is positioned just after the 3′ splice site. cDNA's inserted at this Eco RI site can be transiently expressed at high levels in COS cells. The inserted cDNA is transcribed into a hybrid mRNA such that the cDNA sequence is flanked by the adenovirus tripartite leader at the 5′ side and by the mouse DHFR sequence serving as a nontranslated sequence at the 3′ side. The adenovirus tripartite leader and the VA RNA's increase the translatability (*16, 36*) while the DHFR sequence appears to enhance the stability of the hybrid mRNA (R. Kaufman, unpublished results).

Table 1. CSF activity in supernatants from COS cells transfected with DNA's from the Mo cell cDNA expression library. The Mo cell cDNA expression library in p91023 (*15*) was prepared by standard methods (*30*). Sixty thousand bacterial colonies from the library were replica-plated onto nitrocellulose filters. The colonies from each filter were scraped into L-broth and plasmid DNA was isolated as described (*31*). Each DNA sample was prepared from a pool of 200 to 500 independent clones. We used 5 μg of each DNA sample to transfect a 10-cm dish of COS-1 cells by DEAE-dextran–mediated DNA transfection with the addition of chloroquine treatment (*16*). The transfected COS cell–conditioned medium was harvested 72 hours after DNA transfection and activity was measured in KG-1 CSF assay (*17*). From the primary screen of 200 DNA samples, six pools (A) were found to produce CSF activity in COS cells. These pools were also assayed with the use of 10^4 light-density nonadherent human bone marrow cells as targets (*17*). The bacterial colonies from each of the first three positive pools were picked and placed in square matrices (pool M99 had approximately 340 clones, pool M181 had 370 clones, and pool M195 had 470 clones). DNA was prepared from each horizontal row and vertical column of each matrix, and transfected to produce COS cell–conditioned media samples which were assayed for CSF by the KG-1 cell assay. Two positive samples (B) were obtained from each set of transfections corresponding to each matrix, thereby unambiguously identifying the position of the CSF clone in the matrix. These cloned DNA's induced the expression of GM-CSF when transfected into COS-1 cells (C). NT, samples that were not tested in the bone marrow assay.

A			B			C		
DNA sample (primary pools)	CSF Activity (U/ml)		DNA sample (secondary pools)	CSF activity (U/ml)		DNA sample (isolated clone)	CSF activity (U/ml)	
	KG-1	Bone marrow		KG-1	Bone marrow		KG-1	Bone marrow
M99	40	500	M99-4	>300	1620	pCSF-1	7200	9700
			M99-35	>300	925			
M181	50	450	M181-1	>300	NT	pCSF-2	2400	NT
			M181-3	270	NT			
M195	60	540	M195-58	>300	NT	pCSF-3	2600	NT
			M195-30	300	NT			
M267	50	180						
M286	150	210						
M293	60	300						

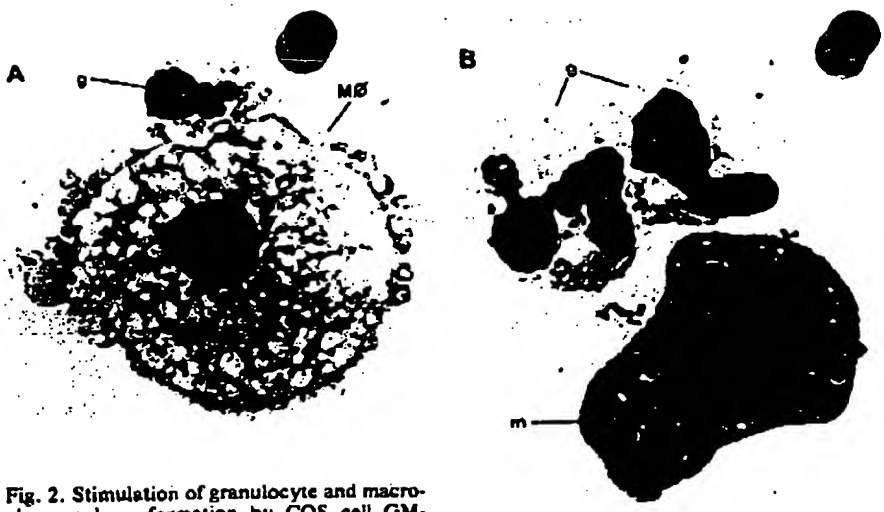

Fig. 2. Stimulation of granulocyte and macrophage colony formation by COS cell GM-CSF. Light-density nonadherent human bone marrow cells were plated (2×10^5 cells per milliliter) with 10 μl of conditioned medium from COS cells transfected with pCSF-1 in 35-mm dishes as described (*17*) except 0.87 percent methylcellulose was used instead of soft agar. More than 25 colonies were stimulated to grow; no colonies were observed in negative control dishes. A number of colonies were picked and the cells were dispersed onto slides and treated with Wright's stain. (A) Field showing a single macrophage (Mϕ) and a mature granulocyte (g); (B) field showing several mature granulocytes (g) and a single myelocyte, a granulocyte precursor (m).

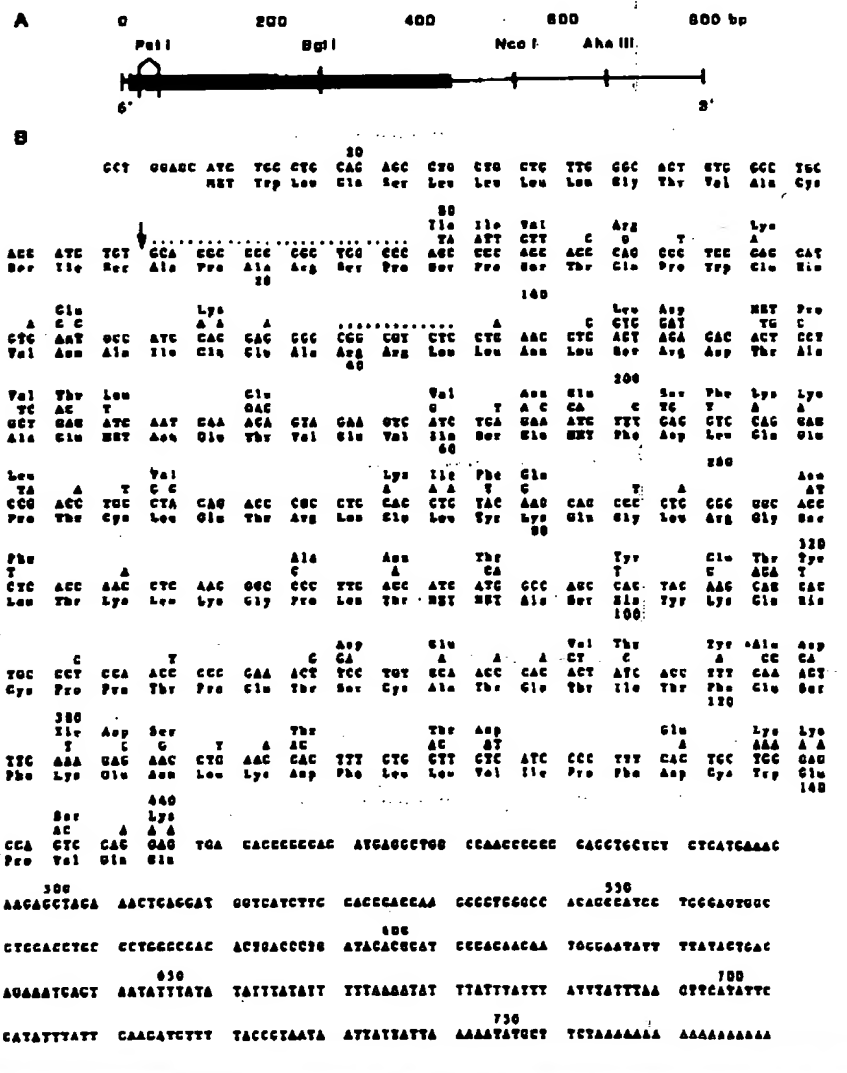

Fig. 3. (A) Restriction map of human GM-CSF and (B) comparison of the sequences of the human and the murine GM-CSF's. (A) The cDNA insert of pCSF-1 is bounded by Eco RI linkers. Other restriction sites found in the sequence are as indicated. The heavy line indicates the position of the open reading frame. (B) The complete sequence of the cDNA insert of pCSF-1 was determined by the dideoxynucleotide chain termination method following subcloning of fragments into M13 vectors (*37*). The predicted amino acid sequence of the single long open reading frame is indicated below the nucleotide sequence. The position of cleavage of the signal peptide, indicated with an arrow, was determined by amino terminal sequencing of GM-CSF isolated from Mo cell–conditioned medium and recombinant GM-CSF from medium conditioned by COS cells transfected with pCSF-1 (*23*). The nucleotide sequence analysis of five independent CSF clones (all from the Mo cell cDNA library) revealed sequence heterogeneity at one position (two clones had the sequence shown while three clones had T at position 358 instead of the C indicated here). The nucleotide sequence of the coding region of murine lung GM-CSF (*8*) along with predicted amino acid changes is indicated above the human sequence. The sequence not indicated (—) is deleted in the mouse sequence relative to the human.

Expression of GM-CSF mRNA. We examined mRNA from several cellular sources known to produce proteins with CSF activity. RNA blot analysis (Fig. 4A) revealed that two mature T-cell lines (Mo and UCD-144-MLA) (*34*), as well as lectin-stimulated peripheral blood lymphocytes (PBL's), synthesized readily detectable levels of a 1-kb mRNA that hybridized with the GM-CSF clone. This messenger could not be detected in RNA samples from the immature T-lymphoblastoid cell line CCRF-CEM (*19*) or from the B-lymphoblastoid cell line Daudi (*20*), neither of which produced measurable CSF (data not shown). Although Mo cells constitutively produce the transcript, treatment with phytohemagglutinin (PHA) and phorbol myristate acetate (PMA) increased the abundance of the message two- to fourfold whereas treatment with the glucocorticoid dexamethasone decreased the level of the CSF mRNA by a similar amount. Analysis of a second HTLV-transformed T-cell line, C10-MJ2 (*21*), confirmed that the CSF gene could be activated by lectin stimulation. In contrast to Mo cells, the level of GM-CSF mRNA detected in RNA obtained from the C10-MJ2 cells was very low in the absence of stimulation but could be increased more than tenfold by treatment of the cells with PHA and PMA. Isolation of further GM-CSF clones from a cDNA library prepared from lectin-stimulated C10-MJ2 cells suggested that the abundance of the CSF mRNA in these cells is 0.05 to 0.1 percent of the total mRNA.

Purification of the natural and recombinant CSF's. The purification f human GM-CSF from T cell–c nditioned medium proved to be difficult for several reas ns. First, the time (10 to 14 days) required for colonies to grow in the bioassay made it difficult to follow the activity through sequential fractionation steps. Second, regardless of the source, GM-CSF is always present as a minor component of the total protein in conditioned medium and extensive purification is necessary to achieve homogeneity. Finally, the molecular heterogeneity of the GM-CSF protein, which is evident as heterogeneity in size, charge, and hydroph bicity [see also (*13*)] made fractionati ns based on these physical properties inefficient. Nevertheless, using conventional column chromatography and tw reversed-phase high-performance liquid chromatography (HPLC) steps, we were able to extensively purify the T cell–derived GM-CSF (*22*). In a typical preparation, 40 liters of starting conditioned medium yielded 4 to 6 μg (about 200 to 400 picomoles) of the natural hematopoietin. Sodium dodecyl sulfate–polyacrylamide gel electrophoresis (SDS-PAGE) of the protein in the most active fraction from the final purification step revealed that the CSF protein migrated as a single diffuse band with an apparent molecular mass of 18 to 22 kilodaltons (Fig. 5, lane 2). This highly purified GM-CSF had a specific activity of 1×10^7 to 4×10^7 units per milligram when assayed with human bone marrow [illegible]t cells and was active at 4 to 20 picomolar c ncentrations in the KG-1 cell assay.

To produce quantities of recombinant GM-CSF, we used DNA transfection to introduce pCSF-1 into large numbers of COS-1 cells (see Fig. 5) which were subsequently allowed to condition medium in the absence of serum. By this procedure we could readily prepare 4- to 5-liter batches of serum-free conditioned medium with CSF activity 10 to 30 times higher than the activity in the T-cell conditioned medium. The recombinant GM-CSF had fractionation properties virtually identical to those of the natural protein as described above. This similarity plus the higher levels of activity generated by COS cells greatly facilitated the isolation of the recombinant GM-CSF (*23*). In fact, gel filtration followed by reversed-phase HPLC yielded 200 μg of recombinant CSF from 4 liters of conditioned medium (Fig. 5, lane 1). One of the most highly purified fractions, when analyzed by SDS-PAGE, migrated as a heterogeneous band with an apparent molecular mass of 18 to 24 kD, a result similar to that obtained with the natural T cell–derived protein (Fig. 5, lane 1). The specific activity of the recombinant CSF was indistinguishable from that of the native protein isolated from Mo cell–conditioned medium. We have been able to prepare milligram quantities of such highly purified material from the transiently expressing COS monkey cells.

The qu[illegible]tics of natural GM-CSF purified from the continuous T-cell line and the larger amounts of recombinant GM-CSF purified from the pCSF-1 transfected COS cells were sufficient for microsequencing of the NH_2-terminus (*24*). The sequence of the first six residues of natural GM-CSF was found to be Ala-Pro-Ala-Arg-Ser-Pro, which is identical to the sequence predicted from the cDNA sequence (Fig. 3) for residues 18 to 23. This confirms our identification of the cDNA as that for GM-CSF and indicates that the signal sequence is removed by cleavage after serine residue 17. With the recombinant GM-CSF we determined the sequence of the 16 residues (Ala-Pro-Ala-Arg-Ser-Pro-Ser-Pro-Ser-Thr-Gln-Pro-Trp-Glu-His-Val) corresponding to the 18th through the 32nd amino acids predicted by the DNA sequence. The fact that the same NH_2-terminal sequence was obtained with both natural and recombinant CSF provides evidence that the observed molecular heterogeneity of the purified proteins is not a result of differential processing at the NH_2-terminus but most likely is a result of heterogeneity in carbohydrate modification of the polypeptide. We cannot rule out the alternative possibility of COOH-terminal processing or other forms of posttranslational modification. In either case, our results demonstrated that the expression of a unique GM-CSF gene in COS-1 cells can produce protein with substantial molecular heterogeneity similar to that observed

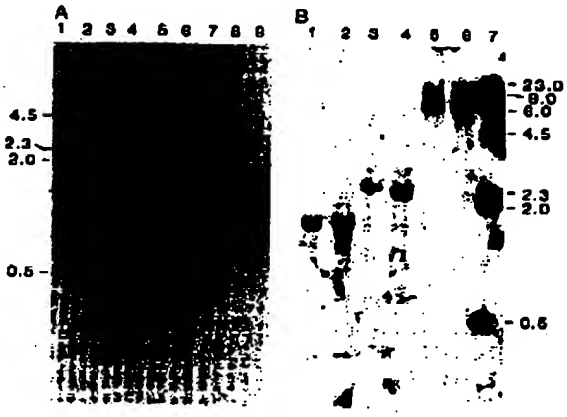

Fig. 4. Nitrocellulose blot analysis of (A) the CSF mRNA and (B) restriction fragments of the human CSF gene region. (A) Polyadenylated cytoplasmic RNA (5 μg), isolated as described (*16*), from Mo cells cultured for 20 hours in the presence of 10 n*M* dexamethasone (lane 1); from Mo cells (lane 2); from Mo cells cultured for 20 hours in the presence of PHA and PMA (see legend to Fig. 1) (lane 3); from C10 MJ2 cells (lane 4); from C10 MJ2 cells cultured for 20 hours in the presence of PHA and TPA (lane 5); from UCD-144-MLA cells cultured for 20 hours in the presence of 5 n*M* PMA (lane 6); from Ficoll-separated peripheral blood lymphocytes (PBL's) (lane 7); and from two different samples of PBL's pooled from four donors and stimulated for 20 hours with PHA and PMA (lanes 8 and 9). The samples were fractionated on a 1 percent agarose gel in the presence of 6 percent formaldehyde and transferred to nitrocellulose as described by Kaufman and Sharp (*16*). The nitrocellulose filter was hybridized with the GM-CSF cDNA clone labeled with ^{32}P to about 5×10^7 cpm/μg with T4 DNA polymerase replacement synthesis (*38*). The hybridization was performed for 16 hours at 68°C in a mixture containing 4× SSC (SSC contains 0.15*M* NaCl, 0.015*M* sodium citrate, *p*H 7.4), 5× PM (PM contains 0.02 percent each of bovine serum albumin, polyvinylpyrrolidone, and Ficoll 400), denatured herring sperm DNA (100 μg/ml), and the labeled probe (10^6 cpm/ml). After hybridization, the filter was washed at 68°C for several hours in 2× SSC with 0.1 percent SDS and for 30 minutes in 0.2× SSC with 0.1 percent SDS. The size markers were denatured λ Hind III fragments. (B) High molecular weight DNA (20 μg) from human liver (kindly provided by J. Toole) and from Mo cells (20 μg) was digested to completion with Eco RI (lane 5, Mo cell DNA; lane 6, human liver DNA), Pst I (lane 3, Mo cell DNA; lane 4, human liver DNA), and with both enzymes (lane 1, Mo cell DNA; lane 2, human liver DNA), fractionated by agarose gel electrophoresis (0.7 percent gel), and transferred to nitrocellulose (*39*). The resulting filter was probed as described above except 1×10^7 cpm of labeled probe per milliliter was used. The size markers are end-labeled fragments of a Hind III digest of λ DNA. Digestion of the human DNA's with Eco RI, which does not cleave within the cDNA sequence, gave a single hybridizing fragment of approximately 6000 base pairs (lanes 5 and 6). Cleavage with Pst I, which cleaves the cDNA twice within a 25 nucleotide sequence near the 5' end of the clone, generates two hybridizing fragments of 3000 and 300 nucleotides respectively (lanes 3 and 4). Since the ^{32}P-labeled cDNA probe only extends 25 nucleotides upstream from the first Pst I site, this probe will not anneal with the genomic Pst I fragment containing the first 25 nucleotides of the cDNA sequences. Therefore, the two hybridizing fragments probably result from an additional Pst I site contained within an intron in the genomic sequence. Cleavage of the genomic DNA's with both Pst I and Eco RI yields two hybridizing fragments, one 2000 base pairs and the other 300 base pairs in length (lanes 1 and 2). From these data we conclude that under the hybridization stringency used here, there is a single human GM-CSF gene that contains at least one intron.

with the natural purified protein.

Discussion. The isolation by expression screening of six virtually identical independent CSF clones from a library of 60,000 clones suggests that the GM-CSF reported here is the major species of CSF produced by Mo cells. Alternatively, CSF's encoded by other mRNA's may be more difficult to convert to full-length cDNA's or more difficult to express in the COS cell expression system and therefore could have been missed in the expression screen. Antibodies to the recombinant GM-CSF protein would help clarify the issue of whether or not there are other human proteins with GM-CSF activity.

We have compared the sequence of human GM-CSF with all the sequences recorded in Genbank including those of oncogenes and such growth factors as γ-interferon, IL-2, and murine IL-3, and with the recently published sequence for murine GM-CSF. The only significant homology that we detected was with the murine GM-CSF, which was recently cloned from murine lung mRNA. Maximum homology of the coding regions of the human and mouse cDNA's was obtained by deleting the codons for amino acids 18 to 23 and 40 to 42 from the human sequences as indicated in Fig. 3. The amino acid sequences are then 60 percent homologous while the nucleotide sequences are approximately 70 percent conserved. The sequence of the murine signal peptide was not reported, but it is interesting that the processing of the human GM-CSF apparently occurs six amino acids before the corresponding cleavage site of the mouse protein. The positioning of the four cysteine residues appears to have been preserved in the two proteins, suggesting some importance for the location of disulfide bridges in the structure of GM-CSF.

The sequences of the 3′ noncoding regions of the murine and human CSF cDNA clones show little homology, with the exception of a long stretch of nucleotides consisting of T's and A's beginning roughly 110 nucleotides before the polyadenylic acid sequence in each clone. The mouse sequence consisting of 59 T's and A's [nucleotides 542 to 620 in (*8*)] contains within it an almost exact replica (93 percent homologous) of a 47-nucleotide sequence (nucleotides 646 to 692) in the human cDNA. Regions rich in A and T which share some homology with this sequence have been found in the 3′ noncoding regions of other cDNA's, notably the human and mouse sequences for interferon α2 (*25*). Other conserved sequences have been observed in 3′ noncoding regions, but the function of such sequence elements remains unclear (*26*).

Another factor produced by M cells, T-cell derived neutrophil migration inhibitory factor (NIF-T), has recently been purified to homogeneity (*27*). NIF-T was identified by its ability to inhibit the migration of human neutrophils in vitro, but the highly purified protein also proved to have GM-CSF activity (*27*). The partial NH_2-terminal sequence determined from the purified NIF-T exactly corresponded with the sequence of the GM-CSF protein reported here. The identity of NIF-T and GM-CSF was confirmed by the demonstration that our recombinant GM-CSF has high levels of NIF-T activity (*27*). Thus a single hematopoietin can not only stimulate the growth and differentiation of progenitor cells in bone marrow but can also activate the biological function of the resulting circulating mature blood cells. These results are consistent with the findings that the purified murine G-CSF and GM-CSF can activate murine neutrophil cytotoxic functions (*28*) and that semipurified human CSF from placental-conditioned medium can enhance the antibody-dependent cell-mediated cytotoxicity of human neutrophils (*29*). Thus GM-CSF and NIF-T may have several functions, including the stimulation of the production of effector cells and ultimately the activation of these cells in the periphery. With the availability of the human GM-CSF cDNA clone it should be possible to produce pure CSF in quantities sufficient to evaluate the relative importance of these activities in vivo and to test the clinical potential of CSF for the treatment and prevention of granulocytopenia and infection.

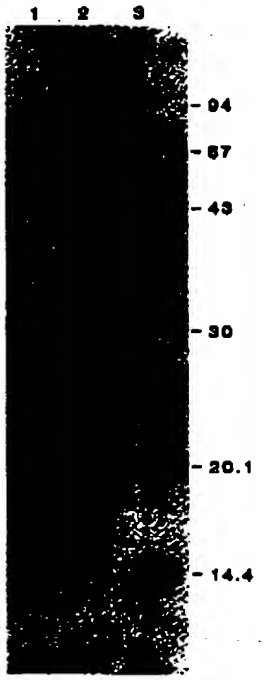

Fig. 5. Electrophoresis (SDS-PAGE) of purified Mo T cell and recombinant GM-CSF. Highly purified Mo GM-CSF (1 μg; lane 2) and recombinant GM-CSF (approximately 4 μg; lane 1) were subjected to electrophoresis (13.5 percent SDS-PAGE) in parallel with the indicated molecular size markers (lane 3) as described (*40*). The protein bands in the gel were visualized by silver staining. The Mo GM-CSF was isolated from 40 liters of serum-free Mo-conditioned medium (*22*). Recombinant CSF was isolated from 4 liters of serum-free conditioned medium from COS-1 cells transfected with pCSF-1 (*23*).

References and Notes

1. D. Metcalf, *Hematopoeitic Colonies. In vitro Cloning of Normal and Leukemic Cells* (Springer-Verlag, New York, 1977); A. W. Burgess and D. Metcalf, *Blood* **56**, 947 (1980); M. A. S. Moore, *Clin. Hematol.* **8**, 287 (1979); N. A. Nicola and M. Vadas, *Immunol. Today* **5**, 76 (1984).
2. J. H. Ihle, L. Rebar, J. Keller, J. C. Lee, A. J. Hapel, *Immunol. Res.* **63**, 5 (1982). D. Metcalf, in *Normal and Neoplastic Haemopoiesis*, D. W. Golde and P. A. Marks, Eds. (Liss, New York, 1983), p. 141.
3. E. R. Stanley, *Proc. Natl. Acad. Sci. U.S.A.* **76**, 2969 (1979); R. K. Shadduck, G. Pigoli, A. Waheed, *J. Supramol. Struct. Suppl.* **4**, 116 (1980).
4. N. A. Nicola, D. Metcalf, M. Matsumoto, G. R. Johnson, *J. Biol. Chem.* **258**, 9017 (1983).
5. A. W. Burgess, J. Camakaris, D. Metcalf, *J. Biol. Chem.* **252**, 1998 (1977).
6. W. Hocking, J. Goodman, D. W. Golde, *Blood* **61**, 600 (1983).
7. J. C. Gasson, I. S. Y. Chen, C. A. Westbrook, D. W. Golde, in *Normal and Neoplastic Hematopoiesis*, D. W. Golde and P. A. Marks, Eds. (Liss, New York, 1983), p. 129.
8. N. M. Gough *et al.*, *Nature* (*London*) **309**, 763 (1984).
9. M.-C. Wu, J. K. Clini, A. A. Yunis, *J. Biol. Chem.* **254**, 6226 (1979); C. Tarella, F. W. Ruscetti, B. J. Poiesz, A. Woods, R. C. Gallo, *Blood* **59**, 1330 (1982).
10. M. Popovic *et al.*, *Science* **219**, 856 (1983); I. S. Y. Chen, S. G. Quan, D. W. Golde, *Proc. Natl. Acad. Sci. U.S.A.* **80**, 7006 (1983).
11. A. J. Saxon, R. H. Stevens, D. W. Golde, *Ann. Intern. Med.* **88**, 323 (1978); V. S. Kalyanaraman *et al.*, *Science* **218**, 571 (1982).
12. D. W. Golde, S. G. Quan, M. J. Cline, *Blood* **52**, 1068 (1978); D. W. Golde, N. Bersch, S. G. Quan, A. J. Lusis, *Proc. Natl. Acad. Sci. U.S.A.* **77**, 593 (1980).
13. A. J. Lusis, D. H. Quon, D. W. Golde, *Blood* **57**, 13 (1980).
14. A. J. Lusis, D. W. Golde, D. H. Quon, L. A. Lasky, *Nature* (*London*) **298**, 75 (1982).
15. Y. Gluzman, *Cell* **23**, 175 (1981).
16. R. J. Kaufman and P. A. Sharp, *Mol. Cell. Biol.* **2**, 1304 (1982); R. J. Kaufman, *Proc. Nat. Acad. Sci. U.S.A.*, in press.
17. H. P. Koeffler and D. W. Golde, *Science* **200**, 1153 (1978); A. J. Lusis and H. P. Koeffler, *Proc. Natl. Acad. Sci. U.S.A.* **77**, 5346 (1980). For the KG-1 CSF assay, 10 μl samples were added to microtiter wells containing 400 KG-1 cells in 140 μl of Iscoves medium with 0.3 percent agar, 20 percent fetal calf serum, and 10^{-4} *M* α-thioglycerol. The assays were scored after 10 to 14 days of incubation at 37°C by determining the increase in the number of KG-1 colonies over background. One unit of KG-1 CSF activity per milliliter is the concentration required to achieve a stimulation of 50 percent of the maximum response achieved when the CSF concentration is saturating. In the bone marrow CSF assay, 10^4 light density nonadherent bone marrow cells from normal human donors were substituted for the KG-1 cells. One unit of CSF in the bone marrow cell assay is that amount which will stimulate the formation of one colony per 10^4 cells above background when the CSF is below saturation levels.
18. R. J. Winzler, in *The Chemistry of Glycoproteins in Hormonal Proteins and Peptides*, C. H.

22. Anderson, W.F., Killos, L., Sanders-Haigh, L., Kretschmer, P.J., and Diacumakos, E.G. (1980). *Proc. Natl. Acad. Sci. U.S.A.* 77:5399–5403.
23. Capecchi, M.R. (1980). *Cell* 22:479–488.
24. Schaffner, W. (1980). *Proc. Natl. Acad. Sci. U.S.A.* 77:2163–2167.
25. Carlsen, S.A., Till, J.E., and Ling, V. (1976). *Biochem. Biophys. Acta* 455:900–912.
26. Corsaro, C.M., and Pearson, M.L. (1981). *Somat. Cell Genet.* 7:617–630.
27. Pellicer, A., Robins, D., Wold, B., Sweet, R., Jackson, J., Lowy, I., Roberts, J.M., Sim, G.K., Silverstein, S., and Axel, R. (1980). *Science* 209:1414–1422.
28. Perucho, M., Hanahan, D., and Wigler, M. (1980). *Cell* 22:309–317.
29. Robins, D.M., Ripley, S., Henderson, A.S., and Axel, R. (1981). *Cell* 23:29–39.
30. Scangos, G.A., Huttner, K.M., Juricele, D.K., and Ruddle, F.H. (1981). *Mol. Cell. Biol.* 1:111–120.

Somatic Cell Genetics, Vol. 7, No. 5, 1981, pp. 617–630

Competence for DNA Transfer of Ouabain Resistance and Thymidine Kinase: Clonal Variation in Mouse L-Cell Recipients

Cheryl M. Corsaro[1] and Mark L. Pearson

Cancer Biology Program, NCI Frederick Cancer Research Center, Frederick, Maryland 21701

Received 7 April 1981—Final 8 June 1981

Abstract—*We have used the calcium phosphate precipitation technique to study the competence of mammalian cell recipients for transformation with genomic mammalian cell DNA. The transformation efficiency for thymidine kinase (tk) varies 10- to 20-fold (up to 10^{-4} transformants/recipient) among different subclones of the LM tk$^-$ Cl 1D mouse fibroblast cell line. Analysis of this phenotype among second-generation subclones indicates that subclones exhibiting high competence tend to breed true, whereas those with low competence do not. Isolation of Tk$^-$ revertants from Tk$^+$ transformants results in the selection of cells with a high-competence phenotype as measured by their subsequent transformation for tk. This phenotype appears to be a general characteristic of such cells because recipients more competent for tk transfer are also more competent for transfer of a second marker, ouabain resistance (oua^R). This codominant marker coding for the Na^+, K^+-ATPase can be transferred at frequencies of 10^{-5} in the high-competence recipients. These results indicate that competence for DNA-mediated gene transfer can be determined in part by genetic factors.*

INTRODUCTION

DNA-mediated gene-transfer methods have been developed that permit the transformation of mammalian cells in culture with the genes encoding thymidine kinase (*tk*) (1, 2), adenine phosphoribosyl transferase (*aprt*) (3, 4), dihydrofolate reductase (*dhfr*) (5, 6), and hypoxanthine-guanine phosphoribosyltransferase (*hprt*) (7–10). Most of these studies used the LM *tk*$^-$ Cl 1D

[1]Present address: Division of Biology, California Institute of Technology, Pasadena, CA 91125.

line of mouse fibroblasts or its derivatives as recipients because these cells appear to be highly competent for DNA transformation. However, little is understood of the mechanisms determining the competence of these cells in particular or other cells in general. The low competence of many interesting cells, including those expressing a differentiated phenotype and those of human origin, is one of the major limitations to the wider use of DNA transformation for the genetic analysis of mammalian cells.

In this study, we have examined the competence of a number of subclones of Cl 1D t determine the extent of cellular variation in this phenotype and also to determine if there were genetic factors affecting competence. First, we compared the transformation frequencies for the *tk* marker among subclones isolated under nonselective conditions. Second, we determined the genetic stability of the competence of these subclones by measuring the transformation frequencies for *tk* in a second generation of subclones. Third, we isolated Tk^- revertants from both a stable and an unstable Tk^+ transformant and used these selected subclones as recipients for the retransfer of the *tk* marker to determine if they were more competent for transformation than the parental Cl 1D line. Finally, we used the transfer of a second independent codominant marker, resistance to ouabain (oua^R)—a specific inhibitor of the Na^+, K^+-ATPase—to determine whether the clonal variation in competence observed for *tk* transfer was a general characteristic of the recipient cells.

MATERIALS AND METHODS

Cells and Media. The LM tk^- Cl 1D mouse fibroblast line deficient in thymidine kinase activity (11) was obtained from Dr. Barbara Migeon. The unselected subclones of Cl 1D (A1, B1, B6, and D4) were isolated by plating Cl 1D cells in growth medium at 0.3 cells/ml/well in 24-well dishes (Linbro Scientific Co.) and trypsinizing cells in wells with single colonies after 12 days of growth. The subclones of A1 and B6 (A1-1, B6-2 etc.) were also isolated by the dilution method described above. CHO RI, a Chinese hamster ovary cell line (CHO pro^- mtx^{RI} oua^R), isolated by Flintoff et al. (12), was obtained from Dr. Peter N. Ray. L6 A49-1, and α-amanitin-resistant mutant with altered RNA polymerase II, was isolated by Dr. Michael Crerar from L6 rat myoblasts (M.M. Crerar, R. Leather, E. David and M.L. Pearson, in preparation). Cells were cultured at 37°C in a 5% CO_2 atmosphere in growth medium: Dulbecco's modified Eagle's medium (DME, glucose 1 mg/ml) supplemented with 10% fetal calf serum (Gibco), 1% nonessential amino acids (Gibco), and gentamicin, 50 μg/ml (Schering Corp.).

DNA Isolation. DNA was isolated as described in the accompanying report (2) from monolayer cultures of L6 A49-1 rat myoblasts and Cl 1D-B6 cells in growth medium and from CHO RI and Cl 1D cells grown in suspension in α-medium (13). The DNA was adjusted to a final concentration of 200 μg/ml in sterile buffer (150 mM NaCl, 10 mM Tris HCl, pH 7.5, 0.5 mM EDTA·Na_2) and stored at 4°C. The 260:280 nm absorbance ratio of the DNA was 1.85–2.0. The same batch of CHO RI DNA was used for the experiments shown in Tables 1, 3, 4, and 5 over a period of one year; no decrease in biological activity was noted over that period of time.

DNA Transformation. The DNA transformation protocol is a modification (2) of the calcium phosphate–DNA precipitation technique of Graham and van der Eb (14) and Wigler et al. (1). Our major modifications were to increase the exposure time of the recipient cells to the calcium phosphate–DNA precipitates to 24–48 h and to increase the expression time to 48 h before selection. The expression time is defined here as length of time from the addition of DNA to the time the cells were changed into selective medium. For selection of the Tk^+ transformants, growth medium was supplemented with 10^{-4} M hypoxanthine, 4×10^{-7} M aminopterin, and 1.7×10^{-5} M thymidine (HAT medium) (15). For selection of the Oua^R transformants, growth medium was supplemented with ouabain (Sigma) at 2.0 mM, unless otherwise noted. The dishes were incubated in HAT or ouabain medium for 17–19 days with only one medium change (on day 12–14) to avoid generating satellite colonies. At that time, individual colonies were picked with sterile cotton swabs, as required, and the remaining dishes were stained with 0.2% methylene blue in 50% methanol and scored for macroscopic colonies.

Isolation of Tk^- Revertants. The Tk^+ transformants of Cl 1D, T6 and T7, were isolated and characterized for the stability of the Tk^+ phenotype as described in the accompanying report (2). After segregation in nonselective medium for 6.5 weeks, the transformants were plated in BrdU medium (containing bromodeoxyuridine, 30 μg/ml) and individual colonies were isolated. These $BrdU^R$ Tk^- revertants were propagated in BrdU medium for 2 weeks and then transferred to growth medium for 4 weeks before being used as recipients for retransformation.

Stability of Transformants. The Oua^R transformant colonies were isolated and grown in ouabain-selective medium for 10 days and then transferred to growth medium. At this time (time 0) and at weekly intervals thereafter, the stability of the Oua^R transformants was tested by plating 50, 500, 2500, and 10^4 cells in 6-well dishes containing growth medium with and without 2 mM ouabain. The dishes were incubated for 10 days, stained with methylene blue, and scored for macroscopic colonies.

RESULTS

We report in the accompanying paper that increasing the DNA exposure time and expression time resulted in a significant enhancement in *tk* transfor-

mation frequencies (2). This improvement in gene-transfer efficiency made it practical to compare the competence of several recipient subclones and to study the pattern of inheritance of this phenotype.

Variation of Competence in Unselected Subclones. Four subclones, A1, B1, B6, and D4, were isolated from Cl 1D under nonselective conditions and used as recipients of the *tk* gene from CHO cell DNA (Table 1). There was at least a 10-fold variation in the transformation frequency among these subclones. One subclone, B6, was transformed with an efficiency 3- to 4-fold higher than the parental Cl 1D line; the other three subclones tested were consistently transformed with efficiencies 2- to 3-fold lower than the LM *tk*$^-$ Cl 1D parent. None of these cell lines ($<2 \times 10^{-7}$) reverted to the Tk$^+$ phenotype when treated with LM *tk*$^-$ DNA nor did their plating efficiencies differ significantly (Table 1). The possibility of artifacts due to variations in the formation of satellite colonies for different subclones is ruled out by our experimental procedure, which minimizes medium changes during selection for HAT^R clones (2), and by the constancy of the plating efficiencies for different subclones. Therefore, we concluded that the observed differences in transformation frequencies reflected differences in the competence of each subclone.

Heritability of Competence in Unselected Subclones. To determine if this phenotype for high or low competence was genetically stable, we obtained comparative *tk* transformation frequencies for a second generation of subclones derived from the low-efficiency subclone, A1, and the high-efficiency subclone, B6 (Table 2). These values ranged from 4×10^{-6} to 10^{-4}. It is clear that the low competence of A1 did not breed true. The five subclones derived from A1 exhibited a wide range of competence phenotypes: two A1 subclones were higher than Cl 1D, two were lower, and one was the same. In contrast, the competence of the high-efficiency recipient, B6, appeared to be relatively stable. All five B6 subclones had mean transformation frequencies higher than Cl 1D, suggesting that there was a genetic basis to the high-competence phenotype of B6. This divergence in competence over the three generations of LM *tk*$^-$ cells is shown schematically in Fig. 1. (The absolute transformation frequencies of A1, B6, and Cl 1D were higher in this experiment than those shown in Table 1, but the relative transformation frequencies were the same.)

Although these results were suggestive, they were not conclusive in establishing whether the high-competence phenotype was heritable. Therefore, we took a more direct approach to this question.

Isolation and Retransformation of Tk$^-$ *Revertants.* If a subset of high-competence recipients exists in the Cl 1D population, and if competence is determined by heritable factors, then it should be possible to select for high-competence recipients by isolating transformants. To test this hypothesis, Cl 1D cells were transformed with *tk*$^+$ DNA from CHO RI cells, and several Tk$^+$ transformants were isolated and characterized for the stability of their Tk$^+$ phenotype in the absence of selective pressure (2). One transformant was stable, and several were unstable. The stable transformant, T6, and one of the unstable transformants, T7, were then subcloned into BrdU

Table 1. Clonal Variation in Transfer of *tk*$^+$ DNA into Unselected Subclones of LM *tk*$^-$ Cl 1D

Tk$^-$ recipient	PE[a] (%)	Transformants × 10^{-6}[b] Exp. 1	Exp. 2
LM *tk*$^-$ Cl 1D, parent	59	7 ± 4	8 ± 4
Cl 1D subclones			
A1	58	<0.1	4 ± 2
B1	51	5 ± 3	3 ± 2
B6	49	20 ± 8	31 ± 21
D4	52	3 ± 1	5 ± 4

[a] Plating efficiencies, PEs, were determined in each experiment by plating 200 cells/100-mm dish in growth medium. The averages for the two experiments are given here.
[b] Colonies/20 μg DNA/10^6 recipient cells/100-mm dish. Each value cited ± standard deviation is the average of 10 dishes in HAT medium for each cell line. The *tk*$^+$ donor DNA was from CHO RI. Controls for Tk$^+$ revertants were determined by treating 5 dishes of each cell line with 20 μg LM *tk*$^-$ Cl 1D DNA/dish and selecting in HAT medium; no colonies were seen ($<2 \times 10^{-7}$).

Table 2. Genetic Stability of Low- and High-Efficiency Recipients

Recipient	Transformants × 10^{-6}[a] Exp. 1	Exp. 2
LM *tk*$^-$ Cl 1D parent	31 ± 8	14 ± 4
Low-efficiency subclone A1	10 ± 3	8 ± 4
A1 subclones		
A1-1	65 ± 7	59 ± 19
A1-3	4 ± 2	9 ± 3
A1-5	30 ± 5	18 ± 3
A1-7	7 ± 3	6 ± 2
A1-9	41 ± 6	43 ± 17
High-efficiency subclone B6	46 ± 11	37 ± 17
B6 subclones		
B6-2	100 ± 13	64 ± 18
B6-4	62 ± 17	62 ± 16
B6-6	34 ± 8	30 ± 10
B6-8	60 ± 10	45 ± 21
B6-10	37 ± 5	19 ± 11

[a] HAT^R colonies/20 μg DNA/10^6 recipient cells/100-mm dish. Each value cited ± standard deviation is the average of 8 dishes in HAT medium. The *tk*$^+$ donor DNA was from L6 A49-1. Control values were determined by treating 4 dishes of each subclone with 20 μg LM *tk*$^-$ Cl 1D-B6 DNA/10^6 recipient cells/dish and selecting for Tk$^+$ revertants in HAT medium. No colonies were seen ($<2 \times 10^{-7}$).

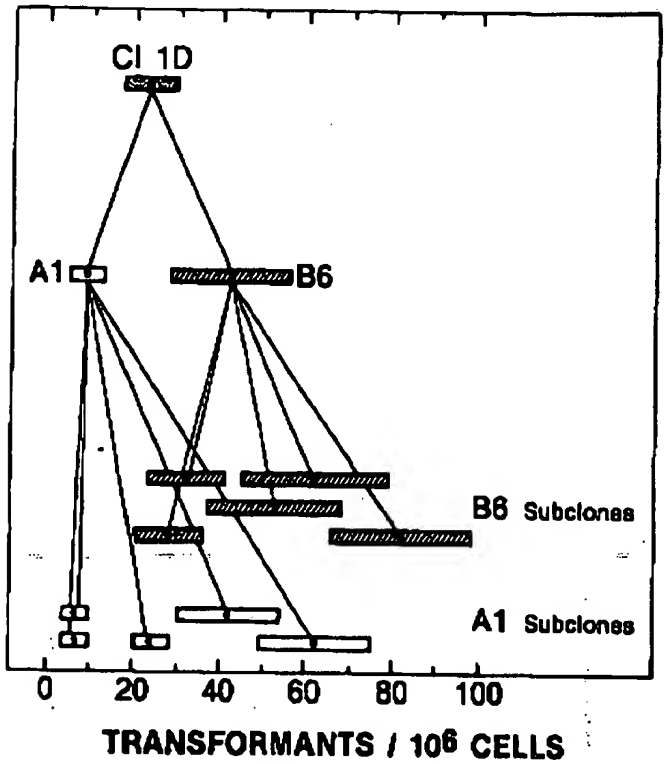

Fig. 1. Heritability of competence for tk^+ transformation in high- and low-efficiency subclones of Cl 1D. The transformation frequencies of each subclone from the two independent experiments in Table 2 were averaged to obtain the mean $\pm SD$ of the number of HAT^R transformants/20 μg DNA/10^6 cells/dish indicated by the dots and the error bars.

medium to select Tk^- revertants. Two $BrdU^R$ subclones of each transformant were isolated and designated T6-BdA, T6-BdC, T7-BdA, and T7-BdC. These Tk^- revertants could then be used as recipients in subsequent *tk* transformation experiments.

These Tk^- revertants were retransformed with tk^+ DNA to see if these selected subclones had higher transformation frequencies than the parental Cl 1D cells from which they were derived (Table 3). The transformation frequency of each f the Tk^- revertant subclones was 3- to 7-fold higher than that of the Cl 1D cells. Note that all four Tk^- revertants were transformed at frequencies higher than Cl 1D, in contrast to the unselected subclones described above (see Tables 1 and 2). These results strongly suggest that the population of Cl 1D cells contains a subpopulation of cells more competent for transformation and that this high-competence phenotype is heritable.

Controls for these experiments included treating 5 dishes of each strain

Table 3. Retransfer of tk^+ DNA into Tk^- Revertants of Tk^+ Transformants

Tk^- recipient	PE[a] (%)	Transformants × 10^{-6}[b] Exp. 1	Exp. 2
LM tk^- Cl 1D parent	59	7 ± 4	8 ± 4
Tk^- revertant subclones from:			
Unstable transformant			
T7-BdA	33	37 ± 9	20 ± 8
T7-BdC	42	49 ± 22	33 ± 14
Stable transformant			
T6-BdA	48	50 ± 14	37 ± 16
T6-BdC	54	26 ± 12	25 ± 10

[a] Plating efficiencies, PEs, were determined as in Table 1.
[b] Colonies/20 μg DNA/10^6 recipient cells/100-mm dish. Each value cited ± standard deviation is the average of 10 dishes in HAT medium for each subclone. The tk^+ donor DNA was from CHO RI. Control values were determined for each experiment by treating 5 dishes of each cell line with 20 μg LM tk^- Cl 1D DNA/10^6 recipient cells/dish and selecting for Tk^+ re-revertants with HAT medium. Colonies were seen only in dishes from the T6-BdA and T6-BdC Tk^- revertant subclones at a frequency of 1 to 3 × 10^{-6}. No colonies were seen in dishes from Cl 1D, T7-BdA and T7-BdC (<2 × 10^{-7}).

with parental tk^- DNA. No HAT^R colonies (<2 × 10^{-7}) were detected in the Cl 1D parent or in the two Tk^- revertants from the unstable transformant, T7-BdA and T7-BdC. The two Tk^- revertants from the stable transformant, T6-BdA and T6-BdC, had re-reversion frequencies of 1–3 × 10^{-6} cells/dish following exposure to tk^- DNA; however, these frequencies were significantly less than those obtained with 20 μg tk^+ DNA (2–5 × 10^{-5}). Furthermore, the enhanced transformation frequency of the Tk^- revertants was not due to an enhanced plating efficiency.

Ouabain-Resistance Transformation. In order to test whether the clonal variation in competence observed for *tk* transfer is a general property of these cells, we wished to measure the competence of these cells for a second independent marker. We selected the ouabain-resistance marker for this

Table 4. Transfer of oua^R and tk^+ Genes into Oua^R Tk^- B6 Recipients

DNA[a]	Transformants × 10^{-6}[b] HAT	Oua
oua^R tk^+	59 ± 19	2.1 ± 1.4
oua^S tk^-	<0.2	0.1 ± 0.3

[a] oua^R tk^+ DNA was prepared from CHO RI. oua^S tk^- DNA was prepared from LM tk^- Cl 1D.
[b] Colonies/20 μg DNA/10^6 recipient cells/100-mm dish. Each value cited ± standard deviation is the average of 6 dishes in HAT medium and 18 dishes in ouabain medium for each type of DNA. The Oua^R transformants were selected in 1.5, 2.0, and 3.0 mM ouabain (6 dishes each); no significant differences in transformation frequency were observed at these different concentrations of ouabain.

purpose because it is codominant (16, 17) and thus does not require prior mutation of the recipient cell. However, first it was necessary to demonstrate that ouabain-resistance could be transferred by DNA. Table 4 shows the DNA-mediated transformation frequencies obtained when the high-efficiency subclone B6 was treated with either *oua*^{R} *tk*$^+$ DNA or *oua*^{S} *tk*$^-$ DNA and then selected in ouabain or HAT medium. The number of Oua^R transformants obtained with *oua*^{R} DNA was 20-fold higher than that obtained with *oua*^{S} DNA. Figure 2 shows that the six Oua^R transformants isolated from dishes treated with *oua*^{R} DNA were unstable, whereas the spontaneous Oua^R mutant from the *oua*^{S} DNA-treated dish was stable. On

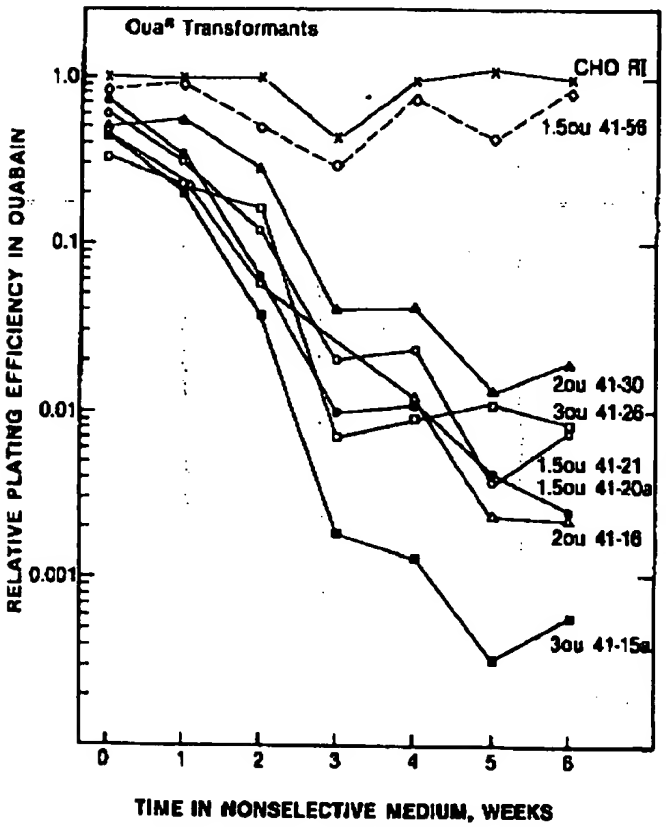

Fig. 2. Stability of the Oua^R phenotype in six *oua*^{R} transformants of the high-efficiency subclone, B6. The relative plating efficiency in ouabain versus nonselective medium is plotted as a function of time after the cells were transferred from ouabain to nonselective medium. Control Oua^R CHO RI cells are shown by the crosses; 1.5ou 41-56 is a spontaneous Oua^R mutant isolated in 1.5 mM ouabain after treatment with *oua*^{S} DNA; 1.5ou 41-21 and 1.5ou 41-20a are transformants isolated in 1.5 mM ouabain; 2ou 41-30 and 2ou 41-16 are transformants isolated in 2 mM ouabain; 3ou 41-26 and 3ou 41-15a are transformants isolated in 3 mM ouabain.

the basis of the increase in apparent transformation frequency obtained with *oua*^{R} vs. *oua*^{S} DNA and the segregation data, we concluded that the *oua*^{R} marker could be transferred by DNA.

Transfer of oua^R *and tk into High- and Low-Efficiency Recipients.* We next measured the independent transformation frequencies for the *tk* and *oua*^{R} markers in the various subclones of Cl 1D to see if the clones that were high-efficiency recipients for *tk* were also high-efficiency recipients for ouabain resistance. Table 5 shows the results of experiments in which *oua*^{R} *tk*$^+$ DNA was used to transform Cl 1D, the four unselected subclones, and the Tk$^-$ revertant, T7-BdC. It is clear that there is a positive correlation in transformation frequencies for the two markers: the clonal derivatives that were high-efficiency recipients for *tk* were also readily transformed to ouabain resistance, whereas the subclones that were low-efficiency recipients for *tk* were also low-efficiency recipients for ouabain resistance. Although the frequency for ouabain-resistance transfer was about 10-fold less than that for *tk* transfer, the *relative* transformation frequencies for both markers were the same in each subclone. Note that the Tk$^-$ revertant, selected first as a Tk$^+$ transformant, was more competent for retransformation with two independent markers.

DISCUSSION

We have used the DNA transfer of the *tk* and *oua*^{R} genes into several clonal derivatives of LM *tk*$^-$ Cl 1D mouse fibroblasts to examine the extent of cellular variation in competence and to determine whether genetic factors

Table 5. Transfer of *oua*^{R} and *tk*$^+$ Markers into High- and Low-Efficiency Recipients

Recipient	Transformants × 10^{-6}	
	HAT	Oua
LM *tk*$^-$ Cl 1D parent	36 ± 17	4 ± 2
Cl 1D subclones		
A1	39 ± 7	3 ± 5
B1	33 ± 12	2 ± 1
B6	122 ± 19	19 ± 4
D4	13 ± 7	1 ± 2
Tk$^-$ revertant subclone, T7-BdC	105 ± 18	13 ± 4

[a] Colonies/20 μg DNA/10^6 recipient cells/100-mm dish. Each value cited ± standard deviation is the average of 4 dishes in HAT medium and 8 dishes in ouabain medium (2 mM ouabain). The *oua*^{R} *tk*$^+$ donor DNA was from CHO RI. Control values were determined by treating 4 dishes with HAT medium and 8 dishes with ouabain medium for each subclone after treatment with 20 μg *oua*^{S} LM *tk*$^-$ Cl 1D B6 DNA/dish. No colonies ($<2 \times 10^{-7}$) were seen in the HAT controls. 0.1 colonies/20 μg DNA/10^6 recipient cells/dish were detected in the Oua controls for the Cl 1D, Cl 1D-B6, and T7-BdC recipients; no colonies ($<10^{-7}$) were observed in the ouabain controls for the other recipients.

might affect this phenotype. Three approaches to this problem were pursued: (1) Comparative transformation frequencies for the *tk* marker were obtained on two generations of subclones that had been isolated under nonselective conditions. (2) Transformation frequencies for *tk* were also compared among a populati n of subclones preselected for *tk* transformation competence. (3) The DNA-mediated transfer of the *oua*^{R} gene was demonstrated and then used as a second independent marker for transformation of the same set of subclones used in the *tk* transfer studies.

Clonal Variation in Competence. We found that randomly isolated subclones of Cl 1D varied as much as 10-fold in their transformation efficiencies, indicating that individual cells differ in their competence phenotype. They could be transformed with either a higher or a lower efficiency than Cl 1D. None, however, were completely defective in transformation. The observation that the high- and low-competence phenotypes of the subclones were reproducible from experiment to experiment suggested that these phenotypes may be heritable. Therefore, a high-efficiency recipient subclone and a low-efficiency recipient subclone were recloned to determine if their phenotypes bred true. Comparative transformation experiments on the next generation of subclones indicated that the competence phenotype of the high-efficiency subclone, B6, was relatively stable. In contrast, that of the low-efficiency subclone, A1, was unstable. These observations indicate that both genetic and physiological factors can influence competence.

Retransformation of Tk$^-$ (BrdU^R) revertants derived from Tk$^+$ transformants provided more convincing evidence that competence is determined in part by genetic factors. All four Tk$^-$ revertants were retransformed at frequencies 3- to 7-fold higher than were the parent Cl 1D cells. These results indicate that some cells in the Cl 1D population are more competent for transformation and that this phenotype is heritable. This conclusion is further substantiated by the enhanced efficiency of transfer of a second marker, *oua*^{R}, into subclones showing an enhanced *tk* transformation frequency. The most informative cell line in this regard was the Tk$^-$ revertant, T7-BdC, for the retransformation experiment demonstrated that a cell line preselected for competence for *tk* transformation was a high-efficiency recipient for both *tk* and *oua*^{R}.

The BrdU^R Tk$^-$ revertants derived from the stable *tk*$^+$ transformant, T6, re-reverted to a HAT^R phenotype at a detectable frequency (approximately 10^{-6}) at least 100-fold higher than that of Cl 1D (2). This indicated that the *tk*$^+$ gene from the first transformation was still present in the T6 cells: the gene was merely inactive and was not permanently lost during the isolation of these BrdU^R subclones. It is conceivable that the elevated frequency of *tk* retransformation is related somehow to the continued presence of the *tk*$^+$ allele in these cells. However, the retransformation

frequencies obtained with *tk*$^+$ DNA were significantly higher than the control re-reversion frequencies obtained with *tk*$^-$ DNA. Furthermore, elevated retransformation frequencies were obtained also with the Tk$^-$ revertants, T7-BdA and T7-BdC, which do not re-revert. The reversible inactivation of *tk* expression after exposure to BrdU noted here for the T6 BrdU^R subclones may be similar to that observed by others in segregants from cell hybrids (18), in Chinese hamster cell variants (19, 20), in herpes simplex virus-infected LM *tk*$^-$ cells (21), and in *tk*$^+$ transformants of LM *tk*$^-$ cells (22) and BRL *tk*$^-$ cells (23).

Wigler et al. (24) have shown that a small selectable subpopulation of cells is highly competent for transformation; the majority of LM *tk*$^-$ cells selected for transformation with the cloned herpes virus *tk* gene also incorporated other exogenous, unselected DNAs (ΦX174, pBR322, rabbit β-globin) added in 100- to 20,000-fold molar excess. However, competence was considered to be a transient phenotypic state of the cell and not stably inherited because the Tk$^+$ transformants showed no increase in transformation frequencies for a second marker (*aprt*$^+$, *hprt*$^+$, or methotrexate resistance) (8, 24). Our finding that competence can be inherited in some instances may simply be a consequence of differences between our experimental conditions for transformation and theirs.

Others have also observed variable transformation frequencies in subclones of other recipient cells. Although virus transformation may involve different biological processes from DNA-mediated transformation, it is interesting that MacPherson and Stoker found a 5-fold variation in efficiency when they analyzed the competence of four unselected clones of BHK21 cells for polyoma virus transformation (25). A 10-fold lower DNA-mediated transformation frequency for *tk* in a mutant *hprt*$^-$ derivative of LM *tk*$^-$ has also been noted by Graf et al. (8). In addition, variable frequencies for both *tk* and *hprt* transfer have been obtained in different cell lines (9, 26, 27). Hanahan et al. (28) also found that SV40 T-antigen expression varied greatly in different clonal isolates transformed with a plasmid DNA carrying the early region of SV40.

Oua^R *Transfer.* As far as we know, this is the first report of DNA-mediated gene transfer of the ouabain-resistance marker. Our evidence for successful transfer is the following: (1) transformation frequencies with *oua*^{R} DNA are 20- to 100-fold higher than with *oua*^{S} DNA, and (2) the *oua*^{R} transformants are unstable when grown in the absence of the selective agent, ouabain. In transferring a marker such as ouabain resistance, which has a detectable mutation frequency, one must distinguish bona fide transformants from spontaneous mutants. Unfortunately, there are no simple biochemical or immunological tests that would allow us to distinguish the Chinese hamster enzyme from the mouse L-cell enzyme. Thus, an alternate means of charac-

terizing the presumptive transformants is necessary. Stability is a characteristic of most (if not all) *oua*^{R} mutants (16, 17). In contrast, transformants can be stable or unstable; more often than not they are unstable (3–5, 7–9). The finding that the six independent *oua*^{R} transformants tested were unstable, in contrast with the mutant arising from a *oua*^{S} DNA-treated control dish, served to distinguish the transformants from the mutant.

The transformation frequency for ouabain resistance in each subclone tested was significantly lower (6- to 25-fold) than that for *tk*, even though both markers were derived from the same preparation of calcium phosphate-precipitated DNA. Because ouabain resistance is a codominant mutation, the mutant cell from which the *oua*^{R} DNA was isolated presumably carried only one copy of the *oua*^{R} allele. Therefore, transformation for the Oua^R phenotype would be expected to be at least 2-fold less efficient than that of the diploid *tk* allele, assuming that the DNA-dependence of the transformation efficiency for the *oua*^{R} marker was similar to that for the *tk* marker (2). The more than 2-fold difference in transformation frequencies observed for the *tk* and *oua*^{R} markers may reflect differences in the relative lengths of these two genes. Large differences in transformation frequencies between two markers from the same DNA—*aprt* and *hprt* (4) and *hprt* and *tk* (8, 9)—have been reported by others.

The difference in competence of one subclone for two different markers (*oua* vs. *tk*) may also reflect differences in the stabilization of the transferred genes in the transformants. For example, we previously found that the majority of the Tk$^+$ transformants of B6 were stable (2), whereas all six Oua^R transformants of B6 analyzed here were unstable. This suggests a correlation between increased competence and increased stability. Similarly, in studies analyzing the difference in competence of two different clones (Cl 1D and B6) for the same marker (*tk*), increased competence appeared to parallel increased stability; the majority of Tk$^+$ transformants from B6 were stable, whereas the majority of Cl 1D transformants were unstable (2). At the same time, we also characterized Cl 1D and the high-efficiency subclone B6 with respect to a number of parameters that might affect cellular competence for transformation, such as growth properties, chromosome number, and dose-response to DNA. No obvious differences in any of these properties were found. However, LM *tk*$^-$ Cl 1D cells are heteroploid and thus, because of chromosomal rearrangements, its subclones are not necessarily genetically identical. Such chromosomal alterations could lead to differences in the number of sites for integration of exogenous DNA sequences or differences in the levels of the gene products whose activity limits successful transformation. Clearly, more direct analysis of the molecular mechanisms limiting transformati n competence and determining the stability of the transferred sequences is required.

Conclusions. This study indicates that genetic factors can contribute to the enhanced transformation competence for *tk* and *oua*^{R} transfer in mammalian cells. A similar dependence of competence on genetic factors is well known in bacterial transformation (29, 30). Our evidence for the involvement of genetic factors in mammalian cell transformation is: (1) the elevated competence phenotype of some unselected subclones is inherited by their progeny, (2) the competence of *tk* transformants for retransformation is high, and (3) the competence for *oua*^{R} transfer is higher in recipients having an elevated competence for *tk* transfer.

Because of the heterogeneity in competence of different subclones noted here, it may be advisable to screen several subclones of other interesting cell types to obtain one more competent for transformation. DNA-mediated transfer of the codominant *oua*^{R} marker may prove useful for such screening, because all mammalian cell recipients are Oua^S and the spontaneous mutation frequency is low. Our data imply further that it may be possible to select an elevated competence phenotype in such cells by using *oua*^{R} transfer to identify transformants that can be used as high-competence recipients in subsequent gene-transfer experiments.

ACKNOWLEDGMENTS

We are grateful for the excellent technical assistance of Jim Dray and Emina David. We appreciate the helpful criticism of Barbara Migeon and Les Krueger. This work was supported in part by grants from the National Cancer Institute of Canada, the Medical Research Council of Canada, and the National Cancer Institute, National Institutes of Health, U.S.A., and in part by a contract NO1-CO-75380 to Litton Bionetics from the National Cancer Institute. C.M.C. was supported during part of this work by a postdoctoral fellowship from the Muscular Dystrophy Association of Canada.

LITERATURE CITED

1. Wigler, M., Pellicer, A., Silverstein, S., and Axel, R. (1978). *Cell* 14:725–731.
2. Corsaro, C.M., and Pearson, M.L. (1981). *Somat. Cell Genet.* 7:603–616.
3. Wigler, M., Pellicer, A., Silverstein, S., Axel, R., Urlaub, G., and Chasin, L. (1979). *Proc. Natl. Acad. Sci. U.S.A.* 76:1373–1376.
4. Lester, S.C., LeVan, S.K., Steglich, C., and DeMars, R. (1980). *Somat. Cell Genet.* 6:241–259.
5. Lewis, W.H., Srinivasan, P.R., Stokoe, N., and Siminovitch, L. (1980). *Somat. Cell Genet.* 6:147–151.
6. Wigler, M., Perucho, M., Kurtz, D., Dana, S., Pellicer, A., Axel, R., and Silverstein, S. (1980). *Proc. Natl. Acad. Sci. U.S.A.* 77:3567–3570.
7. Willecke, K., Klomfass, M., Mitrau, R., and Dahmer, J. (1979). *Mol. Gen. Genet.* 170:179–185.
8. Graf, L.H., Jr., Urlaub, G., and Chasin, L.A. (1979). *Somat. Cell Genet.* 5:1031–1044.

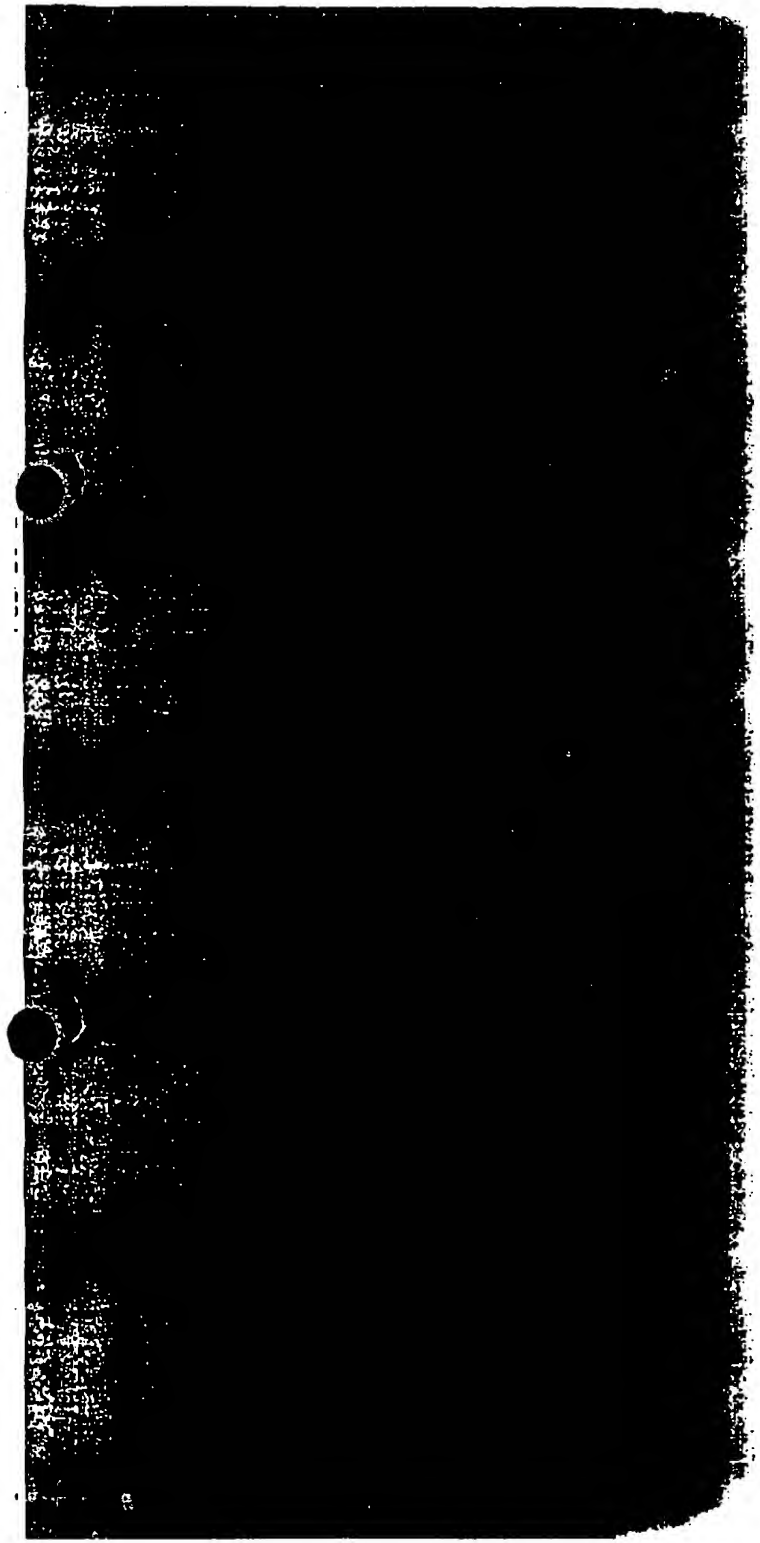

9. Peterson, J.L., and McBride, O.W. (1980). *Proc. Natl. Acad. Sci. U.S.A.* 77:1583–158
10. Liskay, R.M., and Evans, R.J. (1980). *Proc. Natl. Acad. Sci. U.S.A.* 77:4895–4898
11. Kit, S., Dubbs, D., Piekarski, L., and Hsu, T. (1963). *Exp. Cell Res.* 31:297–312
12. Flintoff, W.F., Davidson, S.V., and Siminovitch, L. (1976). *Somat. Cell Genet.* 2:245–26
13. Stanners, C.P., Eliceiri, G.L., and Green, H. (1971). *Nature (London) New Biol.* 230:52–54.
14. Graham, F.L., and van der Eb, A.J. (1973). *Virology* 52:456–467
15. Szybalska, E.H., and Szybalski, W. (1962). *Proc. Natl. Acad. Sci. U.S.A.* 48:2026–2034
16. Baker, R.M., Brunette, D.M., Mankovitz, R., Thompson, L.H., Whitmore, G.F., Siminovitch, L., and Till, J.E. (1974). *Cell* 1:9–21.
17. Corsaro, C.M., and Migeon, B.R. (1978). *Somat. Cell Genet.* 4:531–540.
18. Harris, M. (1975). *J. Cell. Physiol.* 86:413–430.
19. Bradley, W.E.C. (1979). *J. Cell. Physiol.* 101:325–340.
20. Harris, M., and Collier, K. (1980). *Proc. Natl. Acad. Sci. U.S.A.* 77:4206–4210
21. Davidson, R.L., Adelstein, S.J., and Oxman, M.N. (1973). *Proc. Natl. Acad. Sci. U.S.A.* 70:1912–1916.
22. Pellicer, A., Robins, D., Wold, B., Sweet, R., Jackson, J., Lowy, I., Roberts, J.M., Sim, G.K., Silverstein, S., and Axel, R. (1980). *Science* 209:1414–1422.
23. Robins, D.M., Ripley, S., Henderson, A.S., and Axel, R. (1981). *Cell* 23:29–39.
24. Wigler, M., Sweet, R., Sim, G.K., Wold, B., Pellicer, A., Lacy, E., Maniatis, T., Silverstein, S., and Axel, R. (1979). *Cell* 16:777–785.
25. MacPherson, I., and Stoker, M. (1962). *Virology* 16:147–151.
26. Graham, F.L., Bacchetti, S., McKinnon, R., Stanners, C., Cordell, B., and Goodman, H.M. (1980). In *Introduction of Macromolecules into Viable Mammalian Cells, Wistar Symposium Series I*, (eds.) Basergia, R., Croce, C., and Rovera, G. (Alan R. Liss, New York), pp. 3–25.
27. Grodzicker, T., and Klessig, D.F. (1980). *Cell* 21:453–463.
28. Hanahan, D., Lane, D., Lipsich, L., Wigler, M., and Botchan, M. (1980). *Cell* 21:127–139.
29. Tomasz, A. (1969). *Annu. Rev. Genet.* 3:217–232.
30. Smith, H.O., Danner, D.B., and Deich, R.A. (1981). *Annu. Rev. Biochem.* 50:41–68

JOURNAL OF CELLULAR PHYSIOLOGY 126:77–83 (1986)

Recovery of Hormonal Regulation in Protein Kinase Defective Adrenal Cells Through DNA-Mediated Gene Transfer

BERNARD P. SCHIMMER,* MARGARET WONG, DONALEE O'BRIEN, AND PATRICIA SCHULZ

Banting and Best Department of Medical Research (B.P.S., P.S.) and the Department of Pharmacology (B.P.S., M.W., D.O.), University of Toronto, Toronto, Ontario, Canada M5G 1L6

A cAMP-resistant mutant (Kin-8) isolated from Y1 mouse adrenocortical tumor cells harbors a specific lesion in the regulatory subunit of the type 1 cAMP-dependent protein kinase. This mutant also is resistant to the effects of corticotropin and cAMP on steroidogenesis, growth and morphology, suggesting an obligatory role for the protein kinase in regulation of adrenocortical functions. In this study, the cAMP-resistant phenotype of the Kin-8 mutant was reverted by transformation with DNA from cAMP-responsive Y1 cells, and the biochemical basis of the transformation was explored. Initially, Y1 mouse adrenocortical tumor cells were evaluated for their competence as recipients in DNA-mediated transformation experiments, by measuring their ability to incorporate and express a bacterial gene (neo) encoding resistance to neomycin. Y1 cells were transfected with the plasmid pSV2-neo (an SV40-neo hybrid vector designed for expression in animal cells) and screened for resistance to the neomycin analog, G418. Neomycin-resistant transformants were recovered from Y1 cells at a frequency of approximately one per 10^3 cells per 10 μg of DNA, and had specific neo sequences integrated into their high molecular weight (mw) DNA. The Y1 mutant, Kin-8, then was transformed with pSV2-neo DNA plus high mw DNA prepared from cAMP-responsive Y1 cells. Cells competent for transformation were recovered by selective growth in the neomycin analog G418, and these transformants were screened for recovery of morphological responses to cAMP. Several colonies capable of rounding up in the presence of cAMP were recovered after transformation with DNA from Y1 cells. These transformants also recovered the ability to round up in the presence of corticotropin, and were able to respond to both corticotropin and cAMP with increased steroidogenesis. Transformants generated from either Y1 or Kin-8 cells were unstable. Y1 cells lost resistance to neomycin when grown in the absence of G418 at a frequency of 4% per generation. Similarly, Kin-8 transformants lost their sensitivity to cAMP in subsequent culture passages. In some of the cAMP-responsive transformants, cAMP-dependent protein kinase activity was recovered and approached the activity seen in cAMP-responsive Y1 cells. The recovery of a normal protein kinase by transformation appeared to have been sufficient to reverse the cAMP-resistant phenotype of Kin-8 cells. In other cAMP-responsive transformants, protein kinase activity was not appreciably affected by cAMP. In these latter clones the gene encoding responsiveness to cAMP may have been lost in the interval between assays of adrenal-specific functions and protein kinase activity. Alternatively, these clones may have acquired another gene, unrelated to the protein kinase, which was capable of reversing the cAMP-insensitive phenotype.

Cellular genetics has made a significant impact on our understanding of cyclic nucleotide metabolism and the role of cAMP (adenosine 3',5'-monophosphate) in the regulation of various functions in animal cells (e.g., Gottesman, 1980; Bourne et al., 1984). The genetic analysis of cAMP metabolism and cAMP action invariably have been approached by isolating mutants from somatic cells in culture and then by analyzing their biochemical properties or their behavior in cell hybrids (Gottesman, 1980; Bourne et al., 1984; Schimmer et al., 1985). In this regard, the genetic analysis of cAMP action in the Y1 mouse adrenocortical tumor cell line has contributed to the elucidation of the mechanisms in-

Received May 29, 1985; accepted August 29, 1985.

*To whom reprint requests/correspondence should be addressed.

volved in the regulation of adrenocortical functions (Schimmer, 1981). For example, the isolation and characterization of cAMP-resistant, protein kinase-defective mutants from the Y1 adrenal line has helped to establish obligatory roles for cAMP and cAMP-dependent protein kinase in corticotropin's action on the adrenocortical cell (Rae et al., 1979; Williams et al., 1983; Schimmer et al., 1985). Nevertheless, these genetic approaches have been limited by the availability of suitable schemes for the selection of mutants. In addition, the possibility that the phenotypes which arose after mutagenesis and selection resulted from multiple mutational events always had to be considered.

The development of techniques to transform animal cells with isolated DNA (Wigler et al., 1977), has a potential application in the genetic analysis of cAMP metabolism and action in vitro. These techniques permit the introduction of specific genes into cells in order to determine their influences on specific phenotypes and to facilitate the isolation of specific genes for studies of structure and function (see Scangos and Ruddle, 1981, for review). Different cell types, however, differ in the competence to stably incorporate and express exogenous DNA, and only a few differentiated cell lines are available for this type of analysis. Accordingly, most studies of transformation in animal cells have been carried out using fibroblasts from mouse or Chinese hamster ovary cells (Gottesman, 1979). In view of the potential applications of DNA-mediated transformation to studies of corticotropin and cAMP actions, we have evaluated the extent to which mouse adrenocortical tumor cells stably incorporate and express exogenous DNA. In addition, we have used DNA-mediated gene transfer to reverse the cAMP-resistant phenotype associated with protein kinase defective, Y1 adrenal mutants.

MATERIALS AND METHODS

Cells and methods of culture

The Y1 cell line is a stable, ACTH-responsive subclone (Schimmer, 1979) of the mouse adrenocortical tumor cell line originally isolated by Yasumura et al. (1966). The clone designated Kin-8 is a cAMP-resistant mutant of Y1 which has been characterized extensively and which contains a mutation in the gene coding for the regulatory subunit of the type 1 cAMP-dependent protein kinase (e.g., Rae et al., 1979; Doherty et al., 1982; Williams and Schimmer, 1983; Schimmer, 1985). Cells were grown as monolayers in Nutrient Mixture F10 (Ham, 1963), supplemented with horse serum (15%; heat inactivated), fetal bovine serum (2.5%; heat inactivated), penicillin (200 units/ml) and streptomycin (200 μg/ml). A detailed description of the methods used to culture Y1 cells was presented previously (Schimmer, 1979).

Isolation of DNA

Supercoiled pSV2-neo DNA (Southern and Berg, 1982) was isolated from growing cultures of E. coli HB101 using detergent-lysis and centrifugation in CsCl (Maniatis et al., 1982). DNA of high mw was isolated from Y1 adrenal cells as described by Wigler et al. (1979), and was collected by spooling onto sterile glass rods. A 1.8-Kb fragment containing the neo gene segment was purified from pSV2-neo DNA digested with the restriction enzymes, *Hind* III and *Sma* I (Southern and Berg, 1982; Jorgensen et al., 1979). The purified neo fragment was labeled by nick translation with [alpha-^{32}P]dCTP (Maniatis et al., 1975) to a specific activity of approximately 4.0×10^8 cpm/μg DNA.

Transfection of cells with exogenous DNA

Mouse adrenocortical tumor cells were grown in 25 × 150 mm plastic tissue culture dishes to a density of 5×10^6 cells per dish, and transferred to alpha minimal essential medium (αMEM) (Stanners et al., 1971) supplemented with horse and fetal bovine sera. Cells were transformed with pSV2-neo and Y1 DNA using the DNA-calcium phosphate precipitation technique described by Graham and van der Eb (1973). Cells were incubated with the precipitated DNA for 24 h at 37°C, incubated in fresh growth medium for an additional 24 h, and then grown in the presence of the neomycin analog, G418 (100 μg per ml F10 growth medium) for 2–3 weeks. To determine the frequencies of transformation, cells were subcultured into 15 × 100 mm tissue culture dishes at a 1:20 dilution, allowed to attach overnight, and then grown in the presence of G418. Surviving colonies were stained with 1% methylene blue in 70% isopropanol and counted.

Steroid production

Steroid production was measured as described by Gutmann et al. (1978). Cells were incubated in 2 ml of αMEM supplemented with serum for the times indicated. At the end of the incubation, steroids were extracted from the medium with methylene chloride and quantitated by fluorescence in acidic ethanol using corticosterone as a standard.

Protein kinase activity

Protein kinase activity was assayed as described previously (Gutmann et al., 1978) by measuring the transfer of ^{32}P from ATP to histone F2B in the presence of varying concentrations of cAMP. Enzyme activity was assayed at 30°C for 3 min using a 100,000g supernatant fraction prepared from cell homogenates. The reaction mixture contained 35 μg of cellular protein, 100 μg of histone F2B, 150 μg albumin, 10 mM $MgSO_4$, 10 mM dithiothreitol, 0.5 mM 3-isobutyl-1-methylxanthine, 5 mM NaF, 20 μM [gamma-^{32}P]ATP (100 to 200 cpm/pmole), 20 mM 2-(N-morpholino)ethane sulfonic acid (pH 6.5), and cAMP as indicated in a final volume of 250 μl.

Reagents

Powders of Nutrient Mixture F10 and αMEM, sera, G418 (420 μg/mg), and the restriction endonucleases *Hind* III, *Bam* H1, and *Eco* R1 were purchased from Gibco Canada Inc., Burlington, Ontario. Cesium chloride, trizma base, corticosterone, cAMP, 2-(morpholin)-ethane sulfonic acid were obtained from Sigma Chemical Co., St. Louis, Missouri. Bovine serum albumin (Pentax) was from Miles Laboratories Inc., Elkhart, Indiana; 8BrcAMP and the restriction endonuclease *Sma* 1 were from Boehringer Mannheim Canada, Dorval, Quebec; dithiothreitol was from Calbiochem-Behring Corp., La Jolla, California. [alpha-^{32}P]dCTP (3000 Ci/mmol) was from Amersham Canada Ltd., Oakville, Ontari ; [gamma-^{32}P]ATP (20-40 Ci/mmol) was from New England Nuclear, Lachine, Quebec.

RESULTS

Transformation of Y1 cells with pSV2-neo DNA

In order to determine if Y1 mouse adrenocortical tumor cells were competent recipients of exogenous DNA in transfection xperiments, Y1 cells were transfected with pSV2-neo in the absence of carrier DNA and scored for resistance to the neomycin analog, G418. Y1 mouse adrenocortical tumor cells were reproducibly transformed to a neomycin-resistant phenotype with a frequency of 0.8 ± 0.2 transformants per 10^3 cells per 10 μg pSV2-neo DNA (n = 4). Transformants were detectable with 0.05 ug of pSV2-neo DNA per 5×10^6 recipient cells and their number increased with increasing concentrations of plasmid DNA. When transformants were grown in the absence of G418, neomycin resistance was lost at a rate of approximately 4% per generation (data not shown). Sequences homologous to a 1.3 kb segment of the neo gene were detected by hybridization of the probe to DNA prepared from transformed cells, but not by hybridization to DNA prepared from the untransformed Y1 parent. Before digestion with restriction endonucleases, the neo sequences in transformed cells were associated with high mw DNA. After digestion with *Eco* R1 or *Bam* H1, prominent neo sequences were observed on fragments of DNA ranging in size from 2 kb to 14 kb, and linearized pSV2-neo plasmid also was liberated (data not shown). These results indicate that in a large proportion of Y1 transformants, the plasmid was incorporated at multiple sites in the Y1 genome and in many cases, as concatameric structures (Perucho et al., 1980).

Isolation of cAMP-responsive transformants from the protein kinase mutant, Kin-8

cAMP-responsive transformants were generated from the cAMP-resistant mutant, Kin-8, by co-transformation with 40 μg of genomic DNA from cAMP-responsive Y1 cells and 2 μg of pSV2-neo DNA. The pSV2-neo gene provided a dominant selectable marker, facilitating the recovery of those Kin-8 cells able to take up and express exogenous DNA (e.g., Wigler et al., 1979). G418-resistant transformants then were screened for recovery of cAMP-dependent regulatory processes by measuring their ability to round up in the presence of the cAMP analog, 8BrcAMP (Schimmer et al., 1985). The frequency of transformation to G418 resistance measured in the presence of Y1 DNA was seven transformants per 10^3 cells with 2 μg of pSV2-neo DNA. This frequency was much higher than that measured in the absence of Y1 DNA, indicating an enhancing effect of carrier DNA on the transformation process. When the neomycin-resistant transformants were treated with 0.4 mM 8BrcAMP for 24 h and screened by microscopic examination for colonies that rounded up in the presence of the cyclic nucleotide, nine colonies of rounded cells were identified and isolated using stainless steel cloning cylinders. Several of these colonies were replated, screened for sensitivity to 8BrcAMP, recloned and maintained in F10 growth medium supplemented with G418 (100 μg/ml). Rounded colonies of cells were not found among transformants generated with pSV2-neo DNA in the absence of Y1 genomic DNA. The effects of ACTH on the morphology of two transformants recovered after transfection of Kin-8 cells with Y1 DNA are shown in Figure 1. These clones grew as well-stretched monolayers of cells in regular growth medium; however, when treated with ACTH (Fig. 1) or with 8BrcAMP (not shown), the cells retracted from the monolayer and assumed a rounded morphology. These morphological responses to ACTH and 8BrcAMP also were observed in the other transformants recovered in the screening process. In contrast, G418-resistant Kin-8 cells, transformed with pSV2-neo DNA in the absence of Y1 DNA, were resistant to these effects of ACTH (Fig. 1) or 8BrcAMP (not shown) on cell shape.

Steroidogenic activity in cAMP-responsive transformants

In order to determine if the recovery of cAMP-dependent morphological responses in transformants was accompanied by similar recoveries in other adrenocortical functions, the steroidogenic activities of transformed cells were evaluated (Table 1). The transformed cells were divided into two groups and assayed for steroidogenic activity at separate times. The first group was assayed for steroidogenic activity approximately 11 weeks after the clones were isolated. The second group was assayed 16 weeks after the clones were picked. In both sets of transformants, ACTH (10 mU/ml) and 8BrcAMP (1 mM) significantly increased the production of steroids ($p < 0.05$). The effects of ACTH and 8BrcAMP were similar, and resulted in rates of steroidogenesis which were approximately six-fold over the basal level (Table 1). In contrast, steroidogenic activity in the Kin-8 clone transformed with pSV2-neo DNA alone was not stimulated by ACTH or 8BrcAMP (Table 1). The levels of steroids produced by the two groups of clones, however, were significantly different. This difference likely resulted from an instability of the cAMP-responsive phenotype, causing steroidogenic activities to fall approximately four-fold during the 5-week interval between assays (Table 1). The instability of the acquired phenotype also was observed when clone S1 (Table 1) was reassayed for steroidogenic activity. After an additional 11 weeks in culture, clone S1 responded to 8BrcAMP with increased steroidogenesis, but the levels of steroids produced were at least 90% lower than seen in the initial assays (not shown).

cAMP-dependent protein kinase activity in cAMP-responsive transformants

During the 5-week interval between assays of steroidogenic activity (Table 1), the transformants were examined for cAMP-dependent protein kinase activity. Protein kinase activities measured in the transformants were compared with the activities observed in cAMP-responsive Y1 cells and in cAMP-resistant Kin-8 cells (Fig. 2). Protein kinase activity, measured in supernatant fractions prepared from homogenates of Y1 cells, was stimulated approximately ten-fold by cAMP to a maximum of 1050 ± 20 units of enzymatic activity. The concentration of cAMP required to elicit a half-maximal response (ED_{50}) was 0.09 ± 0.01 μM. Protein kinase activity measured in the Kin-8 mutant (transformed with pSV2-neo in the absence of Y1 genomic DNA) was considerably less sensitive to cAMP and was increased approximately two-fold over basal activity at 10 μM cAMP. The protein kinase activities of the cAMP-responsive transformants fell into two groups. In one group (two clones), the protein kinase was stimulated by cAMP to a

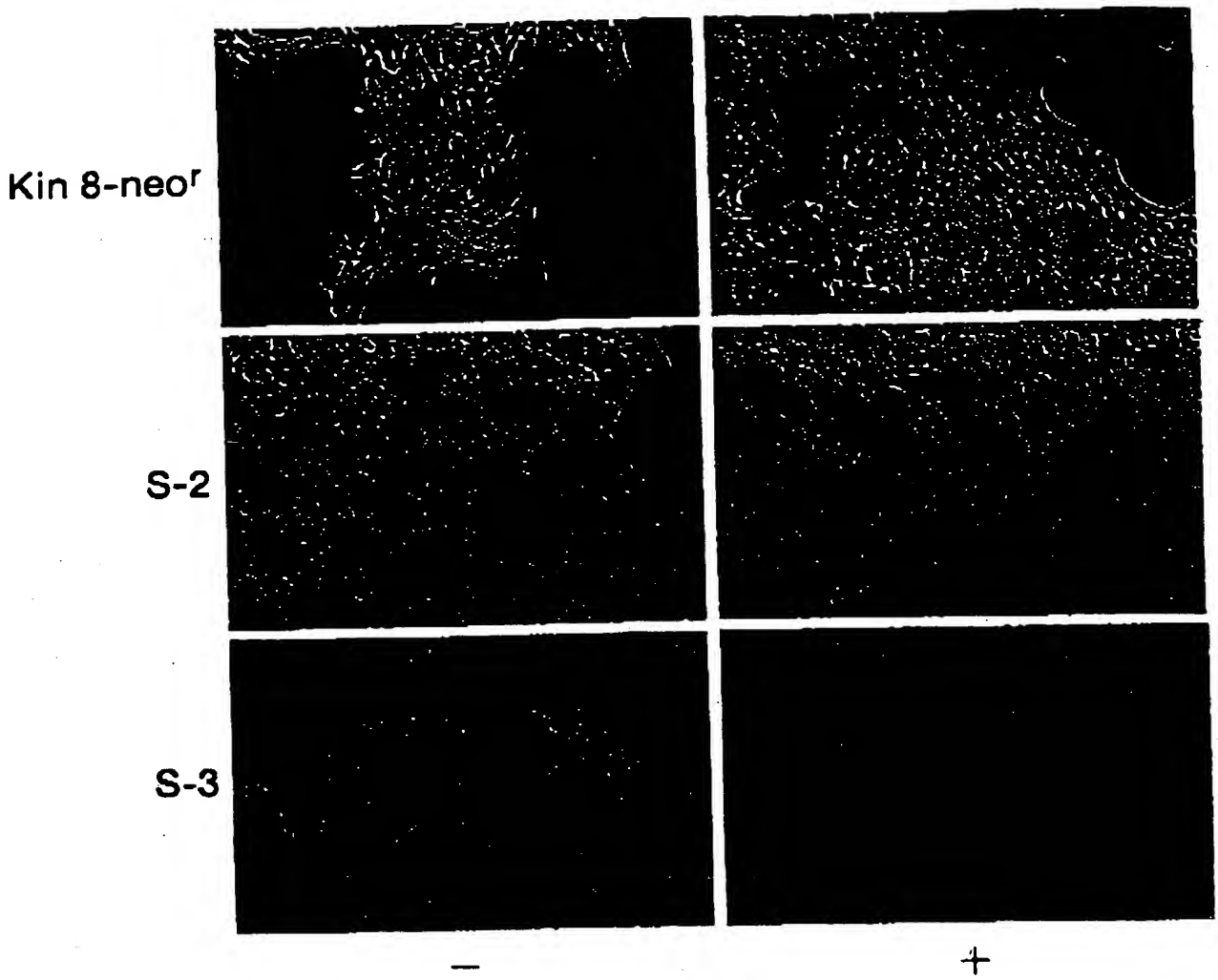

Fig. 1. Effects of ACTH on the morphology of cAMP responsive transformants. Cells were incubated in αMEM plus serum for 24 h in the presence (+) or absence (−) of corticotropin (10 mU/ml), and photographed under phase contrast. Shown are: clones S-2 and S-8—cAMP-responsive derivatives of the cAMP-resistant mutant Kin-8, formed by co-transfection with pSV2-neo DNA and Y1 genomic DNA; Kin8-neo^r—Kin-8 cells transformed to neomycin resistance with pSV2-neo in the absence of Y1 DNA.

greater extent than the enzyme from the mutant Kin-8. In this group, the maximal activity achieved with cAMP approached that obtained with the enzyme from the Y1 parent. The ED_{50} of the enzyme for cAMP (0.25 ± 0.03 μM) was approximately 2.5 times greater that the ED_{50} of the Y1 enzyme (Fig. 2). The cAMP responsive enzymatic activity in this group was unstable, and, after an additional 3 weeks in culture, was lost (data not shown). In the second group of cAMP-responsive transformants (five clones), protein kinase activity was relatively insensitive to cAMP at all times of assay, and was not significantly different from the activity observed in cAMP-resistant Kin-8 cells (Fig. 2).

DISCUSSION

A number of mutants, designated Kin, were isolated from Y1 adrenocortical tumor cells and were shown to be resistant to the effects of ACTH and cAMP on steroidogenesis, growth, and morphology (Schimmer et al., 1977; Rae et al., 1979). Several lines of evidence suggested that the cAMP-resistant phenotype in these mutants resulted specifically from a lesion in the gene coding for the regulatory subunit of the type 1 cAMP-dependent protein kinase: The type 1 enzyme, the major isozyme form in Y1 cells, had a reduced affinity for cAMP in mutant clones whereas the type 2 enzyme behaved normally (Gutmann et al., 1978; Schimmer et

TABLE 1. Steroidogenic activity in cAMP-responsive transformants[1]

Cell line	Steroids (μg/mg protein)		
	Basal	ACTH	8BrcAMP
Kin8-neo[r]	0.1 ± 0.1	0.4 ± 0.4	0.3 ± 0.2
Group 1			
S-1	1.4 ± 0.1	> 10	> 10
S-2	1.1 ± 0.2	6.5 ± 2.8	> 10
S-3	1.8 ± 0.1	> 10	> 10
Group 2			
S-4	0.6 ± 0.1	2.9 ± 1.3	2.9 ± 0.6
S-5	0.4 ± 0.1	3.6 ± 0.1	2.3 ± 0.3
C-1	0.4 ± 0.1	2.6 ± 0.3	2.7 ± 0.2
C-2	0.6 ± 0.2	3.4 ± 0.8	3.1 ± 0.7

[1]cAMP-responsive transformants of the cAMP-resistant mutant Kin-8 were divided into two groups and assayed for steroidogenic activity with an interval of 8 weeks between assays. Steroidogenic activity also was measured in a derivative of the cAMP resistant mutant Kin-8 (Kin8-neo[r]) transformed with pSV2-neo DNA in the absence of Y1 genomic DNA. Steroid production was assayed in triplicate, in cell monolayers containing approximately 1 mg protein per plate. Corticotropin (ACTH), 10 mU/ml, or 8BrcAMP, 1mM, were added as indicated.

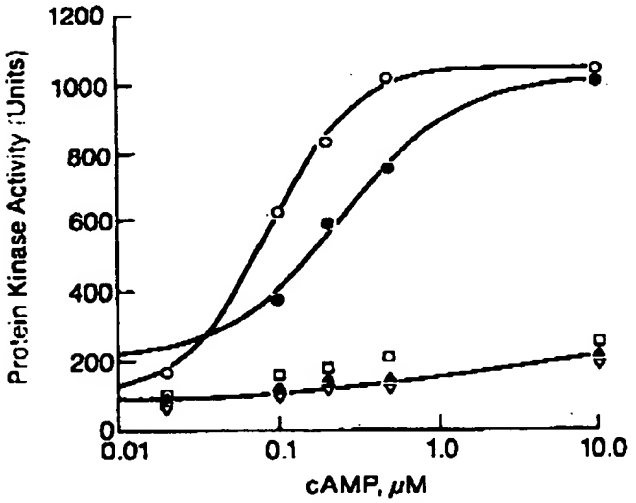

Fig. 2. Protein kinase activity in cAMP-responsive transformants. Protein kinase activity was assayed by measuring the transfer of ^{32}P from ATP to histone F-2B as described in Materials and Methods. One unit of activity equalled 1 pmol P transferred per min per mg protein. Enzyme activity was assayed as a function of cAMP concentration in extracts from Y1 (○), Kin8-neo[r] (▲) and cAMP-responsive transformants S-1 (▽), S-2 (●) and S-3 (□).

al., 1979); the regulatory subunit of the mutant type 1 enzyme was structurally altered and was responsible for the aberrant behavior of the protein kinase (Doherty et al., 1982); the altered structure of the regulatory subunit was seen in cell-free translation systems primed with mRNA from the cAMP-resistant clones (Williams and Schimmer, 1983); provision of normal regulatory subunits to cAMP-resistant clones by cell fusion restored normal cAMP-dependent protein kinase activity, and concomitantly restored the mutants to a cAMP-responsive phenotype (Schimmer et al., 1985).

In this study, we attempted to restore cAMP-dependent regulation in the protein kinase mutants of Y1 cells by transformation with DNA from cAMP-responsive Y1 cells. Based on our previous studies, we predicted that cells which acquired the gene coding for a normal protein kinase regulatory subunit would behave like the original Y1 parent, particularly in terms of characteristic responses to corticotropin or cAMP (Schimmer, 1981). We also considered as possible that the Kin mutants could acquire additional copies of other genes capable of reversing the cAMP-resistant phenotype—e.g., genes coding for components of the cAMP-responsive pathway beyond the protein kinase. In the latter case, other elements of the cAMP responsive domain might be identified. We attempted the transfer of wild-type genes into Kin mutant cells because previous experiments involving cell fusion indicated that the Kin mutation behaved recessively in the presence of additional, wild-type regulatory subunits (Schimmer et al., 1985). In this regard, attempts to transfer cAMP-resistance into Y1 cells using DNA from the mutant Kin-8 were not successful (M. Wong and B.P. Schimmer, unpublished observations).

Experiments were conducted initially to determine the competence of Y1 adrenocortical tumor cells with respect to transformation with exogenous DNA. The results presented here demonstrated that Y1 adrenocortical tumor cells were amenable to transformation with the transducing vector, pSV2-neo (Southern and Berg, 1982). Transformation of Y1 cells to a neomycin-resistant phenotype was dependent upon the concentration of pSV2-neo DNA, and was associated with the uptake and integration of neo sequences into the Y1 genome. The frequency of transformation in Y1 cells, approximately 10^{-3} transformants per cell per 10 μg of DNA, was equivalent to the frequencies reported in fibroblast lines by Southern and Berg (1982). The frequency of transformation appeared to be enhanced 30-fold when transformation was carried out in the presence of carrier DNA. The effect of carrier DNA on frequencies of transformation has been noted previously in fibroblast lines (e.g., Abraham et al., 1982).

Having established that Y1 mouse adrenocortical tumor cells could be transformed with exogenous DNA, we attempted to isolate cAMP-responsive transformants from the cAMP-resistant mutant, Kin-8. Of the Y1(Kin) clones, this mutant was most resistant to cAMP and had the least responsive cAMP-dependent protein kinase activity (Rae et al., 1979). When treated with corticotropin or 8BrcAMP, cells from this clone did not round up; instead they remained flattened on the surface of the culture dish (e.g., Fig. 1). The selection of cAMP-responsive transformants from Kin-8 cells involved cotransfection with pSV2-neo DNA and with Y1 DNA. Cells competent for transformation were selectively grown in the neomycin analog, G418, and then were screened for morphological changes indicative of their responsiveness to 8BrcAMP. Whereas single rounded cells could be seen occasionally in control populations of Kin-8 cells, colonies of rounded cells were observed only in populations transformed with genomic DNA from Y1 cells. Inasmuch as the detection of cAMP-responsive clones was based on a screening process, it was difficult to determine the frequency of transformation to a cAMP-responsive state. Crude estimates suggested that cAMP-responsive clones were recovered from the total population of transformants with a frequency of two to five transformants per 10^4 cells. The spontaneous rate of

reversion to a cAMP-responsive state could not be measured by this screen, but appeared to be lower than the frequency of tr nsformation. These transformants also recovered the ability to respond morphologically to corticotropin (Fig. 1), and to respond to both corticotropin and 8BrcAMP with increased steroidogenesis (Table 1). The cAMP-responsive transformants likely incorporated a large proportion of the Y1 genome randomly (Scangos et al., 1981), and therefore may have expressed many genes from the Y1 cell line. Our results, however, were obtained with seven different transformants suggesting that the recovery of responsiveness both to corticotropin and to cAMP resulted from a single gene, rather than from several genes. Therefore, the data suggest that corticotropin and cAMP act through common pathways to regulate the morphological and steroidogenic responses of the adrenal cell line.

The transformants of mouse adrenocortical tumor cells reported here were unstable. Under non-selective conditions, transformants lost the neo gene with a frequency of 4% per generation. In addition, cells transformed with Y1 DNA lost the potential for steroidogenesis when maintained in culture (Table 1). Unstable transformants have been observed using other cell lines, though stable derivatives eventually emerged from these populations (Scangos and Ruddle, 1981). Whether stable clones will emerge from the cAMP-responsive Kin-8 transformants has yet to be determined. The instability of the transformants suggests that cAMP-responsiveness arose as a consequence of gene transfer rather than spontaneous reversion; however, this instability also has complicated the assignment of specific genes to the cAMP-responsive phenotype. In some clones, the recovery of morphological and steroidogenic responses to ACTH and cAMP were associated with the recovery of cAMP-dependent protein kinase activity (Fig. 2). The apparent affinity of the protein kinase from transformants for cAMP was somewhat lower than that for the enzyme from the Y1 parent. The lower affinity for cAMP seen in transformants may have resulted from competition between wild-type and mutant protein kinase subunits for the holoenzyme as discussed previously (Schimmer et al., 1985). These data imply that the acquisition of a cAMP-responsive protein kinase is sufficient to restore Kin-8 mutants to corticotropin- and cAMP-responsive states. In some cAMP-responsive transformants, the protein kinase was insensitive to cAMP and indistinguishable from the Kin-8 mutant (Fig. 2). These latter clones may have been in a state of transition; initially, these clones may have recovered cAMP-dependent protein kinase activity, but then many cells may have lost the corresponding gene leaving only a residual undetectable level of cAMP-dependent protein kinase activity. Alternatively, these clones may have acquired another gene which was capable of reversing the cAMP-insensitive phenotype.

In view of the foregoing experiments, it may be possible to use DNA-mediated transformation to evaluate the roles of specific, cloned genes in hormonal regulation of adrenocortical functions. It would be of interest to determine: 1) if a cloned gene encoding the regulatory subunit of the type 1 cAMP-dependent protein kinase restores a cAMP-responsive phenotype to these cells; 2) if a cloned gene encoding the regulatory subunit of the type 2 enzyme functions similarly; and 3) if other genes override the mutation affecting the protein kinase and restore responsiveness to corticotropin and cAMP.

ACKNOWLEDGMENTS

This w rk was supported by a research grant from the National Cancer Institute of Canada.

LITERATURE CITED

Abraham, I., Tyagi, J.S., and Gottesman, M.M. (1982) Transfer of genes to Chinese hamster ovary cells by DNA-mediated transformation. Somat. Cell Genet., *8*:23–39.

Bourne, H.R., Casperson, G.F., van Dop, C., Abood, M.E., Beiderman, B.B., Steinberg, F., and Walker, N. (1984) Mutations of adenylate cyclase in yeast, mouse, and man. Adv. Cyclic Nucleotide and Protein Phosphorylation Res., *17*:199–205.

Doherty, P.J., Tsao, J., Schimmer, B.P., Mumby, M.C., and Beavo, J.A. (1982) Alteration of the regulatory subunit of type 1 cAMP-dependent protein kinase in mutant Y1 adrenal cells resistant to 8-bromoadenosine 3':5'-monophosphate. J. Biol. Chem., *257*:5877–5883.

Gottesman, M.M. (1979) Workshop on "Mutation and Gene Transfer in Somatic Cells." Somat. Cell Genet., *5*:665–671.

Gottesman, M.M. (1980) Genetic approaches to cyclic AMP effects in cultured mammalian cells. Cell, *22*:329–330.

Graham, F.L., and van der Eb, A.J. (1973) A new technique for the assay of infectivity of human adenovirus 5 DNA. Virology, *52*:456–467.

Gutmann, N.S., Rae, P.A., and Schimmer, B.P. (1978) Altered cyclic AMP-dependent protein kinase activity in a mutant adrenocortical tumor cell line. J. Cell. Physiol., *97*:451–460.

Ham, R.G. (1963) An improved nutrient solution for diploid Chinese hamster and human cell lines. Exptl. Cell Res., *29*:515–526.

Jorgensen, R.A., Rothstein, S.J., and Reznikoff, W.S. (1979) A restriction enzyme cleavage map of Tn5 and location of a region encoding neomycin resistance. Molec. Gen. Genet., *177*:65–72.

Maniatis, T., Jeffrey, A., and Kleid, D.G. (1975) Nucleotide sequence of the rightward operator of phage λ. Proc. Natl. Acad. Sci. USA, *72*:1184–1188.

Maniatis, T., Fritsch, E.F., and Sambrook, J. (1982) Molecular Cloning. A Laboratory Manual. Cold Spring Harbor Laboratory, Cold Spring Harbor, New York.

Perucho, M., Hanahan, D., and Wigler, M. (1980) Genetic and physical linkage of exogenous sequences in transformed cells. Cell, *22*:309–317.

Rae, P.A., Gutmann, N.S., Tsao, J., and Schimmer, B.P. (1979) Mutations in cyclic AMP-dependent protein kinase and corticotropin(ACTH)-sensitive adenylate cyclase affect adrenal steroidogenesis. Proc. Natl. Acad. Sci. USA, *76*:1896–1900.

Scangos, G.A., Huttner, K.M., Juricek, D.K., and Ruddle, F.H. (1981) Deoxyribonucleic acid-mediated gene transfer in mammalian cells: Molecular analysis of unstable transformants and their progression to stability. Mol. Cell. Biol., *1*:111–120.

Scangos, G., and Ruddle, F.H. (1981) Mechanisms and applications of DNA-mediated gene transfer in mammalian cells—a review. Gene, *14*:1–10.

Schimmer, B.P. (1979) Adrenocortical Y1 cells. Methods Enzymol., *58*:570–574.

Schimmer, B.P. (1981) The adrenocortical tumor cell line, Y1. In: Functionally Differentiated Cell Lines. G. Sato, ed. Alan R. Liss, Inc., New York. pp. 61–92.

Schimmer, B.P. (1985) Isolation of ACTH-resistant Y1 adrenal tumor cells. Meth. Enzymol., *109*:350–356.

Schimmer, B.P., Rae, P.A., Gutmann, N.S., Watt, V.M., and Tsao, J. (1979) Genetic dissection of ACTH action in adrenal tumor cells. In: Hormones and Cell Culture. Cold Spring Harbor Conference on Cell Proliferation. G. Sato and R. Ross, eds. Cold Spring Harbor Laboratory, Cold Spring Harbor, New York, Vol. 6, pp. 281–297.

Schimmer, B.P., Horney, S.J., Williams, S.A., Aitchison, W.A., and Doherty, P.J. (1985) Recovery of cyclic nucleotide regulation in protein-kinase-defective adrenal cells through somatic cell fusion. J. Cell. Physiol., *121*:483–489.

Schimmer, B.P., Tsao, J., and Knapp, M. (1977) Isolation of mutant adrenocortical tumor cells resistant to cyclic nucleotides. Mol. Cell. Endocrinol., *8*:135–145.

Southern, E. (1975) Detection of specific sequences among DNA fragments separated by gel electrophoresis. J. Mol. Biol., *98*:503–517.

Southern, P.J., and Berg, P. (1982) Transformation of mammalian cells to antibiotic resistance with a bacterial gene under control of the

SV40 early region promoter. J. Mol. Appl. Genet., *1*:327–341.
Stanners, C.P., Eliceiri, G.L., and Green, H. (1971) Two types of ribosome in mouse-hamster hybrid cells. Nature New Biol., *230*:52–54.
Wigler, M., Silverstein, S., Lee, L.-S., Pellicer, A., Cheng, Y.-C., and Axel, R. (1977) Transfer of purified herpes virus thymidine kinase gene to cultured mouse cells. Cell, *11*:223–232.
Wigler, M., Sweet, R., Sim, G.K., Wold, B., Pellicer, A., Lacy, E., Maniatis, T., Silverstein, S., and Axel, R. (1979) Transformation of mammalian cells with genes from procaryotes and eucaryotes. Cell, *16*:777–785.
Williams, S.A., and Schimmer, B.P. (1983) mRNA from mutant Y1 adrenal cells directs the synthesis of altered regulatory subunits of type 1 cAMP-dependent protein kinase. J. Biol. Chem., *258*:10215–10218.
Yasumura, Y., Buonassisi, V., and Sato, G. (1966) Clonal analysis of differentiated function in animal cell cultures. I. Possible correlated maintenance of differentiated function and the diploid karyotype. Cancer Res., *26*:529–535.

Crystal structure of an HIV-binding recombinant fragment of human CD4

Seong-Eon Ryu*, Peter D. Kwong*, Alemseged Truneh†, Terrence G. Porter†, James Arthos†, Martin Rosenberg†, Xiaoping Dai‡, Nguyen-huu Xuong‡, Richard Axel*§, Raymond W. Sweet† & Wayne A. Hendrickson*§

* Department of Biochemistry and Molecular Biophysics and § Howard Hughes Medical Institute, Columbia University, New York, New York 10032, USA
† SmithKline Beecham Pharmaceuticals, King of Prussia, Pennsylvania 19406, USA
‡ Departments of Physics, Chemistry and Biology, University of California at San Diego, La Jolla, California 92093, USA

CD4 glycoprotein on the surface of T cells helps in the immune response and is the receptor for HIV infection. The structure of a soluble fragment of CD4 determined at 2.3 Å resolution reveals that the molecule has two intimately associated immunoglobulin-like domains. Residues implicated in HIV recognition by analysis of mutants and antibody binding are salient features in domain D1. Domain D2 is distinguished by a variation on the β-strand topologies of antibody domains and by an intra-sheet disulphide bridge.

CD4, a cell-surface glycoprotein found primarily on T lymphocytes, is required to shape the T-cell repertoire during thymic development and to permit appropriate activation of mature T cells[1]. T cells that recognize antigens associated with class II major histocompatibility complex (MHC) molecules, mainly T helper cells, express CD4. Evidence is accumulating that CD4 and the T-cell receptor coordinately engage class II molecules on antigen-presenting cells to mediate an efficient cellular immune response, and that engaged CD4 may transmit a signal to an associated cytoplasmic tyrosine kinase, p56[kk].

CD4 belongs to the immunoglobulin superfamily of molecules which generally serve in recognition processes[2,3]. The sequence of CD4[4,5] indicates that it consists of a large (~370 residues) extracellular segment composed of four tandem immunoglobulin-like domains, a single transmembrane span, and a short (38 residues) C-terminal cytoplasmic tail. The first domain (D1) shares several features with immunoglobulin variable domains, but the sequence similarities between immunoglobulins and the other extracellular domains (D2, D3 and D4) are more remote.

In humans, CD4 can be subverted from its normal immunosupportive role to become the receptor for infection by the human immunodeficiency virus (HIV)[1,6,7]. Recombinant soluble CD4 proteins bind to the HIV envelope glycoprotein gp120, and can thus inhibit viral infection and virus-mediated cell fusion *in vitro* (refs 8, 9 and references therein). Domain D1 suffices for high-affinity binding to gp120 (ref. 8), and the analysis of substitution mutants further limits the sites of interaction to discrete regions in the domain[9,10–18].

Crystals of whole soluble CD4 (sCD4) molecules have been grown[19,20] but there has been limited success in achieving adequate diffraction order. The high solvent content and weak diffraction of several characterized polymorphs of human sCD4 are compatible with an extended, flexible molecule[19]. From the pattern of proteolytic cleavages that generate stable fragments (refs 21–23 and unpublished results), the main flexibility seems to be at the D2 to D3 junction. We have now crystallized a truncated derivative of CD4 that diffracts well, and here we report its atomic structure. This recombinant fragment[8] as secreted from Chinese hamster ovary (CHO) cells consists of residues 1–183 of human CD4 plus two missense residues, Asp-Thr; and it is unglycosylated. This molecule, which we refer to as D1D2, is as active as sCD4 in binding to gp120 (dissociation constant $K_d = 3$ nM) and retains all antibody epitopes mapped to these domains of CD4 (ref. 8 and unpublished results). Others have crystallized similar fragments from the N-terminal half of sCD4[24,25] and the structure of one is reported in the accompanying paper[43].

Here we describe the D1D2 structure in comparison with that of immunoglobulin domains, provide a geometrical definition for HIV recognition sites, and discuss implications of the structure for normal CD4 function and evolution of the immunoglobulin family. We find that the domains of CD4 are indeed immunoglobulin-like, although there are significant differences from the antibody analogues. The primary sites for HIV interaction are on loops that protrude from the variable-like D1 domain in analogy with immunoglobin complementarity-determining regions (CDRs). The D2 domain, which is intimately associated with D1, resembles constant domains but it is distinguished by a strand topology that is variable-like.

Structure determination

D1D2 protein secreted from CHO cells was purified to homogeneity by following procedures similar to those used for sCD4 (ref. 26). Crystals of this protein grown from polyethylene glycol (PEG) and stabilized at pH 8.2 (Table 1) belong to space group C2 and have unit cell dimensions of $a = 83.71$ Å, $b = 30.07$ Å, $c = 87.54$ Å, $\beta = 117.3°$. They contain one D1D2 molecule per asymmetric unit and 50% solvent. In searching for derivatives, we soaked crystals into stabilization medium doped with various heavy-atom compounds.

Diffraction data for the structure determination (Table 1) were measured at an area detector facility[27] where we collected CuKα data for the native protein and for candidate derivatives. Observable intensities could be recorded to 1.9 Å spacings from fresh native crystals, and even more strongly from the $K_2Pt(NO_2)_4$ derivative. We could also measure multiwavelength anomalous diffraction (MAD) data from this platinum derivative using characteristic gold emission lines which bracket the PtL_{III} absorption edge[28]. Phases were evaluated by both multiple isomorphous replacement (MIR) and MAD methods (Table 1). Electron density maps from MIR phasing (including anomalous data) at 2.7 Å resolution and from MAD phasing at 3.5 Å resolution both showed similar features. We then probabilistically combined MIR and MAD phase information to produce a combined map at 2.7 Å resolution (Fig. 1*a*) which showed distinct solvent channels and an apparent two-domain structure. A complete chain-tracing consistent with the amino-acid sequence for the first domain was possible, but the second domain remained difficult to interpret. By using a hand-drawn molecular envelope, we then performed solvent flattening and density truncation to improve the map further (Fig. 1*b*). This enabled us to trace the chain through the second domain. The C-terminal 12 residues (174–185) could not be seen.

A complete model was built into the solvent-flattened map as displayed by FRODO[29] program on a graphic workstation. Fragments from well-refined structures were fitted onto Cα guide points measured from a minimap and used as the starting point for building. Refinement made use of PROLSQ[30] and XPLOR[31] programs and included several manual rebuildings. Resolution of the analysis was gradually extended to 2.3 Å. After analysis of model 5 (Table 1) at $R = 0.208$, we discovered on comparing manuscripts that this model and one developed by Wang *et al.*[25] differed in the alignments of sequence in two strands (E of D1 and B of D2) and in conformations at residues 1, 103–108, 134–139 and 151–154. We then tested a model with residues 66–73 and 112–120 positioned in the former places of 64–71 and 114–122, respectively, and with the 134–139 region also rebuilt. Further refinement produced model 6 (Table 1) with an R value of 0.196 and stereochemical ideality typified by an r.m.s. deviation of 0.018 Å from ideal bond lengths. Study of this still incompletely refined model confirms the revised

TABLE 1 Statistics from the crystallographic analysis

(*a*) Diffraction data

Derivative	d_{min} (Å)	X-ray line /wavelength (Å)	No. of measurements	No. of reflections	Data coverage (%)	R_{merge}
Native	2.3	CuK_α/1.542	24,407	7,882	92	0.061
$K_2Pt(NO_2)_4$	2.5	CuK_α/1.542	40,130	6,757 (12,667)	99 (93)	0.057 (0.053)
	2.7	$AuL_{\beta1}$/1.084	33,914	5,314 (9,978)	97 (97)	0.069 (0.062)
	2.5	$AuL_{\beta2}$/1.068	43,005	6,639 (12,505)	97 (92)	0.072 (0.085)
	2.7	$AuL_{\alpha1}$/1.276	30,724	5,432 (10,210)	99 (99)	0.062 (0.054)
K_2PtCl_6	2.8	CuK_α/1.542	22,033	4,786 (6,751)	96 (88)	0.094 (0.086)

(*b*) MIR analysis

d_{min} (Å)	11.1	7.7	5.9	4.8	4.0	3.4	3.0	2.7	Total
$K_2Pt(NO_2)_4$									
r.m.s. f_H/E_{iso}	2.18	1.69	2.01	1.48	1.04	1.12	1.24	1.29	1.32
r.m.s. $\Delta F_{calc}/E_{ano}$	0.85	0.88	1.08	1.08	0.79	0.74	0.49	0.37	0.63
K_2PtCl_6									
r.m.s. f_H/E_{iso}	1.54	1.72	1.92	1.52	1.13	1.19	1.23	—	1.35
r.m.s. $\Delta F_{calc}/E_{ano}$	0.45	0.54	0.58	0.39	0.24	0.21	0.14	—	0.23
$\overline{m}$	0.81	0.71	0.75	0.71	0.58	0.57	0.51	0.37	0.53

(*c*) MAD analysis

λ (Å)	Observed ratio 1.542	1.084	1.068	1.276
1.542	0.043	0.066	0.057	0.069
1.084		0.038	0.029	0.030
1.068			0.038	0.036
1.276				0.037

(*d*) Solvent flattening

Shell/cycle	R	$\Delta\phi$
1/1	0.31	28.2
1/5	0.24	35.5
3/5	0.23	37.0
7/5	0.22	43.8
13/10	0.21	63.4

(*e*) Refinement

Step	Program	Data range (Å)	*B*-value refinement	Rebuilding	H_2O	R	$\Delta\sigma$ (Å)
0	PROLSQ	10.0–2.7	No	No	0	0.447	0.044
1	PROLSQ	5.0–2.7	No	No	0	0.271	0.025
2	PROLSQ	10.0–2.3	Yes	Yes	0	0.273	0.024
3	XPLOR	10.0–2.3	No	Yes	0	0.268	0.024
4	PROLSQ	10.0–2.3	Yes	Yes	0	0.250	0.023
5	PROLSQ	10.0–2.3	Yes	Yes	106	0.208	0.020
6	XPLOR/PROLSQ	10.0–2.3	Yes	Yes	72	0.196	0.018

Crystallization. D1D2 was purified in sequential steps of ion-exchange chromatography[28] involving S-Sepharose capture at pH 5.2, Q-Sepharose passage at pH 9.0 and a final elution from S-Sepharose at pH 6.0 in 0.6 M NaCl. Crystallization was carried out at 20 °C by equilibration against reservoirs of 20–25% PEG 3350 starting from hanging droplets composed of protein at ~20 mg ml^{-1} in PBS at pH 7.0 and equal volumes from the reservoir. Collected crystals were transferred to a stabilization medium (30% PEG 3350, 80 mM Tris buffer, pH 8.2). Typical crystals have dimensions of 0.5 × 0.3 × 0.2 mm. Diffraction data for MIR phasing and for refinement were measured with CuKα X rays generated by a Rigaku RU200 rotating anode and detected on two multiwire chambers on the Mark III system at UCSD. All data were collected at or near 20 °C. The inverse beam method was used to collect Bijvoet mates; that is settings were changed from (ω, χ, φ) to (ω, −χ, φ + π) after rotations at each crystal orientation. Data for MAD phasing were collected on the Mark II area detector system. A graphite monochromator was used to select specific characteristic lines produced from a gold-plated anode installed on an Elliot GX-6 generator. The monochromator was tuned to 50% intensity at one side or the other of the unresolved $L_{\beta1}/L_{\beta3}$ doublet for selection of a primary monochromatic component. The UCSD area detector processing package was used for the reduction of all data. Values given inside of parentheses for numbers of reflections and R_{merge} are without merging of Friedel mates ($R_{merge} = \sum |I_{obs} - I_{avg}| / \sum I_{avg}$). MIR analysis. Heavy-atom positions were determined from Patterson syntheses. The refinement of heavy-atom parameters and the phase calculations were performed with a version of program PHARE modified by Z. Otwinowski (personal communication) for an improved error treatment. Relative occupancies for the $K_2Pt(NO_2)_4$ and K_2PtCl_6 derivatives were (1.00, 0.94) and (0.53, 0.51, 0.25, 0.22, 0.19), respectively. The first two heavy-atom sites of the K_2PtCl_6 derivative are in common with the sites of the $K_2Pt(NO_2)_4$ derivative. Parameters cited in the table are: f_H, calculated heavy-atom structure-factor contributions; ΔF_{calc}, calculated Bijvoet difference; E_{iso}, r.m.s. isomorphous closure error; E_{ano}, r.m.s. anomalous closure error; and $\overline{m}$, mean figure-of-merit. MAD analysis. The MADSYS system of programs[54] was used to produce initial MAD phases. Phase combination between MIR and MAD was performed by the combination of ABCD coefficients[55]. But in this case it was necessary to modify the original MAD refinement formulation[54] so as to produce phases for the native non-anomalously scattering component[56] of the platinyl CD4 complex. The previously used method for extracting ABCD coefficients[57] proved to be ineffective in this case. Instead these phasing coefficients were extracted directly from MAD phases and figures-of-merit[57]. MIR and MAD phases were combined at 20.0–3.5 Å; MIR phases were used alone for the 3.5–2.7 Å data. Observed anomalous diffraction difference ratios are given for the data between 20.0–3.5 Å. Bijvoet (diagonal elements of matrix) and dispersive (off-diagonal elements) difference ratios represent r.m.s. ($\Delta F_{\pm h}$)/r.m.s. (F) and r.m.s. ($\Delta F_{\lambda\lambda}$)/r.m.s. ($F$), respectively. Solvent flattening was performed following procedures used in the structure analysis of myohemerythrin[58]. After interpretation of the first domain, a molecular envelope was delineated which included 56% of the asymmetric unit of the crystal (as compared with 50% for the true solvent content) to ensure that all protein density was included. After subtraction of the mean solvent density and truncation of the lowest density values within the molecular boundary, the contents of the modified density function were Fourier-inverted. Phasing coefficients from the inversion were reduced by 0.5 before combination with ABCD values from MIR. A truncation level to eliminate the lowest 20% of molecular points (as compared with 0% and 10%) was chosen as giving the best definition for known features in domain D1. The phase refinement was carried out starting from the 20.0–4.5 Å shell and including higher angle reflections successively until finally reaching 2.7 Å spacings. Five cycles of solvent flattening were carried out for each shell between shell 1 and shell 12 and 10 cycles were run for shell 13. R, Crystallographic R value between observed structure factor magnitudes and calculated values from the solvent-flattened map. $\Delta\phi$, Phase differences between phases from MIR plus MAD and phases from the solvent flattened map. Refinement. Selected points along the course of refinement are listed. For all steps the data having $F_{obs} > 4\sigma(F_{obs})$ were included. Step 0 refers to the unrefined starting model after adjustment of the scale factor only. From step 2 onward the data between 10.0 and 5.0 Å were included which helped to achieve better connectivities in $2F_{obs} - F_{calc}$ maps. The final model at 2.3 Å resolution is based on the 5,889 reflections (64%) which met the 4σ criterion. This partially refined model includes the 1,420 atoms from residues 1–173 plus the 72 water sites. Thermal parameters were restrained as typified by an r.m.s. discrepancy of 1.27 Å^2 in B values between bonded main-chain atoms. $R = \sum |F_{obs} - F_{calc}| / \sum F_{obs}$; $\Delta\sigma$, r.m.s. bond deviation from ideality (Å).

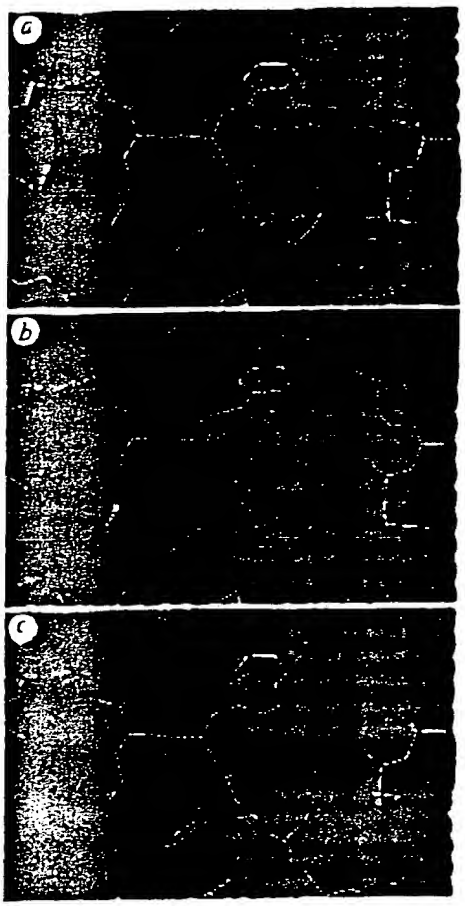

FIG. 1 Electron-density distributions used in the structural determination. The portion displayed in each panel includes the segment Phe 26-His 27-Trp 28-Lys 29 with the partially refined model 5 (yellow) superimposed on the density (blue). *a*, Experimental map at 2.7 Å resolution based on combined MIR plus MAD phase information; $\overline{m}=0.58$. *b*, Experimental map at 2.7 Å resolution after phase refinement by solvent flattening and density truncation; $\overline{m}=0.66$. *c*, Refined map with model phases after refinement at 2.3 Å resolution; $R=0.208$.

alignment in D1 and supports the changes made in D2, although several loops in D2 remain ill-defined. All conclusions drawn from model 5 remain unchanged, but the precise numerical quantities and Figs 2*b*, 4 and 5*a* were redone from model 6.

Overall structure

The D1D2 structure is of the all-β type. It consists of two intimately associated domains, each of which is a β sandwich folded with immunoglobulin-strand topology. The polypeptide folding is shown in Fig. 2. The first domain (D1) comprises residues 1–98 disposed in nine β strands, and the second domain (D2) contains residues 99–173 and has seven β strands. These domain boundaries are in striking correspondence with intron boundaries immediately after residues 100 and 177 in the gene structure[5]. The suggestion that J-like regions follow these introns is not borne out by the structure.

The last strand of D1 continues straight into the first strand of D2, running for a length of 49 Å from residues 88–103. This tandem association of domains leads to a rod-shaped molecule of dimensions roughly 25 × 25 × 60 Å. By comparing the solvent-accessible surface area of D1D2 with that of the separated

FIG. 2 Backbone structure of the D1D2 fragment of CD4. *a*, Schematic diagram (copyright Yarmolinski and Hendrickson, 1990). *b*, Stereodiagram of the α-carbon backbone. Positions of residue numbers divisible by ten are indicated by small spheres, sulphur atoms in disulphide bridges are indicated by larger spheres. The point of view is down the Z″ axis after rotations about X(100°), Z′(−30°), Y′(−90°) and X″ (10°) starting with the frame having X, Y, Z along a, b and c*.

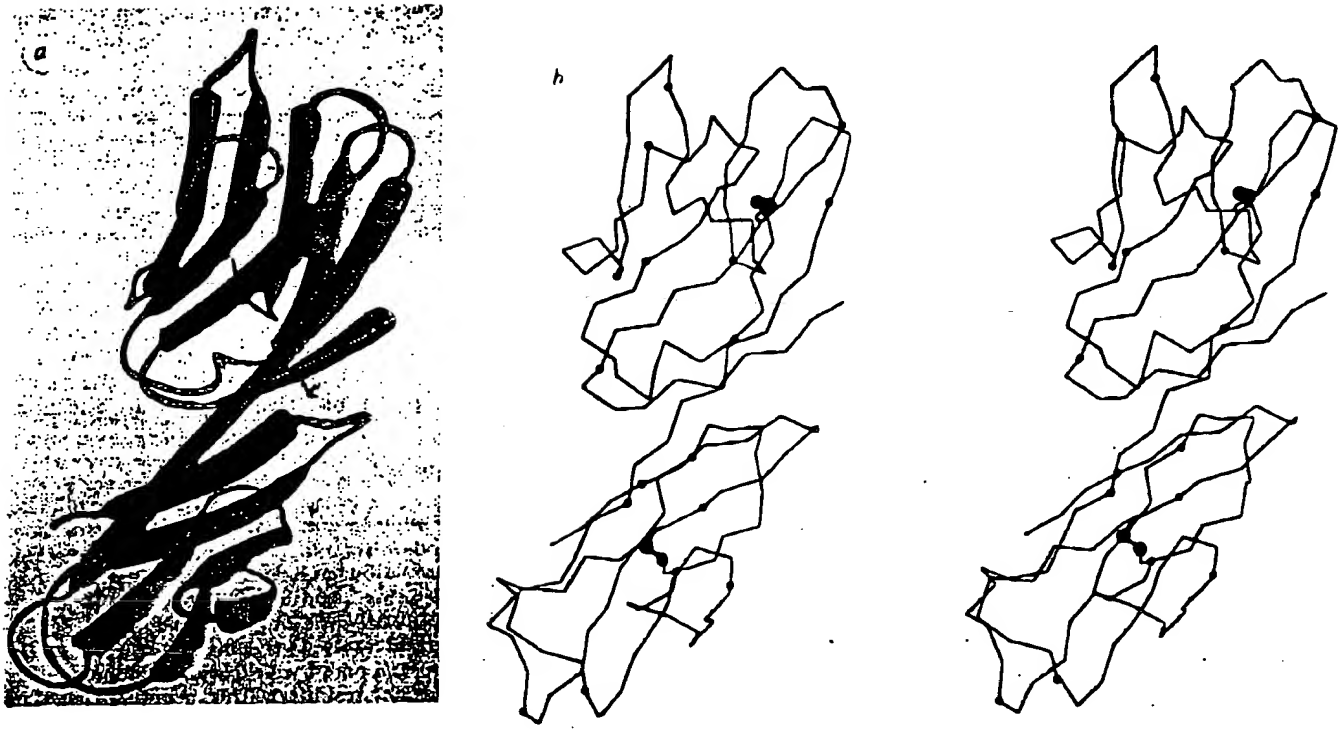

domains, we found that 310 Å² from each domain is buried in the interface. This compares with 110 Å² for the VH–CH1 interface of Fab New[32]. Interdomain contacts are largely hydrophobic. Residues involved in interdomain contacts include Val 3, Leu 5, Ile 76, Leu 90, Val 97 and Phe 98 from D1, and Glu 119, Pro 121, Gln 163, Val 166 and Phe 170 from D2. The surface of D1D2 has many positively charged amino acids (the calculated pI of residues 1–183 is 10.0), and the electrostatic potential surface[33] computed from the model is mostly positive at neutral pH. There are, however, two prominent patches of negative potential: one is associated with Glu 89, Glu 87 and Asp 88 and the other is from Asp 105, Asp 153 and Asp 173.

TABLE 2 Residues implicated in HIV recognition by point mutation in D1 of CD4*

Amino-acid residue	Fractional solvent accessibility†	Effect on gp120 binding‡				Effect on syncytium formation‡‖			Ref.
K29	0.30	A	■□□						16
G30	(0.91)	E	═	E	■■□	E	□□		16,18
Q40¶	0.85	F	┌┐	H	┌─┐	F	■□		10,12
		H	□□	H	□JU				8,18
		A	▭						16
G41	(0.93)	S	■□□						18
S42	1.00	T	■□□	A	□□□				16,30
F43	0.90	V	■■	I	■□□	V	■■		8,15
		L	┌┐			L	□□		10
L44	0.38	S	■■□	A	■■┌┐				15,18
T45	0.69	F	▬	G	■□□	F	■■		10,15
		I	□□	A	□□□	I	□□		8,16
G47	(0.43)	E	┌─┐	S	■■□	E	■□		10,15
		R	▬			R	■■		10
S49	0.58	T	□□□	Y	■■┌┐				15
		A	■□□						16
N52	0.73	N	□□□	A	■□□				16,18
A55	0.00	F	■■			F	■■		8
R58	0.73	G	■□□	A	□□□				15,18
R59	0.82	G	■□□	A	■■┌┐				15,18
Q64	0.84	E	□□□	A	■□□				15,16
		N	┌─┐						12
F67	0.00	L	■■□						15
E77	0.97	A	■□□						16
T83	0.55	A	■■■						16
E85	0.59	A	■■□						16
E87	0.53	K	┌─┐			K	■□□□		10,17
		A	□□□			G	■■■■		16,17
						N	■□□□		16,17
D88	0.71	A	□□□			L	■■■□		10,17
Q89	0.80	L	┌─┐			K	■■□□		16,17
		A	□□□						

* Within the 98 amino-acid residues of the D1 domain there is no mutational information on residues 3–6, 12, 14, 15, 16, 26, 69–71, 78, 83, 84 and 97. However, the binding of gp120 to Rhesus CD4[10] and to the human–rat chimaeric protein eliminates 12, 14, 16 and 76 from this list. Mutations which caused global alteration of structure, as evidenced by reduced binding of several anti-CD4 monoclonal antibodies were not considered[7,8,18]. Such mutations were the only data for 13 amino acids and thus led to exclusion of residues 7, 13, 35, 36, 37, 54, 57, 62, 75, 79, 82, 93 and 95. Thus, in total, 25 amino acids are excluded from consideration.

† Fractional solvent accessibility was calculated as the ratio of solvent-accessible surface area for atoms of an amino-acid residue X in the protein to that area obtained after reducing the structure to a Gly–X–Ala tripeptide[34]. Values listed are for side-chain atoms except in the case of glycine residues where main-chain values are given.

‡ Mutants are identified by single-letter code. Mutational effects are symbolized by blackening in steps proportional to the quantitations' sensitivity of the assays as reported. Only single amino-acid substitutions are included. The results from double substitutions largely confirm these data. Certain double mutations are of particular note. A G25S/K30I severely disrupts binding[35], emphasizing the significance of F43. S, L31M/A55T does not affect binding[35], indicating that the severe effect by the A55F substitution is conformational in nature. E87G/K90G[18] and D88N/Q89R[8] do not affect binding, further indicating that this region is not involved in initial binding to gp120.

§ Relative effects of the indicated mutations on virus[35] or gp120[18] binding to cell surface CD4 or gp120 binding to soluble CD4 proteins[8,35,36]. The results shown are an interpretation of the primary data and comparisons among the results from the different laboratories are approximate.

‖ Relative ability of cells bearing CD4 mutant proteins to form syncytium with cells expressing virus envelope proteins[8,35,37] or of soluble CD4 proteins to inhibit syncytium[8].

¶ The Q40A mutation increases binding affinity to gp120 twofold.

The D1D2 crystal lattice contains diad axes that could accommodate a dimeric molecule. However, contacts across screw axes dominate the lattice interactions and the only diad-mediated interface (between D1 domains) seems unlikely to persist in solution. The lattice interactions of D1 are more extensive than those of D2 which is reflected in molecular mobilities of the domains: the average B value is 19.9 Å² for D1 compared with 37.8 Å² for D2. This accounts for our greater difficulty in tracing the D2 chain.

CD4, like many members of the immunoglobulin superfamily, is a single-chain cell-surface receptor composed of tandemly repeated domains. Some of these domains have been assigned as V-like and others as C-like or in the 'C2 set'[34]. The D1D2 domain of CD4 contains both types and, apart from the similarity of CD5 with the PapD bacterial chaperone protein[35], this is the first three-dimensional structure for such members of the family.

Variable-like domain D1

As anticipated by sequence comparisons, D1 is similar to the variable (V) domains of antibodies. A schematic drawing of the folding pattern with standard immunoglobulin designations for the secondary structural elements is shown in Fig. 3. Strands B, D and E make up one β sheet, and strands A, C, C', C'', F and G are in the other sheet of the β sandwich. In immunoglobulin V domains, the first half of strand A is hydrogen-bonded to strand B of the outer sheet but the second half switches to the inner sheet. Strand A of D1 is foreshortened and occupies only the 'inner-sheet' position, hydrogen-bonded in parallel with strand G. D1 preserves the inter-sheet disulphide bridge and several other elements of the hydrophobic core characteristic of the immunoglobulin framework. Starting from these alignments we have superimposed D1 onto representative immunoglobulin V domains from Bence-Jones protein Rei ($V_{L\kappa}$)[36], and Fab New ($V_{L\lambda}$ and V_H)[32]. The structurally aligned sequences are shown in Fig. 4. D1 superimposes remarkably well onto the β-sheet framework of all V domains, with a best match to Rei bringing 72 Cα atoms to an r.m.s. discrepancy of 1.22 Å from expert superposition.

In striking contrast with the conserved core of β strands, several loops between strands in CD4 are quite different from those in immunoglobulin V domains. In particular, loop CC' is shortened by four residues and loop FG (immunoglobulin CDR3) is shortened by four to six residues from canonical immunoglobulin lengths. These loops mediate V_H–V_L dimerization in immunoglobulins, an interaction that does not occur with CD4. One addition, important for gp120 binding, is the lengthening of loop C'C'' (immunoglobulin CDR2) by three residues in CD4 compared with κ light chains such as Rei. In this regard, CD4 more closely resembles V_H domains even though overall it superposes best with Rei. This CDR2-like loop interacts with Trp 62, not found in antibodies, and juts out at the tip. Few of the loop changes in D1 were detected in previous alignments with Rei, and consequently structural predictions based on Rei[37] have failed to capture the essence of CD4. The salience of the CDR2 analogue of CD4 and the diminutive nature of the CC' loop and the CDR3 analogue are evident in Figs 2 and 3.

Distinctive domain D2

Domain D2 of CD4 has a tertiary folding that can readily be recognized as resembling immunoglobulin constant domains. Again following standard immunoglobulin nomenclature (Fig. 3), one β sheet of the sandwich-like structure contains strands A, B and E, and the other sheet has strands C, C'', F and G. Despite the general similarity of D2 to constant domains, details of the folding are considerably divergent. First, the size of D2 is small (75 residues) compared with that of immunoglobulin constant domains (~100 residues). This manifests itself in shorter strand lengths. A second variation is that strand C',

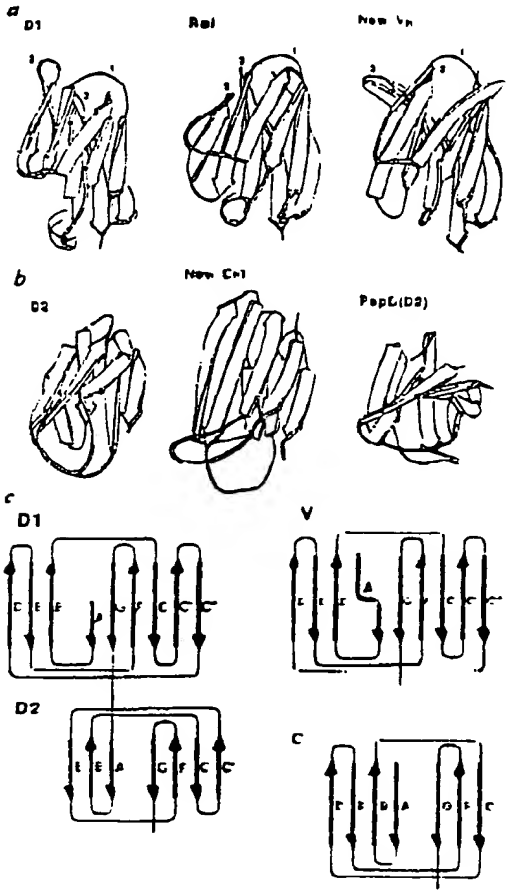

FIG. 3 Schematic comparisons between domains of CD4 and other immunoglobulin-folded domains. a, Ribbon diagrams comparing D1 with a variable λ light-chain domain and a variable heavy-chain domain. The point of view is as in Fig. 2; the CDR loops of immunoglobulins and their analogues in D1 are indicated by numerals. b, Ribbon-diagram comparisons of D2 with a constant domain and with domain D2 of the bacterial chaperone protein PapD. c, Topology diagrams and strand nomenclature for the β sheets in CD4 and in variable and constant domains of immunoglobulins.

which corresponds sequentially to the D strand of normal constant domains, joins the β sheet consisting of strands C, F and G, rather than being hydrogen-bonded to strand E in the other sheet. In this respect, D2 is V-like. A final striking difference from immunoglobulins is that D2 has its disulphide bond between strands in the same sheet, that is strands C and F (Fig. 2), rather than between sheets as is usual. This feature, which is unusual but not unprecedented[38], had been predicted[34]; however, strand C' was not anticipated. The hydrophobic core of immunoglobulin domains is preserved in D2 despite the unusual disulphide connection (Fig. 4). Leu 116 on strand B occupies the position of a normal cysteine partner for Cys 159 on strand F. The inward orientation of the intra-sheet disulphide bridge makes it an important member of the hydrophobic core even though it does not join the sheets.

D2 can be structurally aligned with the CH1 domain of Fab New (Fig. 4), but the resulting spatial superposition is not as close as for D1 comparisons with V domains. Only six of the seven strands superimpose at a 2.5 Å stringency for matches, and this gives 33 matches with an r.m.s. discrepancy of 1.59 Å. D2 superimposes somewhat less well with the Rei variable domain (30 matches within 2.5 Å for 1.68 Å r.m.s. discrepancy). In fact, D2 is actually more similar to the domains of PapD[35] than to immunoglobulin domains. As in the D2 topology, PapD domains also exhibit sheet switching (partially in D1(PapD), fully in D2(PapD)), and 39 Cα atoms of D2 (CD4) superimpose on D1(PapD) with an r.m.s. discrepancy of 1.55 Å. Drawings of the aligned structures are shown in Fig. 3.

Binding site for gp120

The initial molecular event in HIV infection is the binding of gp120 on the viral envelope to CD4 on the cell surface. The high affinity of this interaction, at least for several laboratory strains of the HIV-1 virus[39], has permitted a detailed mapping of the binding site. More than 200 mutant CD4 recombinants have been constructed and tested for gp120 affinity (refs 8, 10-18, J. Arthos *et al.*, manuscript submitted, and unpublished results). Some of these mutant proteins have also been used to map the CD4 epitopes of a battery of monoclonal antibodies. In Table 2 we distil the mutation results to those point mutants in D1 which impair gp120 binding without causing extensive disruptions of structure as judged by antibody binding. Analyses have been reported for mutations at 80 of the 98 residues in D1, but only 19 positions among them have impact on gp120 binding without apparent global conformational change. Thirteen of these are in the span from 38 to 59. Completely buried

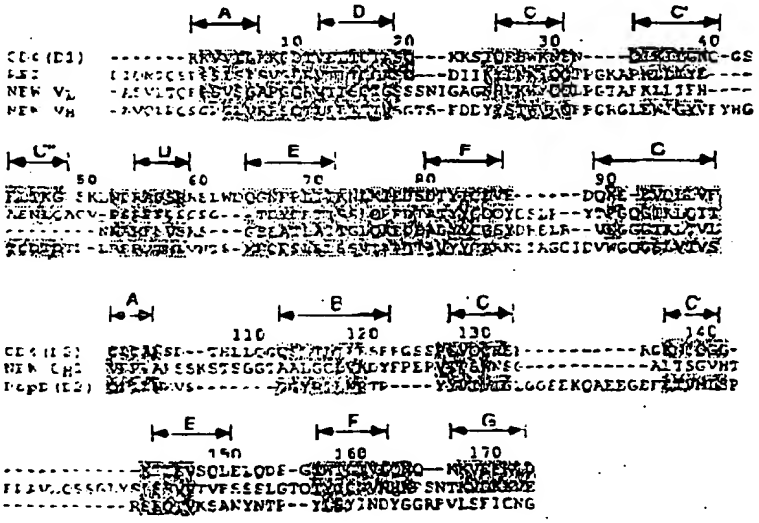

FIG. 4 Structural alignment of the amino-acid sequences of CD4 domains with other immunoglobulin-related domains. Shaded residues have Cα positions within 2.5 Å of corresponding CD4 positions after optimal superposition of all shaded residues for a given pair of domains. (Exceptions up to 2.60 Å were allowed for residues in the middle of strands.) Each superposition relates a certain number of positions N within the specified 2.5 Å limit and these match at a certain r.m.s. discrepancy, Δ. For the match of D1 with Rei ($V_{L\kappa}$), N = 75 and Δ = 1.22 Å; for D1 versus New ($V_{L\lambda}$), N = 66 and Δ = 1.12 Å; and for D1 versus New (V_H), N = 68 and Δ = 1.25 Å. For the match of D2 with New (C_H1), N = 33 and Δ = 1.59 Å; for D2 versus PapD(D2), N = 37 and Δ = 1.26 Å; for D2 versus PapD(D1), N = 35 and Δ = 1.55 Å; and for D2 versus Rei ($V_{L\kappa}$), N = 30 and Δ = 1.65 Å. The alignments of D2 versus PapD(D1) and D2 versus Rei ($V_{L\kappa}$) are not shown.

residues can be discounted as direct participants in binding because their exposure would require major conformational change, which is without precedent for immunoglobulin domains. We have calculated the degree of exposure for each residue in D1 (Table 2), and find that three of the gp120-sensitive residues, Gly 28, Ala 55 and Phe 67, are inaccessible. It seems unlikely that either Lys 29 or Gln 64 is critical for binding because there is no effect for mutations at the more exposed neighbours of Lys 29 or for single or multiple mutations at 64, except alanine. Thus only the alanine replacements at 77, 81 and 85 fall outside of the 41–59 span. The distribution of binding mutants is shown in Fig. 5*a*, *b*.

The importance of the 41–59 region in HIV binding is corroborated by a chimaeric CD4 in which the human sequence from 36 to 62 has been inserted into rat CD4 (A. F. Williams, personal communication). This imparts full gp120 binding activity on the normally unreactive rat CD4 molecule. It also shows that 33 additional side chains which differ in rat and human CD4, including Gln 64, are not absolutely essential for the binding[4]. But, Glu 77, Thr 81 and Glu 85 are among the residues conserved between rodents and primates. Thus, whereas the 41–59 region is positively identified as being involved in gp120 binding, participation of the 77–85 region cannot be excluded.

Antibody binding studies also help to define the gp120 binding site (refs 10, 40, and our unpublished results), pointing especially to the CDR2-like region. Two major groups of D1-binding monoclonal antibodies have been described and their epitopes are illustrated in Fig. 5*c*. The epitope of one cross-blocking group, typified by Leu3a, maps to the CDR2-like loop and usually includes portions of the CDR1-like loop. These antibodies also block gp120 binding. The epitope of the second group, typified by monoclonal L71, includes the CDR3-like loop and sometimes a portion of the strand G. These antibodies inhibit viral infection and cell fusion, but do not efficiently block gp120 binding; some even form ternary complexes with gp120 and CD4 (A. Truneh *et al.*, manuscript submitted).

The CDR2-like region that is strongly implicated in gp120 binding is also very prominent in the CD4 structure (Figs 3 and 5). The C'–C" hairpin loop at Gln 40–Phe 43 is almost completely exposed. Most strikingly, the hydrophobic side chain of Phe 43 juts out into the solvent as shown in Fig. 5*e*, *f*. The involvement of a phenyl group in binding is also suggested by peptide inhibition studies[41,42]. If the 77–85 span were also to be directly involved in gp120 binding, this would present a puzzle because this site is on a face nearly opposite from the CDR2-like region (the vector from the molecular centre of D1 through Cα43 makes an angle of 152° with the similar vector through Cα81), and no intervening residues have been implicated in gp120 recognition.

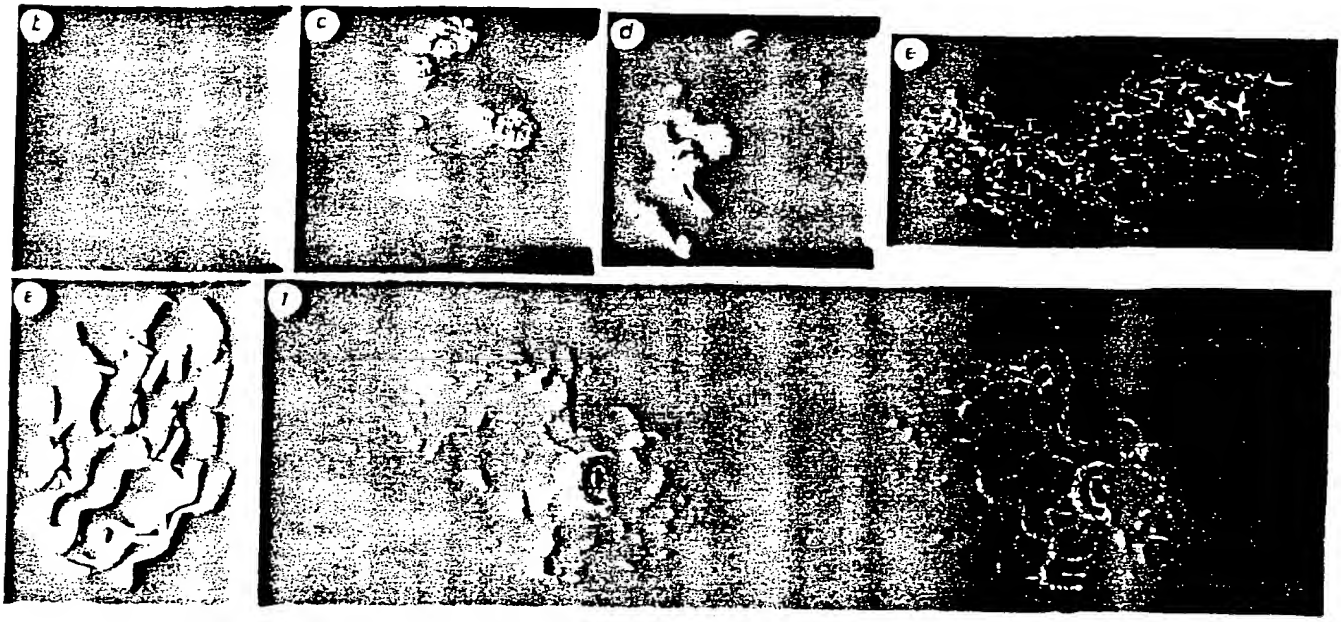

FIG. 5 Images of CD4 relating to sites of interaction with HIV. *a* Cα backbone of D1 with sites implicated by mutational and structural analysis to affect high-affinity gp120 binding (see Table 2). Non-buried residues that show reduction in binding without global disruption of structure (as judged by antibody binding) are coloured red-orange (26, 41, 42, 43, 44, 45, 47, 49, 52, 55, 56, 77, 81 and 85) on a backbone drawn by WORM (L. Andrews). The orientation is as in Figs 2 and 3. *b*, Van der Waals' surface of D1 with side chains of gp120-sensitive residues coloured. Those showing marked reductions are in pink (43, 44, 45, are visible) and those showing moderate effects are in purple (55, 42 are visible). The point of view is from above *a* looking down at the tips of CDR-like loops. *c*, Van der Waals' surface of D1 with side chains of antibody epitopes coloured. Residues identified with epitopes of the Leu3a family and shown in purple (24, 25, 27, 42, 43, visible) and those identified with the L71 family are shown in yellow (66, 68, visible). The view is roughly as in *b*. *d* Electrostatic potential surface computed with DELPHI[35] at neutral pH and displayed with AAK (A. Nicholls and B. Honig) at the levels of the solvent-accessible surface with a probe radius of 1.4 Å. Blue represents positive potential, red negative, and white neutral. The negative patch is associated with residues 25, 27 and 28. The view is approximately as in *b*, *c*. An all-atom representation of D1D2. Residues in the gp120-binding region, from residue 41 to 59, are drawn in red. The direction of view is roughly as in Fig. 2, but the molecule has been rotated by ~90° about this view axis. This view illustrates the exposed nature of Phe 43. The actual conformation of this phenyl side chain in the crystal is at least partly determined by lattice interactions, but its highly exposed nature would also be expected to persist in other conformations accessible in solution. *f*, Stereoview of the molecular surface in the major gp120-binding region of D1. Atoms are drawn as in *e*, and are enveloped by the surface in contact with a probe sphere of 1.4 Å radius as displayed by QUANTA (Polygen). This view is taken after rotation from *e* by ~90° about the horizontal axis.

Fusion determinants

After the initial binding event, entry of virus into the cell occurs through fusion of cellular and viral envelope membranes. In addition, HIV-infected cells fuse with uninfected $CD4^+$ cells to form syncytia, a process mediated by interactions between HIV envelope protein expressed on the infected cell surface and CD4 on the uninfected cell. Syncytium formation is thought to mimic viral entry and could be an important mode of viral spreading. Chimpanzee CD4, which binds to HIV but does not support syncytium formation, has Gly replacing Glu at residue 87. This replacement in human CD4 abolishes syncytia formation while preserving gp120 binding[17] and, curiously, normal viral infection kinetics. Residues 88 and 89 are also implicated in this process by mutation (Table 2). These residues lie at the β-turn tip of the CDR2-like loop in D1 and are part of a patch of negative potential on the otherwise mostly positive D1D2 surface (Fig. 5*d*). The CDR2-like loop is spatially separated from the CDR2-like loop implicated in high-affinity binding to gp120 ($C\alpha$87 is 17 Å from $C\alpha$43). In accord, monoclonal antibodies of the L71 family block syncytium formation although they permit gp120 binding to CD4. So, it seems that the CDR2-like loop is necessary for secondary interactions between the viral envelope and CD4 before fusion. This could relate to CD4-induced release of gp120 from virus and infected cells[43–45] and exposure of a fusogenic domain on the membrane envelope protein gp41.

Immune response interactions

The observation that $CD4^+$ lymphocytes react only with class II-bearing target cells suggests that CD4 associates directly with class II MHC, and it is thought that CD4 may also have a role in signal transduction. There is evidence from cellular assays to support the association of CD4 with class II MHC molecules[46], the T-cell receptor[47], and the $p56^{lck}$ kinase[48], as well as other CD4 molecules[49]. Except for the interaction of CD4 with $p56^{lck}$, however, these associations are necessarily weak and thus difficult to measure. Mutagenesis *in vitro* has been used to identify the sites on CD4 that interact with class II MHC molecules. On the basis of assays of either cell adhesion[16,50] or interleukin-2 production[18], large separated expanses of the CD4 molecule, involving regions on D1, D2 and D3, have been implicated in the CD4–MHC interaction. These findings are not easy to reconcile with the structure of CD4. Some of the disruptive mutations occur in contact or bridging regions between the domains. Perhaps some of the other disruptions reflect complications from the diverse components of the cellular system rather than direct binding. For example, self-associations of CD4[19] might be involved in signal transduction and possibly in class II binding.

Evolutionary implications

There is little doubt that CD4 and immunoglobulins have evolved from a common ancestor: intron and domain boundaries coincide and, although the sequences are highly divergent, superimposable strand topologies and a common hydrophobic core are preserved. It seems likely, however, that evolution to the antibody family, with its vast repertoire of dimeric receptor units, was a later event, and that CD4 is more prototypical of immunoglobulin superfamily receptors which are often monomeric and nonpolymorphic. The absence from CD4 of J-like regions, which impart diversity in antibodies, is consistent with this. The progenitor of the diverse immunoglobulin superfamily of the present may have its vestige in the gene structure of D1, which is split by an intron (at position 47) as are genes for other immunoglobulin-like domains[51,52]. A quasi-diad axis, perpendicular to the sheets and passing midway between strands B and E on one sheet and between strands C and F on the other, can be used to superimpose successive strands in the first exon on those in the second exon. An immunoglobulin progenitor produced by a gene duplication event[53] might have been V-like, but a D2-like progenitor that would evolve to V and C domains is also a possibility.

Whatever the course of evolution, it is remarkable that molecules that function in recognition are often members of the immunoglobulin gene family. Clearly the immunoglobulin fold provides a facile framework from which a variety of loops with distinctive characteristics can be elaborated. These loops can have distinct functions, as in binding to gp120 at the CDR2-like loop and effecting fusion from the CDR3-like loop, and such modularity might have evolutionary advantage. Similarly, the quasi-symmetric nature of the immunoglobulin motif, with N and C termini at opposite ends, facilitates the concatenation of tandem, flexibly linked modules that can have distinct roles. In the case of CD4, one domain might be involved in class II binding whereas another domain might effect self-associations of the kind found in crystalline polymorphs[19], and these could be essential for signal transduction. Indeed, in an alignment of D3 with D1, dimerization loops of immunoglobulin V domains would not be foreshortened in D3 as they are in D1. Such modules could evolve separately and be recombined by exon shuffling to integrate complex recognition and effector functions. □

Received 12 October; accepted 29 October 1990.

1. Robey, E. & Axel, R. *Cell* 60, 697–700 (1990).
2. Maddon, P. J. *et al. Cell* 42, 93–104 (1985).
3. Williams, A. F. & Barclay, A. N. *A. Rev. Immun.* 6, 381–405 (1988).
4. Clark, S. J., Jefferies, W. A., Barclay, A. N., Gagnon, J. & Williams, A. F. *Proc. natn. Acad. Sci. U.S.A.* 86, 1649–1653 (1987).
5. Maddon, P. J. *et al. Proc. natn. Acad. Sci. U.S.A.* 84, 9155–9159 (1987).
6. Dalgleish, A. G. *et al. Nature* 312, 763–767 (1984).
7. Klatzmann, D. *et al. Nature* 312, 767–768 (1984).
8. Arthos, J. *et al. Cell* 57, 469–481 (1989).
9. Capon, D. J. *et al. Nature* 337, 525–531 (1989).
10. Peterson, A. & Seed, B. *Cell* 54, 65–72 (1988).
11. Landau, N. R., Warton, M. & Littman, D. R. *Nature* 334, 159–162 (1988).
12. Clayton, L. K. *et al. Nature* 335, 363–366 (1988).
13. Mizuguchi, T., Fuerst, T. R., Berger, E. A. & Moss, B. *Proc. natn. Acad. Sci. U.S.A.* 86, 9273–9277 (1989).
14. Chao, B. H. *et al. J. biol. Chem.* 264, 5182–5186 (1989).
15. Brodsky, M. H., Warton, M., Myers, R. M. & Littman, D. R. *J. immun.* 144, 3078–3086 (1990).
16. Ashkenazi, A. *et al. Proc. natn. Acad. Sci. U.S.A.* 87, 7150–7154 (1990).
17. Camerini, D. & Seed, B. *Cell* 60, 747–754 (1990).
18. Lamarre, D. *et al. Science* 245, 748–746 (1989).
19. Kwong, P. D. *et al. Proc. natn. Acad. Sci. U.S.A.* 87, 6423–6427 (1990).
20. Davis, S. J. *et al. J. molec. Biol.* 213, 7–10 (1990).
21. Richardson, N. E. *et al. Proc. natn. Acad. Sci. U.S.A.* 85, 5102–5106 (1988).
22. Berglu, C. C. *et al. J. immun.* 142, 2250–2256 (1989).
23. Healey, D. *et al. J. exp. Med.* 172, 1233–1242 (1990).
24. Chirnow, S. M. *Biochemistry* 29, 9885–9891 (1990).
25. Wang, J. *et al. Nature* 348, 411–418 (1990).
26. Carr, S. *et al. J. biol. Chem.* 264, 21286–21295 (1989).
27. Xuong, Ng.h., Sullivan, D., Nielsen, C. & Hamlin, R. *Acta crystallogr.* B43, 267–269 (1985).
28. Ashford, V., Del, R., Nielsen, C., Sullivan, D. & Xuong, Ng.h. *Acta crystallogr.* A46, C-15 (1990).
29. Jones, T. A. *J. appl. Crystallogr.* 11, 268–272 (1978).
30. Hendrickson, W. A. & Konnert, J. H. in *Computing in Crystallography* (eds Diamond, R., Ramaseshan, S. & Venkatesan, K.) 13.01–13.22 (Indian Institute of Science, Bangalore, 1980).
31. Bringer, A. T., Kuriyan, J. & Karplus, M. *Science* 235, 458–460 (1987).
32. Saul, F. A. *et al. J. biol. Chem.* 253, 585–597 (1978).
33. Gilson, M., Sharp, K. & Honig, B. *J. comp. Chem.* 8, 327–335 (1987).
34. Williams, A. F., Davis, S. J., He, C. & Barclay, A. N. *Cold Spring Harb. Symp. quant. Biol.* 54, 637–647 (1989).
35. Holmgren, A. & Brändén, C.-I. *Nature* 342, 248–251 (1989).
36. Epp, O. *et al. Eur. J. Biochem.* 45, 513–524 (1974).
37. Bates, P. A., McGregor, M. J., Islam, S. A., Sattentau, Q. & Sternberg, M. J. E. *Protein Eng.* 3, 13–21 (1989).
38. Wilson, I. A., Stanfel, J. J. & Wiley, D. L. *Nature* 289, 366–373 (1981).
39. Das, E. S., Xi, L. L., Moudgil, T. & Ho, D. D. *Proc. natn. Acad. Sci. U.S.A.* 87, 6574–6578 (1990).
40. Sattentau, Q. J. *et al. J. exp. Med.* 170, 1319–1334 (1989).
41. Lifson, J. D. *et al. Science* 243, 712–714 (1989).
42. Fisberg, R. W. *et al. Science* 249, 287–291 (1990).
43. Kirsh, R. *et al. AIDS Res. hum. Retroviruses* 6, 1209–1215 (1990).
44. Moore, J. P., McKeating, J. A., Weiss, R. A. & Sattentau, Q. J. *Science* (in the press).
45. Hart, T. K. *et al. Proc. natn. Acad. Sci. U.S.A.* (in the press).
46. Doyle, C. & Strominger, J. L. *Nature* 330, 256–259 (1987).
47. Chuck, R. S., Cantor, C. R. & Tax, D. B. *Proc. natn. Acad. Sci. U.S.A.* 87, 8021–8025 (1990).
48. Turner, J. M. *et al. Cell* 60, 755–765 (1990).
49. Veillette, A., Bookman, M. A., Horak, E. M., Samelson, L. E. & Bolen, J. B. *Nature* 338, 257–259 (1989).
50. Clayton, L. K., Sieh, M., Pious, D. A. & Reinherz, E. L. *Nature* 339, 548–551 (1989).
51. Owens, G. C., Edelman, G. M. & Cunningham, B. A. *Proc. natn. Acad. Sci. U.S.A.* 84, 294–298 (1987).
52. Lemke, G., Lamar, E. & Patterson, J. *Neuron* 1, 73–83 (1988).

53. Bourgois, A. *Immunochemistry* 12, 873–878 (1975).
54. [illegible] W. A. *Trans. Am. crystallogr. Assoc.* 21, 33–?3 (1985).
55. Fehler, A., Smith, J. L. & Hendrickson, W. A. *Acta crystallogr.* A46, 537–540 (1990).
56. Karle, J. *Int. J. quant. Chem. Symp.* 7, 357–367 (1980).
57. Hendrickson, W. A. *Acta crystallogr.* B27, 1472–1473 (1971).
58. Hendrickson, W. A., [illegible] C. L. & [illegible] R. B. *Proc. natn. Acad. Sci. U.S.A.* 72, 2160–2164 (1975).
59. Sheriff, S., Hendrickson, W. A., Stenkamp, R. E., Sieker, L. C. & Jensen, L. H. *Proc. natn. Acad. Sci. U.S.A.* 82, 1104–1107 (1985).

ACKNOWLEDGEMENTS. We thank M. Sumner, D. Sullivan, V. Ashford and C. Nelson for help in data collection [illegible] for help in protein preparation and purification; C. Ogata for helpful discussions, Z. Otwinowski for his phasing program, C. Brändén and M. Amzel for supplying PepC and Fab New coordinates, respectively; A. Williams, Q. [illegible], F. Sjoholm and D. Capon for communicating results before publication and R. Yermolinsky for her drawing. This study was supported in part by the National Institutes of Health (W.A.H.) and by the [illegible] Foundation (N.-h.X.); the area detector facility at UCSD is an NIH Research Resource (N.-h.X.). Atomic coordinates have been deposited in the Protein Data Bank with entry name 1CD4 for release one year after publication of this paper.

LETTERS TO NATURE

Entropy production as the selection rule between different growth morphologies

Adrian Hill

Physiological Laboratory, Downing Street, Cambridge CB2 3EG, UK

CRYSTALLIZATION of a solid phase from a melt or solution is a special case of pattern formation in which the dissipation of energy across the free energy gradient between the two phases can give rise to various growth morphologies in the steady state[1]. Experimental studies of crystallization from undercooled solutions[2], electrolytic deposition[3,4] and the formation of fluid patterns in a Hele–Shaw cell[5] have revealed faceted, dendritic, 'dense-branching' and fractal morphologies[6]. For a system with fixed anisotropy and interfacial tension, changes in the driving force for the transition (such as the degree of undercooling) can cause changes in growth morphology which are usually accompanied by changes in growth rate. The selection rule that determines these morphologies remains unclear, although a recent suggestion[3,4] is that it is based on the growth velocity. Here I propose that selection is governed by the rate of entropy production per unit area of the different growth patterns. This principle allows accurate prediction of the morphology transition observed for the crystallization of NH_4Cl (ref. 2). I suggest that it may reflect a more general thermodynamic principle underlying a wide range of natural processes.

Consider the formation of a generalized 'crystal' in which the driving force X (ignoring surface terms) is proportional to either supersaturation, pressure or other fields. The form of the crystal involves many surface orientations which have a different surface free energies. Denoting this surface free energy f by

$$f = u - Ts \quad (1)$$

where u and s are the surface energy and entropy of the crystal, the velocity V representing the rate of crystallization is expressed as a linear function

$$V = L(X - \theta) \quad (2)$$

where X is the difference between the free energies of the dissolved solute and the bulk solid and θ is the free energy required to increase the area, so that $X - \theta$ is the total driving force, and L is the rate coefficient reflecting the growth rate of a particular morphology and its rate of entropy production. The dissipation is given by

$$\phi = dS/dt = V(X - \theta) = L(X - \theta)^2 \quad (3)$$

where θ is a linear function of f and S is the entropy created in the crystallization. A model of the process of growth that relates velocity to driving force is a model of the rate coefficient and a link between the kinetics and the entropy production. Ben-Jacob and Garik[6] suggest that there must be a conjugate variable to the average rate of crystal growth. This conjugate variable is the force $(X - \theta)$. Equations (2) and (3) assume linear phenomenological relations but these are merely convenient and not essential: they almost certainly do not hold far from equilibrium or when chemical reactions occur.

The dissipation functions of two morphologies formed by adjacent steady states will in general have crossover points (Fig. 1). It follows directly from equation (3) that the crossover point for adjacent morphologies occurs at the driving force

$$X_c = \frac{(L_1\theta_1 - L_2\theta_2) \pm (\theta_1 - \theta_2)\sqrt{(L_1L_2)}}{(L_1 - L_2)} \quad (4)$$

There are entropic crossovers because equation (3) is a parabola in the $\phi - X$ plane: the section between $X = 0$ and $X = \theta$ represents a disaggregation of the crystal structure. This does not normally occur in experiments unless crystals are initially present, in which case one morphology disappears as the other is formed. As ϕ is always positive, I consider for the moment only the parts of the entropy curves with positive gradients because these represent crystallization, that is, the forward reaction driven by X. Reference to Fig. 1 shows that if a crossover point is to occur in this domain when $\theta_1 < \theta_2$ then $L_1 < L_2$. At higher driving forces new crossovers occur if there are steady states that can exist by creating other morphologies with higher values of L. When the driving force is reduced from a high value, the principle of selection for the steady state with highest value of ϕ predicts that at the crossover points (c_1 and c_2 in Fig. 1) transitions occur to different steady states producing different crystal morphologies. In the linear regime these transitions cannot occur without discontinuities in the rate of crystallization because, as follows from equations (2) and (4), the only point free from such discontinuity is the trivial one

$$(\theta_1 - \theta_2)\sqrt{(L_1L_2)} = 0 \quad (5)$$

in which the rates are zero. Small differences in entropy production rates at a crossover, however, could lead to small changes in slope together with small discontinuities which may be masked by variation in the data. Discontinuities are indeed a striking feature of morphology changes in various experimental

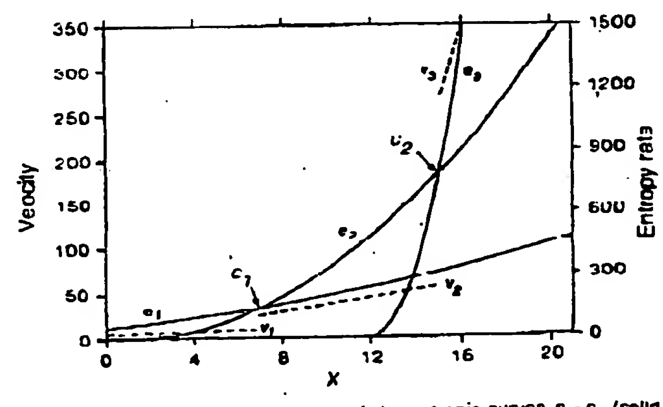

FIG. 1. The crossing points c_1 and c_2 of the entropic curves e_1–e_3 (solid lines) of three morphologies. The associated velocities v_1–v_3 (dashed lines) are also shown. The constants for the three entropic curves are $L_1 = 0.5$, $\theta_1 = -10$; $L_2 = 4$, $\theta_2 = 1$; $L_3 = 87$, $\theta_3 = 12$.